NASA TECHNICAL MEMORANDUM

NASA TM X-52290

NASA TM X-52290

GPO PRICE $ ________

CFSTI PRICE(S) $ ________

Hard copy (HC) 3.00

Microfiche (MF) .65

ff 653 July 65

CENTAUR AC-6 NOSE FAIRING SEPARATION TESTS

by Jack C. Humphrey and Charles W. Eastwood, Jr.
Lewis Research Center
Cleveland, Ohio

N67-35375 (ACCESSION NUMBER) 1 (THRU)
10 (PAGES) (CODE)
31 (CATEGORY)
(NASA CR OR TMX OR AD NUMBER)
FACILITY FORM 602

NATIONAL AERONAUTICS AND SPACE ADMINISTRATION · WASHINGTON, D.C. · 1967

3 CENTAUR AC-6 NOSE FAIRING SEPARATION TESTS 6

by Jack C. Humphrey and Charles W. Eastwood, Jr.

Lewis Research Center
Cleveland, Ohio

NATIONAL AERONAUTICS AND SPACE ADMINISTRATION

E-3897

CENTAUR AC-6 NOSE FAIRING SEPARATION TESTS

by Jack C. Humphrey and Charles W. Eastwood, Jr.

Lewis Research Center
National Aeronautics and Space Administration
Cleveland, Ohio

Summary

The flight qualification tests of the AC-6 Centaur nose fairing by simulated separation of the fairing from the Centaur vehicle are described. It was necessary to qualify several new parts of the nose fairing not qualified in previous tests and to determine loads imposed by the fairing on the Centaur forward bulkhead during separation. The tests were conducted under pressure conditions encountered by Centaur at the time of nose fairing flight separation (approximately the pressure at 350,000 foot altitude) but without simulation of the actual flight acceleration (approximately 1.25g). Data presented give pressures, forces, displacements, and accelerations encountered by the nose fairing during separation in each test.

It was determined by these tests that all parts of the nose fairing in the final test configuration were suitable for their proposed use. In addition, it was determined that the loads transmitted through the nose fairing hinges to the Centaur tank during separation were within the allowable loads for the tank. Because of these tests, it was necessary to change the envelope within the nose fairing due to static interference and possible dynamic interference between thermal bulkhead struts and the Surveyor envelope.

Introduction

Previous flight qualification tests (ref.1) conducted in support of Atlas/Centaur flight AC-4 showed that shrapnel came from the parts used on the nose fairing split line latches and the plug assembly of the thruster bottle nozzles. Since this shrapnel could damage the Surveyor payload, it was necessary to redesign the parts releasing the fragments and to qualify these parts for use with the nose fairing. Other parts not included in the AC-4 qualification tests were added to the nose fairing for tests reported herein.

Since the AC-6 flight was to be the first flight with new Centaur tanks in which the tank wall thickness was to be decreased from 0.016 inches to 0.014 inches, a more precise verification of the dynamic loads on the tank caused by nose fairing separation was required.

A payload envelope inside the nose fairing was defined and agreed upon by those involved in the construction of the Surveyor and the Centaur vehicles. In certain areas, it was necessary to determine if the nose fairing parts encroached upon this envelope.

Objective

The purposes of the tests were to (1) determine if there were any underdesigned parts, (2) to flight qualify all parts, (3) to determine dynamic loads imposed by the nose fairing on the Centaur vehicle, and (4) to determine if necessary clearance existed between the nose fairing and either the Centaur vehicle or the Surveyor dynamic envelope during separation.

Test Article

The nose fairing, forward bulkhead model, equipment shelf, and payload adapter described in reference 1 were also used in the tests reported herein, but with modifications and additions. These changes are presented in table I. Before use in this series of tests, the nose fairing was repaired and modified at the General Dynamics, Fort Worth plant, and all possible new parts were installed there. The new parts that could not be installed at Fort Worth were installed at LeRC under the supervision of the contractors' personnel familiar with the installation of the parts.

The Centaur forward bulkhead model was modified for tests LA-3 and LA-4 so as to allow installation of a load cell to measure the radial load applied by the fairing through the hinge to the forward bulkhead. This was accomplished by elongating the hinge shear pin holes in the 219 ring so as to allow rotation of the hinge under load. This freedom of motion allowed the hinge to transmit the fairing loads to a load cell placed between it and the rigid pipe structure of the forward bulkhead model. Figure 13 shows this installation for test LA-3, figure 14 shows the calibration curve for the load cell, and figure 15 shows the deflection curve for the load cell for test LA-3. Further modification of the forward bulkhead was made for test LA-4A so that the spring constant of the structure supporting the load cell would be close to the spring constant of the forward bulkhead during the flight. It was necessary to make this spring constant non-variant, and therefore it differed from the spring effect of the actual flight tank bulkhead which deflected at a varying rate as the load changed. Figure 16 shows the deflection curves of the hinge supporting structure compared to a deflection curve of the hinge point of the Centaur tank. To effect this change, the 219 ring and the outer skin of the forward bulkhead were cut away 60 degrees on each side of the hinge point. The load cell was removed from the bulkhead structure and was supported on a beam having a spring constant of 8000 pounds per inch deflection. Figures 17 and 18 show this modification.

Facility

The facility arrangement for the AC-6 separation test was the same as the arrangement in reference 1 for tests 8 through 13. Briefly, the fairing was mounted on a model of the Centaur forward bulkhead. The quad II-III fairing half was mounted on facility hinges and stopped by large pads cushioned by aluminum honeycomb to lower the deceleration of the fairing. The quad I-IV fairing half was jettisoned into a net. Figure 19 shows the facility arrangement.

For this test, no Surveyor model was mounted inside the fairing. A pipe tower containing three cameras was mounted in its place.

A separate test was also run to compare the thrust developed by the thrust bottle using the AC-4 type nozzle with that developed by the thrust bottle using the AC-6 nozzle. For this test the thruster bottle was attached to a steel frame work by the mounting arms used in the nose fairing. These arms were strain gauged so as to measure the thrust of the bottles. A calibration of these gauges was made using a load cell and hydraulic ram to transmit known forces to the nozzle of the thruster bottle. Figure 20 shows the arrangement of the test set-up and figure 21 shows the calibration curves for the strain gauges used in the tests. The test stand was located in an altitude chamber capable of being evacuated to a simulated 100,000 foot altitude.

Facility Electric System

The electrical activation system for the tests was designed so that after all circuits were armed by a key switch, a program timer with attached transistor type relays was energized by another key switch to give power to the various electrical devices in the test system. The timer and system was arranged so as to turn on the lights and cameras immediately and to fire the thruster bottle squib one second after start of the cameras. Separate toggle switches for energizing the shaped charge and the split line latches could be used before actuation of the timer. Figure 22 shows a schematic diagram of the electrical system.

Facility Instrumentation and Cameras

The instrumentation and the cameras are similar to that used in the test reported in reference 1. Figure 23 shows a block diagram of the instrument system. Figure 24 shows the location of all transducers used in these tests and Table II relates the transducer number and transducer position as well as the number of the tests in which the transducer was used, its range, and its accuracy. Figure 25 shows the camera positions and Table III gives the camera positions used for each test.

The jettison bottle test equipment had strain gauges mounted on the support arm and a pressure pick up connected to the bottle. This instrumentation is shown in figure 20. These instruments were recorded on the same equipment used for fairing separation tests.

TEST DESCRIPTIONS

General

Table III lists the test hardware, its arrangement, and the facility configuration for each test.

Thrust tests of Jettison bottles

A comparison of the new type exhaust nozzle (Part no.-55.08019) used on the jettison bottle was made with the nozzle used on the AC-4 jettison bottle by exhausting the bottle from 2500 pounds per square inch to a pressure equivalent to that found at approximately 100,000 feet altitude with each of the nozzles. Two tests were performed using the AC-4 nozzle and one test was performed using the AC-6 nozzle. Figure 26 shows the test arrangement. Data for the nozzle tests are shown in figure 27.

Test LA-1

Before installation of the fairing into the test chamber, strain gauges were installed on the Quad I-IV barrel section of the fairing, the two halves of the flight hinge, (Part No. 55-72075 and 55-72979) and one of the thermal bulkhead struts (Part No. 55-71297). In each location on the fairing wall one gauge was installed on the outside and another gauge was installed on the inside. The two gauges were wired to form two active arms of a bridge circuit. The location of these gauges is shown in figure 24b and a photograph of the gauges before and after installation of a protective metal sheet is shown in figures 28a and b. The tank half of the hinge (strain gauge no. 117) was calibrated by applying stepped loads up to 5000 pounds on this half of the hinge in a downward direction while mounted on the forward bulkhead model. The calibration of the fairing half of the hinge (strain gauge no. 118) was accomplished by forcing this hinge half radially inward against its mating half mounted on the forward bulkhead. The same load increments were used for both hinge calibrations. Calibration of the tank half of the hinge is shown in figure 29. Figure 30 shows the calibration for the fairing hinge half.

Previous calibrations of the thermal bulkhead strut strain gauges established that the load in the strut could be calculated by use of the known gauge factor and the known parameters of the strut with less than 1 percent error, consequently no calibration was made of these gauges.

Before test LA-1, several changes not accomplished at the contractor's factory were made and some fitting of parts was required. Defective parts were observed as follows:

1. The new 218.90 ring (55-72969) and tank half of hinge (55-72979) and the anvil ring (55-72975) were installed on the forward bulkhead model. During the installation four nut plates were damaged and were not used for future tests.

2. Because of the addition of the new pyrotechnic valve and nozzle to the jettison bottle, the bottle location had to be changed to eliminate interference with the seal bulkhead (Part no. 55-72030, located at top of Quad II-III fairing half). Figure 6 shows this change.

3. After installation of the fairing on the 218.90 ring the tension strap (55-7214), shaped charge (55-74382), seal retainer (55-71217), seal (55-72166), and skirt (55-71210) were installed. Hand fitting of the wiring tunnel bulkhead was required before installation of the shaped charge. After fitting, the shaped charge was installed with no trouble and the tension strap was fitted with no more than 0.05 inch clearance at any point around the circumference. Figure 31 shows the fit between the wiring tunnel bulkhead and the tension strap (Part no. 55-71214). Fitting was also required before installation of the shaped charge detonators as seen in figure 32.

4. During installation of the split line latches, galling occurred between one of the lugs and nuts used on the latches. This lug and nut were replaced with spares and no further difficulty arose. Installation of two of the squibs used in the latch pin puller assemblies was made with difficulty due to insufficient clearance between the squib and clevis.

Testing of the shaped charge and split line latches was conducted in a separate test from the fairing separation test so as to prevent particles from the shaped charge getting into the facility diffusion pumps required for the separation test. For this test the laboratory central vacuum system which is capable of evacuating the test chamber to a maximum altitude of approximately 100,000 feet was used instead of the diffusion pumps. The shaped charge was fired and 24 seconds later the split line latches were fired while at the rated altitude of the pumping system. After returning the test chamber to a sea level condition it was found that the latches and shaped charge had performed their functions satisfactorily with only minor damages noted. The shaped charge retainer was delaminated. Parts of the retainer and the seal were scattered at random locations about the test chamber. Bolts holding the skirt assembly were ejected in three places and partially ejected in six places. The plastic bolt hole inserts originally glued to the skirt were all loosened during explosion of the shaped charge. The bottom of the detonator was tilted outboard by the explosion and screws holding the detonator had pulled partially through the mounting block. A screw used to hold the detonator fairing was ejected from each fairing. Figure 33 shows some of the post test details. The tension strap cut, although continuous, was not sharp. A rolled effect, as seen in figure 34, was observed at all sections. Although the flight hinges were installed with a gap between the top of the fairing half pin and the tank half socket, no gap existed after the tension strap was cut, due to the release of tension on the 208 seal ring.

Examination of the fairing after firing of the pyrotechnics also revealed that the gap between the fairing halves at the top of the cone was 1.2 inch between the Quad I and II longerons and 1.1 inch between the Quad III and IV longerons. The gap with latches attached had been less than 0.2 inch. Figure 35 shows the gap.

No effort was made to decrease the gap at this time. The chamber was cleaned so as to be able to use the diffusion pumps and then evacuated to 348,000 feet altitude. Separation was accomplished and only minor damage was sustained. The gasket glued to the payload adapter air conditioning disconnect was broken from its attachment point and was found lying on the equipment shelf. The A frame attached to the Quad II-III deflector bulkhead was bent as shown in figure 36. A crack was observed in the deflector bulkhead upper fibre glass angle ring that ties the bulkhead to the conical section. This crack was very close to the XX axis in Quad II as shown in figure 37. Figure 38 shows plots of the data taken during this test and figure 39 shows the flight trajectory of the fairing.

Test LA-2

The bent deflector bulkhead A frame was removed, a new part was riveted to the A frame assembly, and the whole assembly was then replaced. The gasket on the payload adapter air conditioning disconnect was glued to the male part of the disconnect instead of the female part. The current measuring circuit of the pyrotechnic electrical system was altered by placing relay contacts in the circuit so that current could not be measured until the arming circuit was energized as shown in the wiring schematic, figure 22. The flight hinge was relocated so that no gap existed between the top of the tank half of the hinges and the bottom of the 218.90 splice plate, and a gap of 0.070 inch between the bottom of the hinge pin and the hinge socket was set.

New parts not on the previous test were installed on the nose fairing. These parts were the payload hazard detection system, as shown in figure 9, TV light assembly (minus the electrical harness) as shown in figure 5, and the thruster bottle pressure pickup. (A photograph of the hazard detection probe in the air conditioning nozzle is shown in figure 49.)

To determine if clearance existed between the Centaur nose fairing and the volume reserved for the Surveyor payload, a wood model of the aft end of the Surveyor envelope was fabricated at LeRC to dimensions given by the General Dynamics drawing number 55-00050. This model was clamped to the payload adapter inside the nose fairing and 1.0 inch thick honeycomb was glued to the outer rim of the underside of this model. Measurements of the envelope revealed that after installation all parts of the envelope were within 0.06 inches of proper station.

Later efforts to close the fairing halves revealed a definite static interference between the strut on the YY axis between the II and III quads and the payload envelope model. To put the Quad II-III fairing half in its proper position, it was necessary to cut a slot in the envelope to give this strut clearance. This slot was approximately 1.5 inches wide and penetrated the bottom envelope surface 3.5 inches. To assemble the Quad I-IV half of the fairing, it was necessary to remove the bottom surface

of the envelope located at station 135 and in the YY axis area. It was also necessary to cut the edge of the envelope back about 2 inches, and for a length of 4 inches around the circumference directly above the air conditioning duct (enlarged section located on top of the thermal bulkheads). These clearances were necessary only during the assembly operation and would not be needed if the assembly were made using the fixtures provided for in flight assembly. Figure 41 shows the installation on the payload adaptor and modifications to the envelope model.

Four new nut plates on the barrel section channel were installed and the shaped charge was installed without a seal under the tension tie. A new skirt was used for this test because of damage to the original skirt. A strengthened detonator fairing was installed over each detonator. The shaped charge was fired at 108,000 feet altitude pressure, and the tension strap was cut all along its length. Again the cut left a turned over edge which in some places was broken in two places so as to form a loose sliver of metal as shown in figure 42. Bolts and the inserts of the skirt assembly were loosened or completely pulled out in numerous places. Figure 43 shows the skirt damage for all shaped charge tests. Three bolts in the detonator fairing were also loosened. The detonator was completely separated from its mounting pad as shown in figure 44.

For the second shaped charge test, the same skirt assembly, 218.90 ring and detonator fairings were used. The skirt assembly was repaired by glueing new plastic inserts in the old locations. Washers with 0.562 inch outside diameter were placed under the bolts holding the Quad I, III, and IV skirts and with 0.625 inch outside diameter under bolts for Quad II skirt. It was more difficult to screw bolts through the skirt and the tension strap in this assembly than in previous assemblies. The shaped charge was fired at sea level for this test and the tension strap was completely cut. A rolled edge at the cut was again observed. Bolts and inserts were again damaged on the skirt assembly, but damage was not as great as in previous tests. Examination of the anvil ring after this test showed that it had become deformed from repeated shaped charge firing. The bottom of the anvil ring section was bent inward approximately 0.06 inches all around its circumference. The detonator again pulled away from its support plate and was only held by its electrical connection. Figure 43 shows the skirt positions with the bolt damage.

Immediately after firing the shaped charge, the test chamber was closed and evacuated to a pressure equivalent to 94,000 feet altitude. The latches were then fired and all separated with no damage to the latch fairings. The fairing halves again had sprung apart upon latch separation. A gap 2.25 inches wide between the longerons was found at the top of the cone.

It was desired to make a comparison between the flight trajectory and a computed trajectory based on having this gap closed (highest pressures

and accelerations would be obtained for this case). Interference between the two halves of the knee joint latch brackets had been observed when the fairings were held together by the latches. These brackets were ground so as to remove 0.25 inch of metal from the interference points. Latches were installed on the brackets and tightened to bring the fairing halves together and then slowly loosened. The gap between the longerons after procedure was 1.1 inch at the top of the Quad III-IV joint. Although this gap was still too large, it was decided to make corrections on the next test. The chamber was then cleaned and evacuated to a pressure simulating an altitude of 348,000 feet. Separation was accomplished, but the strut in Quad III parallel to the X axis was broken at its midpoint as shown in figure 45. Crushing of the honeycomb installed on the underside of the envelope model gave evidence that this strut had hit the envelope. The honeycomb in Quad II and IV was also crushed, but these spots were not crushed as deeply as the spot in Quad III. The air conditioning duct glue joint holding it to the thermal bulkhead was cracked under the broken strut. Figure 46 shows the data for this separation and figure 47 gives plots of the Quad I-IV fairing trajectory.

Test LA-3

Measurements of impingement pressure from the jettison bottle were made in tests LA-1B and LA2D at a point on the Y axis four inches inboard from the cone wall. A transducer installation for these tests is shown in figure 48a. Calculated values were made for a point at the cone wall. To check the calculated values, the cone wall was cut and pressure pickups were mounted flush with the cone wall as shown in figure 48b. The back end of the pressure pickups protruded outboard of the outer surface of the cone and was supported there by a bracket. Figure 48c shows this external arrangement. The catcher shoe of the deaccelerating device was modified by placing an additional strip of aluminum honeycomb (3 inches thick x 12 inches wide) down the center of the shoe. In the area where the pickup and bracket was expected to contact, all of the honeycomb was cut away. Figure 48d shows the modification to the catcher shoe. This honeycomb cutaway section was approximately 6.0 inches square.

Radial stress measurements made on the fairing hinges in previous tests never measured pure radial stress. The measurements taken were affected by vertical stresses as well as radial stresses. In order to measure pure radial stress, a load cell was fabricated by placing strain gauges on a metal block. The load cell was mounted on the structure of the forward bulkhead model as shown in figure 13. The load cell was adjusted so that the tank half of the flight hinge was held in a vertical position when forced against the load cell by the fairing separation forces. Holes in the 218.9 ring splice plates used to position the hinge were slotted so that all radial load was transmitted to the load cell. A plot showing calibration of the load cell output with radial load is given in figure 14.

To close the gap between the fairing halves experienced in the previous tests, metal shims were placed between the flanges at the knee joint of the

Quad II-III fairing half. The shims tapered from .375 inch at a point 1 foot on each side of the Y axis to 0 at the split line. The foam rubber on the X axis joint of the thermal bulkhead in the Quad I and II area was removed and the foam rubber on the air-conditioning duct joint to the payload adapter was cut to 1 inch thickness (originally 1.5 inches). Before closing the fairing halves a new strut was installed to replace the one broken in the previous test. The honeycomb on the payload envelope was replaced and toothpicks were placed on the guidance platform to give an indication of the clearance between the platform and the thermal bulkhead.

The fairing halves were closed, pulled together by latches, and then the latches slowly loosened and removed. After this procedure, the gap measurements (distance between longerons) at various stations along the fairing were as follows:

Station	I-II Gap	III-IV Gap
203	0	0
147	0.27	0
74	0.35	0.05
-2	0.20	0
-17	0.20	0
-28	0.10	0

After making this change to the fairing, evacuation was started. At a pressure equivalent to an altitude of 351,000 feet separation was initiated. The fairing wall in the area of the newly installed pressure transduced measuring jettison bottle total pressure on the II-III fairing wall was cracked. Examination of the catcher shoe revealed that the bracket and transducer on the outside of the fairing did not hit the catcher in the honeycomb cutaway area and thus transmitted highly concentrated impact loads to the fairing structure. Figure 49 shows the crack in the fairing wall caused by the forces transmitted by the transducer. Figure 50 shows the misalignment of the transducer contact point and the space provided for it on the catcher pad.

Toothpicks were broken on the guidance platform (as shown in figure 51) due to motions of the thermal bulkhead. The aluminum honeycomb on the payload envelope showed evidence of contact by the struts in the III and II quads, but no struts were broken. Figure 52 shows the crushed honeycomb caused by strut contact. The hinge pad fairing on the Quad I-IV half was broken during this test as shown in figure 53.

Figure 54 shows the data taken during this separation and figure 55 is a series of plots describing the trajectory.

<u>LA-4</u>

Due to the fact that fabrication of a newly designed shaped charge was to be completed at a later date, it was decided to make a separation test before the shaped charge test.

Repair of the damage to the nose cone structure in the area near the jettison bottle pressure transducer was accomplished by filling the honeycomb interior of the wall with the mixture of Epon 828, Versamid, and hardener through holes in the exterior skin. Three layers of fibre glass cloth were then glued over the exterior skin.

Vibration tests of the jettison bottle structure by the contractor resulted in failure of a part in the bottle support structure. Because of these results, a redesign of the support structure was made and the redesigned parts were installed for this test.

It was suspected that the radial hinge loads measured on the last test, LA-3, might not be the same as those experienced during flight because the spring constant of the structure supporting the hinge for the test was stiffer than that supporting the hinge during flight. It was also desired to measure the total vertical load of the fairing during jettison. In order to simulate the spring constant of the hinge support point, the structure used to support the hinge in the previous test was replaced by a steel beam with a spring constant of 8,000 pounds per inch in the direction of inboard radial loads. In order to place all the vertical load on the hinge, the station 219 ring was cutaway for 60° on either side of the I-IV fairing hinge. It was also necessary to remove a section of the forward bulkhead wall under the removed section of the 219 ring because this wall would have resisted some of the radial load from the hinge load cell. Figures 17 and 18 show this alteration. A calibration of load against displacement of the new load cell system is shown in figure 16.

The fairing halves were then assembled. The gap between the halves was essentially the same as that in the previous run. After assembly, it was noted that the hinge was not in contact with the load cell. The load cell was adjusted so that contact was made with the hinge. The test chamber was evacuated to a pressure simulating an altitude of 348,000 feet and separation was initiated. The strut on the Y-axis of the quad II-III fairing half was broken during this test. This damage was caused by rebound from the catcher system and contact with the payload envelope model. Small damage also occurred to the quad I-IV barrel section caused by facility parts. Data for this test may be seen in figure 56 and plots of the trajectory may be seen in figure 57.

To conduct the shaped charge tests, it was necessary to replace the cutaway sections of 219 ring and forward bulkhead. This was done by adding a circumferential pipe inside the model, installing supports between the cutaway piece and the new and existing circumferential pipe rings, and holding the whole repair in place by fiberglass lay up. A new anvil ring of the same design as used in previous tests was installed on the 218.9 ring. New nut plates were installed on the barrel section 218.9 channel.

New design tension straps, shaped charges, and skirts were received. The tension strap and the shaped charge were installed to check the fit before

the inner hinge pod fairings were installed. The fit was perfect at this time. The shaped charge was removed and new hinge pod fairings (Part no. 55-72152) were installed. An attempt then was made to install the shaped charge and it did not fit. It was necessary to remove the new hinge pod fairing on the I-IV half and install the old hing pod fairing that had been previously damaged. The shaped charge then was able to be installed. To complete bolting the shaped charge at this time, it was necessary to ream two of the shaped charge bolt holes 1/32 inch larger. The skirt was installed with 5/8 inch outside diameter aluminum washers under the bolts. The detonators used in this test were screwed to their mounting plates by larger screws and larger bolts were used to attach the detonator fairings to the structure. After completion of the 218.9 area assembly, the chamber was evacuated to a pressure equivalent to that at 111,000 feet altitude. The shaped charge was fired and cut the tension strap at all spots. The skirt had only two bolts loose and only three inserts started to come loose as shown in figure 43. No damage occurred on the detonator fairings and the detonators did not come loose from their mounting plates on this test. The redesign of the tension strap improved the cutting effort of the shaped charge since no curled edge was observed at the cut in this test.

Discussion

Comparison of AC-4 Thrust Bottle Valve With AC-6 Pyrotechnic Valve

The tests conducted using the AC-4 and AC-5 type jettison bottle valves show that the thrust developed by the jettison bottles using the two types of valves differed by no more than 200 pounds at any instant. Figure 58 shows thrust versus time for all three tests. The test using the AC-6 type nozzle allowed a higher flow than the flow seen in the tests with the AC-4 type nozzle as shown in figure 59.

Deflector Bulkhead and Payload Cavity Pressures

Tests LA-1B, LA-2D, and LA-4A were made with jettison bottle pressures of 2460 $\pm$ 10 psi. Pressures on the deflector bulkhead varied between 11 to 18 psia for these tests as read on transducer No. 1, figure 38a; transducer No. 1, figure 46b; and transducer No. 35, figure 56d. For the same conditions in the AC-4 tests, the deflector bulkhead pressures varied between 14 to 15 psia. Test LA-3 was run at a jettison bottle pressure of 2960 psi, and in this test the deflector bulkhead pressure was 19.7 psia as read on transducer 35, figure 54b compared with an 18 psia bulkhead pressure for the AC-4 overpressure test (2700 psi bottle pressure and 1.063 diameter nozzle). These pressures were well within the design pressure loads (40 psi at the location of the transducers).

The addition of the pyrotechnic valve on the jettison bottles brought the exit nozzles of the bottles closer to the opposite cone walls. An effort was made to determine pressures in these areas. Pressure transducers were located on the center lines of each of the jettison bottle valves at different distances from the valve in each of the tests. In test LA-1B full size pressure transducers were used with the sensitive pressure element located 4.0 inches from

the cone wall, and the measured pressures were 114 psi on the quad II-III side of the fairing and 83 psi on the I-IV side of the fairing. The pressure on the quad II-III fairing half was measured by transducer No. 20 and the pressure on the quad I-IV fairing half was measured by transducer No. 19, as shown in figure 38c. In test LA 2D, the transducer on the II-III side was changed to a wafer strain gauge type with the sensitive element 0.1 inch from the cone wall. This transducer (No. 27) measured 62 psi; whereas, the full size transducer (No. 19) on the I-IV fairing half measured 81 psi. Both of these measurements are shown on figure 46b. In test LA-4A, the transducers were of the full size type mounted on the outside of the fairing and projecting through holes cut in the cone wall so that the sensitive pressure element was flush with the inside cone wall. In this test, the maximum reading on the quad II-III wall was 29 psi (transducer No. 37) and that on the quad I-IV wall was 49 psi (transducer No. 38). Both records can be seen in figure 56d. In the overpressure test, LA-3, the transducers were of the full size type and located with the element flush with the inside cone wall. The maximum pressure measured on the quad II-III cone wall was 64 psi (transducer No. 37) and on the quad I-IV cone wall was 72 psi (transducer No. 38). Both records can be seen in figure 54b. It should be noted that these pressure readings were made in a complicated and varying pressure field (on the exhaust center line of jettison bottles) and the absolute values of pressure should be regarded as only approximate.

A complicating factor in the nose fairing cavity pressure measurements was the fact that the two halves of the fairing did not meet and seal along the vertical longerons. The maximum gap occurred at the top of the fairing in the vicinity of the jettison bottles. During tests LA-1 and LA-2, this gap had a maximum dimension of 2.25 inches.

Shims were placed between the cone and barrel section of the II-III fairing half and the gap between halves was decreased as described in the previous description of the LA-3 test.

Theoretically the larger the gap, the lower the pressure in the jettison bottle compartment should be. Pressures records did not substantiate this conclusion. The trajectory of the fairing also should be affected by the larger gap and again no apparent change in trajectory was noticed. In fact, test LA-2 which had the largest gap, had the highest angular velocity of the standard pressure tests.

<u>Pyrotechnic Devices (shaped charge, split line latches, and jettison bottle valves)</u>

The shaped charge used to cut the tension tie which holds the nose fairing to the 218.9 ring on the vehicle tank, was tested four times in the AC-6 test series. Three of these tests were at simulated attitudes above 93,000 and one test was conducted at ambient pressure. In all tests, the tension tie was completely cut and in test LA-1A, the only test in which the fabric

seal was placed under the tension tie, the tension tie and the seal were both completely cut so that separation of the nose fairing could be accomplished. In shaped charge tests LA-1A, LA-2A, and LA-2B, the tension ties were examined after being cut and were found to have a rolled over edge at the cut as shown in figure 34.

In test LA-2A, the rolled edge was cracked at its junction with the main body of the tension strap and a possibility existed that it could break off and provide flying strips of metal that might endanger the payload. Figure 60 shows a detailed cross section of the groove under the shaped charge for the tension ties used in tests LA-1A, LA-2A, and LA-2B and for the redesigned tension tie groove used in test LA-4B. In the original groove if the shaped charge was located off center, the cut could be made at one end of the thin flat section and cause the rolled effect. In the new design the 0.060 inch long thin flat section does not exist, thereby eliminating the tendency to roll. In addition, a more accurate location of the shaped charge with respect to the groove is made, thus assuring that the strap is cut at the thinnest point. The rolled edge was not seen on the tension ties of test LA-4B with this new design.

An effort was made on test LA-1A to determine if particles of the shaped charge or any other part of the fairing invaded the payload, equipment shelf, or jettison bottle areas. There areas were cleaned and vacuumed before the fairing halves were assembled. Examination after the fairings were jettisoned revealed small particles throughout the interior of the fairing. These particles were as large as 0.03 inches and none seemed to be from the shaped charge (figure 61 shows some of the particles on protective paper covering placed over the equipment shelf before the test); however, the manner in which the tests were conducted was not similar to flight firing of the shaped charge in that it was necessary to clean the test area of all shaped charge debris outside the fairings so as to not damage the test chamber vacuum pumps during the nose fairing jettison test. Thus, it was not possible to jettison the fairing halves in the same time sequence as the flight time sequence.

Although the shaped charge completely separated the fairings from the vehicle, it also caused damage to the skirt assembly (a plastic structure protecting the shaped charge) as shown in figure 10. The effect of the explosion was to force the skirt outward and thus to shear inserts. These inserts were glued to the foamed plastic body of the skirt and were used to provide bearings for the bolts holding the skirt to the 219 ring. Figure 43 shows the developed surface of the skirts used in each of the tests and indicates the position of each of the bolt-insert points on the skirts. This figure lists all damage seen after each of the shaped charges were fired. As can be seen in test LA-1A and LA-2A, very few of the inserts were intact after the test. In test LA-1A five of the insert-bolt points were undamaged and in test LA-2A, eleven were undamaged. Damage varied from partial cracking of the glue joint between the insert and the skirt body as shown by the symbol marked "incipient failure" to bolts completely blown from their thread fasteners or inserts with no effective glue joint, as shown by the symbol marked "failure". Test LA-2B was made with the skirt body used in test LA-2A. New inserts were glued in the skirt using a mixture containing 50

parts by weight of Epon 828, 50 parts by weight of Versamid, and 10 parts by weight of hardener. This mixture was very fluid and probably held the inserts better than the adhesive used in tests LA-2A, thus partially accounting for the improved performance in tests LA-2B. In test LA-2B, washers were placed under the head of the bolts to give a larger bearing area than that provided by the inserts. Washers in quads I, III, and IV were of 0.562 inch diameter while those in quad II were of 0.625 inch diameter. Greatly improved performance was noted in all parts of the skirt but the skirt in the quad II area with the 0.625 inch washers had 93 percent undamaged connection points while the skirts in the other quads had only 67 percent undamaged connection points. Test LA-4B was run with 0.625 inch washers under all bolt heads and had 94 percent of the connection points undamaged, the damaged connection points had only incipient failure.

Damage was also sustained by the fairing used to cover the shaped charge detonators and by the detonators. Figure 33b shows the detonator fairing after the explosion. Some damage to the detonator fairing structural fiberglas was observed after the first two tests, but this was eliminated by adding more layers to the fiberglas. Bolts were completely ejected by the explosion during some of the tests, but use of longer bolts eliminated this problem. During the first three tests, the screw holding the dual detonator to a plastic mounting plate failed in tension. Views of this failure are shown in figure 33d and figure 44. Larger screws were used in test LA-4B and no failure occured.

The thruster bottle nozzle and valve assembly shown in figure 1 replaced the design used on the AC-4 vehicle so as to eliminate possible metallic shrapnel. In all tests, the valve operated perfectly. No shrapnel was evident and no failures of the pyrotechnic actuated shearing pin occurred.

The redesigned split line latches are shown in figure 3. In all tests of the latches, operation was without failure. No shrapnel from the latches was observed; however, in assembly of the latches, the lug and nut galled on one latch and interference between the pin puller and the clevis was noticed on two other latches. Better inspection, closer tolerances, and better lubrication eliminated these difficulties on the remaining tests.

Pyrotechnic electrical system

The electrical system harness arrangement was changed for AC-6 due to the fact that all pyrotechnic devices for the split line latches were located on the quad I-IV fairing half and not on both fairing halves as in the AC-4 flight. All explosion initiators were of the type that would not fire if 1 watt or 1 ampere of electrical current was applied.

The voltage and total current records may be seen in figures 38, 46, 51, 54, and 56 for all tests and values for maximum voltage or current may be seen in Table 4. Voltage drop varied with the type of test run (shaped charge, split line latch, or thruster bottle valve) and the load associated

with the pyrotechnic devices fired. For two tests in which the shaped charge was the only device fired the maximum drop was 12 volts and the duration of the drop was 0.01 second for one test and 0.05 seconds on the other test. In the one test in which voltage was measured for split line latch firing, the maximum voltage drop was 16 volts. In the four tests in which the explosive squib actuating the thruster bottle valve was fired, the maximum voltage drop was 13 volts and the duration of the drop was approximately 0.01 seconds. The current level for the various tests varied from a low of 9 amperes for the thruster bottle valve tests to a maximum of 47 amperes for the shaped charge and the split line latch tests.

Hinge Loads

Three methods were used to determine hinge and 218.9 ring loads imposed by the fairing during jettison. Strain gauges were placed on the inner and outer fiberglas surface of the fairing at a distance 8 inches above the 218.90 ring to measure the vertical loads through the barrel are of the fairing, strain gauges were placed on the tank half of the hinge to measure the vertical loads seen by the hinge, and a load cell was placed so as to support the tank half of the hinge in a radial inboard direction and to measure radial loads on this half of the hinge (this load cell was supported by a stiff column in test LA-3 and was supported by a less stiff beam with a spring constant of 8,000 pounds per inch in test LA-4A).

The strain gauges on the fairing skin were placed as shown in figure 24b. Tests with these strain gauges were made to determine if concentrated and distributed vertical loads placed on the barrel section of the fairing by a hydraulic ram and measured by a load cell could also be measured by the barrel strain gauges. The concentrated load was applied vertically on the half of the hinge attached to the fairing in 1,000 pound increments up to 5,000 pounds. A load distributed over 30 degrees of the fairing circumference was applied vertically in 2,000 pound increments to 10,000 pounds. This load was applied at four different locations about the circumference. In each case, the total load was calculated from the strain gauge records by the following formula.

$$P = \Sigma_{0^{\circ}}^{180^{\circ}} \frac{1.066}{2} \; E t \epsilon \Delta\theta$$

where

P = Total load, pounds
E = Modulus of elasticity, pounds per square inch
t = Sum of skin thickness
ϵ = Strain, inches per inch

1.066 = Inches per degree on circumference of fairing
$\Delta\theta$ = Degrees on circumference between gauges

It was assumed that all axial loads were transmitted through the fiberglas exterior covers of the fairing and none through the interior honeycomb core.

For the strains gauges located in Quad I and Quad IV, the parameters are as follows, except for the area about the YY axis:

$$E = 3.5 \times 10^6 \text{ psi}$$
$$t = 0.08 \text{ inches}$$

The area located 3" on either side of the Y-Y axis is a combined fiberglas and steel structure. This area has the following parameters:

$E_1 = 3.5 \times 10^6$ psi for fiberglas
$E_2 = 25.5 \times 10^6$ psi for 301 CRES 1/2 hd.
$t_1 = 0.200$ inch for fiberglas
$t_2 = 0.063$ inch for steel

The term Et for the load equation in this area is computed as follows:

$$Et = E_1 t_1 + E_2 t_2$$

The loads as calculated from the strain gauges by use of the preceding equations and parameters were within 5 percent of the concentrated applied load and within 5 percent of the distributed load.

The equations given for the calibration tests were used for calculating the loads on the separation tests. The strain on each of the fairing gauges was obtained from the data at a given time. A sample plot of the strains at a given time and the calculations used to determine the total load through the barrel of the fairing at that time is shown in figure 62. Figure 63 and 64 gives the total load in the barrel for various times and also a curve showing the vertical load felt by the hinge throughout the first 0.20 seconds of jettison in tests LA-1B and LA-2D. In each of the tests, the maximum total load seen by the fairing is equal to or greater than the load seen in the hinge at the same time (as would be expected, since part of the total load must be born by the 218.9 ring). Some discrepancies exist between the hinge vertical loads and the total loads seen by the gauges on the fairing. Strain gauges were installed inside and outside the fairing and wired in a bridge circuit so as to remove any symmetrical bending strain and only indicate the axial component of strain. In the area of the hinge, the skin structure is non-symmetrical due to a thin sheet of steel on the inner surface of the fairing and therefore, the bending strains were not removed. Because of these bending strains, the fairing load data can be used only to determine the extent of the circumferential loading caused by fairing jettison. The axial loads on the hinge shown in figure 65 and 66 are believed to be accurate. The strain gauges were placed on the hinge as shown in figure 24C and calibration of these gauges is shown in figure 29. The maximum load varied between 2,500 and 9,500 pounds and occurred between 0 and 1.5 degrees of hinge rotation (rotation at the top of the fairing started up to 0.02 seconds before rotation at the hinge). An approximation of the way the axial load is shared between the tank half of the hinge and the 218.90 ring during the first 4 degrees of fairing rotation may be obtained by noting the maximum axial loads of tests LA-1B, LA-2D, and LA-4A. In each of

these tests, the jettison bottle pressure was the same, but in test LA-2D, which had a maximum axial load of 8,000 pounds, the tank half of the hinge was raised so that it was in contact with the 218.90 ring and in test LA-4A, which has a maximum axial load of 9,500, the 218.90 ring was completely removed for 60 degrees on either side of the quad I-IV hinge (strain gauged). In contrast to the loads on these two tests, the load for test LA-1B was only 3,200 pounds. In this test the hinge was separated from the 218.90 tank ring by a gap of 0.050 inches. This gap allowed the tank ring to deflect and wear a greater share of the vertical load before it was applied to the hinge. The effect of increasing jettison bottle pressure may be seen by comparing the load of 3,400 pounds found in test LA-3 (jettison bottle pressure 2,940) with test LA-1B having a 3,200 pound load.

In all tests, by 12 degrees of hinge rotation the load in the hinges had reversed and was in a forward direction. The maximum forward hinge load for each test varied from 1,800 pounds to 5,600 pounds. Again, the highest maximum was in test LA-4. In this test, reversal of load took place four times, the earliest reversal taking place at about 5 degrees of hinge rotation.

Revisions were made to the forward bulkhead and to the vertical hinge support before test LA-3 (as previously described in the test set up section of this report) in order to measure radial loads applied through the hinge by the fairing. Further, revisions were made before test LA-4 to make the spring constant of the hinge support more nearly equal to that of the actual flight forward bulkhead. The results of these additions are shown in the radial fairing load curves of figures 65 and 66. In test LA-3, the maximum radial load was about 3750 pounds occurring at about 0 degrees of rotation of the hinge. This load was working against the spring of the forward bulkhead which has a constant of 110,000 pounds/inch as determined in previous tests (Ref. 1). Test LA-4, in which the hinge and fairing were supported by a beam with an 8,000 pound per inch spring constant, showed lower maximum loads of 2500 pounds occurring at about 2 degrees of hinge rotation. The radial and vertical hinge loads observed in these tests at no time exceeded the structural capability of the actual Centaur hinge as established by contractor tests (Ref. 2).

Nose Fairing Trajectory

Figure 67 is a comparison of the AC-4 and the AC-6 series of tests. The small differences in weight and in thrust between the AC-4 and the AC-6 nose fairing tests would indicate that the trajectories in the two series of tests would be about the same; and this conjecture was proved correct. In the AC-6 standard pressure tests the range of maximum angular velocities was from 191 to 196 degrees per second for the AC-4 standard pressure the range of maximum angular velocities was from 165 to 195 degrees per second. Figures 39, 47, and 57 show the trajectories for the AC-6 standard pressures tests. Figure 55 shows trajectory data for the jettison bottle over-pressure test

LA-3. The over-pressure test for the AC-4 configuration achieved a higher maximum angular velocity, 232, degrees per second, than did the AC-6 over-pressure test, 209 degrees per second. This is accounted for by the fact that in the AC-4 type test, not only was the pressure increased in the jettison bottles from 2500 to 2700 pounds per square inch, but the diameter of the nozzle orifice was increased from .828 to 1.063 inches. In the AC-6 over-pressure test the bottle pressure was 2940 pounds per square inch but the nozzle diameter stayed at .824 inches. Due to the small changes in the structure of the fairing between the AC-4 and the AC-6 tests, no jettison test with a single bottle firing was conducted. It was concluded that the trajectory with both standard jettison bottle configuration and with a single jettison bottle would allow the nose fairing to separate from the main vehicle without contact.

Clearance Between Surveyor and Nose Fairing

Addition of an omni-directional antenna to the AC-6 Surveyor model created a clearance problem during assembly and jettison of the nose fairing. A redesign of the deflector bulkhead A frame solved the assembly problem, but verification of the clearance during jettison was required. To obtain this verification a wood model of the antenna was made and mounted on a pipe platform which was held by the payload adapter. The antenna was located at the precise position it would occupy during flight. Small dowels were mounted on the antenna and high speed cameras were used to photograph the antenna and the adjacent deflector bulkhead during jettison tests. The cameras recorded no interference and none of the dowels were harmed. Figure 68 shows the model of the omni-directional antenna used in these tests.

A layout of the nose fairing and the bottom of the contractual Surveyor envelope showed encroachment or near interference between the model and the thermal bulkhead struts with geometric rotation and no dynamic motions such as would be encountered during jettison. A wooden model of the bottom of the envelope was fabricated according to General Dynamics drawing number 55-00050-Chg W. This model was made so that it could be attached to the payload adapter. Figure 69 shows the model as fabricated, the areas of subsequent change, and the areas where aluminum honeycomb was installed to determine if contact between the model and the fairing struts occurred during separation of the fairing. Figure 41 shows the assembly of the model and the fairing. Measurements were taken after assembly of the envelope model on the payload adapter and those measurements showed that the envelope was located so that no part was more than .06 inches from its true flight position. After assembly of the envelope an effort was made to install the fairing halves in their flight position around the envelope. It was found that in the flight position the thermal bulkhead strut in No. 3 locations (location shown in figure 24c) interfered with the bottom of the evnelope on the YY axis, quad II-III half. A rectangular slot approximately 3.5 inches deep and 2.0 inches wide was removed from the envelope. The quad II-III fairing half was then slowly

rotated into position. At an angle of 15 degrees from its closed position the No. 1 and No. 5 struts (location shown in figure 24c) came to the position at which they were the closest to the envelope. At this point these struts cleared the envelope by 1.0 inch. On installing the quad I-IV half of the fairing it was necessary to make the alterations to the envelope in quads I and IV as shown in figure 69 to provide clearance between the envelope and the air-conditioning duct during installation. An examination of the envelope with the quad I-IV fairing in place revealed that no intereference with the unaltered envelope would have existed after installation. Interference occurred only because of the assembly method required by the test facility. Assembly of the fairing cone around the payload before erection on the fairing barrel (method used before flights) would have been possible without violating the payload envelope.

Strips of 1 inch thick aluminum honeycomb were glued to the bottom of the envelope in the areas where the struts were expected to be the closest during jettison to provide evidence of any contact between the struts and the envelope. During jettison test LA-2D (first separation test after installation of the envelope), strut No. 1 was broken. The honeycomb covering the suspected contact area on the envelope near this strut was crushed at three spots as though the strut had nearly contacted the envelope two times before it finally hit the envelope and broke the strut. (Figure 70 shows the area of contact). The honeycomb in the suspected contact areas for struts No. 5 and No. 6 also was crushed. These crushed areas indicated that the struts must have beein within 0.5 inch of contact. No struts in these areas were broken in future tests although the honeycomb in the II and III quads showed evidence of near contact in both tests LA-3 and LA-4. Figure 41 shows the honeycomb installation after Test LA-2D in the area above strut No. 1. Figure 45 shows the strut broken during test LA-2D. A strut located in No. 3 position (YY axis envelope cut out) was broken during test LA-4A but examination of the edge of the envelope model showed that it had been hit in a position slightly to one side of the strut clearance slot and it was concluded that the fairing had hit the facility catcher, rolled, and bounced back far enough for the strut to hit the unslotted area of the envelope.

Conclusions

1. Vertical and horizontal loads transmitted by the hinge to the tank structure were determined to be within the allowable limits.

2. A definite interference was discovered between a thermal bulkhead strut (located at the interface between Quad II and Quad III) and the Surveyor envelope (even during static conditions).

3. A possible dynamic interference was discovered between the four thermal bulkhead struts adjacent to the X-X axis and the Surveyor envelope.

4. All other parts were determined to be acceptable for the environment.

LIST OF TABLES

TABLE I

Nose Fairing part changes or additions between AC-4 and AC-6

General Area	Part	Report Fig. No.	Description and Reasons for Change
Cone	Jettison bottle pyrotechnic valve and nozzle.	1a 1b	This valve replaced the plug and arm used in previous tests so as to eliminate shrapnel. The valve consists of a nozzle with same diameter as in previous tests and a seal diaphragm that is sheared and removed by the action of a pyrotechnic propelled pin, thus allowing flow of gas thru the nozzle without release of shrapnel.
Cone	"A" frame on Deflector bulkhead.	2	This change was a dimensional change to previous part to provide clearance between it and the Surveyor antenna.
Cone	Thruster bottle fill and bleed plate.	-	This modification provided access for pyrotechnic checkout.
Cone	Thruster bottle pressure transducer.	-	Pickup installed on bottle support frame to monitor bottle pressure.
Cone	Separation Latches..	3a 3b	This change was made to eliminate shrapnel from the latches. A lug and clevis held together by a pin actuated by an explosive device was used to hold the fairings together.
Cone	Air conditioning duct (on cone).	4	In previous separation tests this ducting was not used.
Cone	TV lights.	5	These lights are used to illuminate targets painted on the cone for test photographs by the Surveyor TV cameras.
Cone	Jettison bottle relocation.	6	The jettison bottle in the Quad I-IV fairing was lowered 1/2 inch to provide more clarance between the bottle nozzle and seal bulkhead frame.

General Area	Part	Report Fig.No.	Description and Reasons for Change
Thermal Bulkhead	Air conditioning duct (on thermal bulkhead)	7a 7b	This part of duct was used in tests of Ref. 1 and was attached to the thermal bulkhead. Modification was made to increase the clearance over the guidance platform and the auto pilot gyro, both located on the equipment shelf.
Thermal Bulkhead	Air conditioning nozzles (outer perhiphery of bulkhead)	8a	These nozzles were not installed in the AC-4 fairing test
Thermal Bulkhead	Air conditioning nozzles (central area of bulkhead)	8b	A modification was made to these nozzles to keep them from becoming detached from the bulkhead during separation
Thermal Bulkhead	Hazard detection system	9	This system is used to determine leakage of Surveyor propellants
Fairing Barrel Section	218.90 barrel section channel	10 11	A modification to this channel was made so as to provide proper fit with the changed tank 218.90 ring
Fairing Barrel Section	Air conditioning door and ducts	-	A modification was made to permit air conditioning prior to launch
Fairing Barrel Section	Sta 208 seal angle (barrel section)	-	This part was not previously used
Fairing Barrel Section	Shaped charge detonator fairing	-	Strengthened by addition of more material
Forward Bulkhead	Sta 208 seal angle	-	This part was an addition and not used in previous tests
Forward Bulkhead	Tank half of fairing hinge	12	This part modified so as to better transmit loads to tank
Forward Bulkhead	218.90 ring	10 - 11	This part modified so as to better transmit loads to tank
Forward Bulkhead	Liquid hydrogen vent duct	-	A modification was made to the duct to provide capability of more evenly distributing the exhaust to eliminate unbalanced thrust

General Area	Part	Report Fig.No.	Description and Reasons for Change
219 Hardware	Tension Tie	10 - 11	Modified to provide better cutting by the shaped charge
219 Hardware	Shaped charge and detonators	10 - 11	Modified to allow helium purge
219 Hardware	Skirt Assembly	10 - 11	Modified to allow helium purges
Payload Adapter	Seal (adapter to thermal bulkhead)	-	A change was made to provide better fit
Whole Fairing	Pyrotechnic electrical system		Since the separation latch changes required all of the explosive devices to be mounted on the clevis part of the latch (located on the II-III half of the fairing) the harness was completely rearranged. The system was also changed to provide for use of 1 watt - 1 amp explosive squibs.

TABLE II. - TRANSDUCER INFORMATION - a) PRESSURE, POSITION, OR ACCELERATIONS (LOCATION OF TRANSDUCERS SHOWN IN FIG. 24(a))

Trans-ducer No.	Type measure-ment	Vendor	Vendor model No.	Vendor range	Calibrate range	Direc-tion of measure-ment	FLAT frequency range, cps	Overall accuracy of test, %	Tests in which transducer was used: 1A	1B	2A	2B	2C	2D	3	4A	4B	Recording Device
1	pressure	Statham	---	2-50 psia	0-30 psia	+Z	0-600	±6	X				X					Recording oscillograph 1000 cps
2			---	0-100 psia	0-100 psia	-Z		±3	X									
3			PA208	0-5 psia	0-3 psia	+Z		±4	X				X	X	X			
4			PA208	0-5 psia	0-3 psia	+Z		±4	X									
5			PA208	0-5 psia	0-3 psia	+Z		±4	X				X	X				
6	motion	Spacecraft	VEL101A	0-98 inch	0-98 inch	Y		±3	X									
7			VEL101A	0-98 inch	0-98 inch	Y		±3	X									
8			VEL101A	0-98 inch	0-98 inch	Y		±3	X									
9			VEL101A	0-98 inch	0-98 inch	Y		±3	X									
10	accel.	C.E.C.	4-280	0-400 g	0-100 g	Y	2-100	±6	X									FM tape
11	battery voltage	---	---	----	0-36 volt	--	0-600	±3	X	X	X	X	X	X	X			Recording oscillograph -light type
12	battery voltage	---	---	----	0-36 volt	--	0-600	±3	X	X	X	X	X	X	X			Recording oscillograph -light type
13	pressure	Alinco	151	0-4000 psi	0-3000 psi	--	0-60	±1	X				X	X	X			Recording oscillograph 60 cps
14	pressure	Alinco	151	0-4000 psi	0-3000 psi	--		±1	X				X	X	X			
15	motion	Markite	---	0-4 inch	0-4 inch	Y		±2	X				X	X	X			
16		Markite	---	0-10 inch	0-10 inch	X		±1	X				X	X	X			
17		Markite	---	0-10 inch	0-10 inch	X		±1	X				X	X	X			
19	pressure	Alinco	151	0-100 psia	0-100 psia	Y	0-600	±2	X				X					Recording oscillograph, 1000 cps
20	pressure	Alinco	151	0-100 psia	0-100 psia	Y	0-600	±2	X									Recording oscillograph, 1000 cps
21	battery current	---	---	----	0-20 amp	--	0-60	±5	X	X	X	X	X	X	X			Recording oscillograph, 60 cps
22	battery current	---	---	----	0-20 amp	--	0-60	±5	X	X	X	X	X	X	X			Recording oscillograph, 60 cps
23	accel.	C.E.C.	4-280	0-400 g	0-100 g	Y	2-1800	±6	X				X	X				FM tape
24	accel.	C.E.C.	4-280	0-400 g	0-100 g	Z	2-1800	±6	X				X	X	X			
25	pressure	Scientific Advance	SA-M-6	0-150 psia	0-150 psia	Z	0-600	±2							X			
26	accel.	C.E.C.	4-280	0-400 g	200 g	Z	2-1800	±6					X					FM tape
27	pressure	Scientific Advance	SA-M6	0-100 psia	0-100 psia	Z	0-600	±2					X					Recording oscillograph, 1000 cps
28	accel.	ENDEVCO	2225	±1000 g	±100-±1000 g	Y	2-1800	±2										FM tape
29			2225			X		±2										
30			2242C			Z		±2										
31			2225			Y		±2										
32			2225			X		±2										
33			2242C			Z		±2										
34	pressure		14032	0-100 psia	0-100 psia	-Z	0-600	±2					X	X				Recording oscillograph, 1000 cps
35		C.E.C.	4326-0003	0-25 psia	0-25 psia	+Z								X	X			
36		Statham	14032	0-100 psia	0-100 psia	-Z								X				
37		Alinco	152	0-150 psia	0-100 psia	Y								X	X			
38		Alinco	152	0-150 psia	0-100 psia	Y								X	X			
39		Scientific Advance	SAM6	0-100 psia	0-100 psia	Y									X			

TABLE II. - TRANSDUCER INFORMATION - b) STRAIN GAGES
All gages installed to read compression positive and tensions negative, all gages recorded on FM tape. All gages have two active arms.

Gage No.	Fig.* No.	Vendor	Model No.	Gage Factor	Gage resistance, ohms	Calibrated range (microinch)/inch & test used+							
						Test 1B	Range	Test 2D	Range	Test 3	Range	Test 4A	Range
101	24b	Baldwin-Lima Hamilton	DLB-PT - 100-8A	3.95	1000	X	4000	X	3000		3000		9000
102	24b		DLB-PT - 100-8A	3.95	1000	X	4000	X	3000		3000		9000
103	24b		DLB-PT - 100-8A	3.95	1000	X	8000	X	3000		3000		9000
104	24b		DLB-PT - 100-8A	3.95	1000	X	8000	X	3000		3000		9000
105	24b		DLB-PT - 100-8A	3.95	1000	X	8000	X	3000		3000		9000
106	24b		DLB-PT - 100-8A	3.95	1000	X	8000	X	3000		3000		9000
107	24b		DLB-PT - 100-8A	3.95	1000	X	8000	X	3000		3000		9000
108	24b		DLB-PT - 100-8A	3.95	1000	X	8000	X	3000		3000		9000
109	24b		DLB-PT - 100-8A	3.95	1000	X	8000	X	3000		3000		9000
110	24b		DLB-PT - 100-8A	3.95	1000	X	4000	X	3000		3000		9000
111	24b		DLB-PT - 100-8A	3.95	1000	X	4000	X	3000		3000		9000
112	24b		DLB-PT - 100-8A	3.95	1000	X	4000	X	3000		3000		9000
113	24b		DLB-PT - 100-8A	3.95	1000	X	4000	X	3000		3000		9000
114	24b		DLB-PT - 100-8A	3.95	1000	X	3000	X	3000		3000		9000
115	24b		DLB-PT - 100-8A	3.95	1000	X	3000	X	3000		3000		9000
116	24c	Budd	C-12-121	2.07	350	X	8000						
117	24c	Budd	C-12-121	2.07	350	X	1200	X	1200	X	1200	X	2400
118	28a	Budd	C-12-121	2.07	350	X	2000	X	1000	X	1000	X	2000
119	17	Budd	C-12-121	2.07	350					X	1186	X	1186

* This column gives report figure showing gage location.

\+ X indicates use in the indicated test.

TABLE III. - TEST CONDITIONS, CONFIGURATION OF FACILITY AND NOSE FAIRING AND DAMAGE SUSTAINED BY FAIRING

1 Test No.	2 Test Date	3 Test Chmbr. Altitude, miles	4 Thruster Bottle Pressure, psi	5 Type Test	6 Fairing Structure	7 Payload Envelope Model	8 Thermal Bulkhead	9 Jettison Bottle Assembly Config.	10 Deflect. Bulkhd.	11 Split Line Latches	12 Equipment Shelf Simulation	13 Payload Simulation	14 Forward Blkhd. Config.	15 Sta. 208 Seal Gasket	16 Camera Positions as per Fig. 18	17 Film No.	18 Max. Gap at XX axis between half, in.
1A	5-12-65	19.5	Not used	Shaped chg. and latch	Barrel EID55-72086-1 Cones EID55-72008-7 EID55-72008-9	Not used	AC-6 design as per Table I	New pyrometics valve. I-IV bottle height lowered from AC-4 conf.	AC-6 config.	AC-6 design using lug, clevis & Conax pin puller. Fairing at knee jt. chg.	Only guid. pltfm. mtd. on shelf. Toothpicks mtd. on top	Only Surveyor Omni directional antenna used & mounted on pipe platform	AC-6 type St. 219 ring installed. St. 208 ring installed.	Seal gasket used.	Not used	Not used	1.2
B	5-14-65	65.8	2460	Separation											1,3,4,6,7 8,9	MPD 703	
2A	5-26-65	20.5	Not used	Shaped chg.	Same as above.	Envelope installed. Found static interference of envelope and Y axis strut of II-III half	Same as above.	Same as test 1 except flight pressure transducers added & rear support for II-III bottle strengthened.	Same as above.	Same as above.	Same as above.	Same as above.	Same as above.	Seal not used.	Not used.	Not used.	0.1
B	5-28-65	Sea level	Not used	Shaped chg.											5	MPD 712	0.1
C	5-28-65	17.8	Not used	Latch											1	MPD 712	2.25
D	6-2-65	65.8	2460	Separation											1,3,4,6,11	MPD 712	2.25
3	6-10-65	66.4	2940	Separation	Same as above.	Same as above.	Same as above.	Same as test 2.	Same as above.	Not used.	Same as above.	Same as above.	Slotted 219 ring at hinge att. jt. & installed load cell to suppt. hinge in radial direction.	Seal not used.	1,3,4,6,8, 9,11	MPD 713	0.35
4A	6-25-65	65.8	2460	Separation	Same as above.	Same as above.	Same as above.	New thrust bottle fill & bleed plate. Bottle attachment to support bracket strengthened.	Same as above.	Not used.	Same as above.	Same as above.	Cut out bulkhd. & 219 ring 60° each side of Y axis.	Seal not used.	1,3,4,5,8, 9,11	MPD 714	0.35
B	7-16-65	19.7	Not used	Shaped chg.	Same as above.	Same as above.	Same as above.								5,2	MPD 722	0

Test No.	19 Repairs and Alternations	20 Test Damage	21 Poorly Designed Parts	22 Flight Hinge Installation	23 Shaped Charge
1	Nose fairing structure repaired and altered at Ft. Worth, General Dynamics plant.	Four nut plates on the barrel 219 channel destroyed on assembly. Plastic inserts pulled loose when shaped charge fired. Two bolts on detonator fairing pulled loose. Found A frame, attached to deflector bulkhead, buckled. See Fig. 36. Gasket on air conditioning dust nozzle pulled out during separation.	One lug of split line latch became pulled on assumbly. Poor fit of bulkhead found on assembly. Bracket for detonator housing designed so as to have misfit. See Fig. 32.	Hinge pin at top of socket. Gap between hinge and splice plate was 0.050 inch.	Shaped charge. Installed for 1A.
2	Added TV lights and hazard detection system to cone. Installed new air conditioning dust nozzle and glued gasket to nozzle. New A frame installed on deflector bulkhead.	Found skirt plastic inserts pulled out during shaped charge test as shown in Fig. 45. Same skirt used in each shaped charge test but inserts glued in place after first test. Struts on X axis on II-III half broken. Air conditioning duct cracked away from thermal bulkhead.	None	Hinge pin 0.070 inch from bottom of socket. Hinge installed touching splice plate.	Installed for 2A and 2B.
3	Replaced strut. Reglued air conditioning duct. Gap between fairings decreased by putting shims between barrel and cone sections. Installed pressure pickup flush with inside of cone and protruding 4 inches from outside.	Facility catcher plate damaged cone wall in area of newly installed pressure pickup.	None	Same as test 2 except 219 ring and splice plates slotted for hinge pins and hinge supported in new load cell.	Not used.
4	Made forward bulkhead cutout. Repaired damage to cone. After separation test returned forward bulkhead to original configuration.	Strut on Y axis of II-III half broken during separation test. Two bolts in skirt pulled loose.	Tee fitting for thruster bottle not made as per design.	Installed spring behind hinge load cell. Hinge pin on bottom of socket.	New design with helium purge duct installed for test 4B.

TABLE IV. - PYROTECHNIC ELECTRICAL SYSTEM VALUES FOR ALL TESTS

Test No.	Electrical equipment operated	Max. Current		Voltage Values					
		Bat. 1	Bat. 2	Battery 1			Battery 2		
		amps	amps	Start	Min.	Finish	Start	Min.	Finish
LA1-B	Thruster valve	10	10	34	30	34	22	22	23
LA2-A	Shaped charge	47*	35	32	30	31	33	20	27
LA2-B	Shaped charge	23*	47	34	33	34	34	22	34
LA2-C	Latches	45	47	34	20	27	34	18	19
LA2-D	Thruster valve	43	41	36	26	36	36	31	35
LA3	Thruster valve	10	9	34	22	--	35	30	--
LA4-A	Thruster valve	33	37	34	26	34	34	27	34

* These readings believed to be false due to induction.

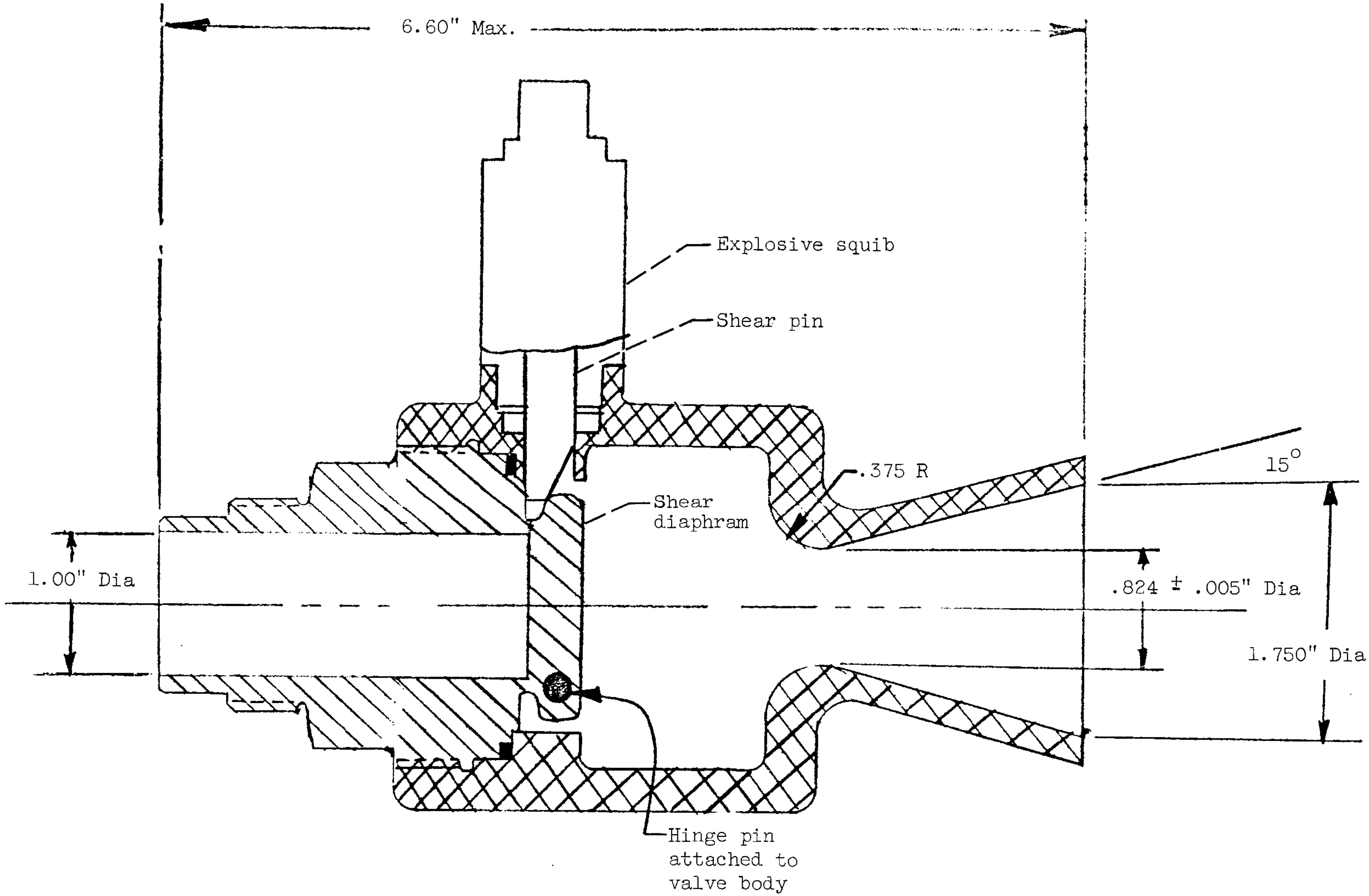

(a) Detail.

Figure 1. - Jettison bottle pyrotechnic valve and nozzle.

E-3897

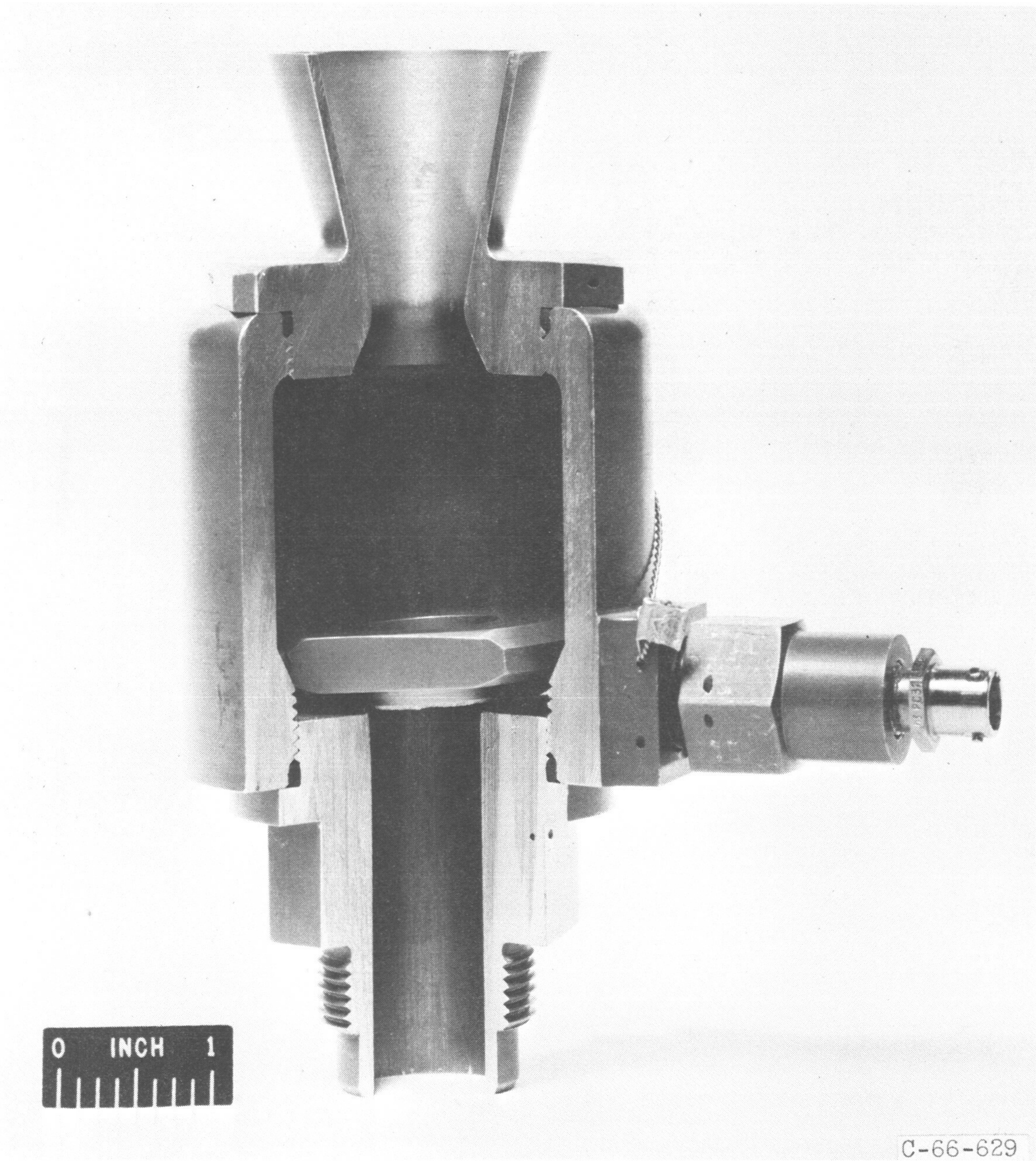

C-66-629

(b) Photos of sectioned valve and nozzle.

Figure 1. - Concluded. Jettison bottle pyrotechnic valve and nozzle.

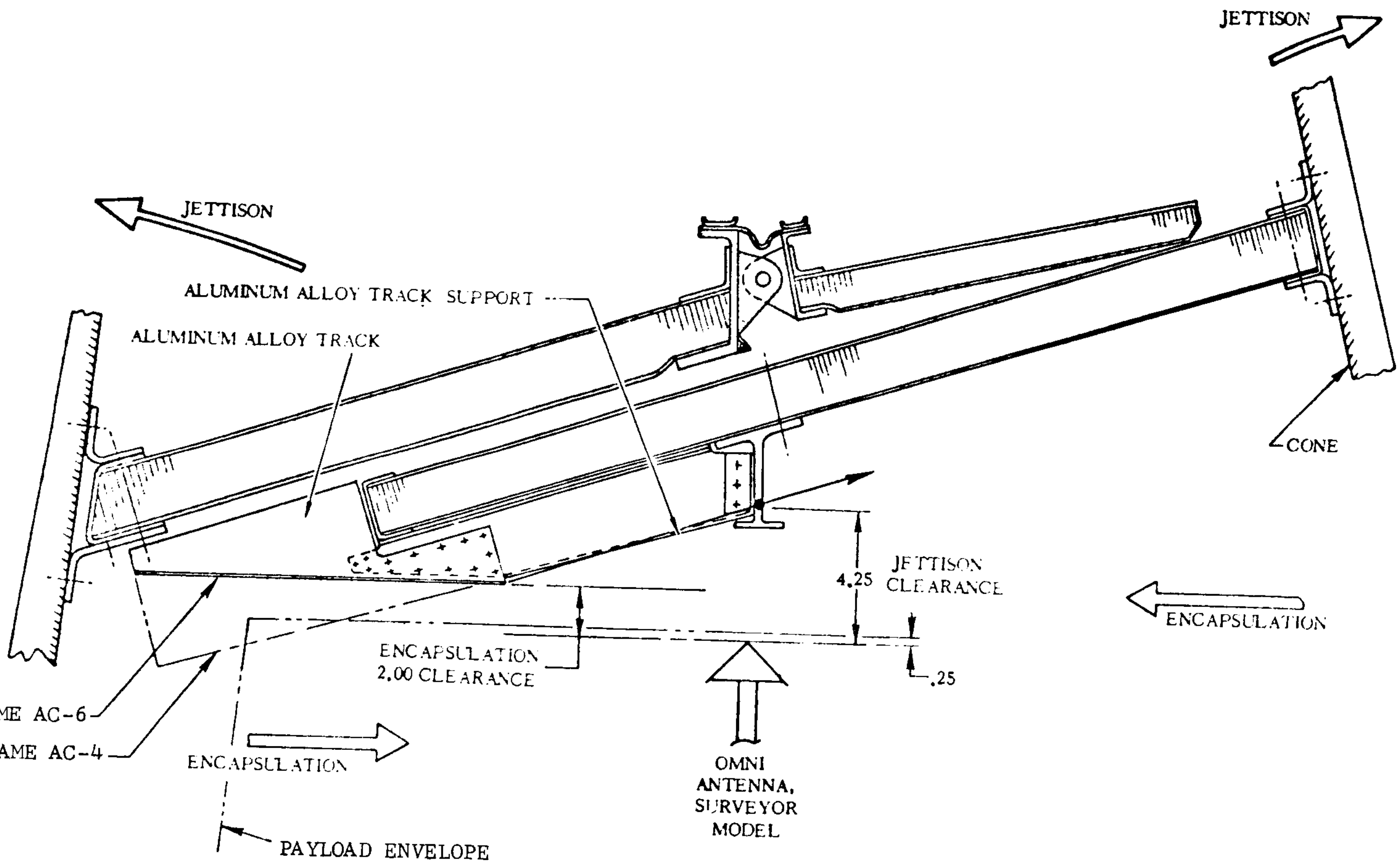

Figure 2. - Deflector bulkhead "A" frame modification.

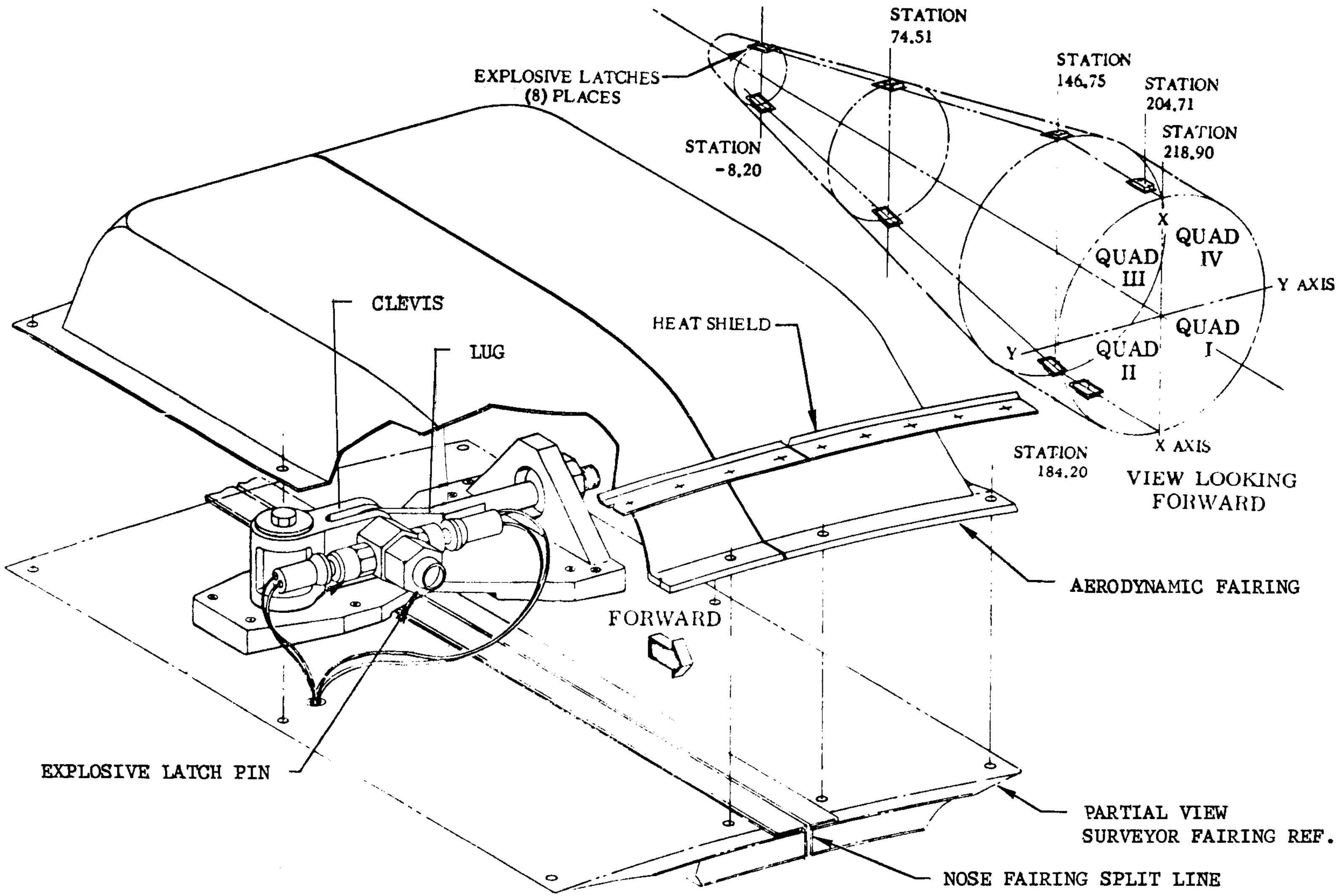

(a) Installation, AC-6.

Figure 3. - Separation latches.

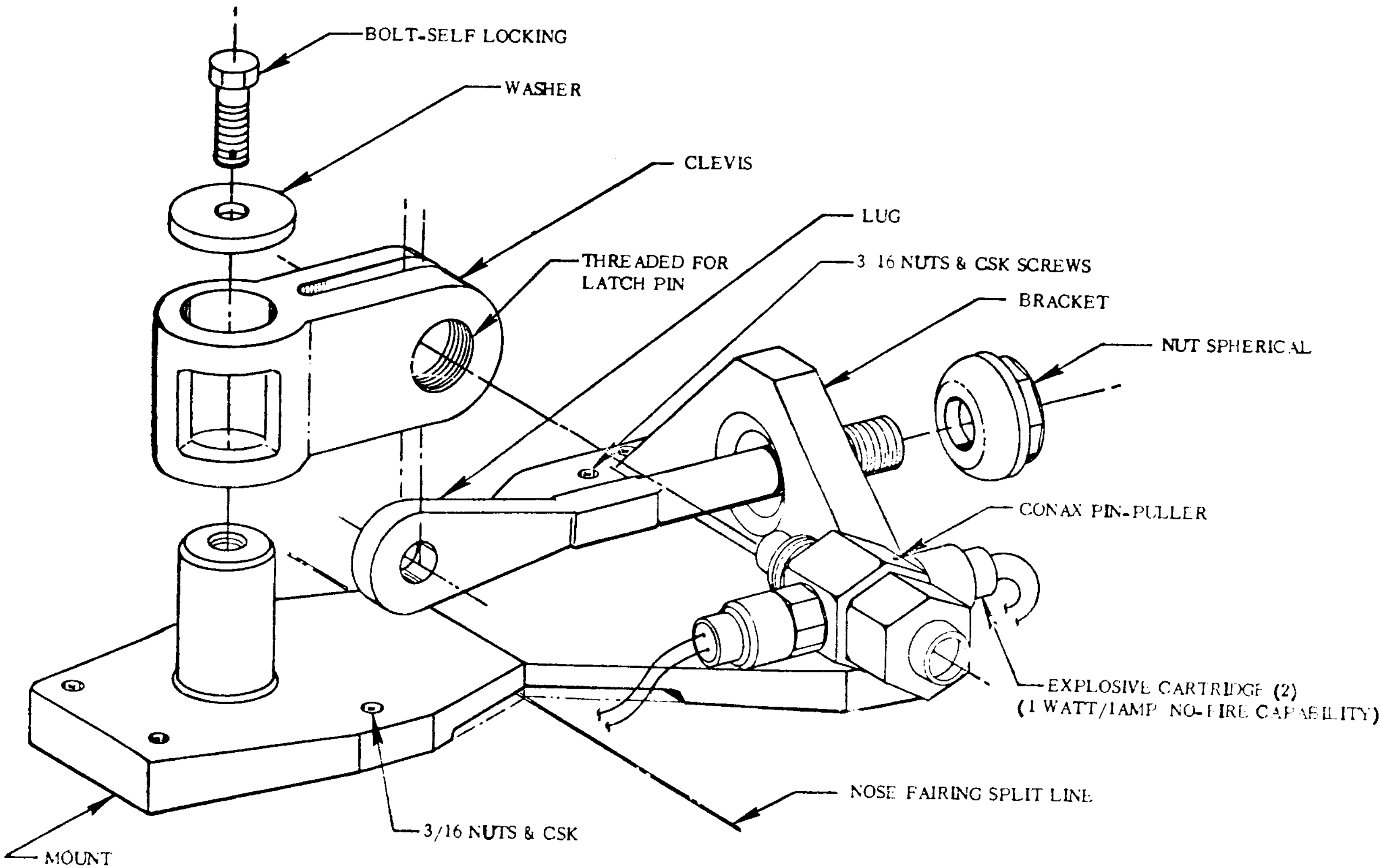

(b) Detail.

Figure 3. - Concluded. Separation latches.

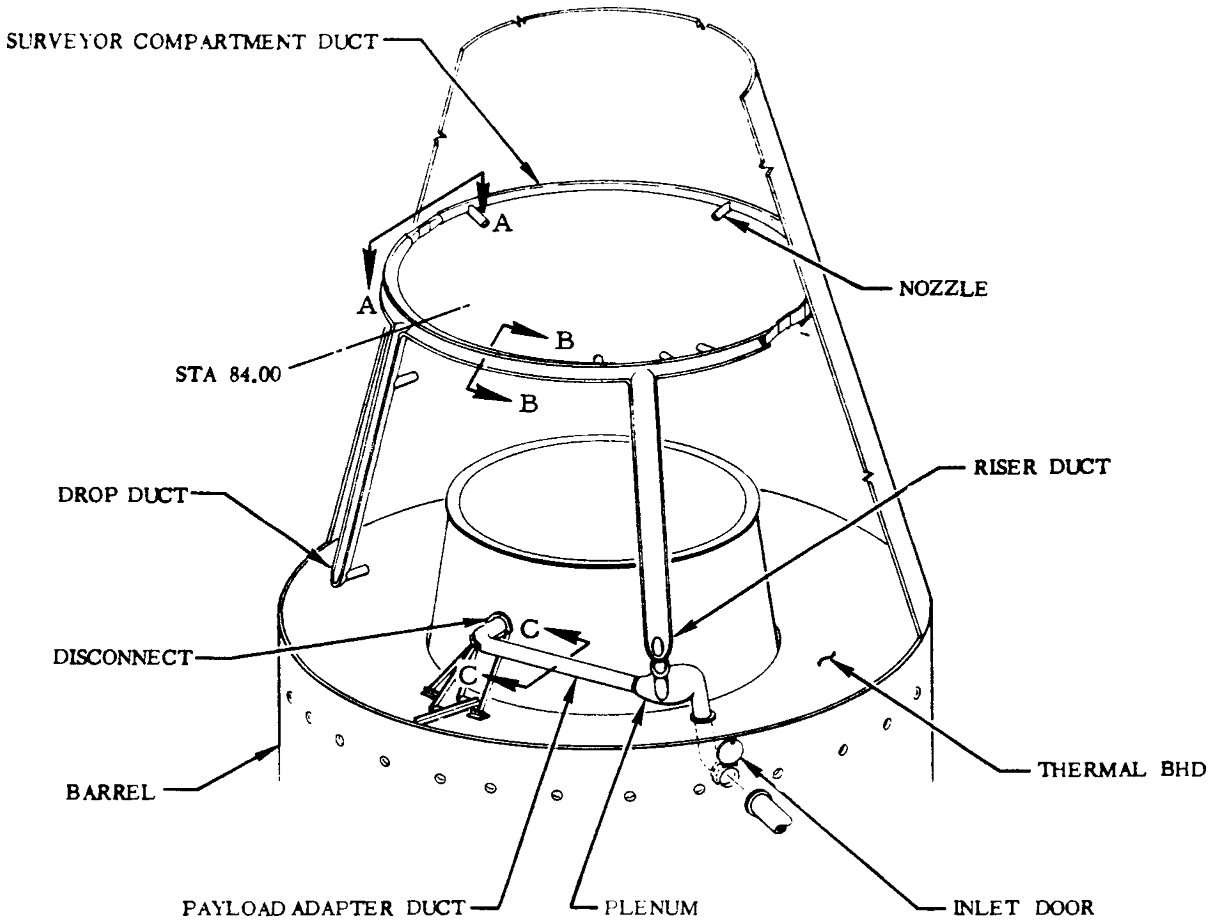

Figure 4. - Payload air-conditioning ducts.

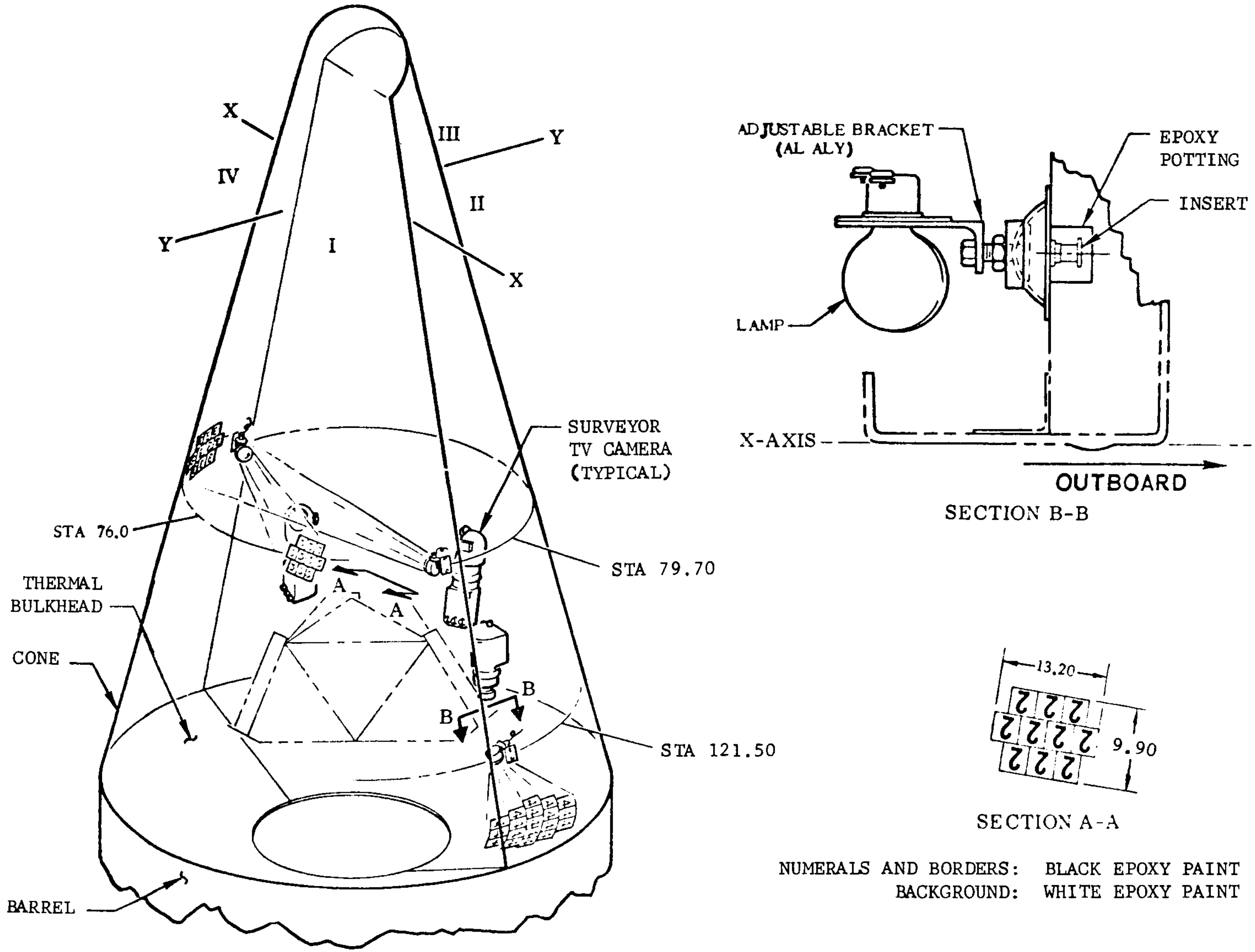

Figure 5. - TV lights and targets.

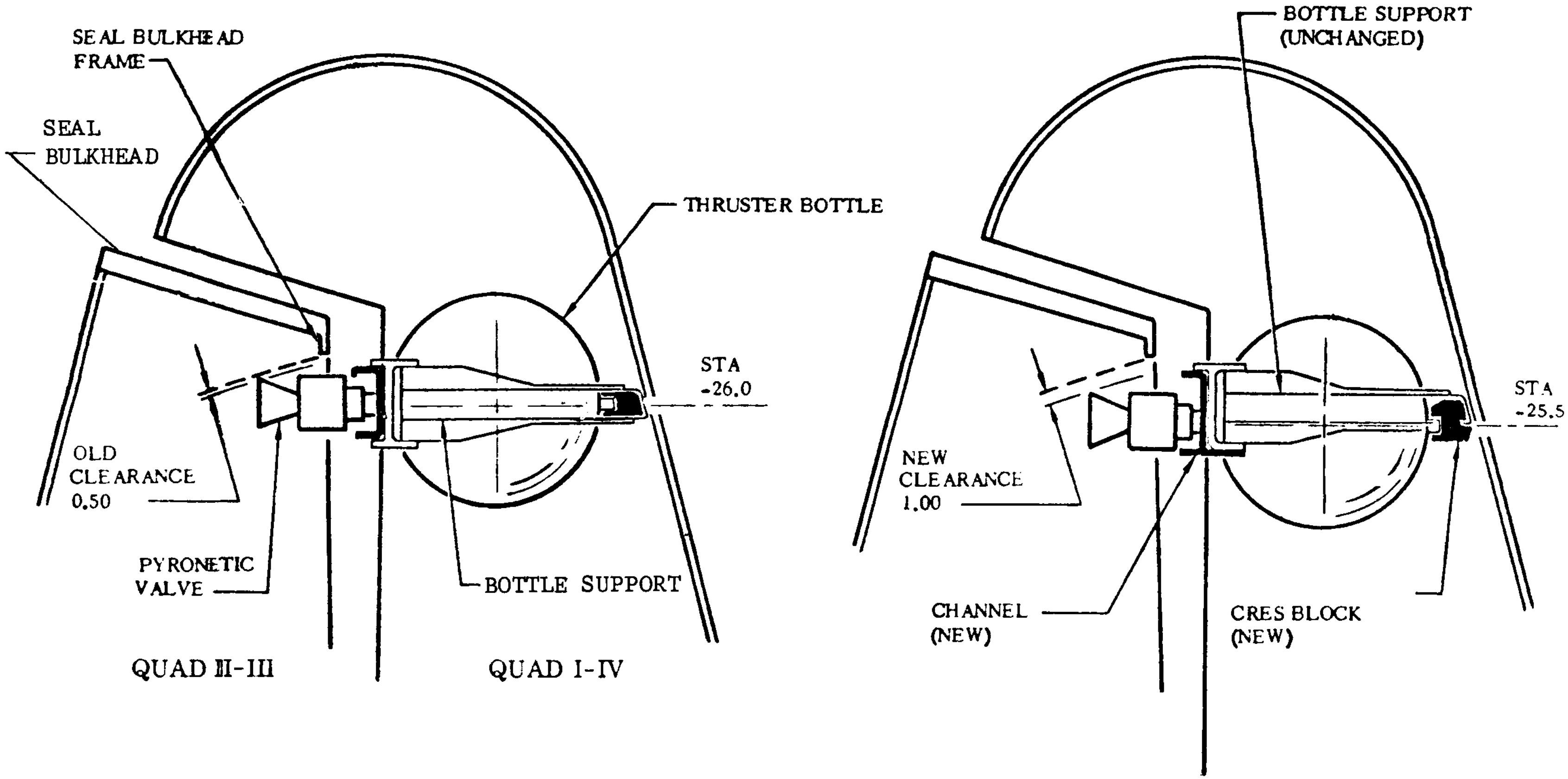

Figure 6. - I-IV Jettison bottle relocation.

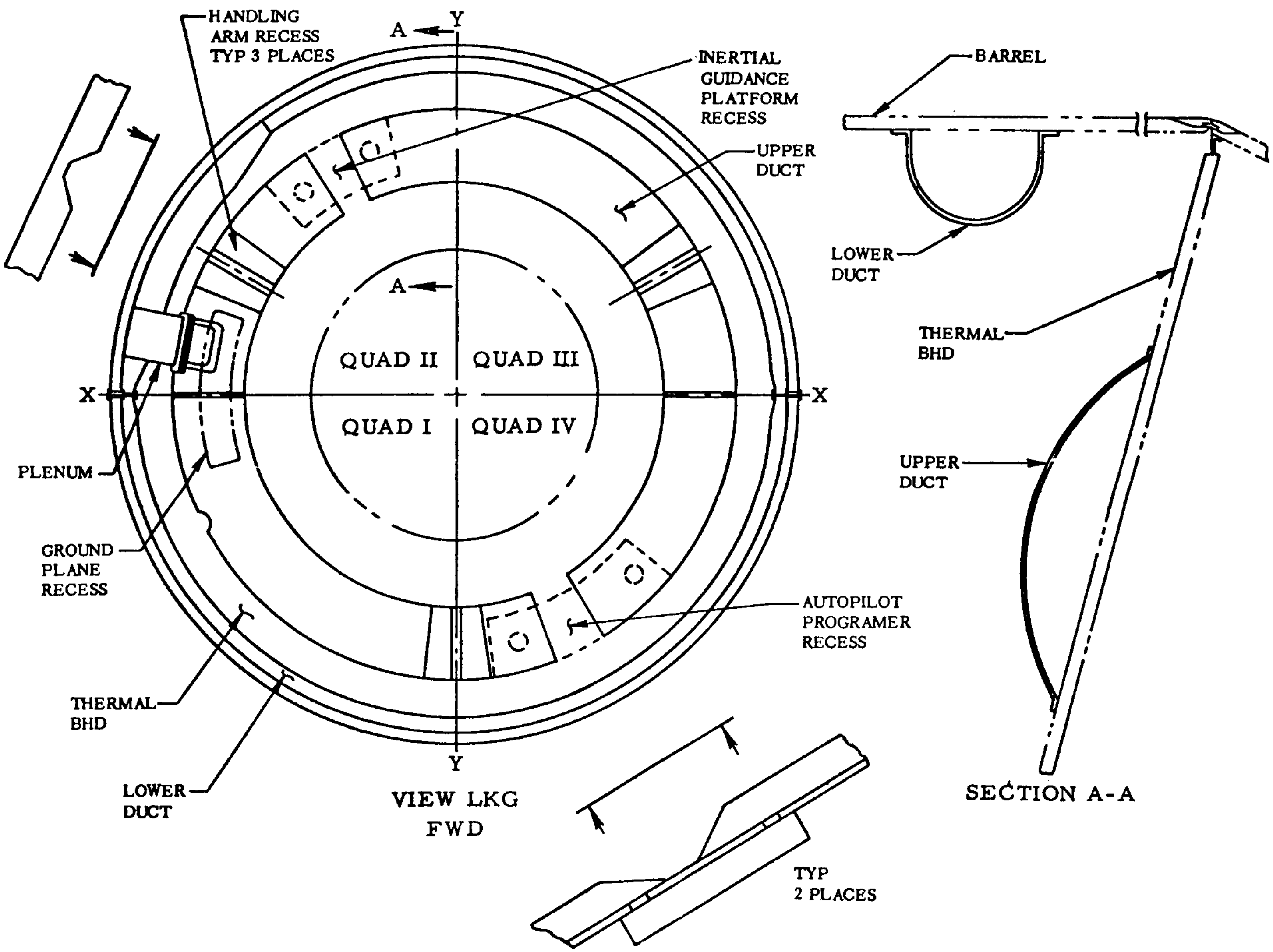

(a) AC-4 configuration.

Figure 7. - Modification of air conditioning ducts attached to the thermal bulkhead.

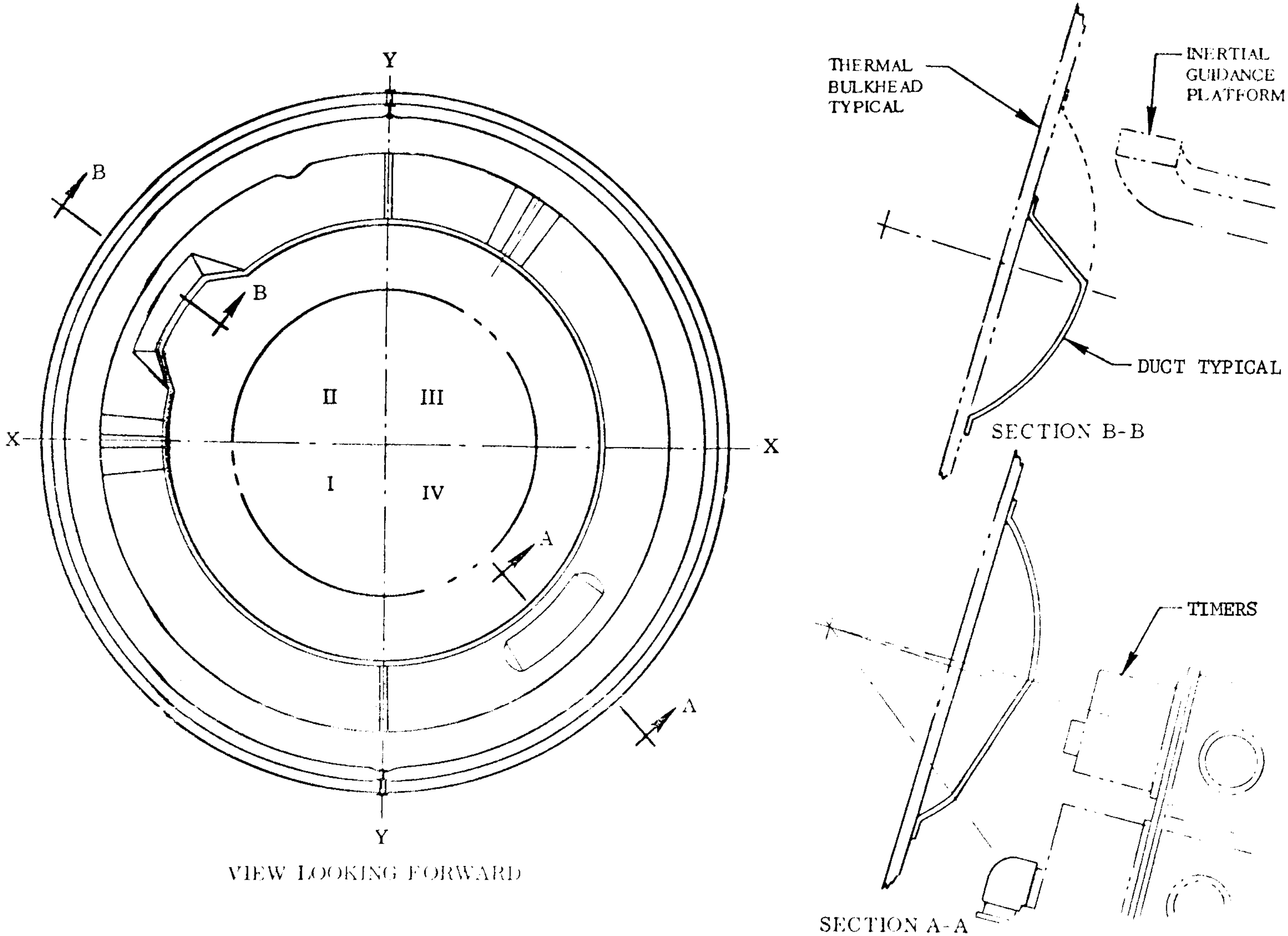

(b) AC-6 configuration

Figure 7. - Concluded. Modification of air conditioning ducts attached to the thermal bulkhead.

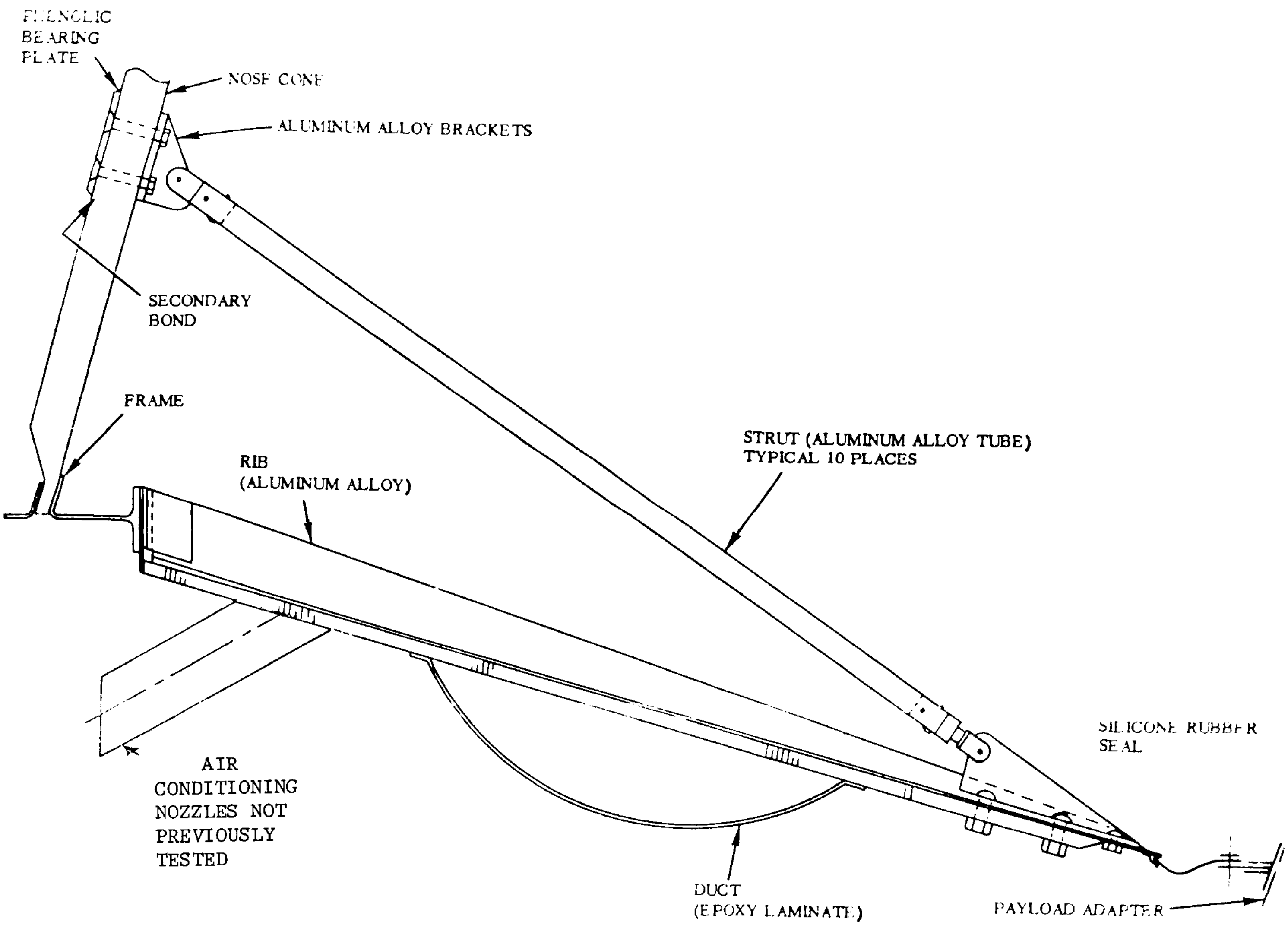

(a) Outer periphery of thermal bulkhead.

Figure 8. - Air conditioning nozzles.

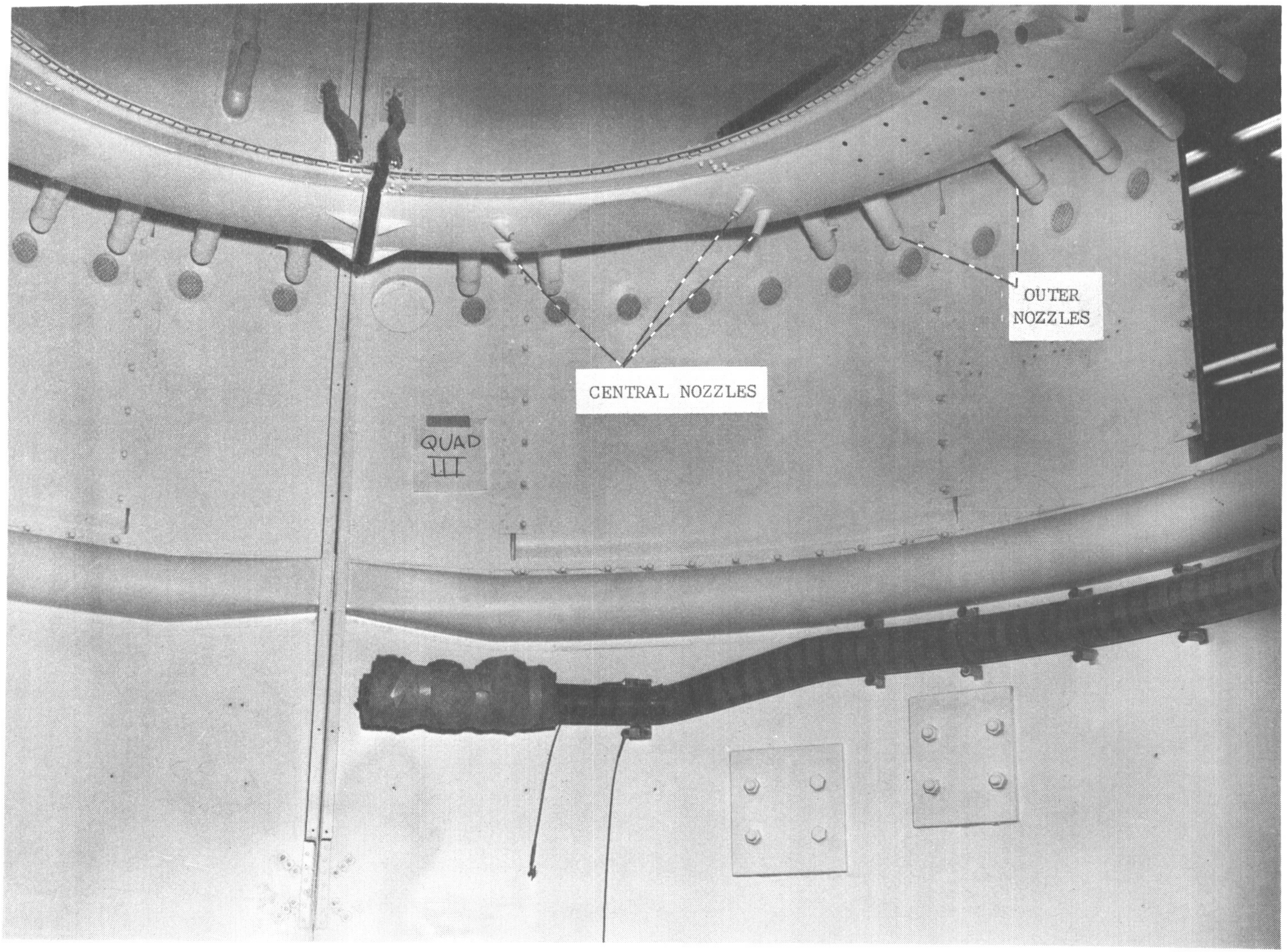

(b) Nozzles to central and outer section of instrument shelf.

Figure 8. - Concluded. Air conditioning nozzles.

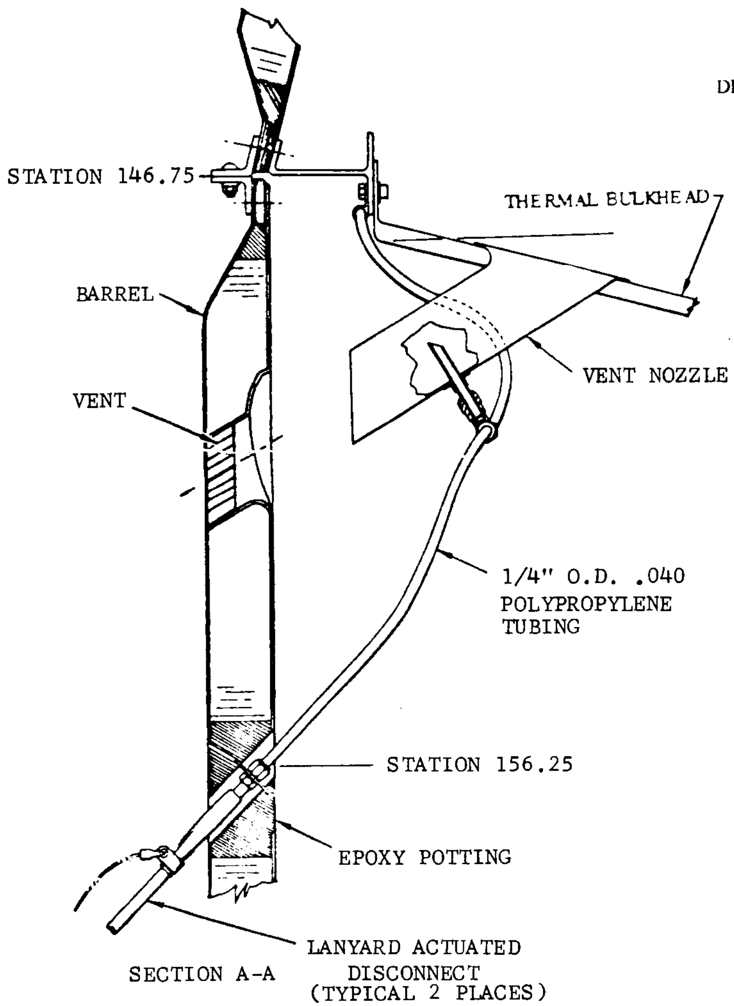

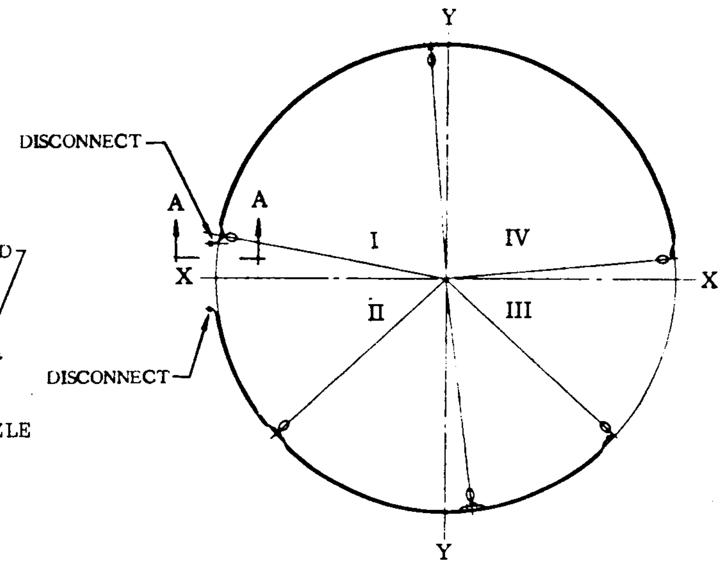

VIEW LOOKING AFT

PURPOSE OF SYSTEM:

TO SAMPLE PAYLOAD AIR CONDITIONING EXHAUST GASES FOR ANALYSIS BY TOXIC GAS DETECTOR, LOCATED ON UMBILICAL TOWER.

2.5 PPM N_2O_4 OR 0.5 PPM MMH FROM THE SURVEYOR ATTITUDE CONTROL SYSTEM IS TOXIC.

Figure 9. - Hazard detection system.

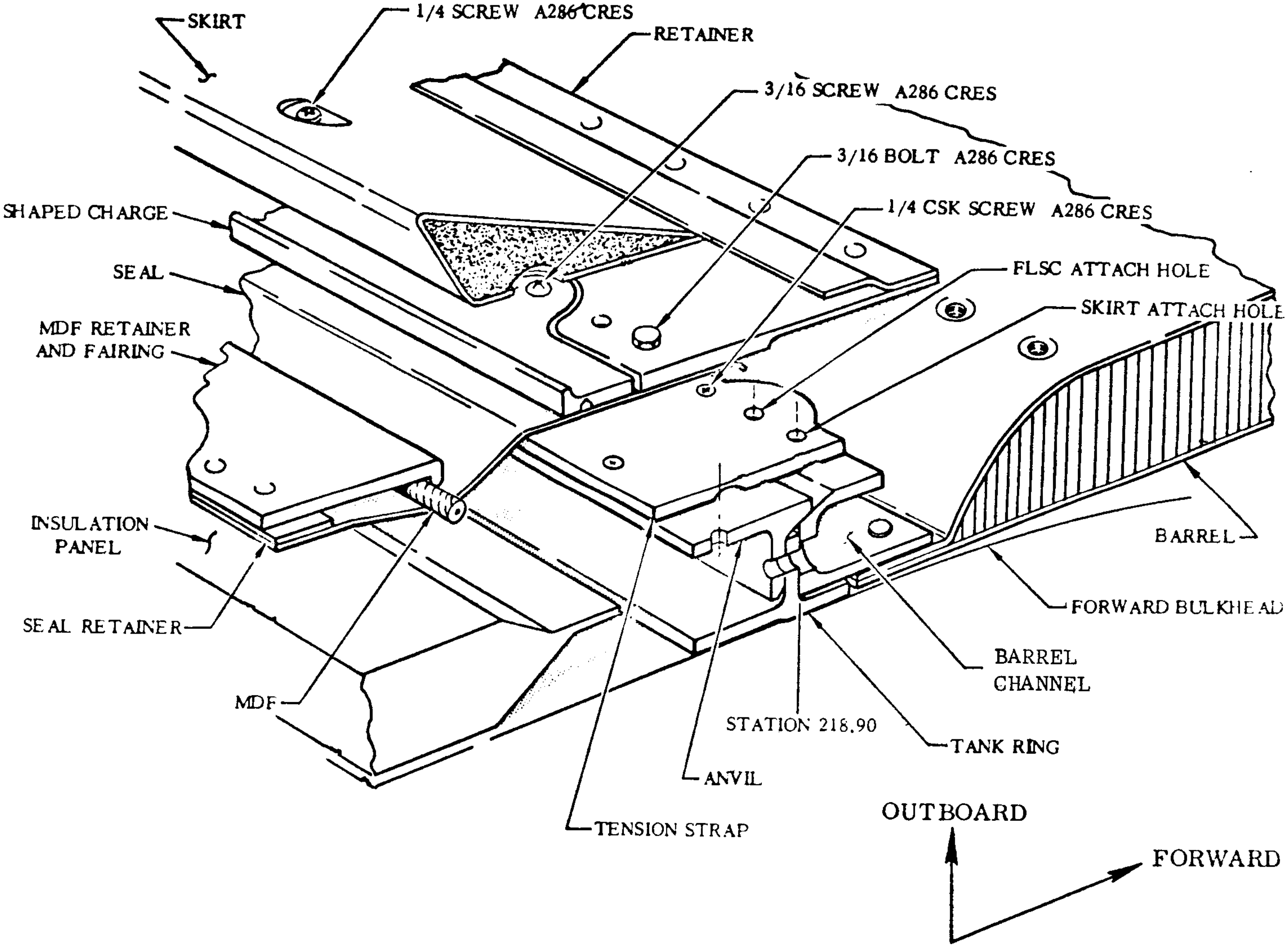

Figure 10. - Station 218.90 areas installation.

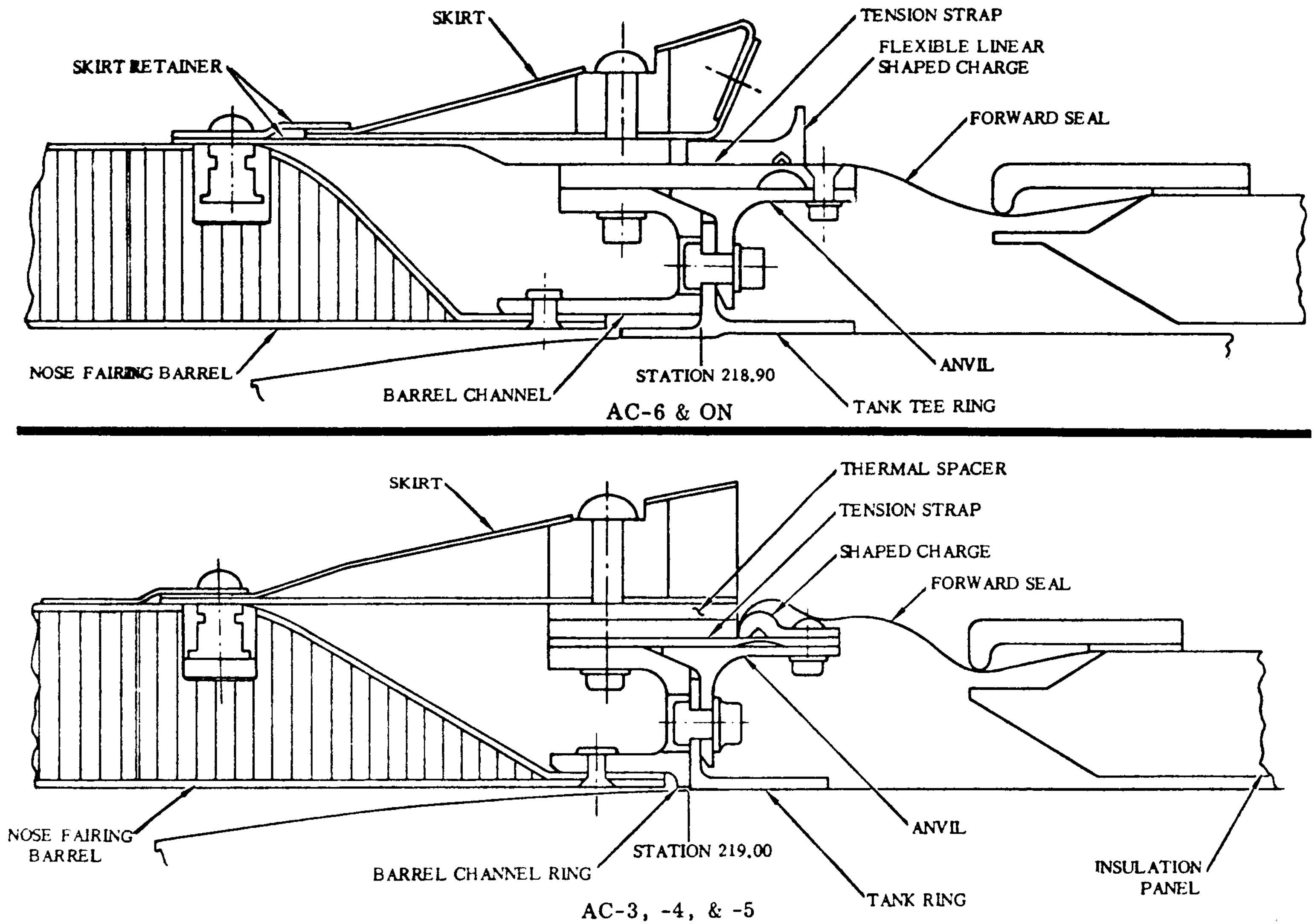

Figure 11. - Station 218.90 details.

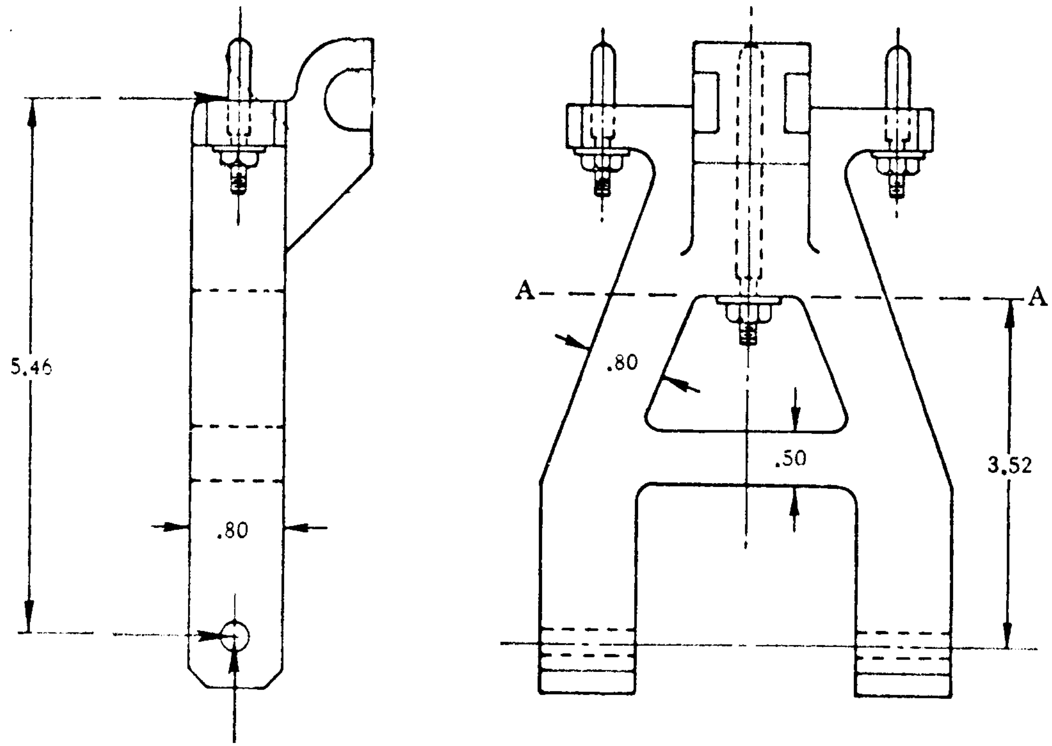

Figure 12. - Tank half of fairing hinge.

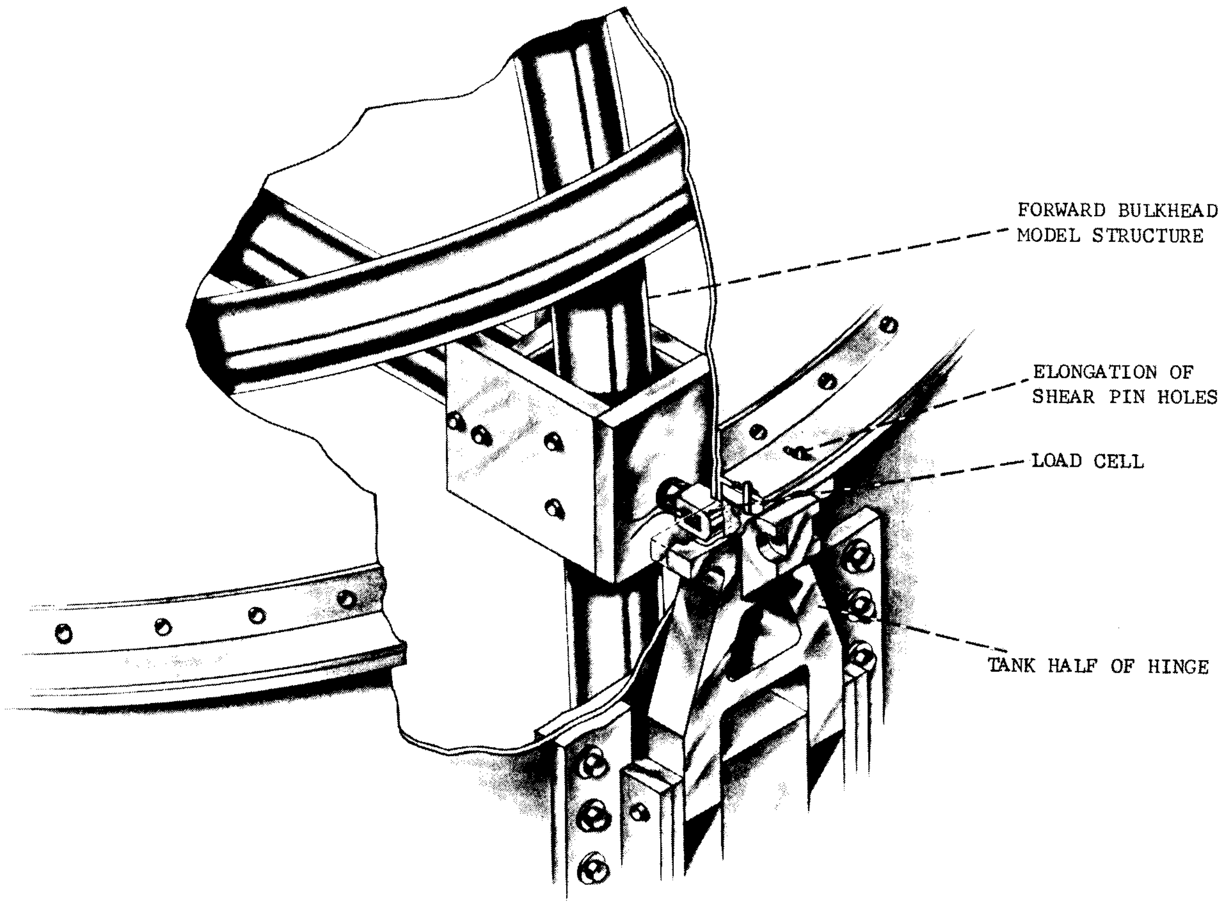

Figure 13. - Modification of fairing hinge support to measure hinge radial loads, test LA-3.

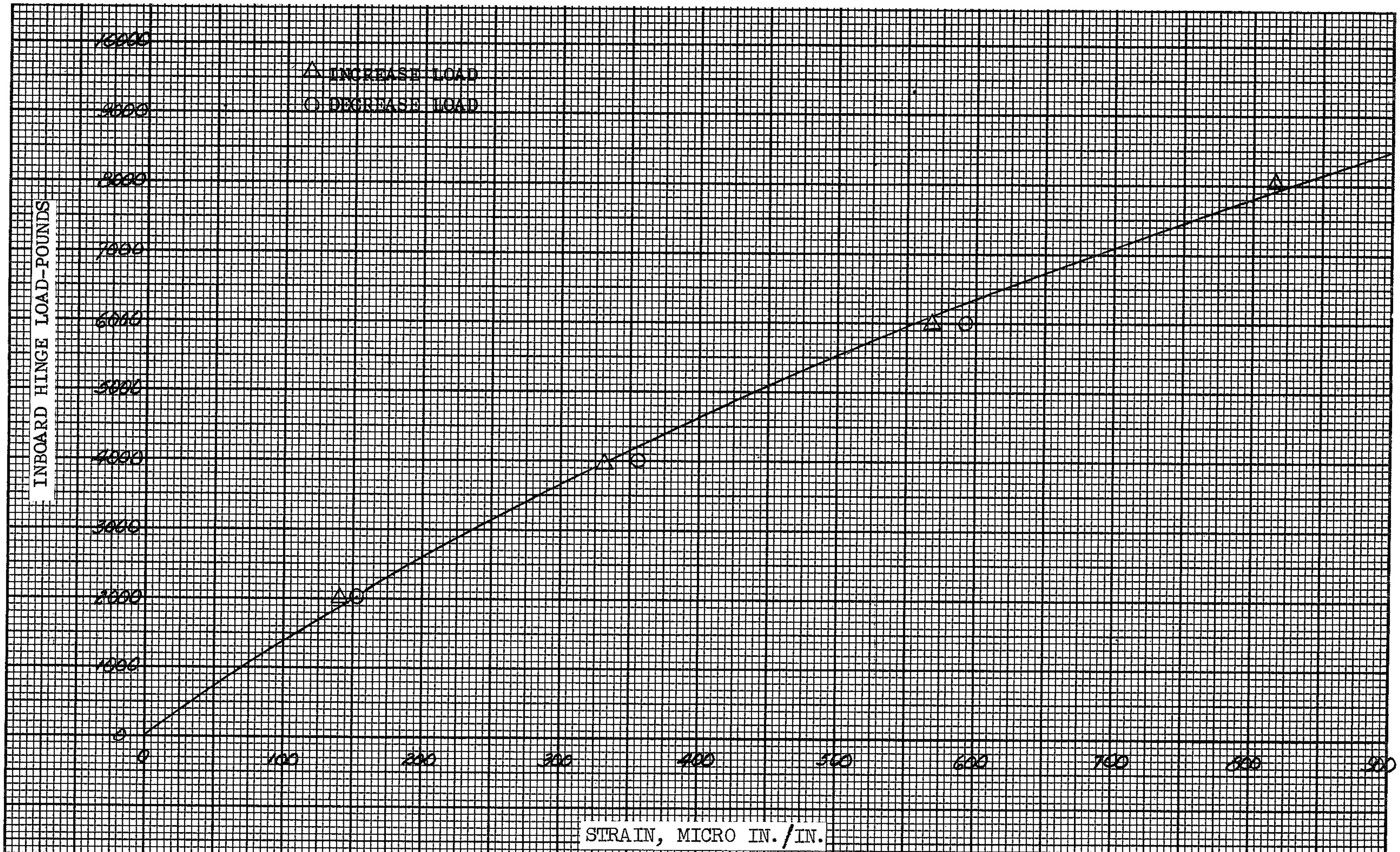

Figure 14. Calibration curve for loadcell (Transducer LA119S).

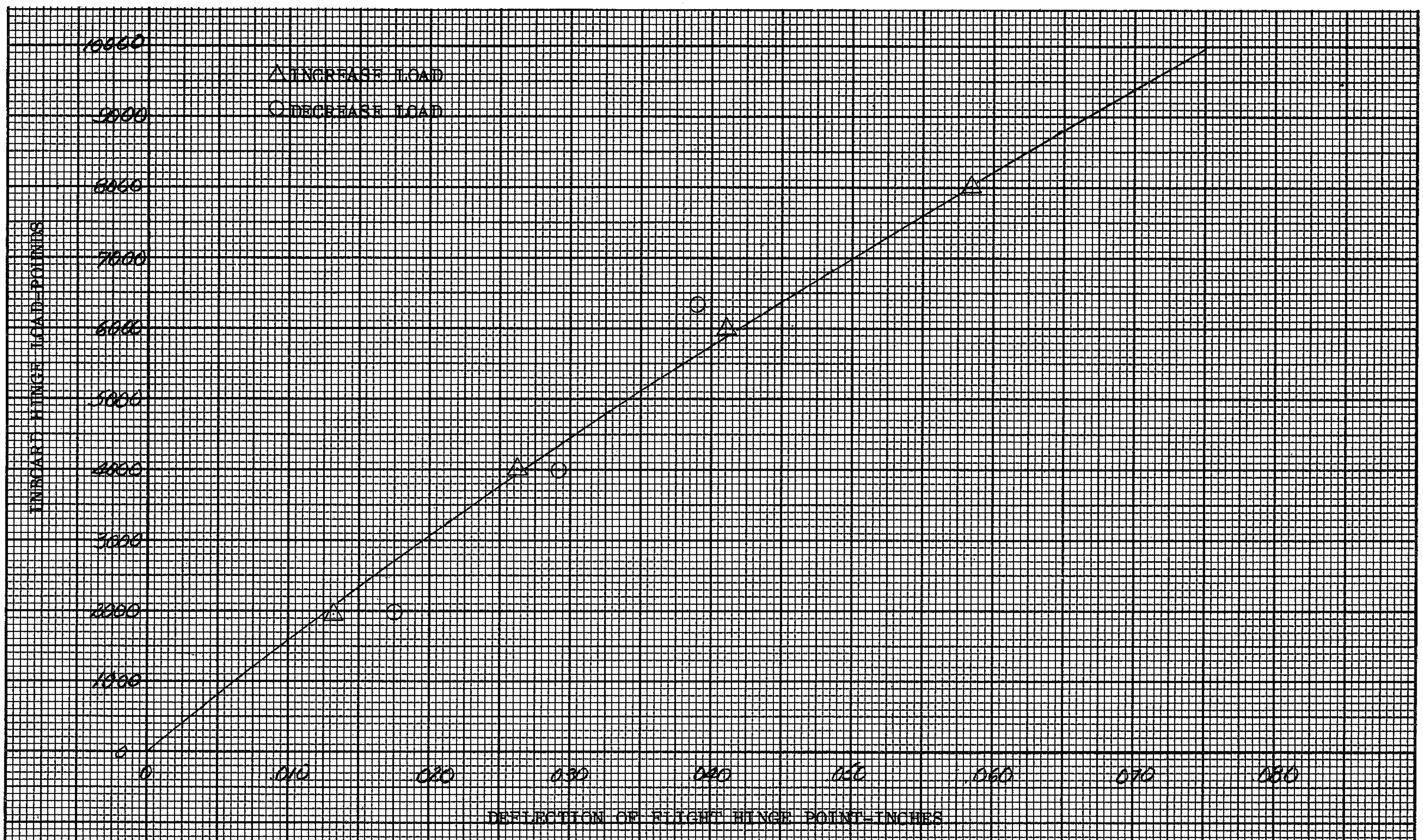

Figure 15. - Deflection versus load of loadcell, test 1A-3.

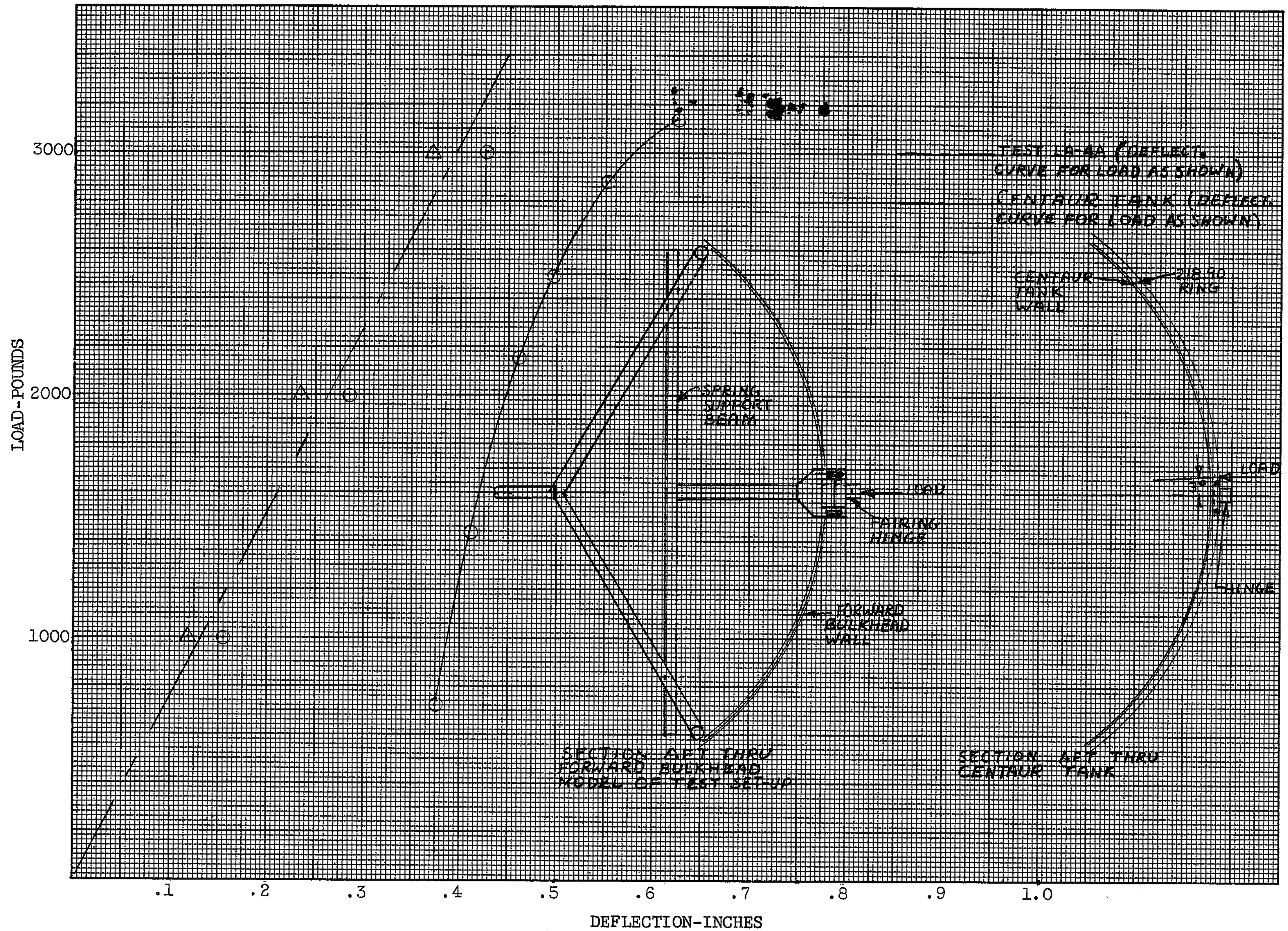

Figure 16. - Deflection versus load comparison between hinge supporting structure of test LA-4A and Centaur tank.

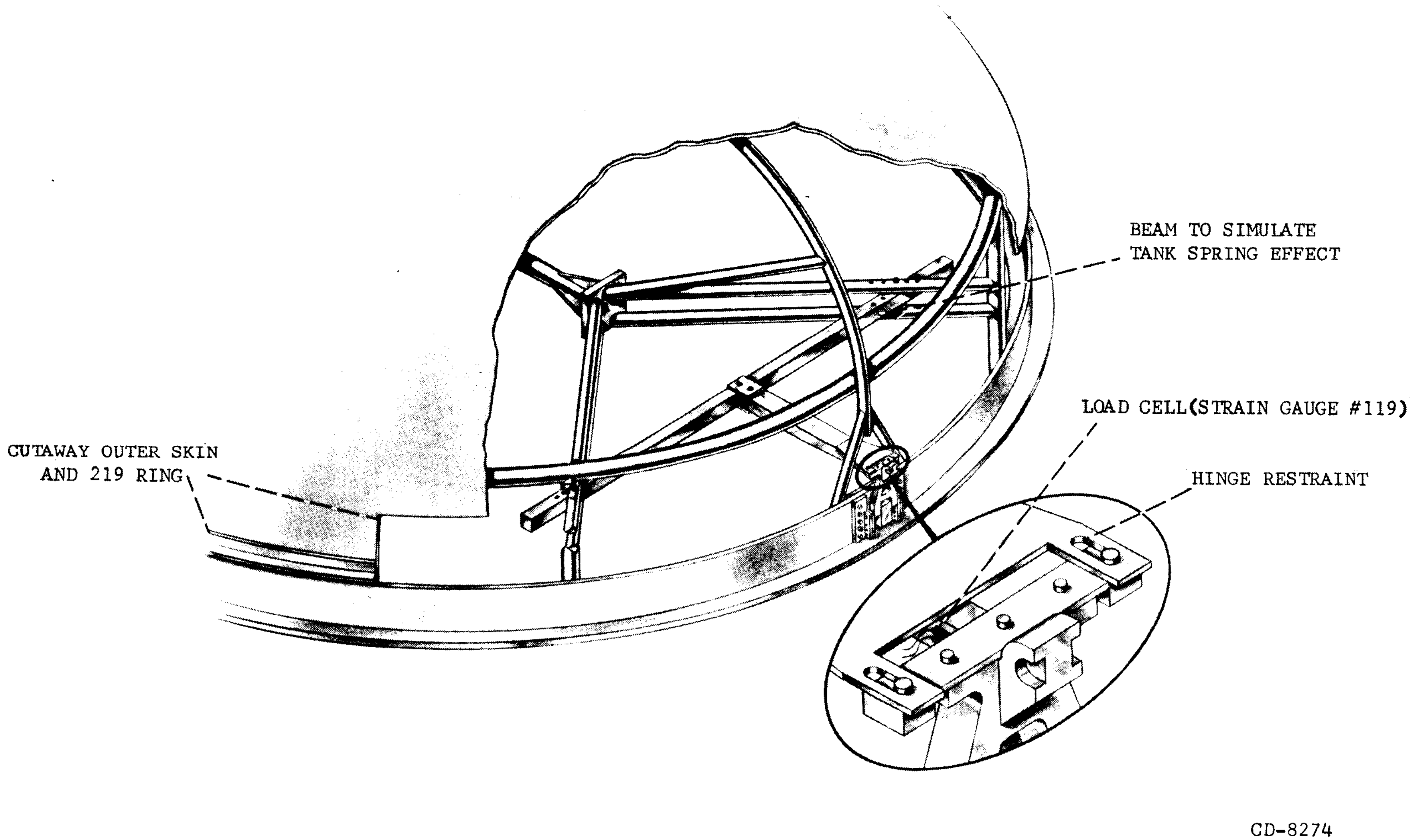

Figure 17. - Modification of tank hinge support to measure hinge radial loads against simulated tank spring effect, test LA-4A.

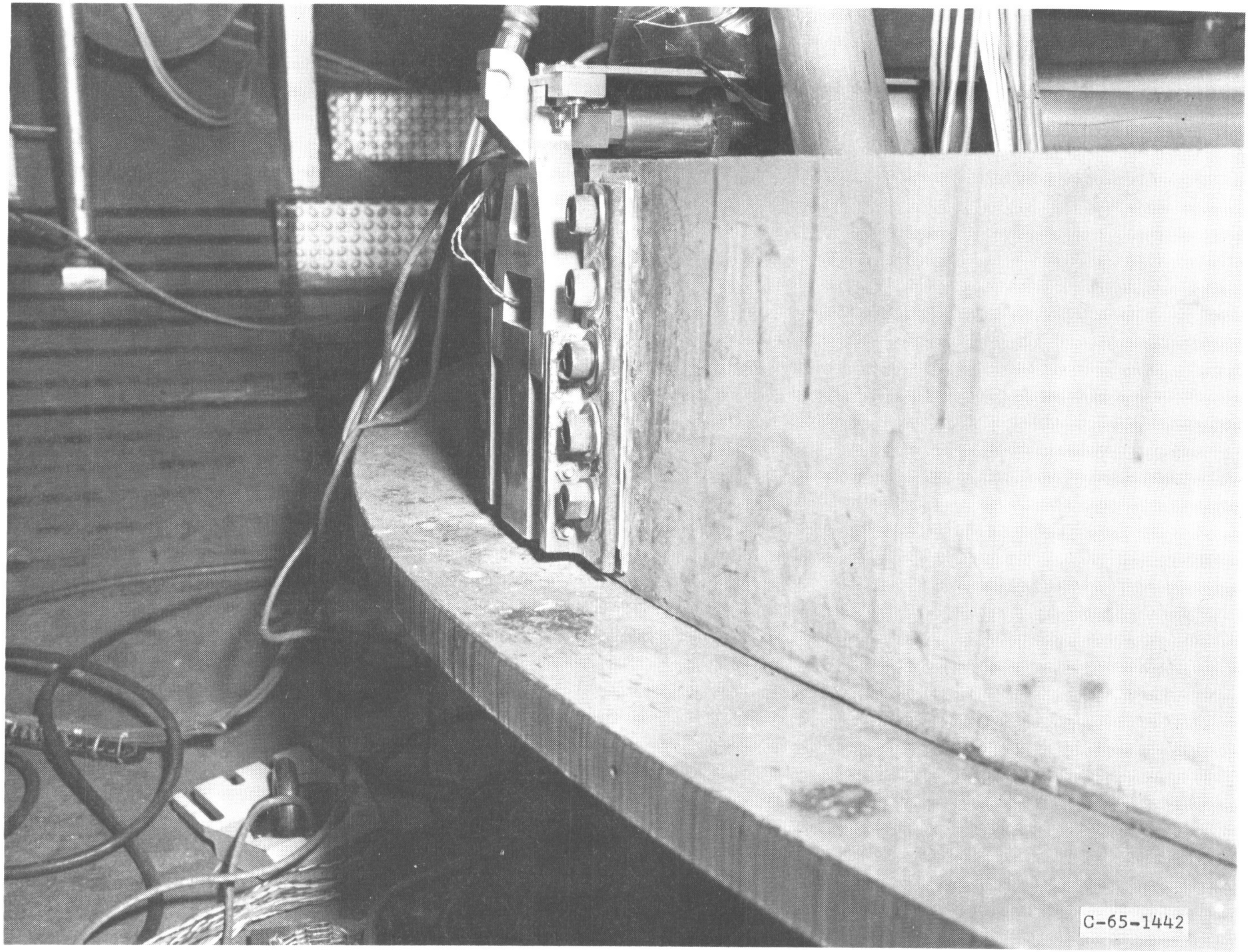

Figure 18. - Modified tank hinge support, test LA-4A.

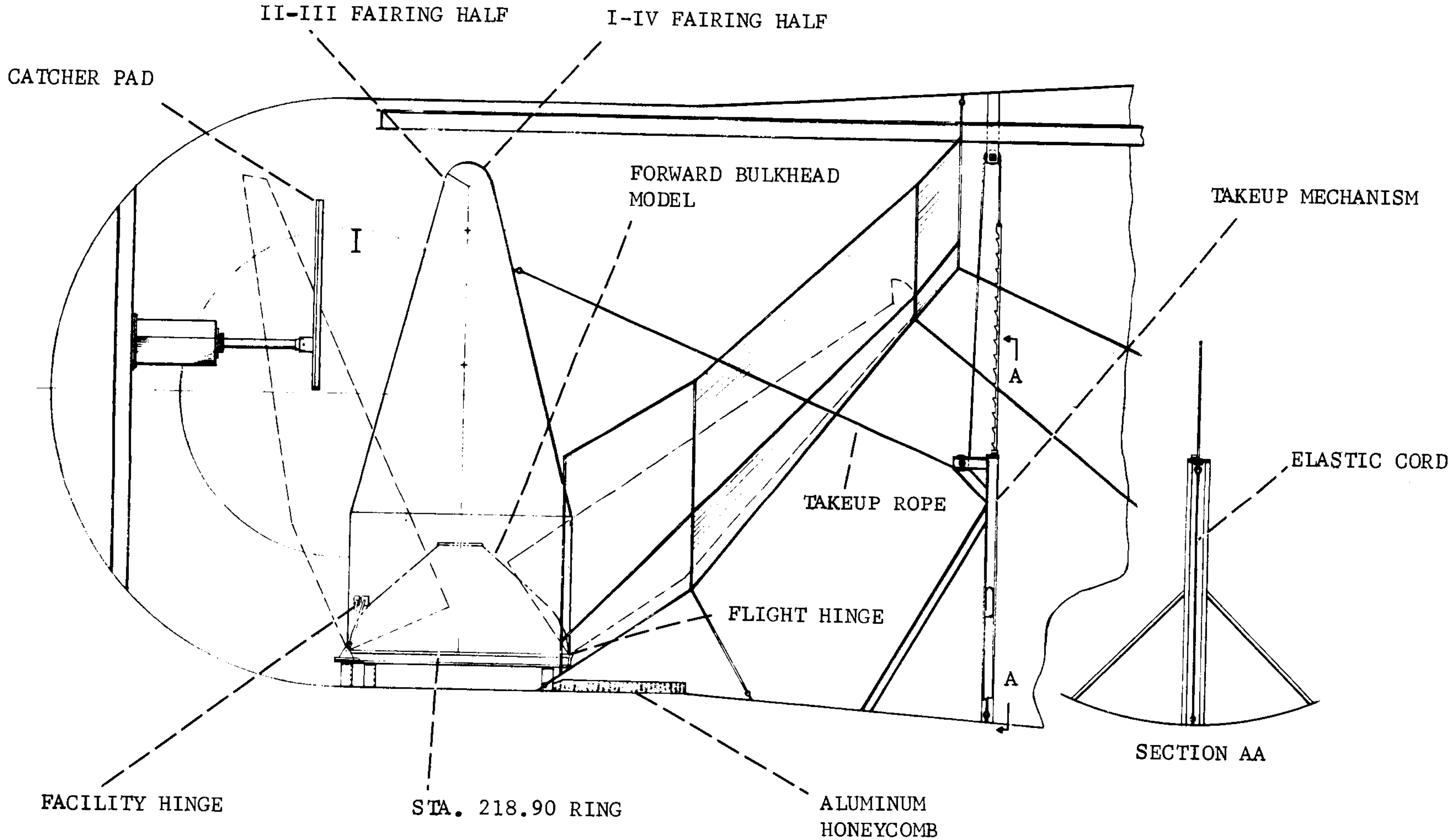

CD-8003

Figure 19. - Facility configuration for fairing tests LA-1 through LA-4.

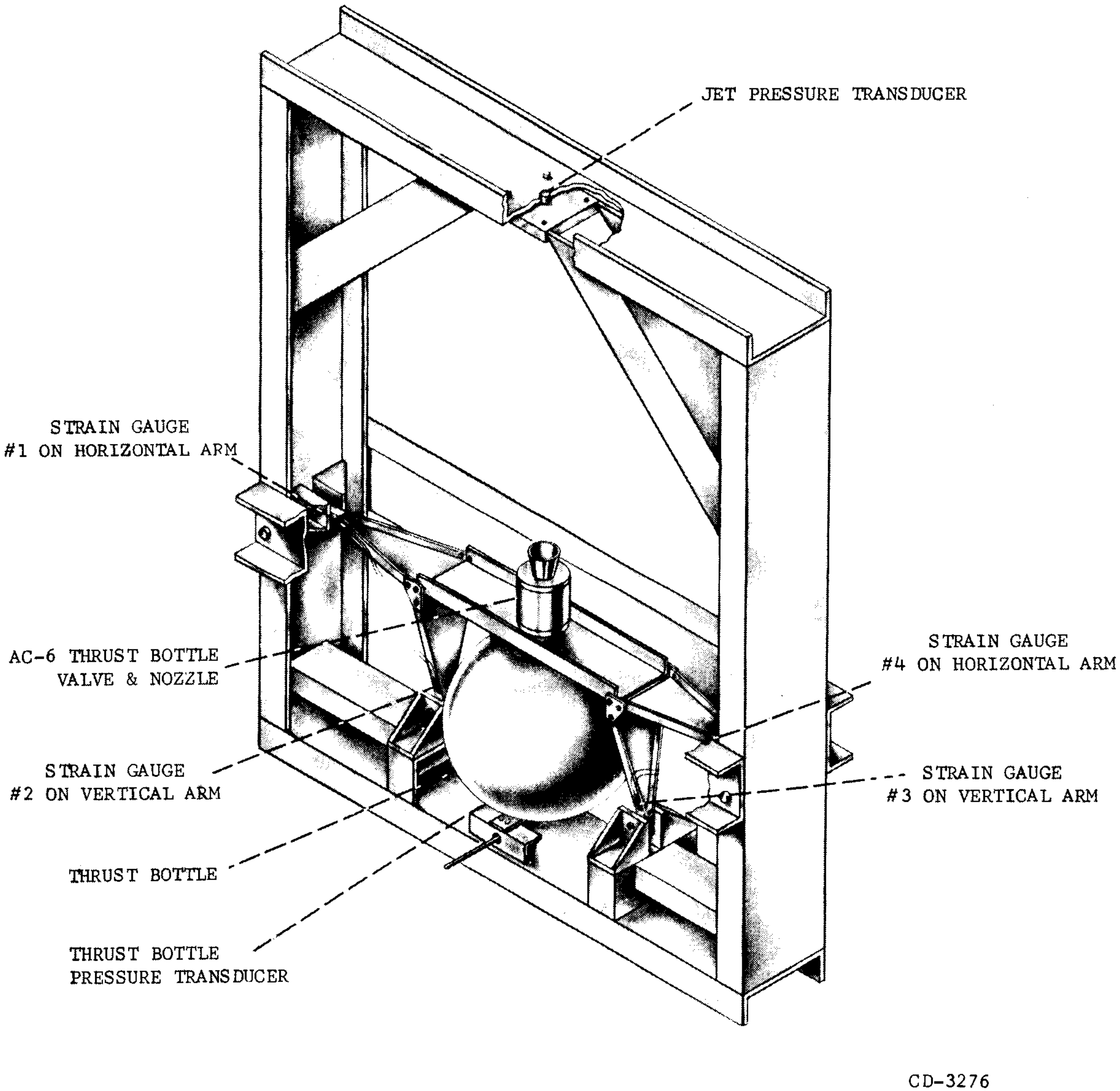

Figure 20. - Thrust bottle test stand.

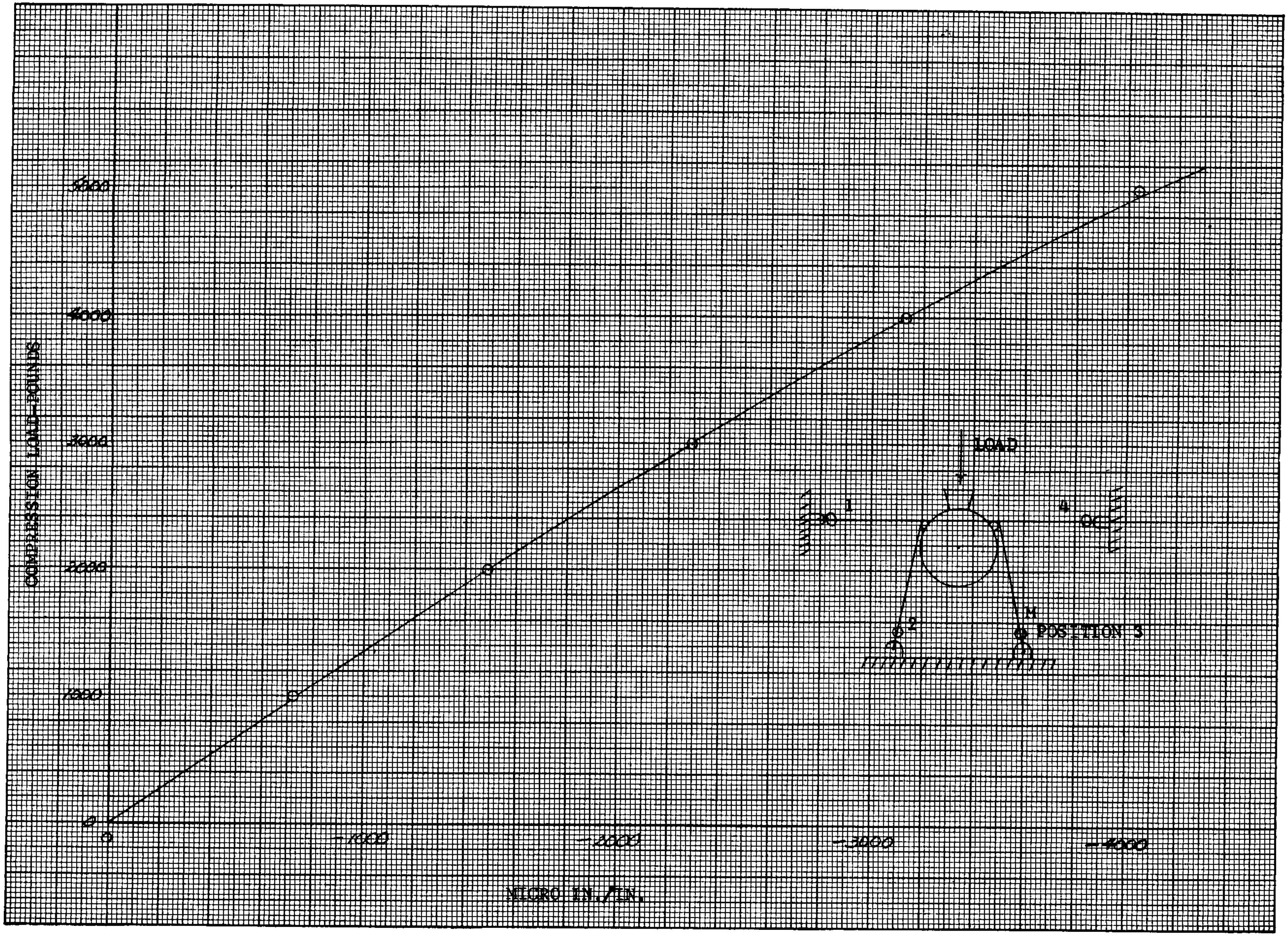

(a) Strain gauge positions 2 and 3.
Figure 21. - Load vs. strain calibration of thrust bottle test stand.

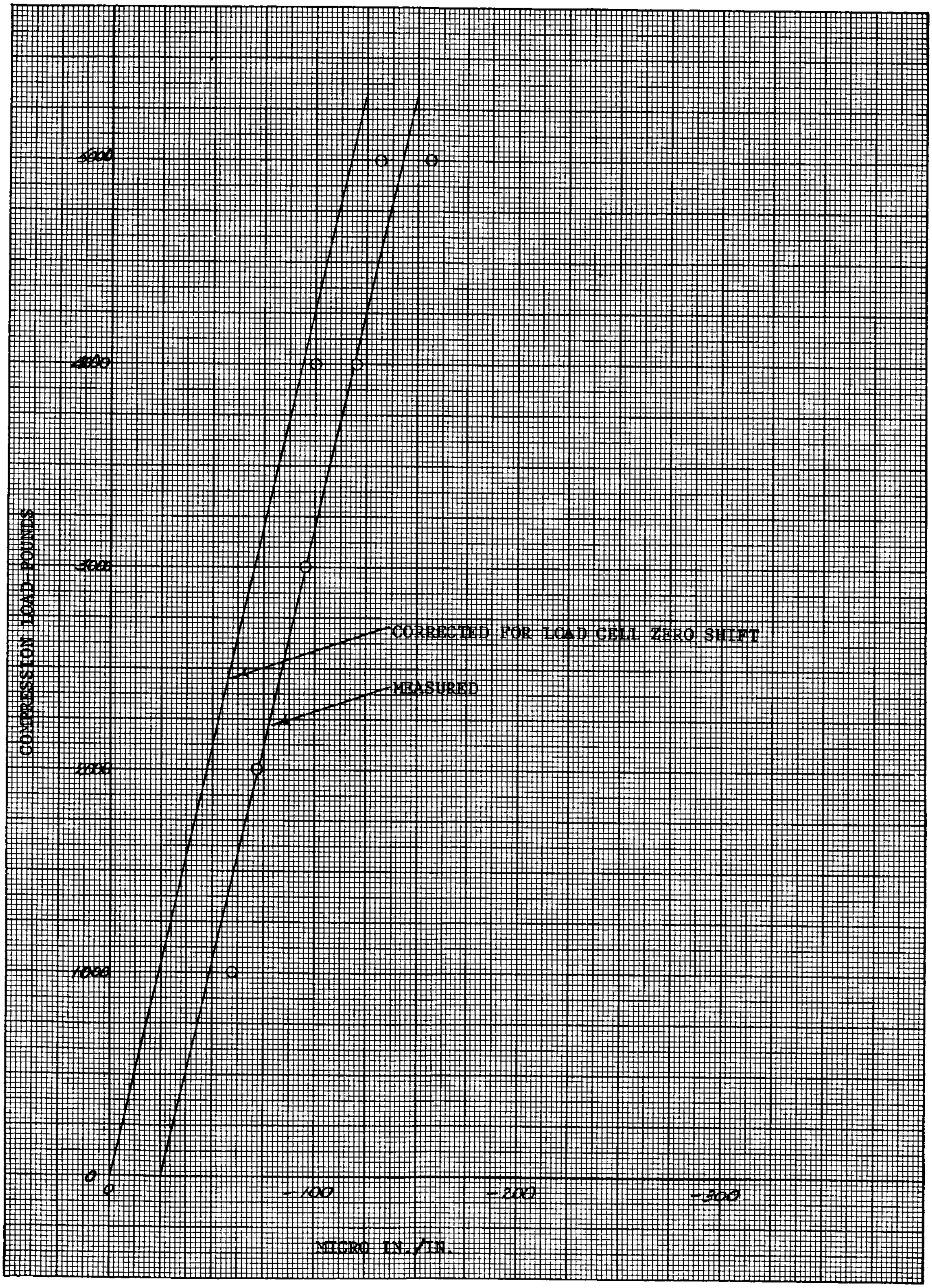

(b) Strain gauge positions 1 and 4.
Figure 21. - Concluded. Load vs. strain calibration of thrust bottle test stand.

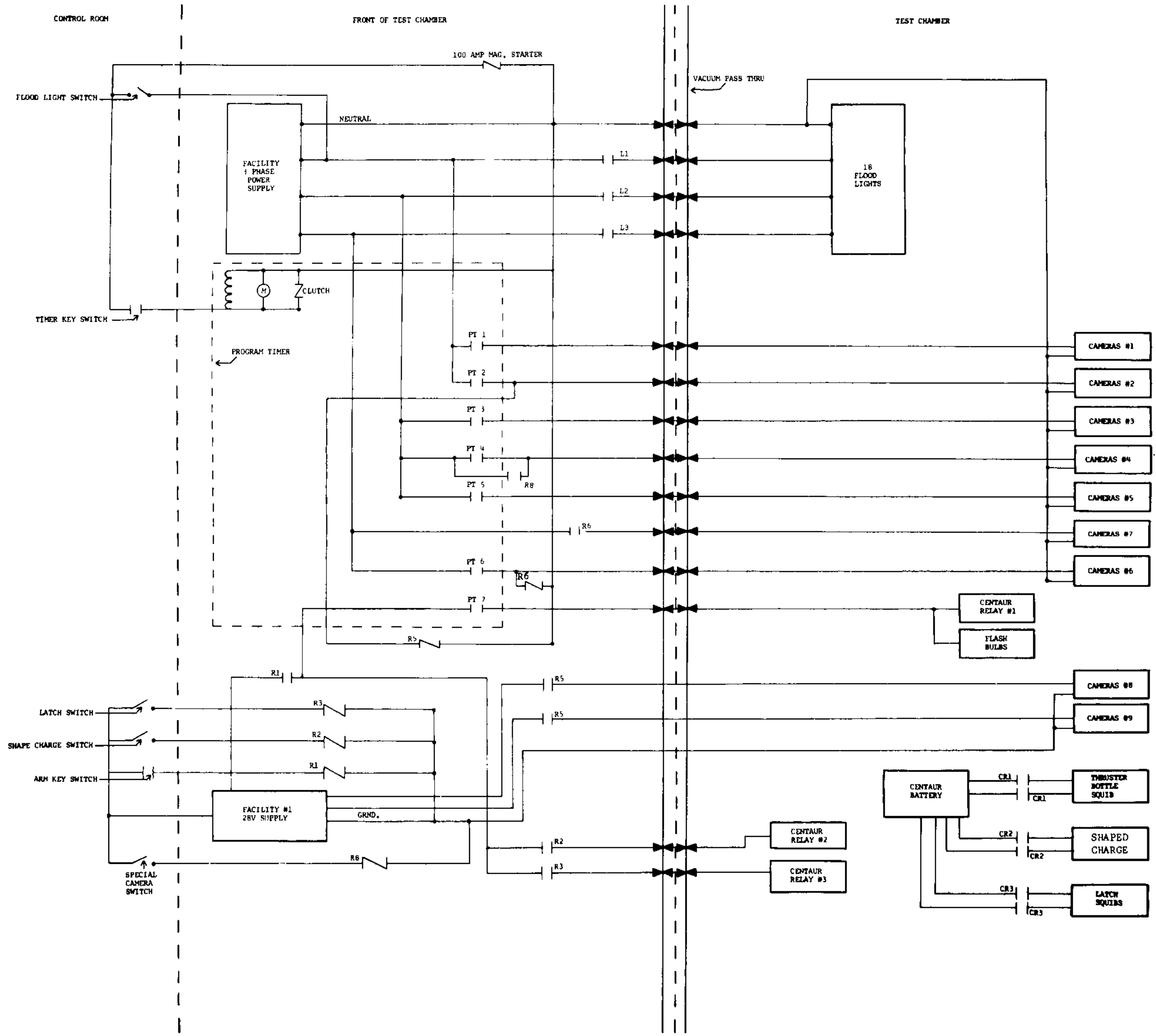

Figure 22. - Schematic diagram of the facility electrical system.

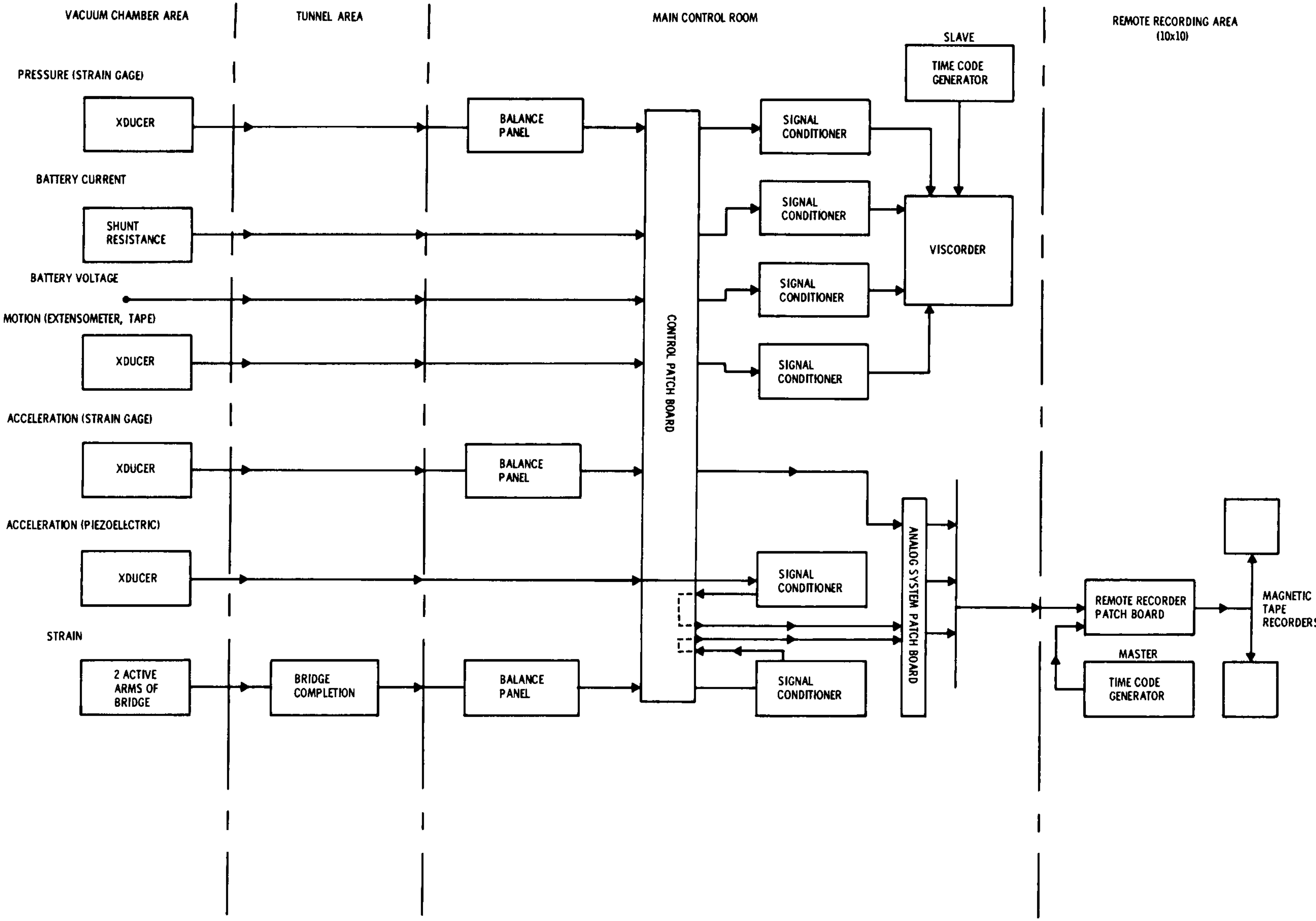

Figure 23. - Block diagram of the instrument system.

E-3897

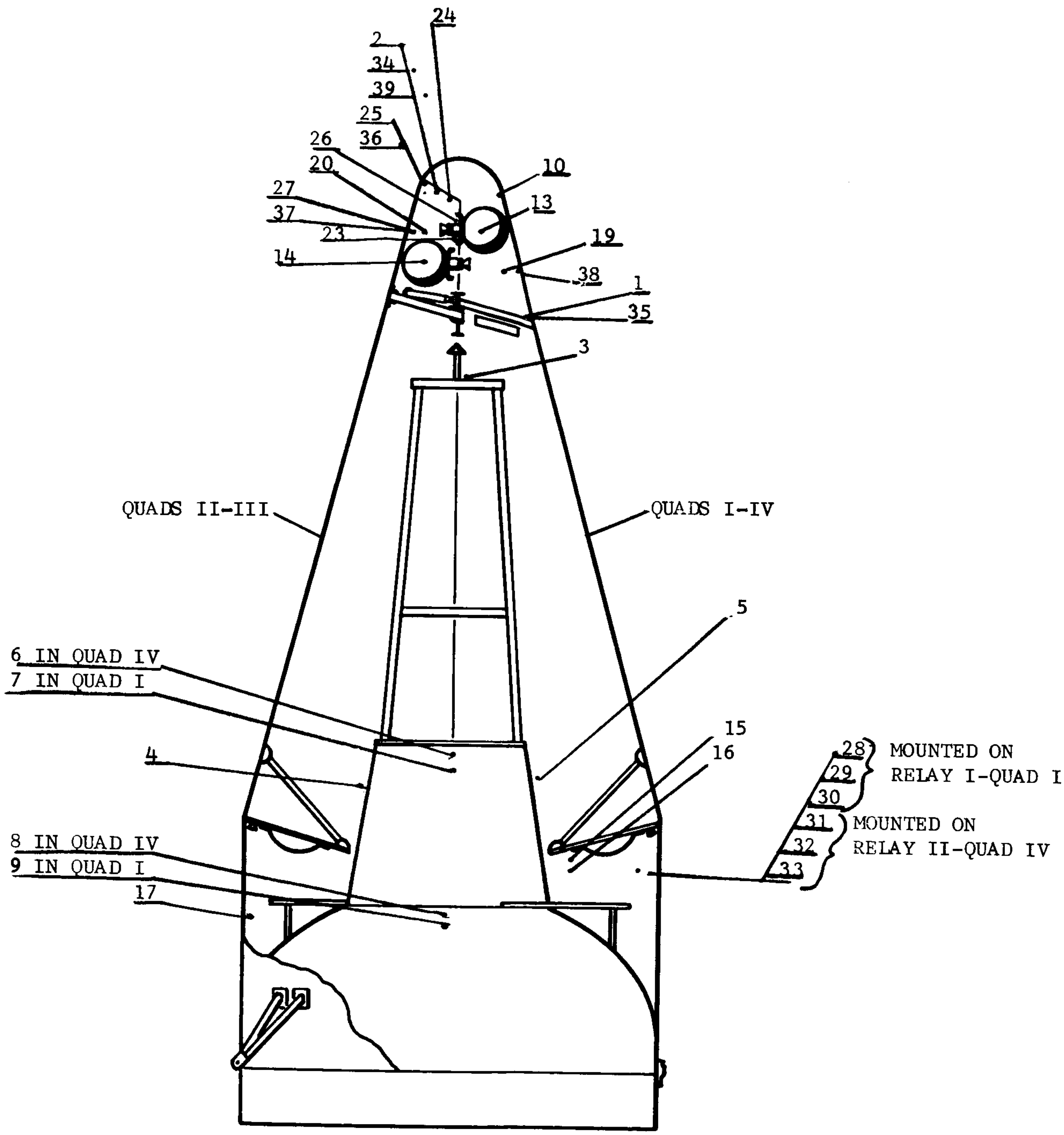

(a) Pressure, motion, and acceleration.

Figure 24. - Location of transducers.

E-3897

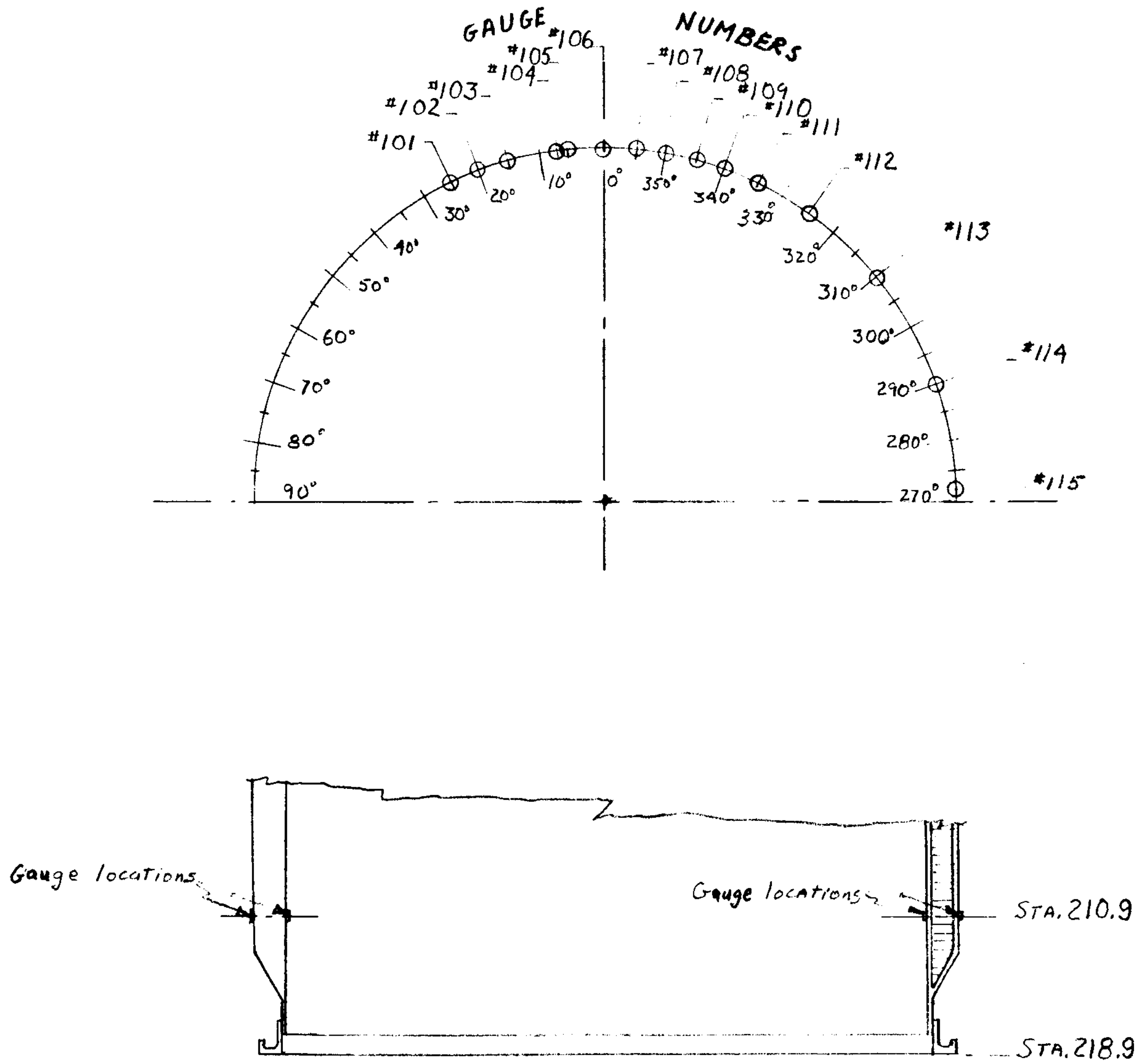

(b) Strain gauges at station 210.90 of fairing.

Figure 24. - Continued. Location of transducers.

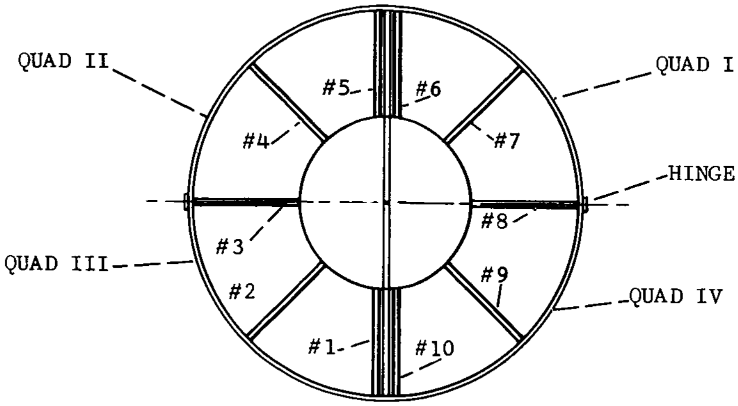

Location of struts and hinges

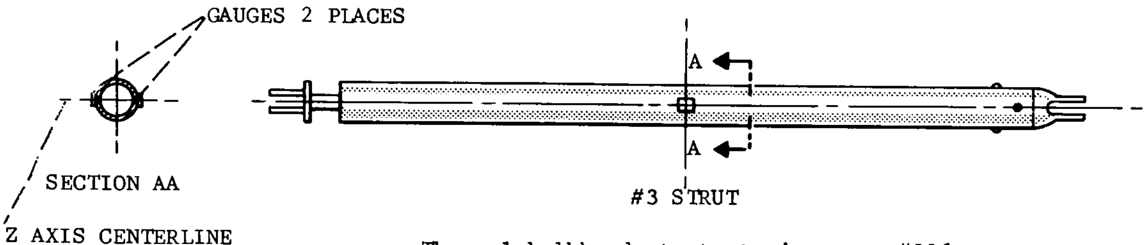

Thermal bulkhead strut strain gauge #116

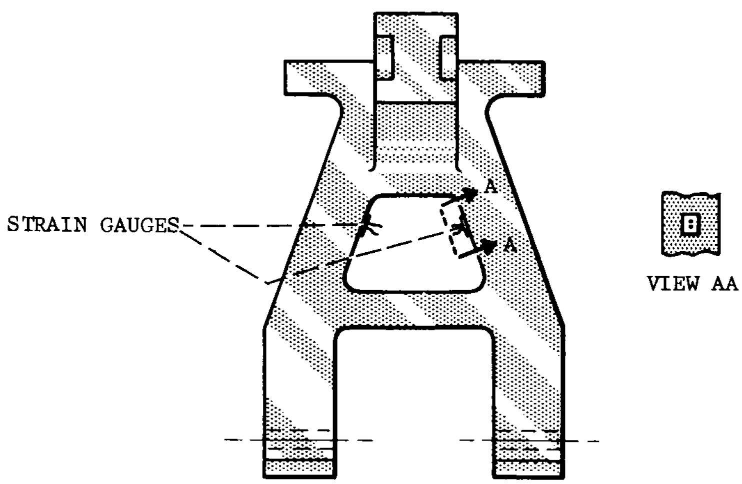

Hinge strain gauge #117

CD-8406

(c) Other strain gauges.

Figure 24. - Concluded. Location of transducers.

E-3897

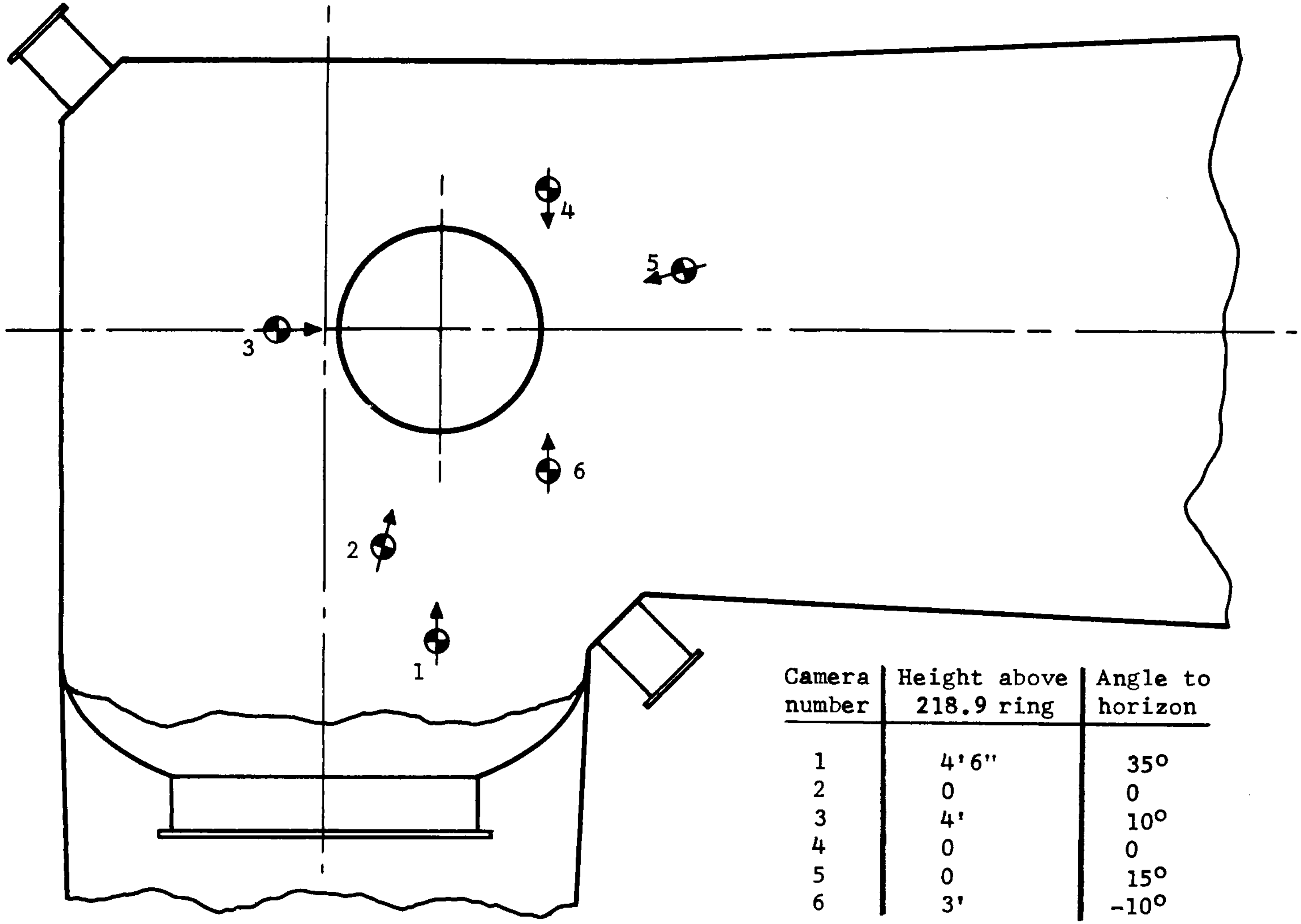

Camera number	Height above 218.9 ring	Angle to horizon
1	4'6"	35°
2	0	0
3	4'	10°
4	0	0
5	0	15°
6	3'	-10°

CD-8273

(a) Outside fairing.

Figure 25. - Camera positions.

Camera number	Height above 218.9 ring	Angle to horizon
7	16.7'	+69°
8	13.8'	-62°
9	14.1	-70°
10	14.1	-70°
11	16.7	69°

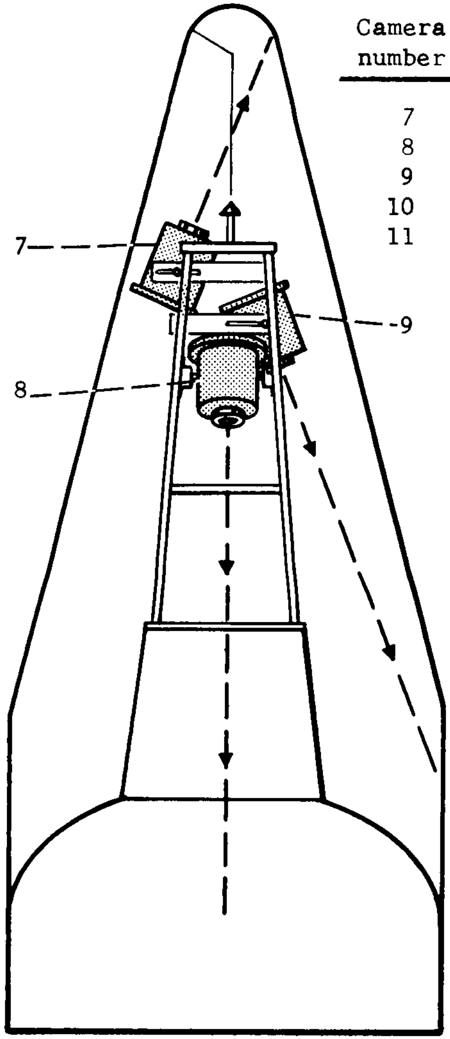

Test LA1

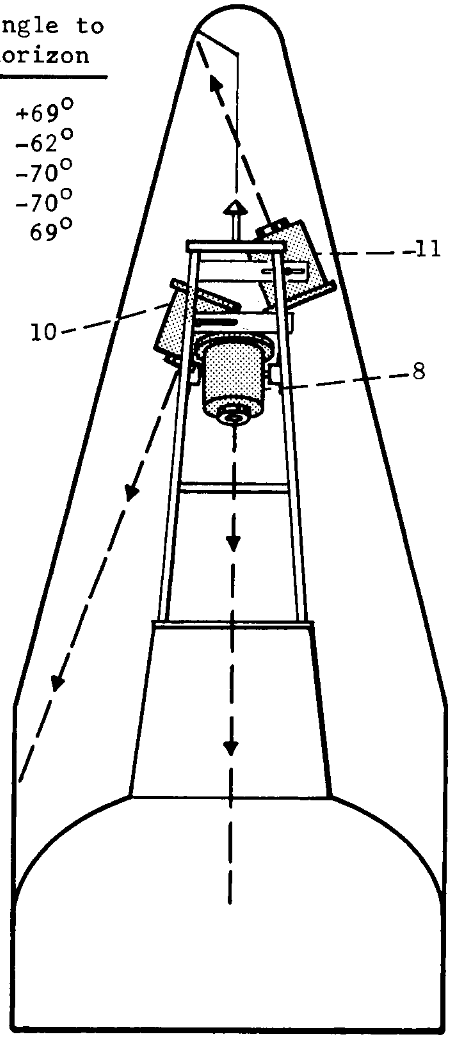

Tests LA2 thru LA4

(b) Inside fairing.

CD-8272

Figure 25. - Concluded. Camera positions.

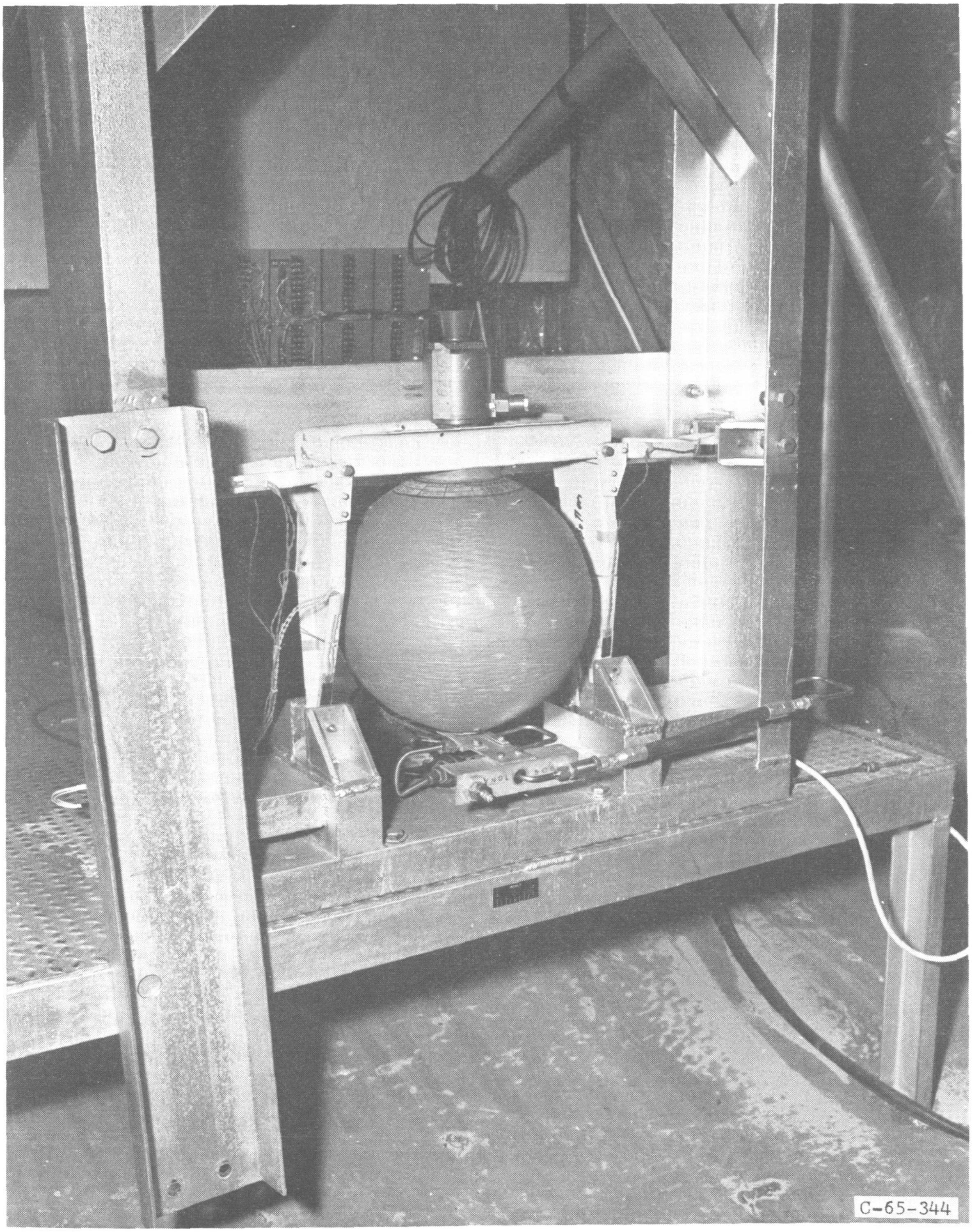

Figure 26. - Jettison bottle thrust test stand.

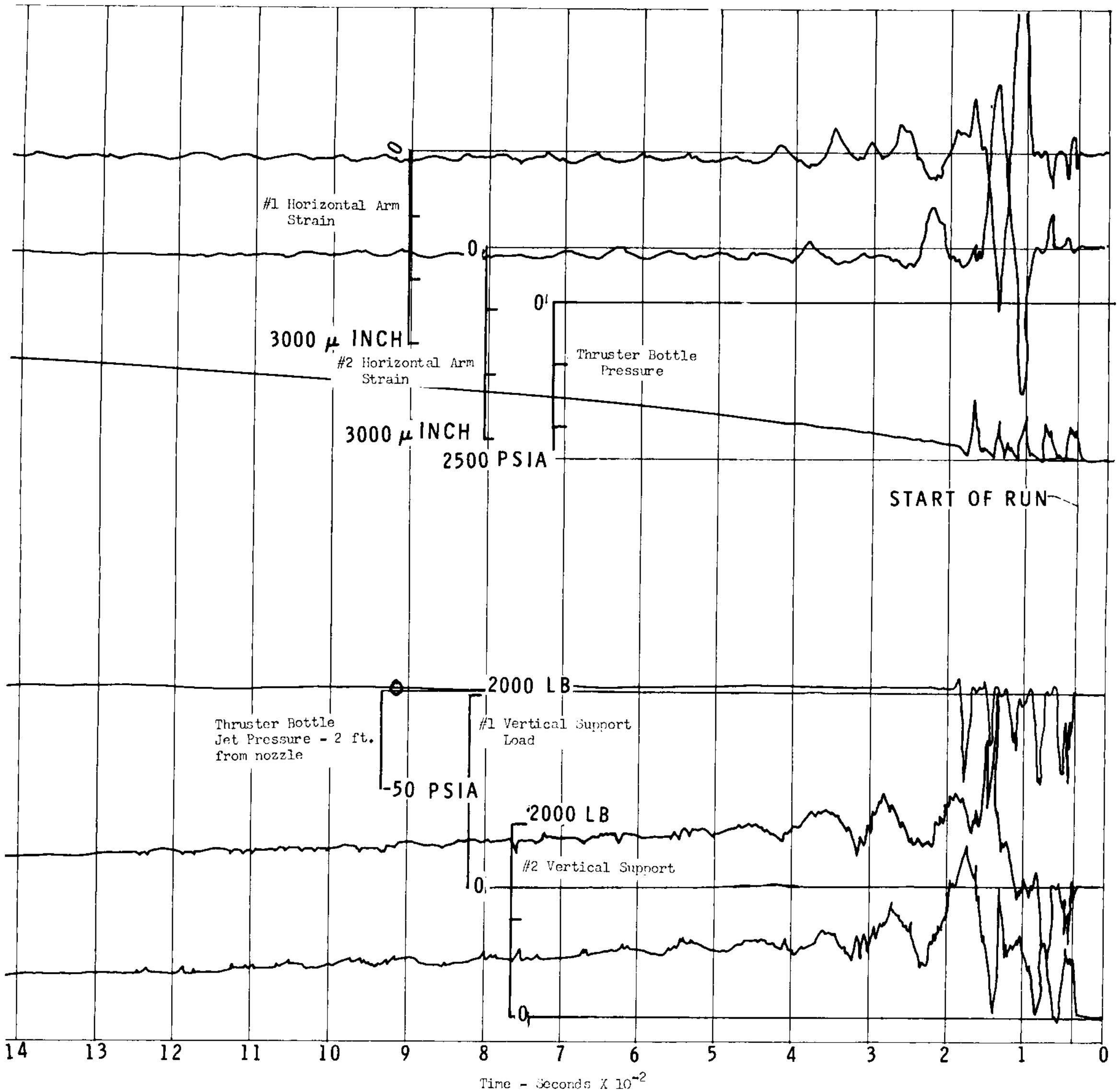

(a) AC-4 type nozzle, test 1.

Figure 27. - Jettison bottle thrust test data.

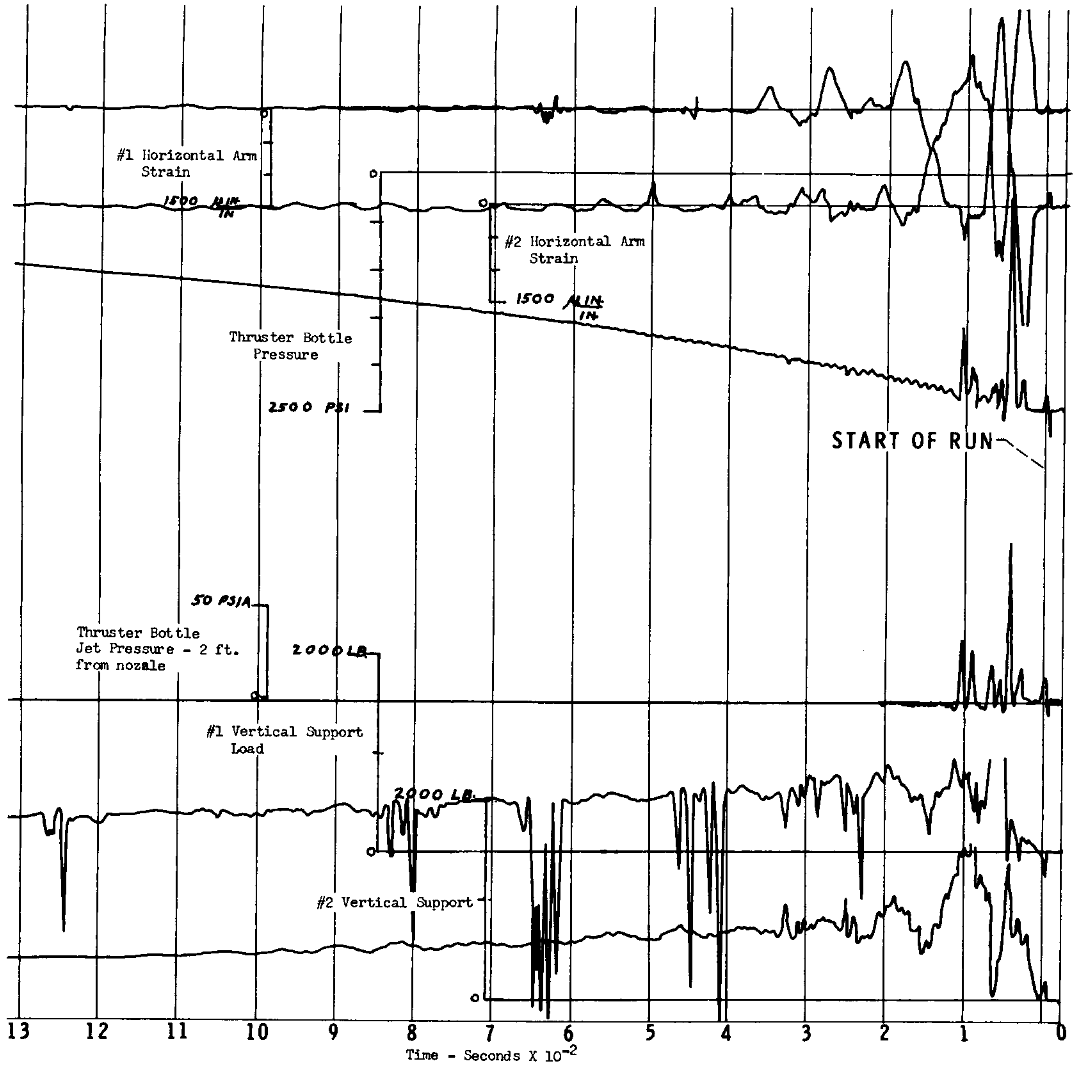

(b) AC-4 type nozzle, test 2.

Figure 27. - Continued. Jettison bottle thrust test data.

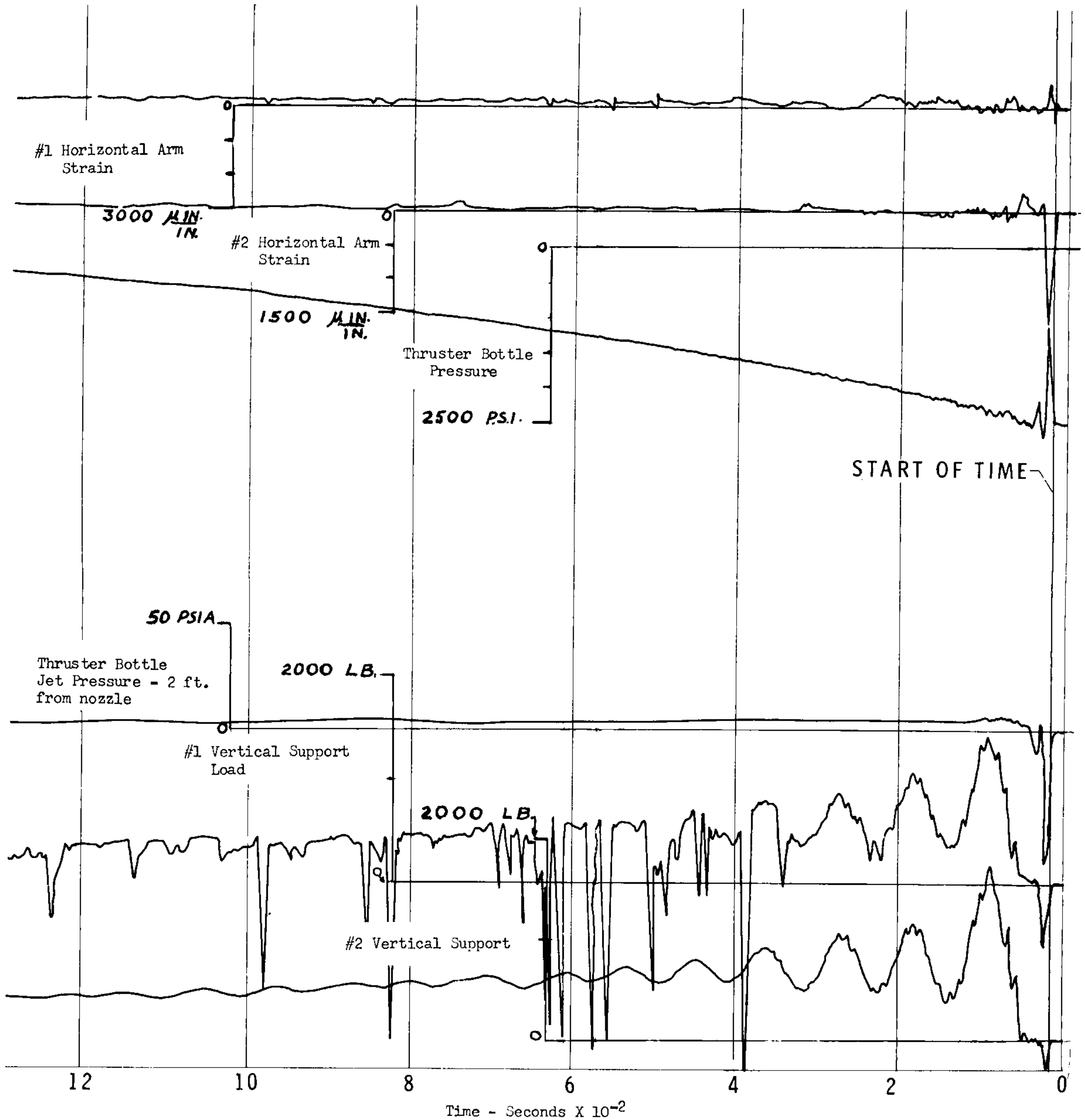

(c) AC-6 type nozzle, test 3.

Figure 27. - Concluded. Jettison bottle thrust test data.

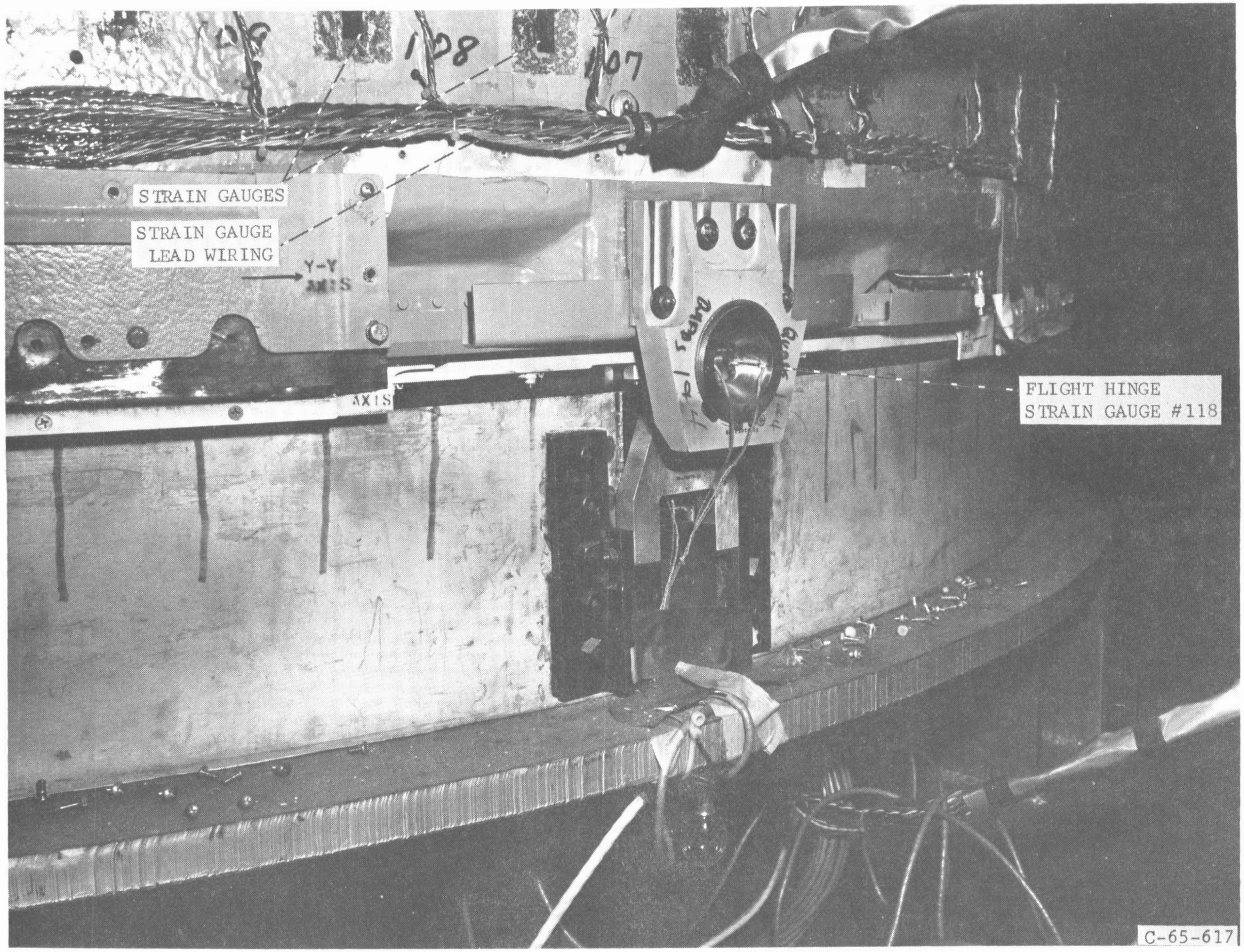

(a) Without metal protective sheet.

Figure 28. - Fairing strain gauge installation.

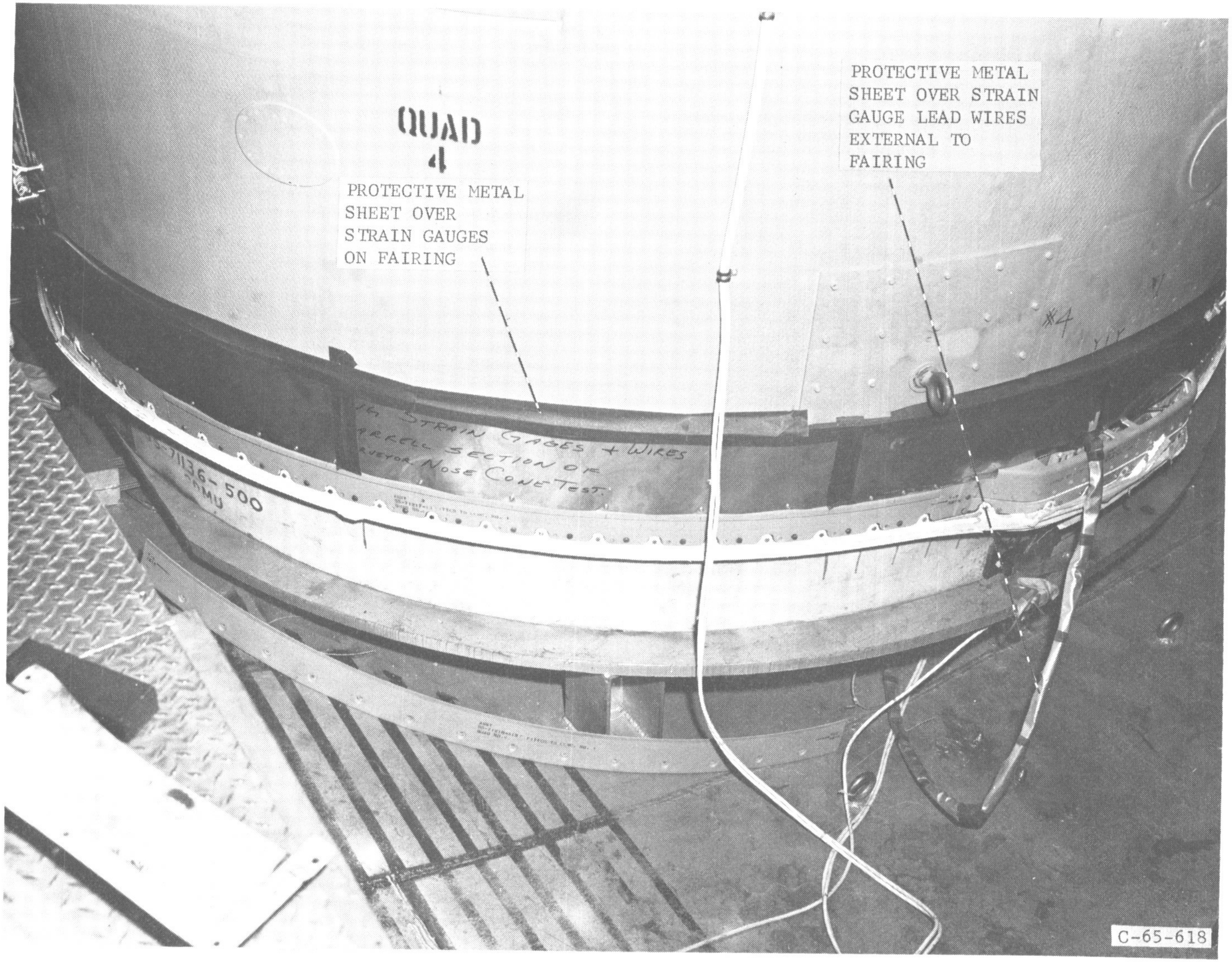

(b) After installation of protective metal sheet.

Figure 28. - Concluded. Fairing strain gauge installation.

E-3897

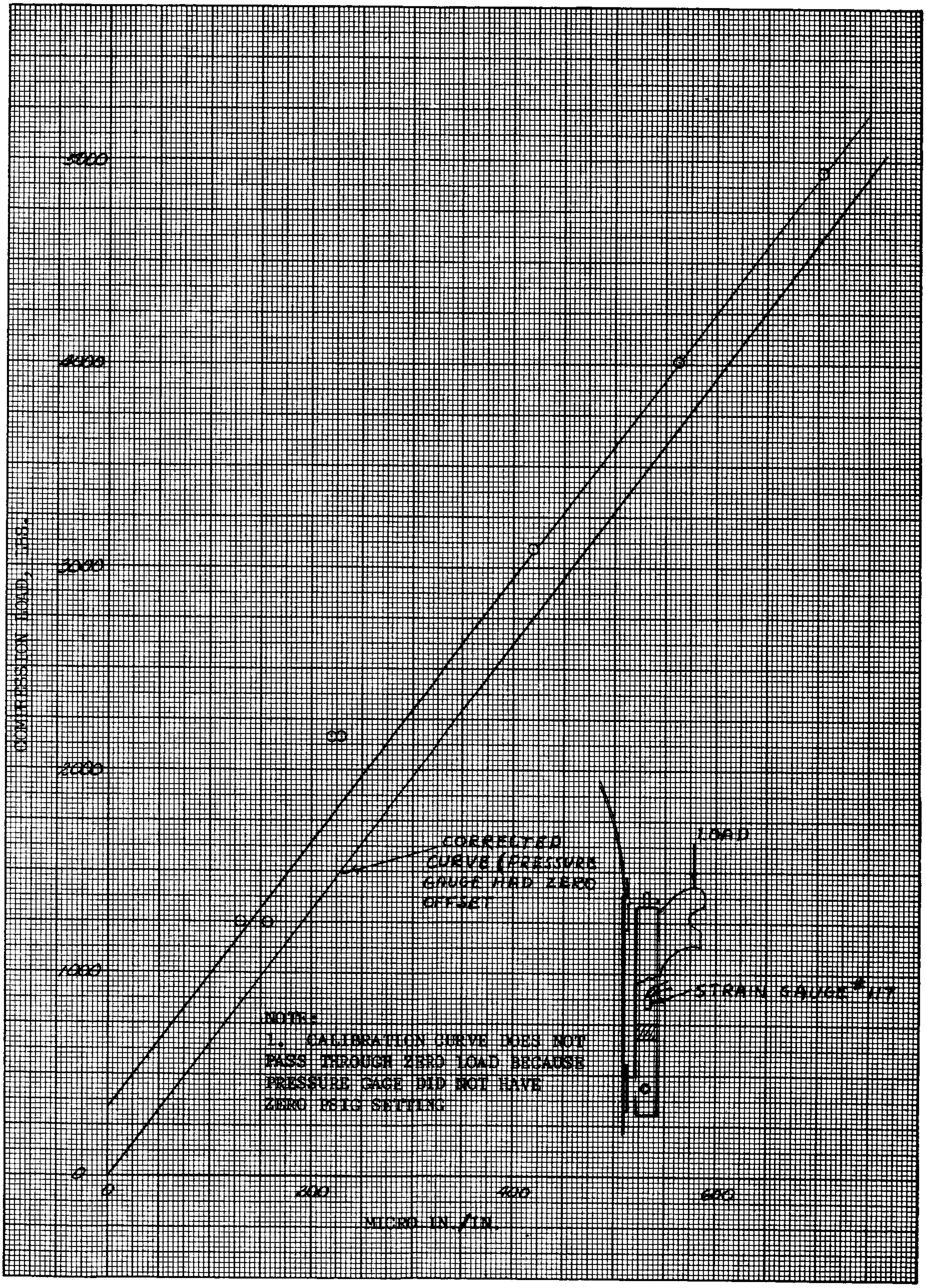

Figure 29. - Calibration of the tank half of the hinge by applying a vertical load.

E-3897

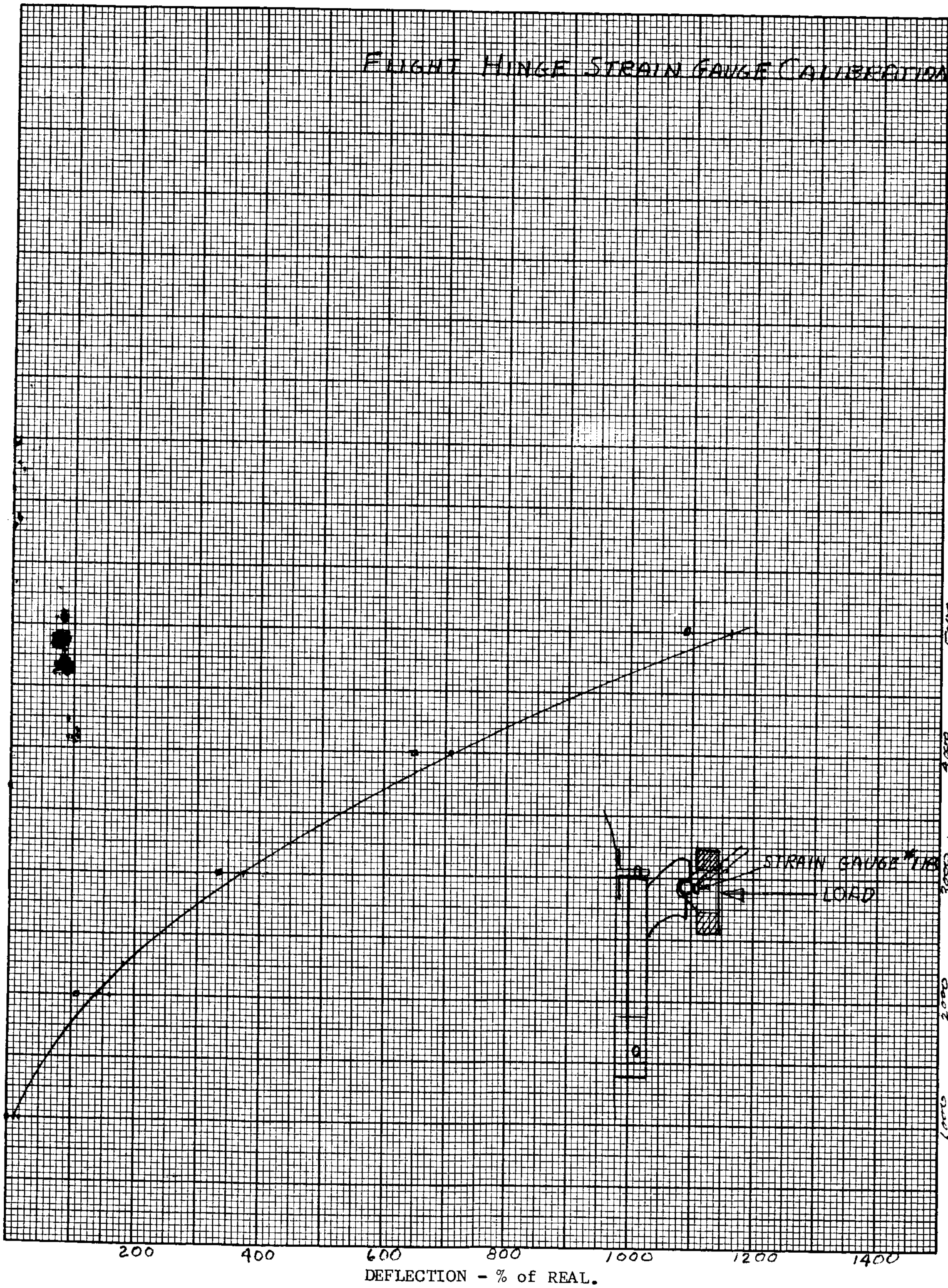

Figure 30. - Calibration of the fairing half of the hinge by applying radial load.

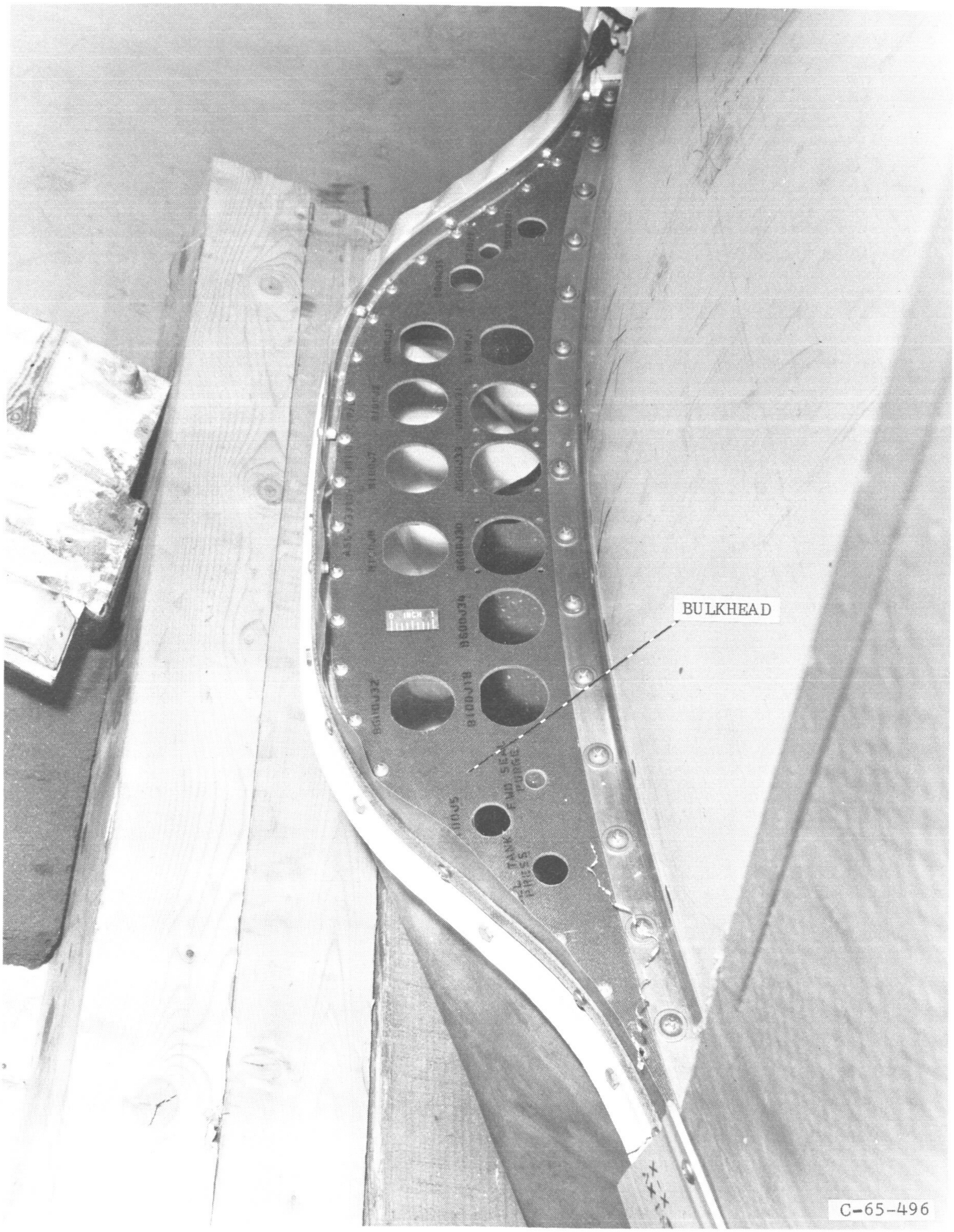

Figure 31. - Wiring tunnel bulkhead installation after the hand fit.

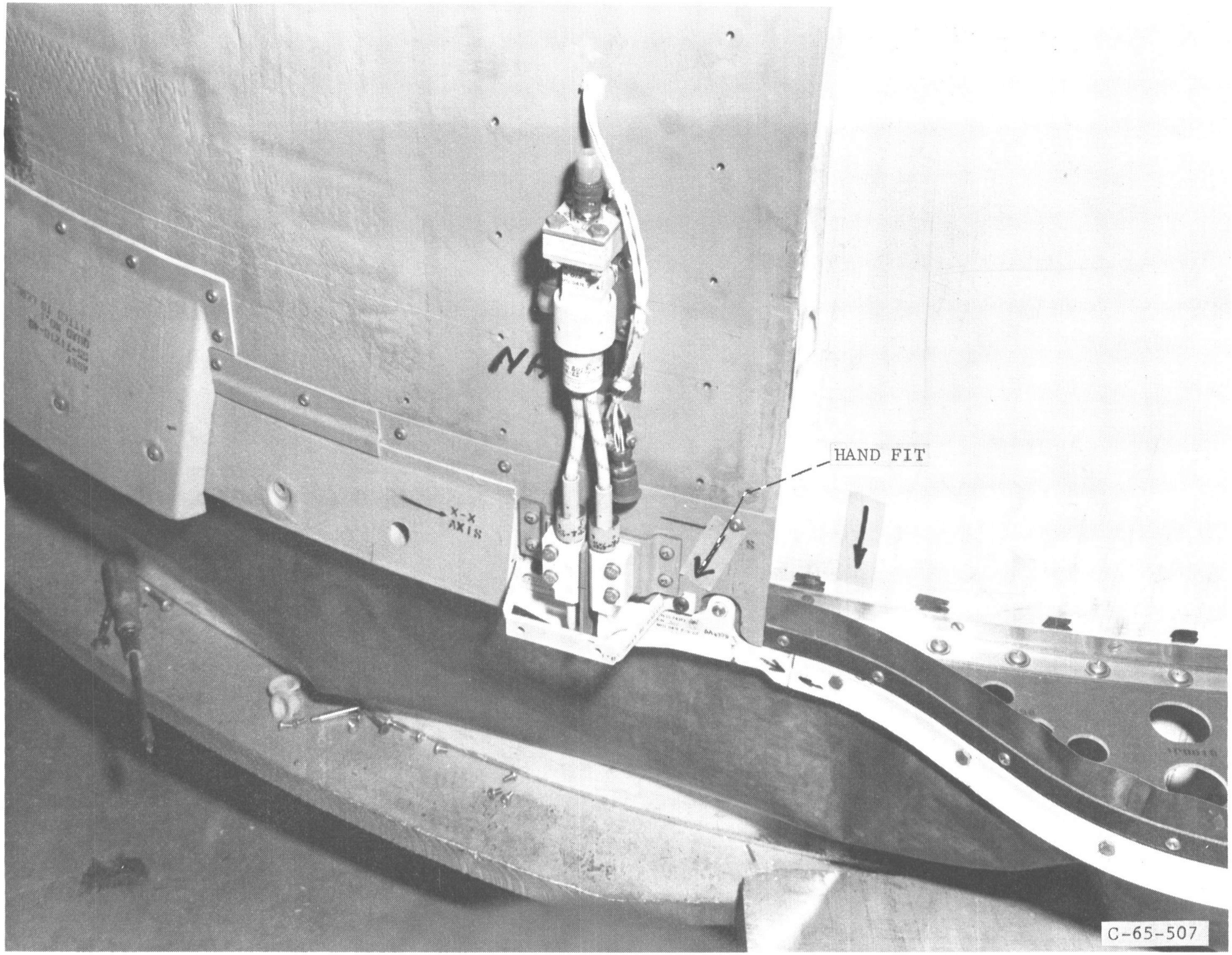

Figure 32. - Shaped charge detonator installation after the hand fit.

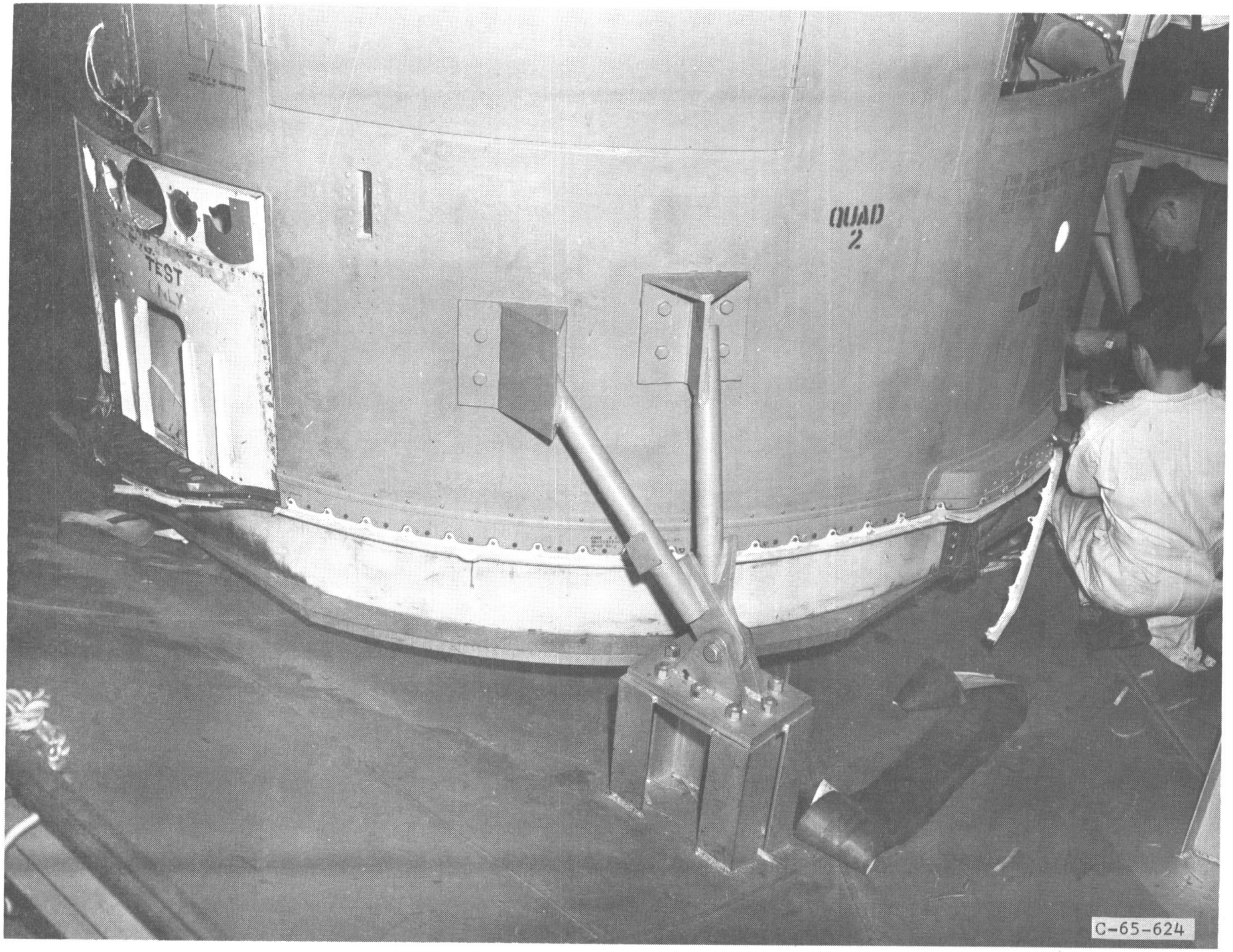

(a) After the removal of skirt.

Figure 33. - Shaped charge test damage, LA-1A.

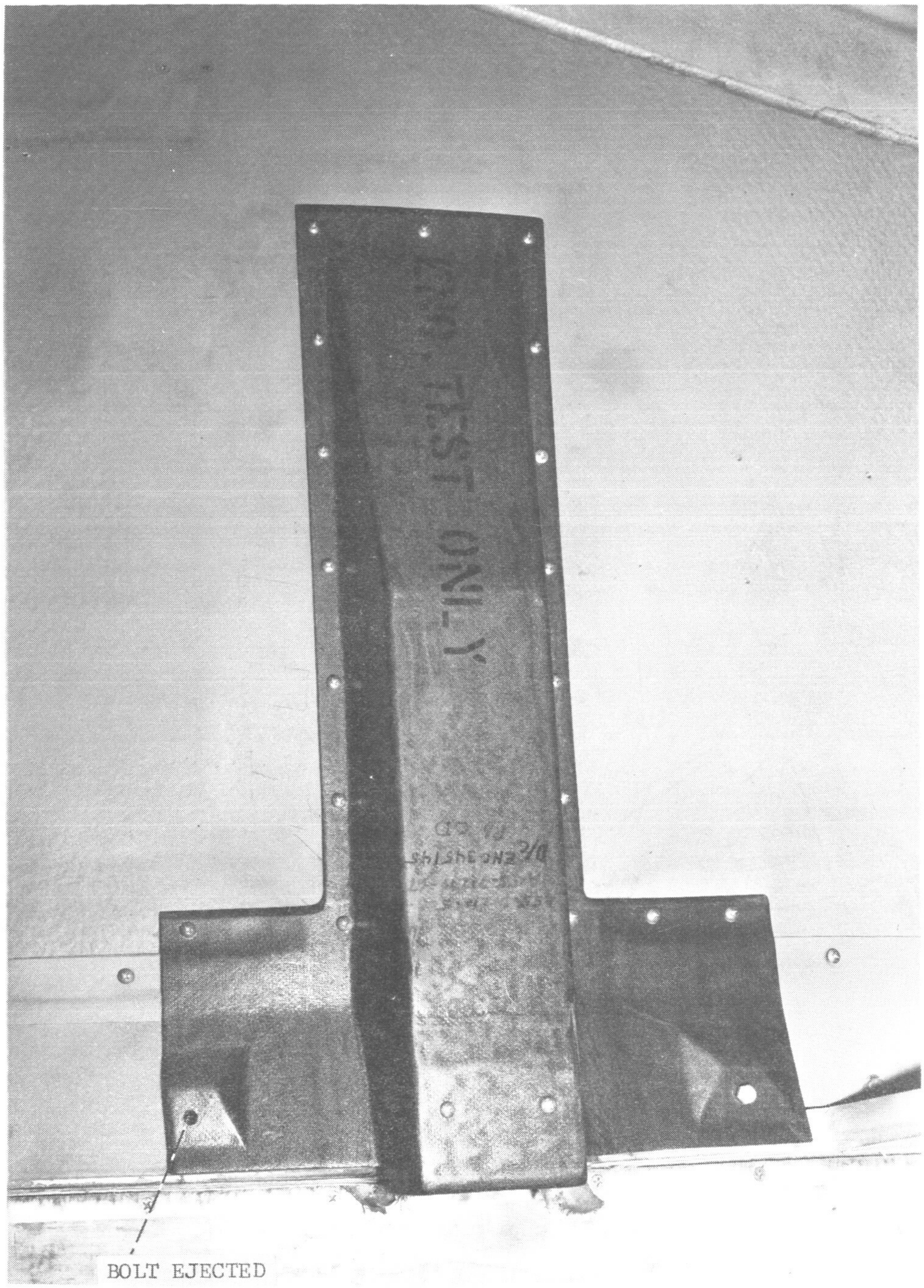

C-65-641

(b) Detonator fairing.

Figure 33. - Continued. Shaped charge test damage, LA-1A.

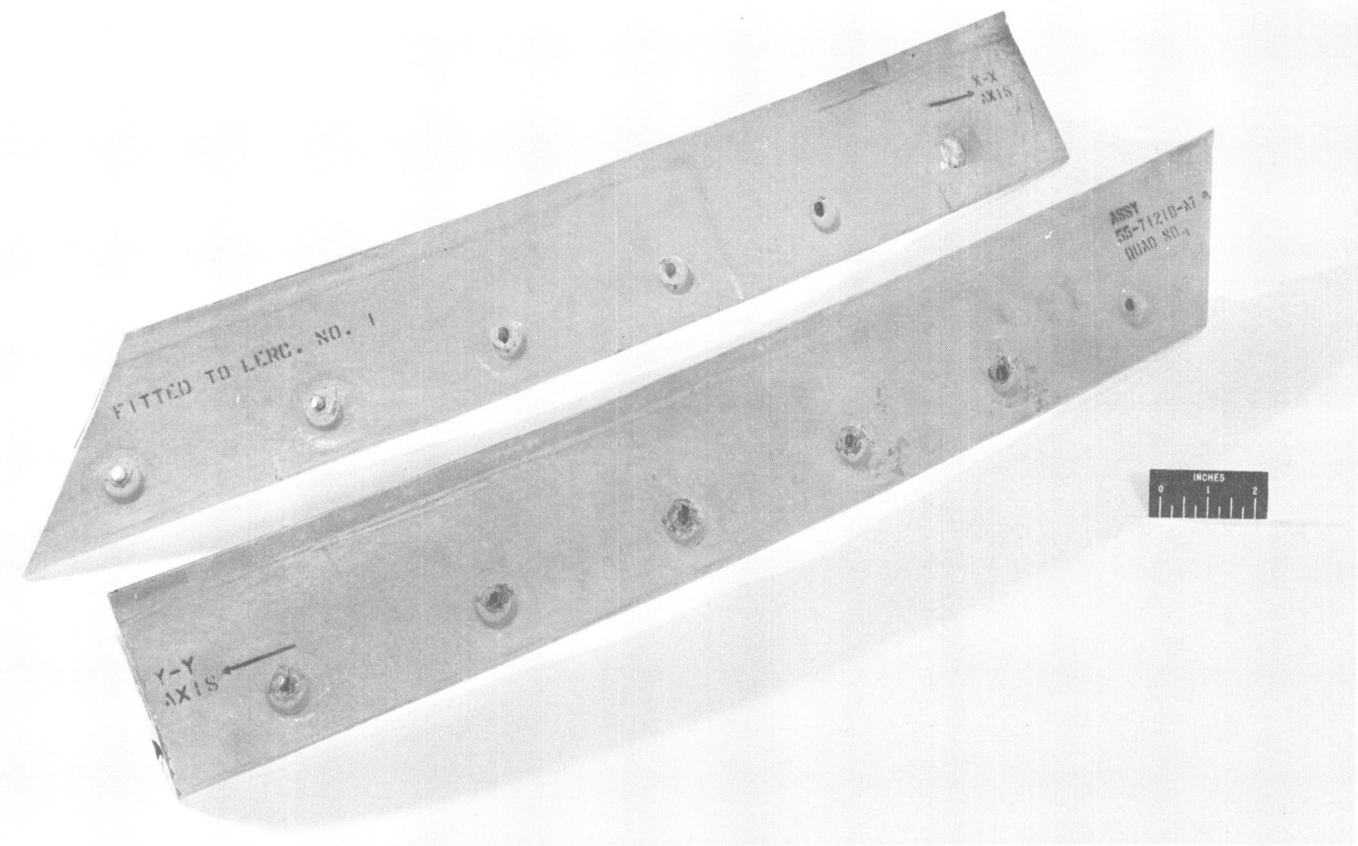

C-65-741

(c) Damaged inserts on the skirt.
Figure 33. - Continued. Shaped charge test damage, LA-1A.

E-3897

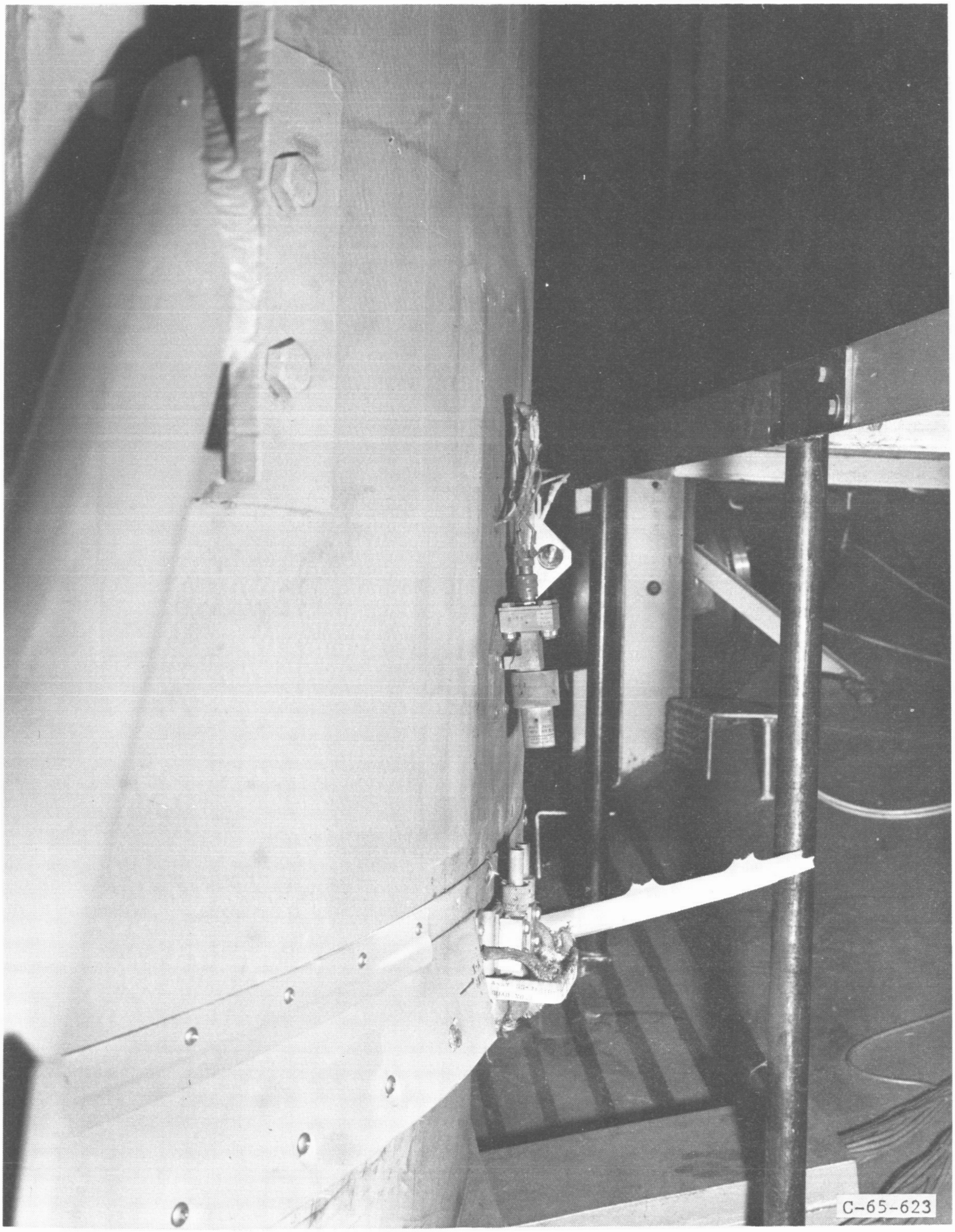

(d) Damage to the detonator mount.

Figure 33. - Continued. Shaped charge test damage, LA-1A.

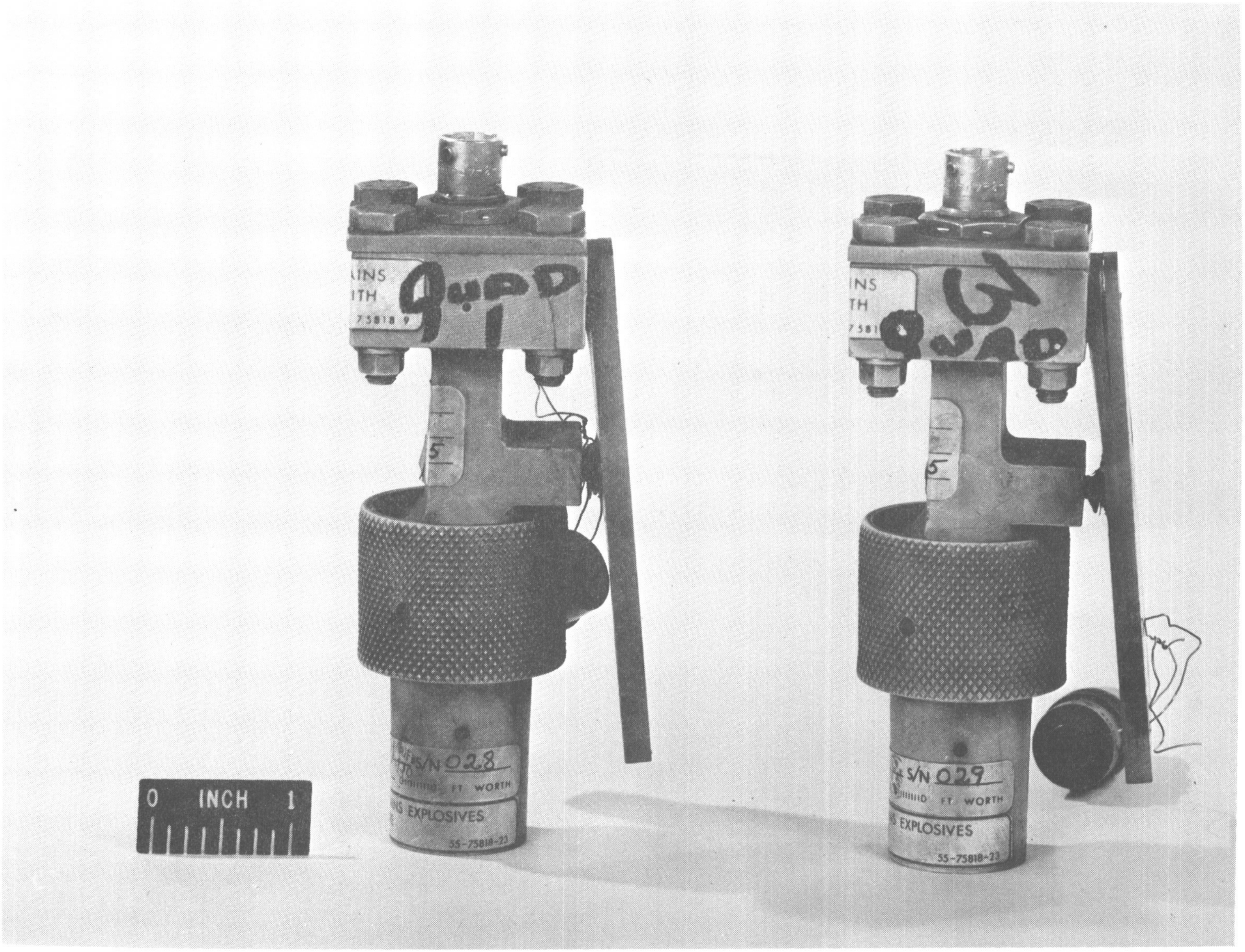

(e) Closeup of the damage to the detonator mount.

Figure 33. - Concluded. Shaped charge test damage, LA-1A.

E-3897

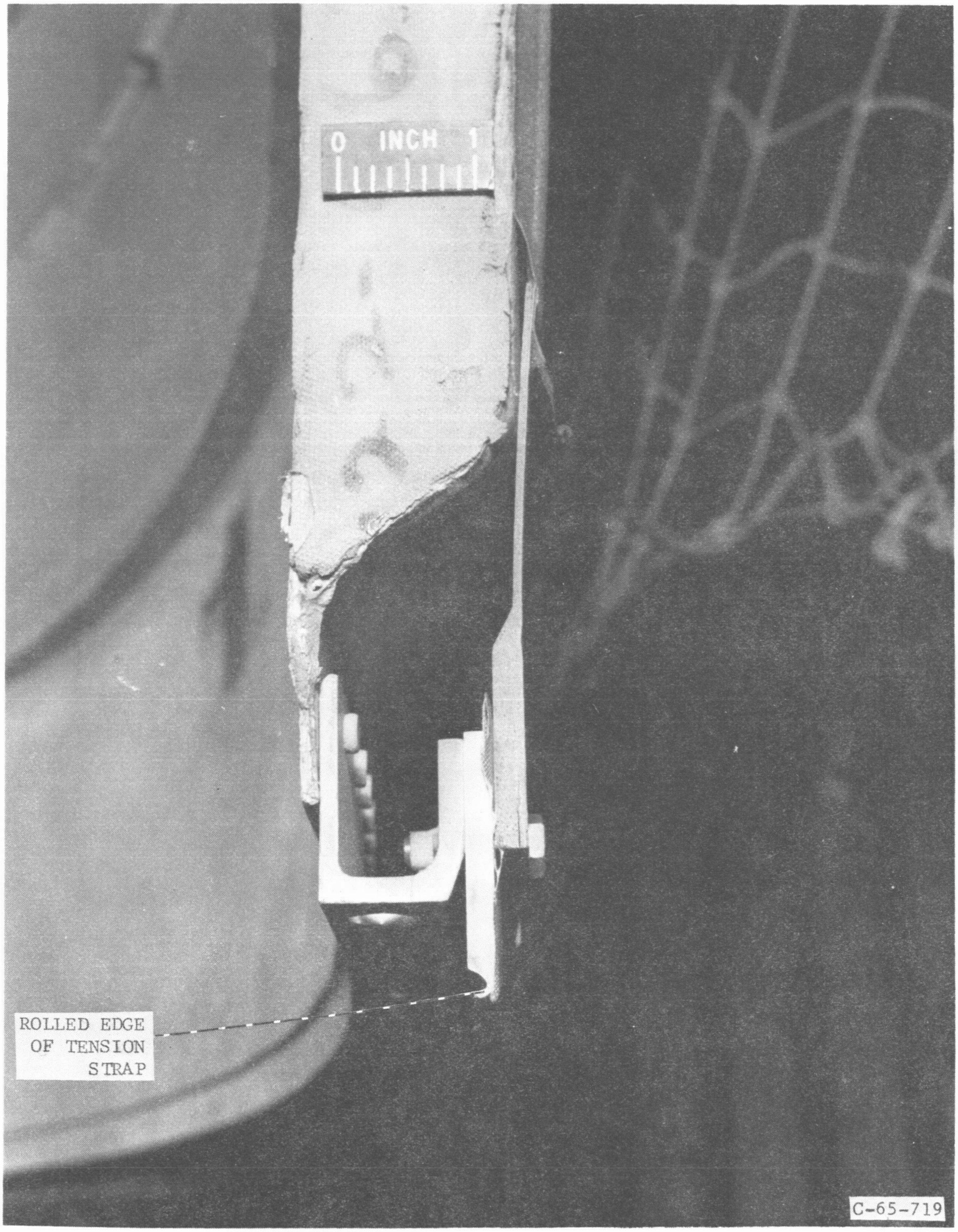

Figure 34. - Tension strap after being cut by the shaped charge, test LA-1A.

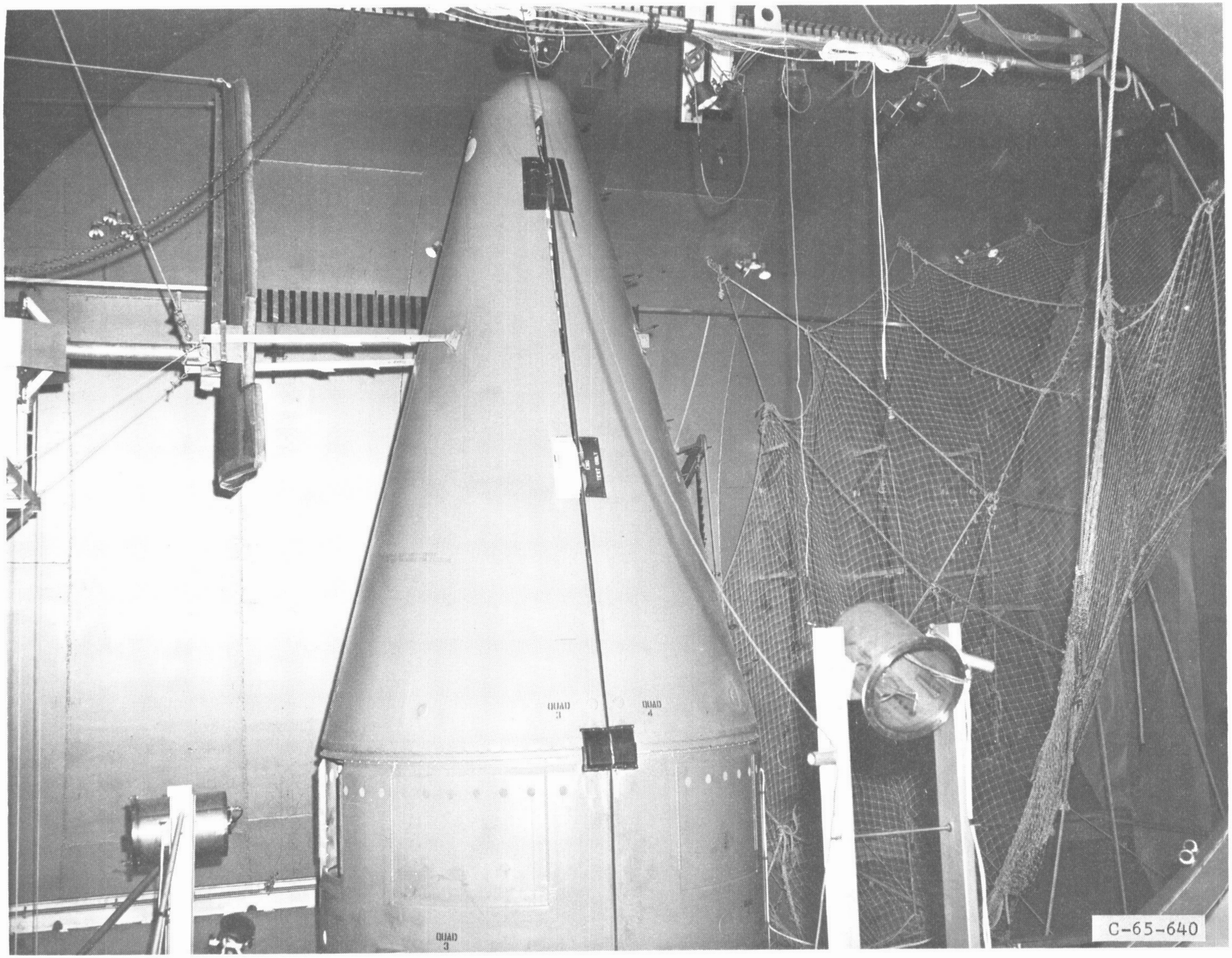

Figure 35. - Gap between fairing halves after the latch separation, test LA-1A.

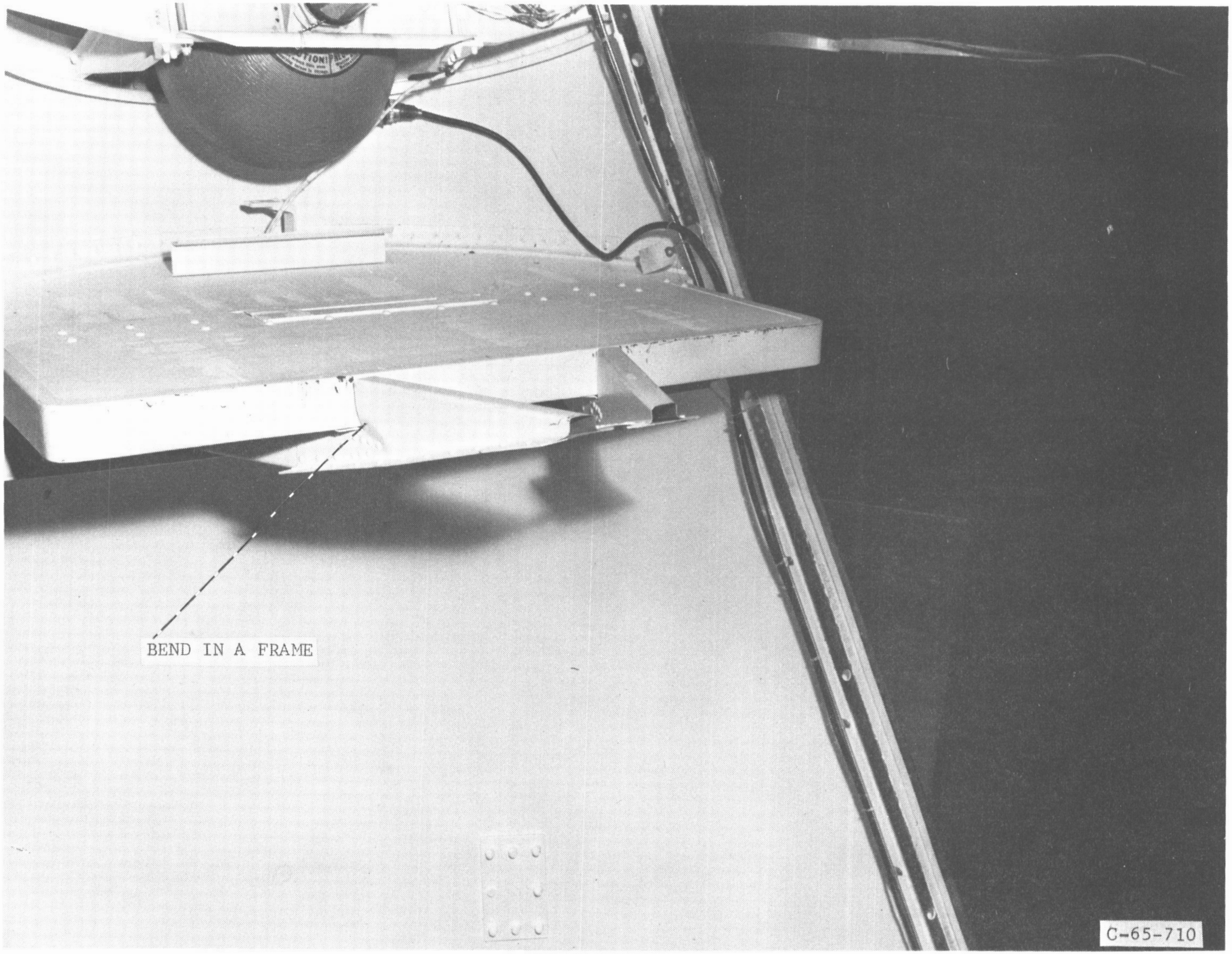

Figure 36. - Damage to the deflector bulkhead A frame, test LA-1B.

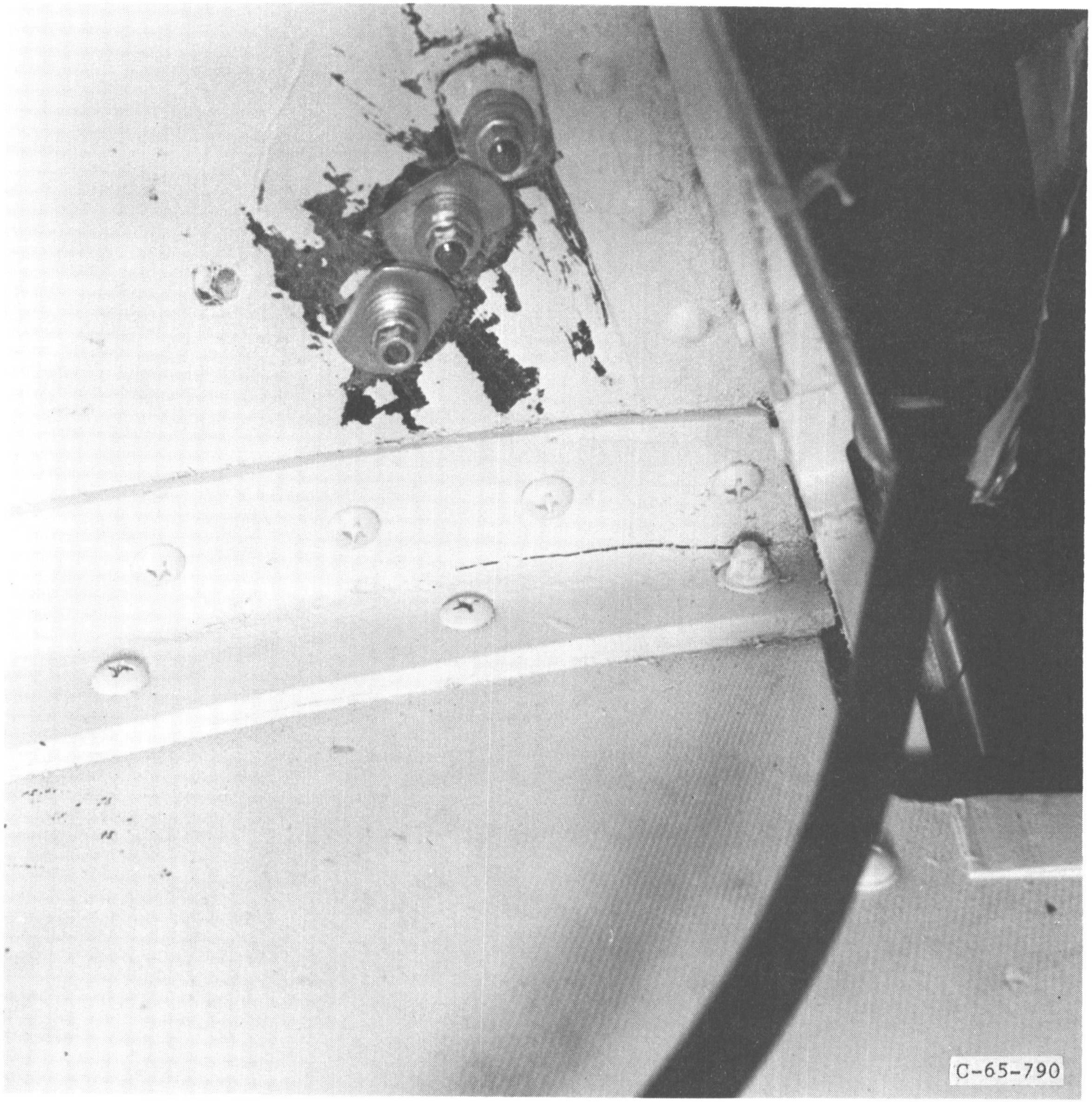

Figure 37. - Crack in the deflector bulkhead on supporting angle, test LA-1B.

E-3897

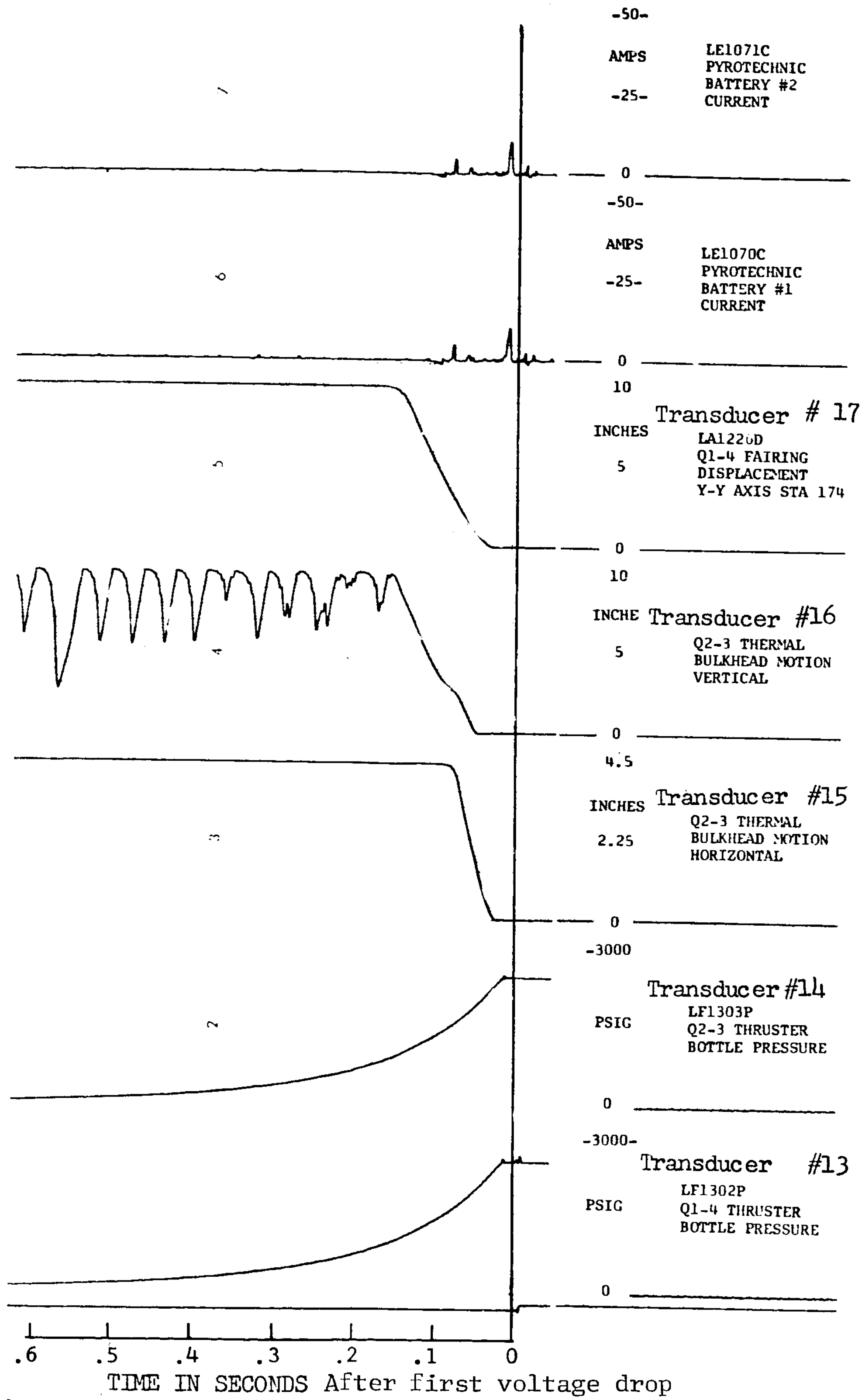

(a) Transducers 13, 14, 15, 16, 17, and battery currents.

Figure 38. - Data for test LA-1B.

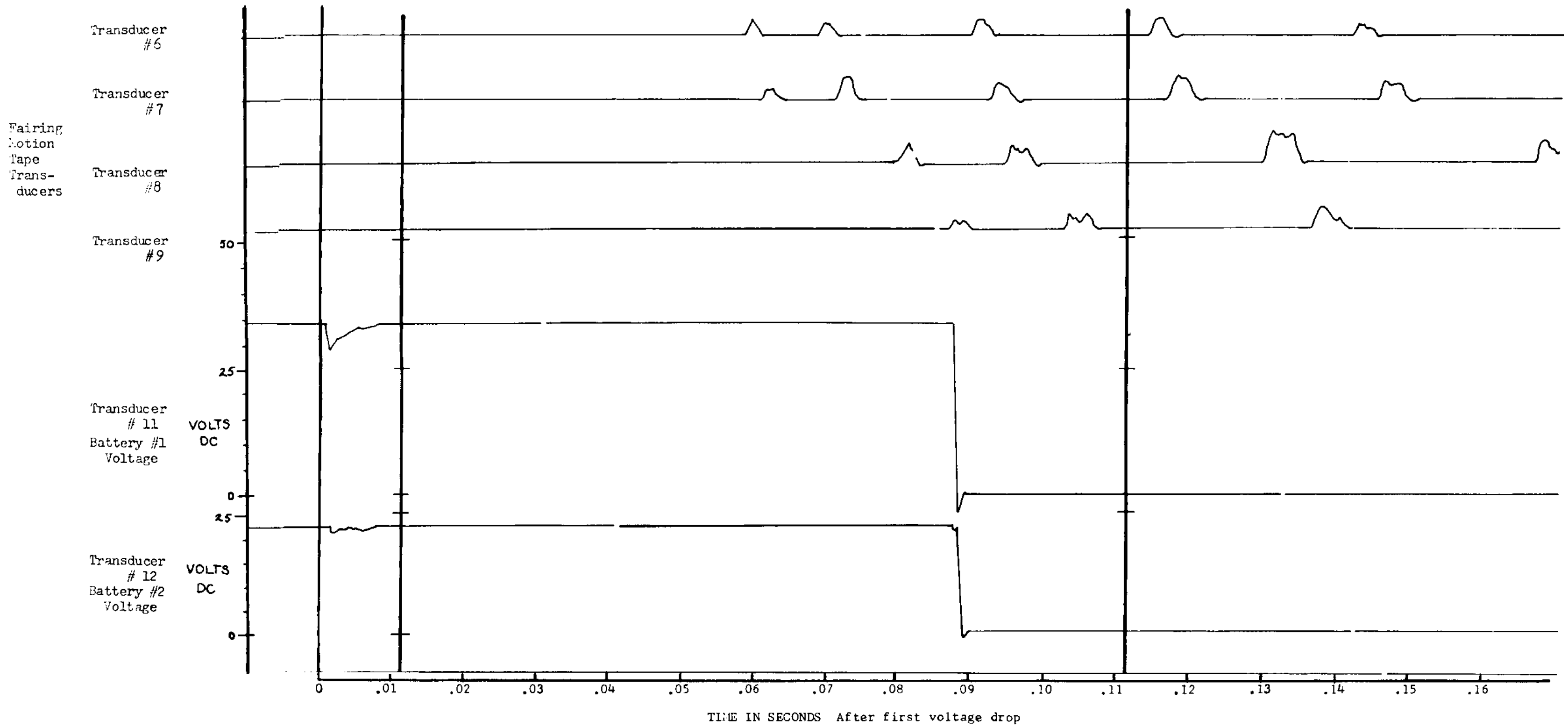

(b) Transducers 6, 7, 8, 9 and battery voltages

Figure 38. - Continued. Data for test LA-1B

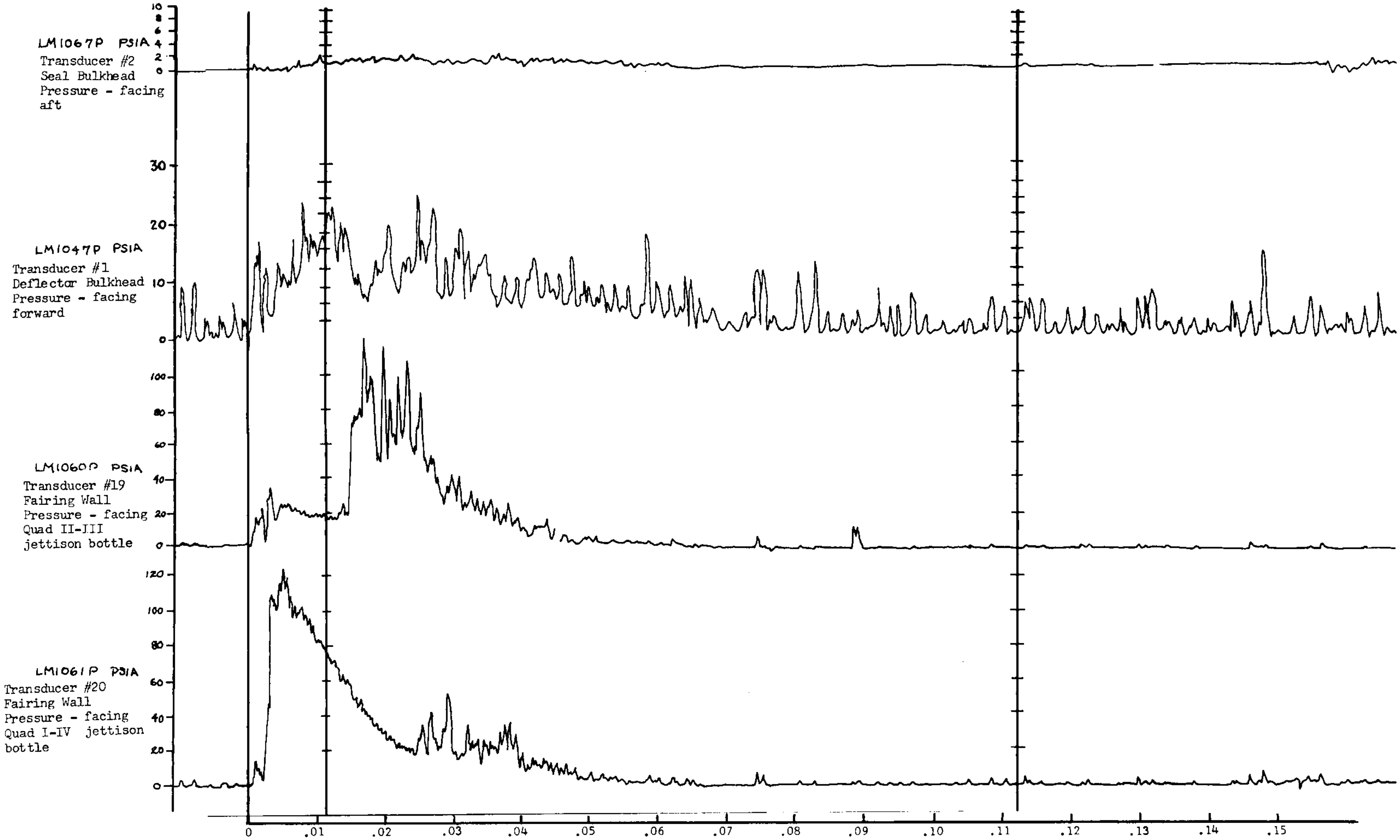

(c) Transducers 1, 2, 19 and 20.

Figure 38. - Continued. Data for test LA-1B.

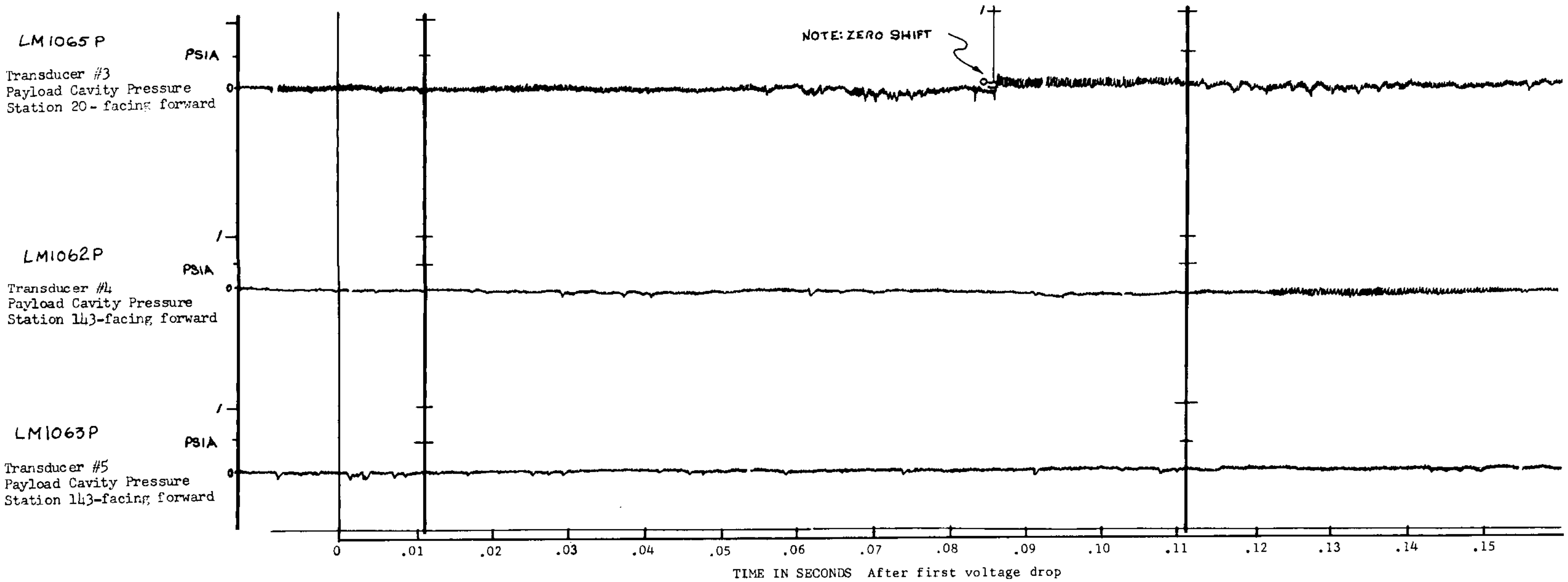

(d) Transducers 3, 4, and 5.

Figure 38. - Continued. Data for test LA-1B.

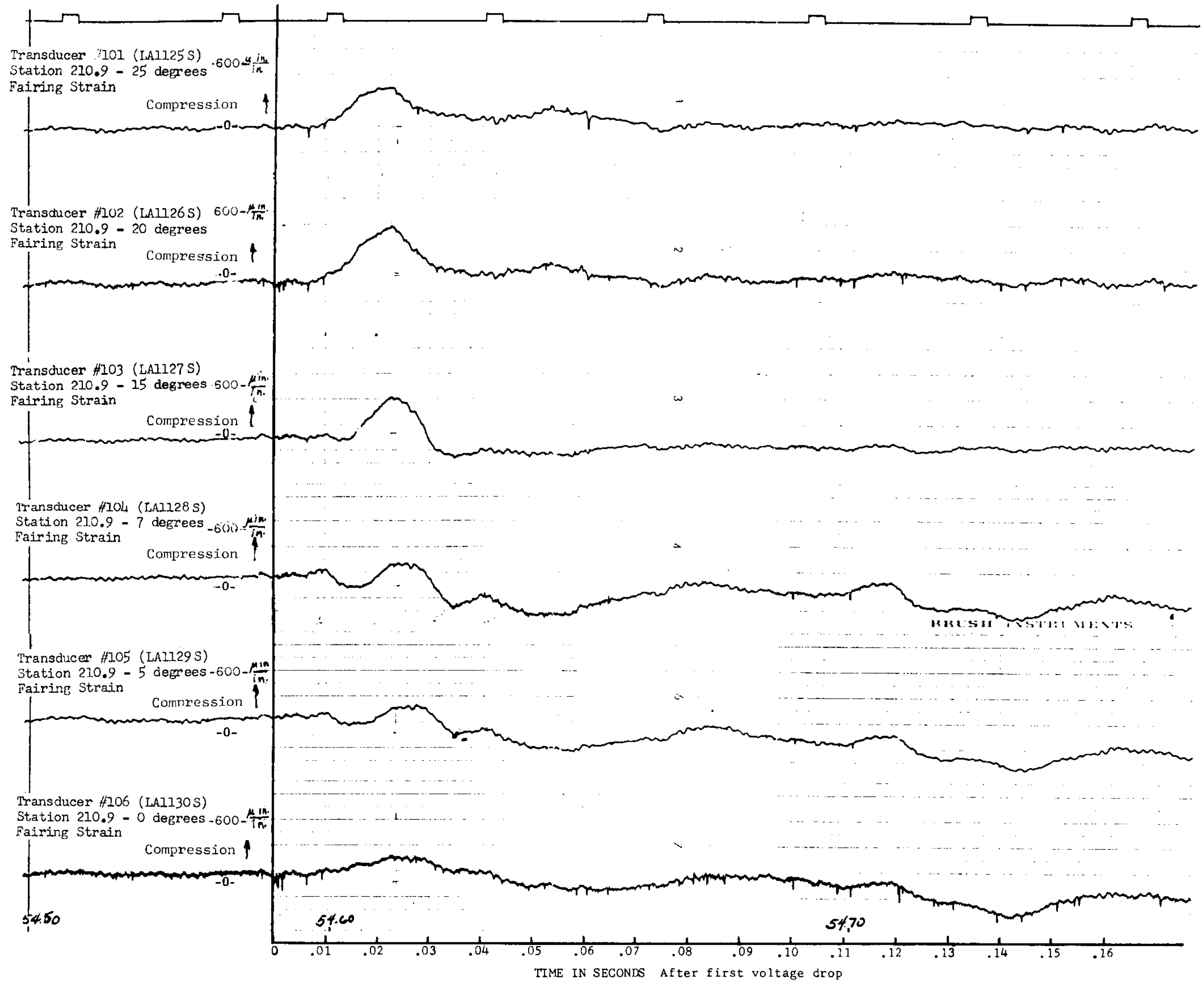

(e) Transducers 101, 102, 103, 104, 105 and 106.

Figure 38. - Continued. Data for test LA-1B.

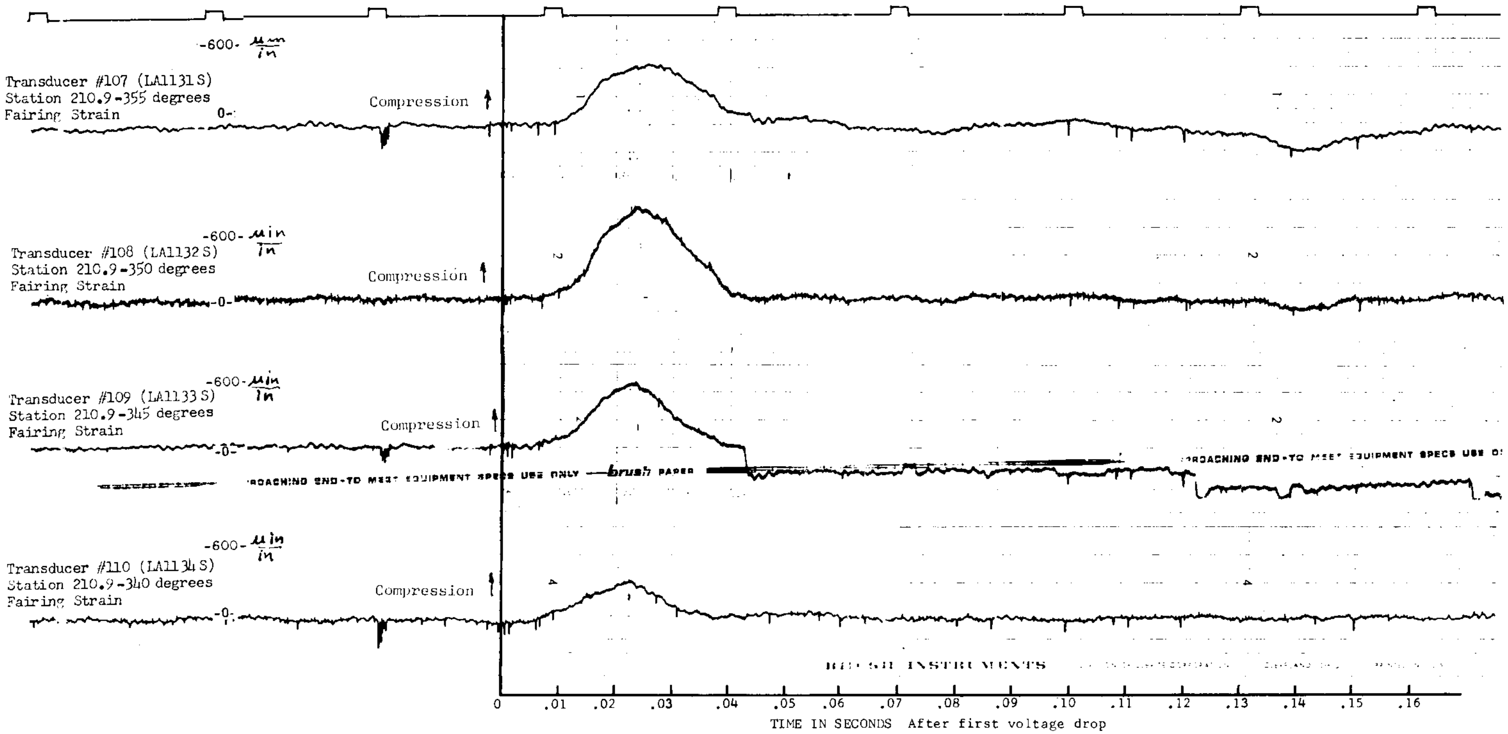

(f) Transducers 107, 108, 109 and 110.

Figure 38. Continued. Data for test LA-1B.

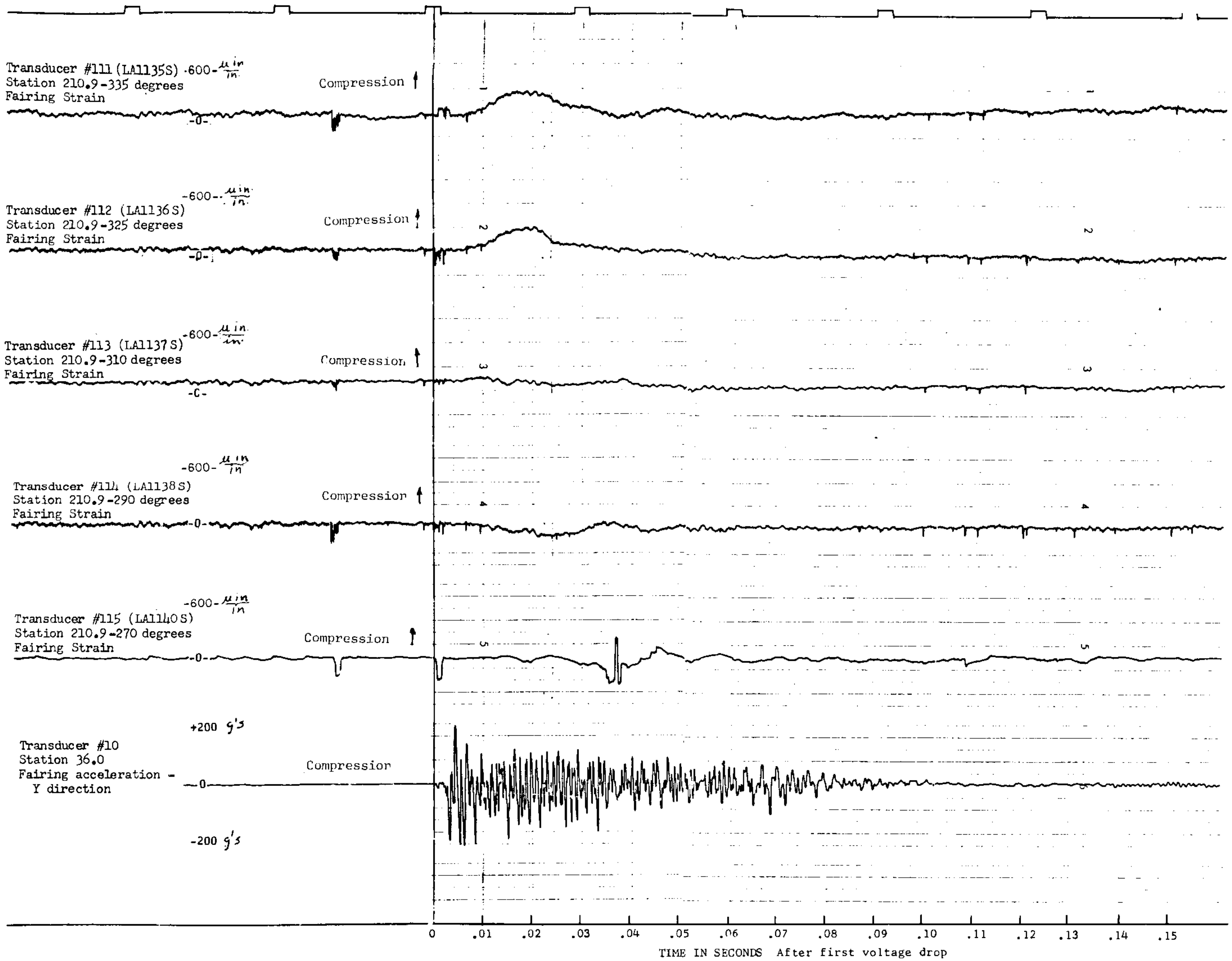

(g) Transducers 10, 111, 112, 113, 114, and 115.

Figure 38. Continued. Data for test LA-1B.

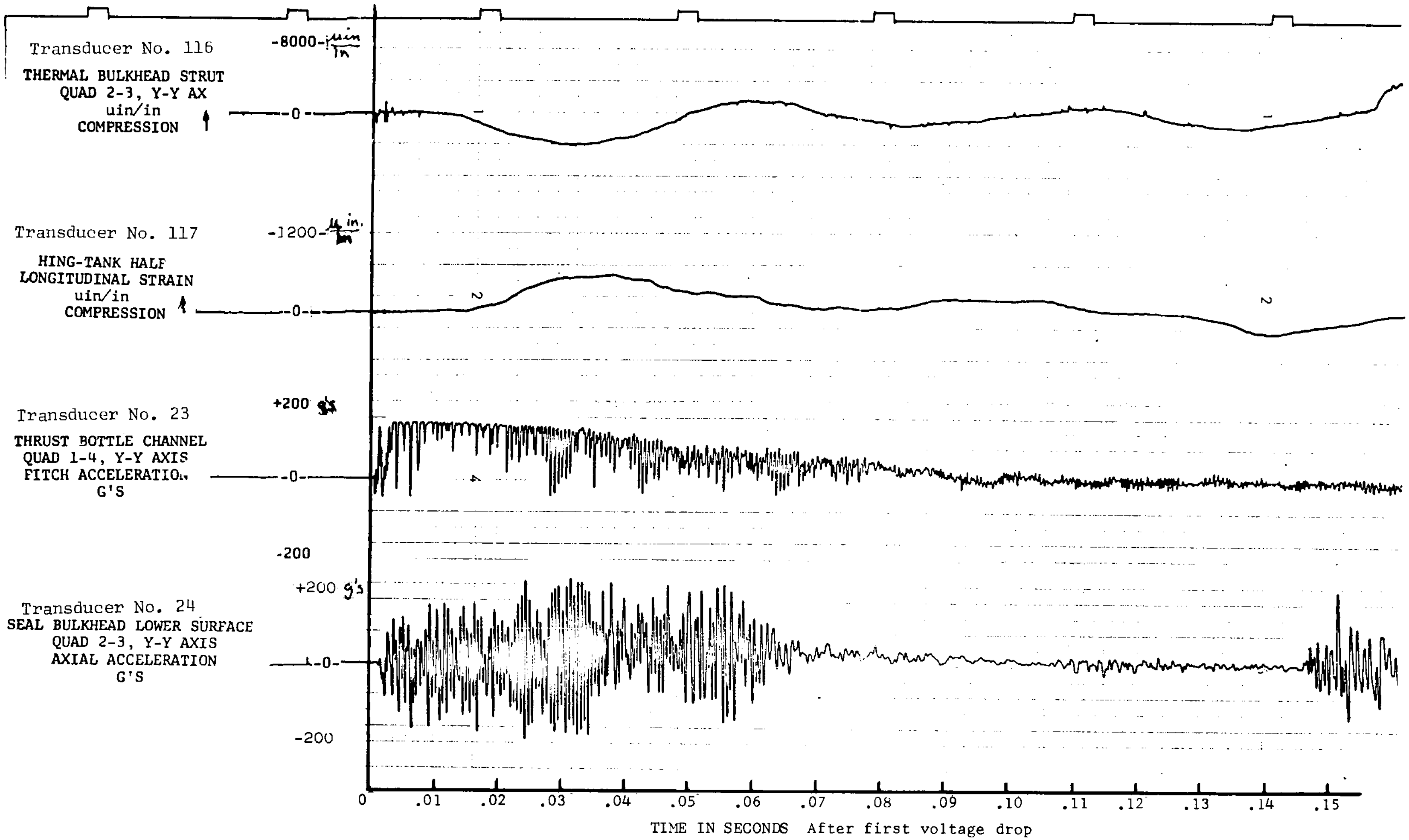

(h) Transducers 23, 24, 116 and 117.

Figure 38. Concluded. Data for test LA-1B.

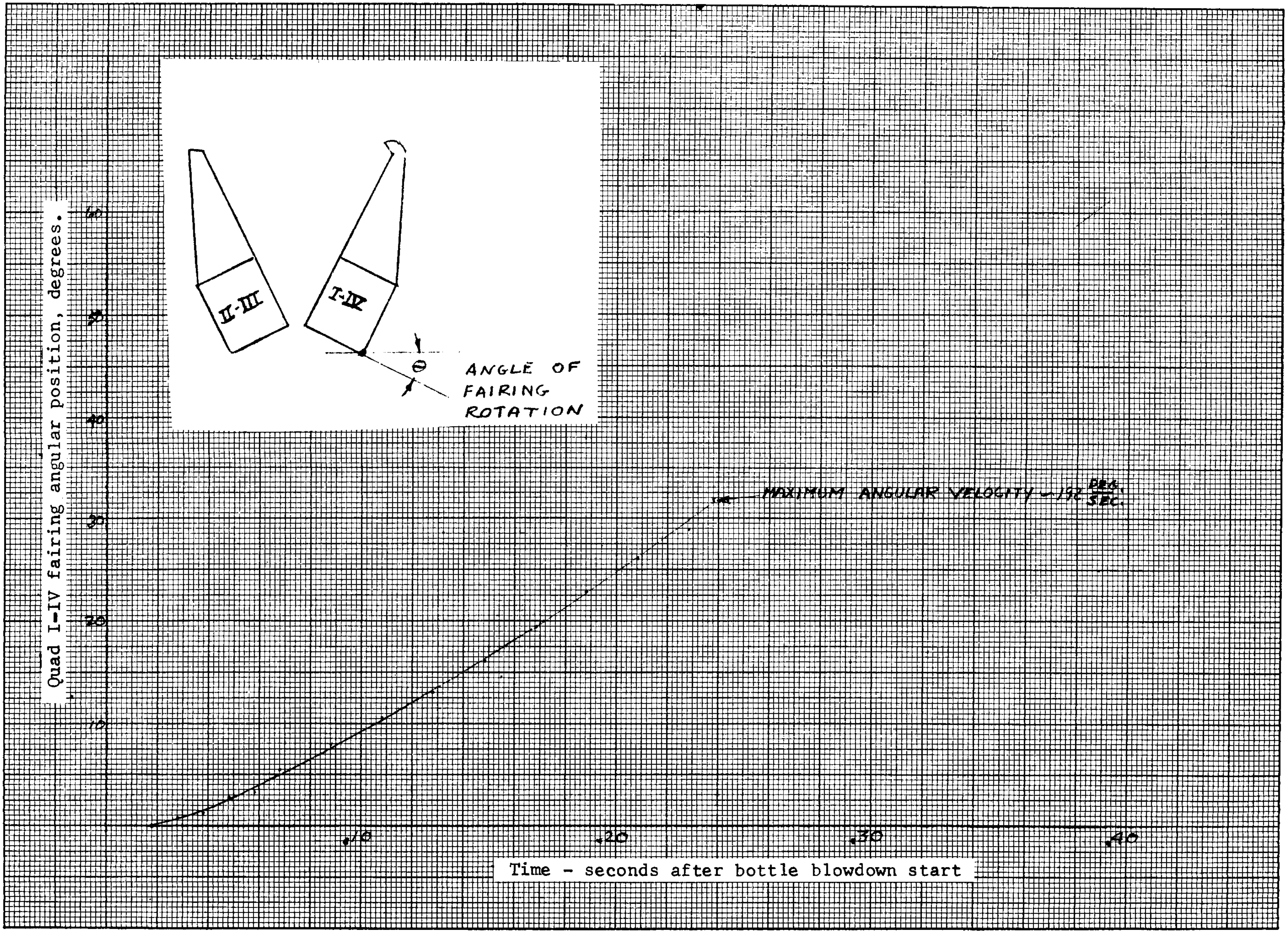

Figure 39. - Nose fairing angular position vs. time test LA-1B (measurement at the I-IV hinge point).

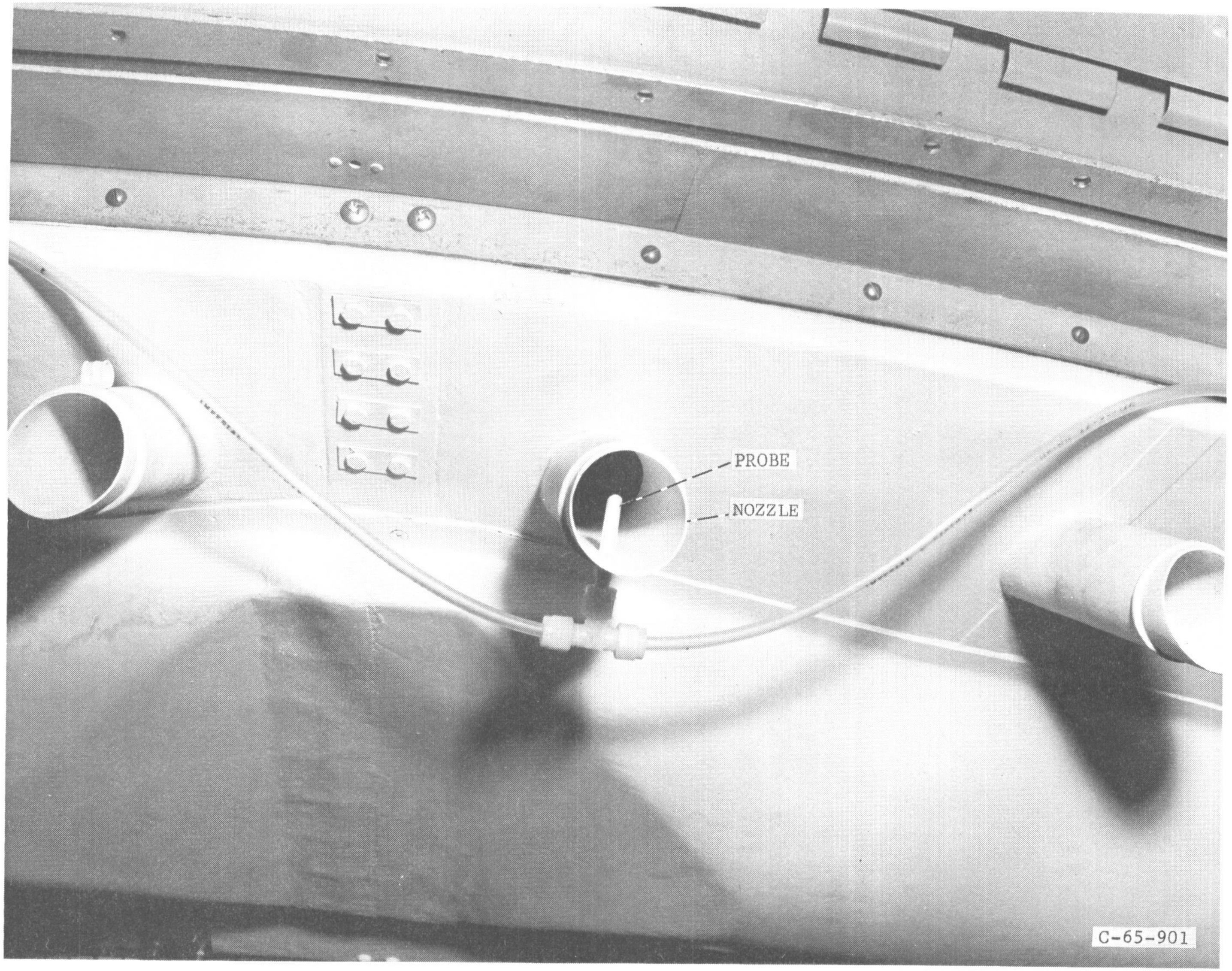

Figure 40. - Hazard detection probe installed in the air-conditioning nozzle.

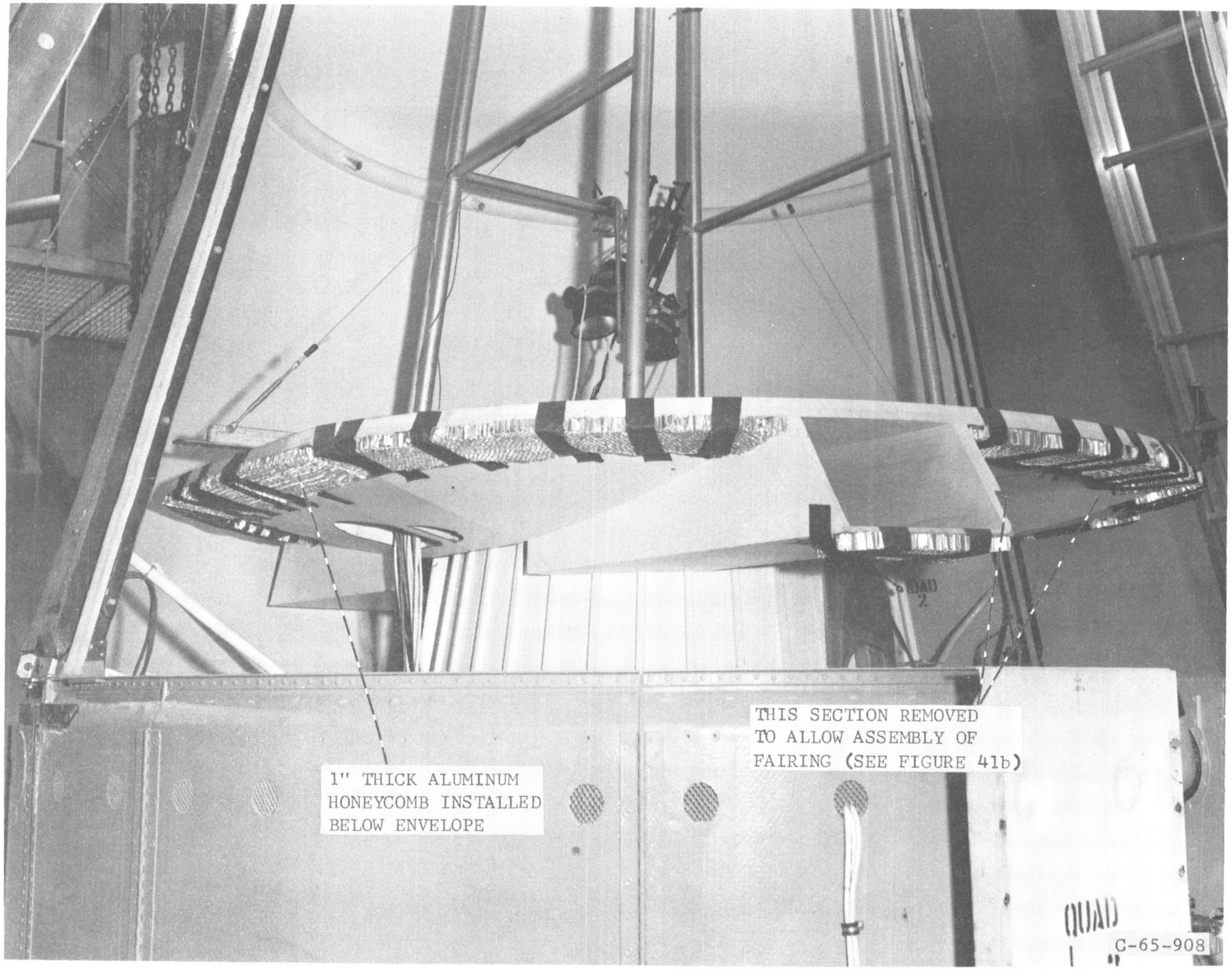

(a) Viewed radially inward from Quad IV.
Figure 41. - Installation of wood model Surveyor envelope.

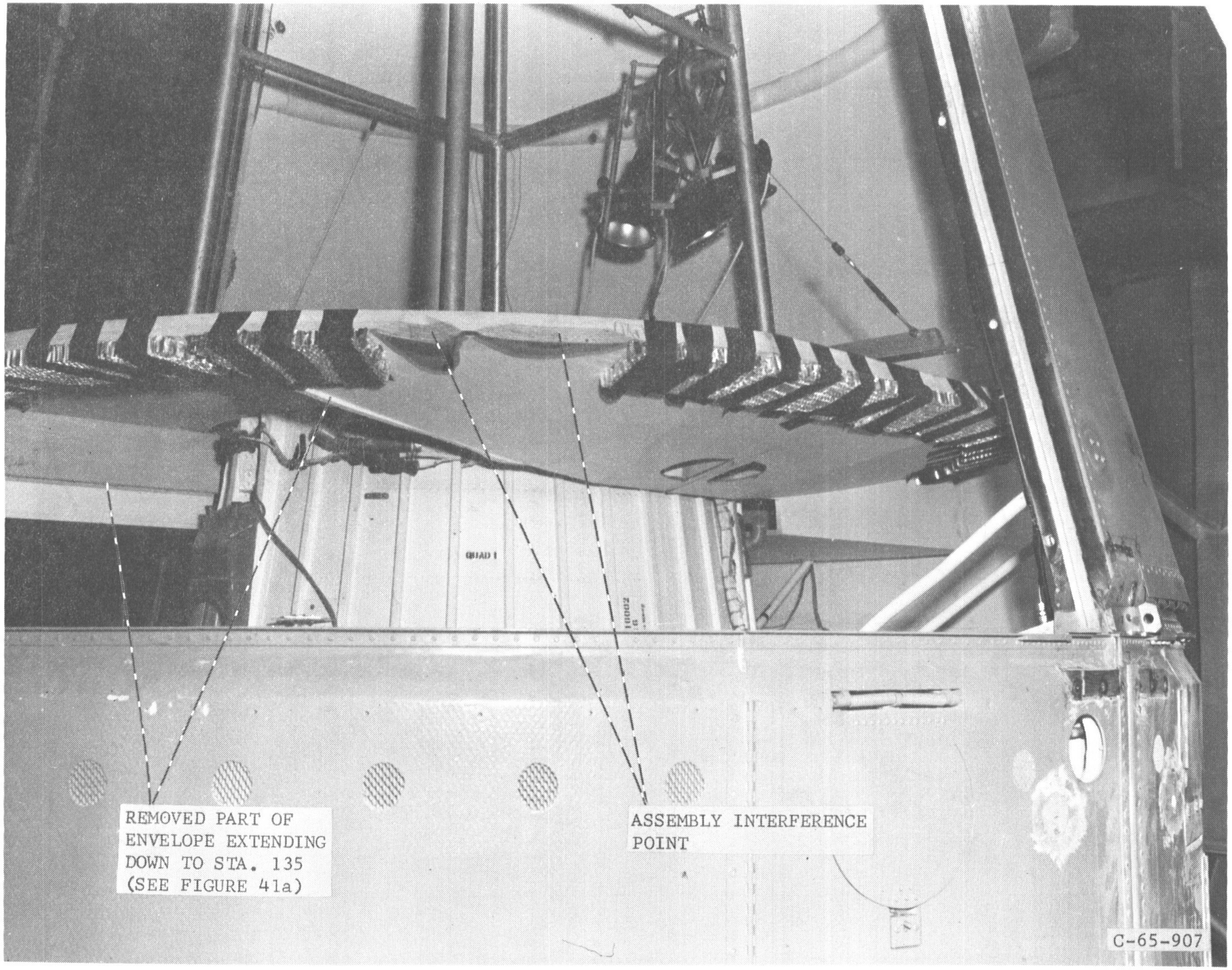

(b) Viewed radially inward from Quad I.

Figure 41. - Concluded. Installation of wood model Surveyor envelope.

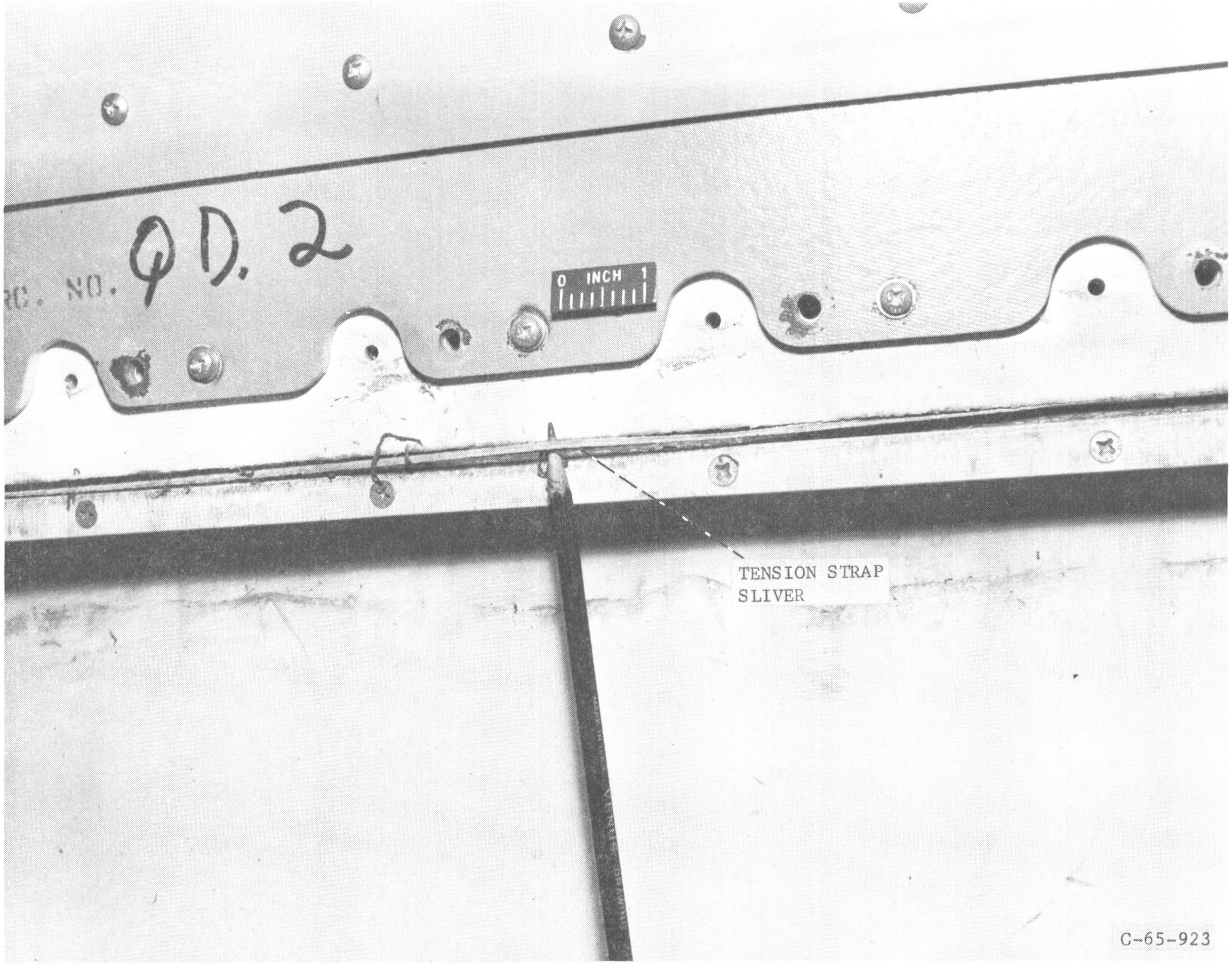

Figure 42. - Sliver of metal formed by the cut made on the tension tie by the firing of the shaped charge, test LA2-A.

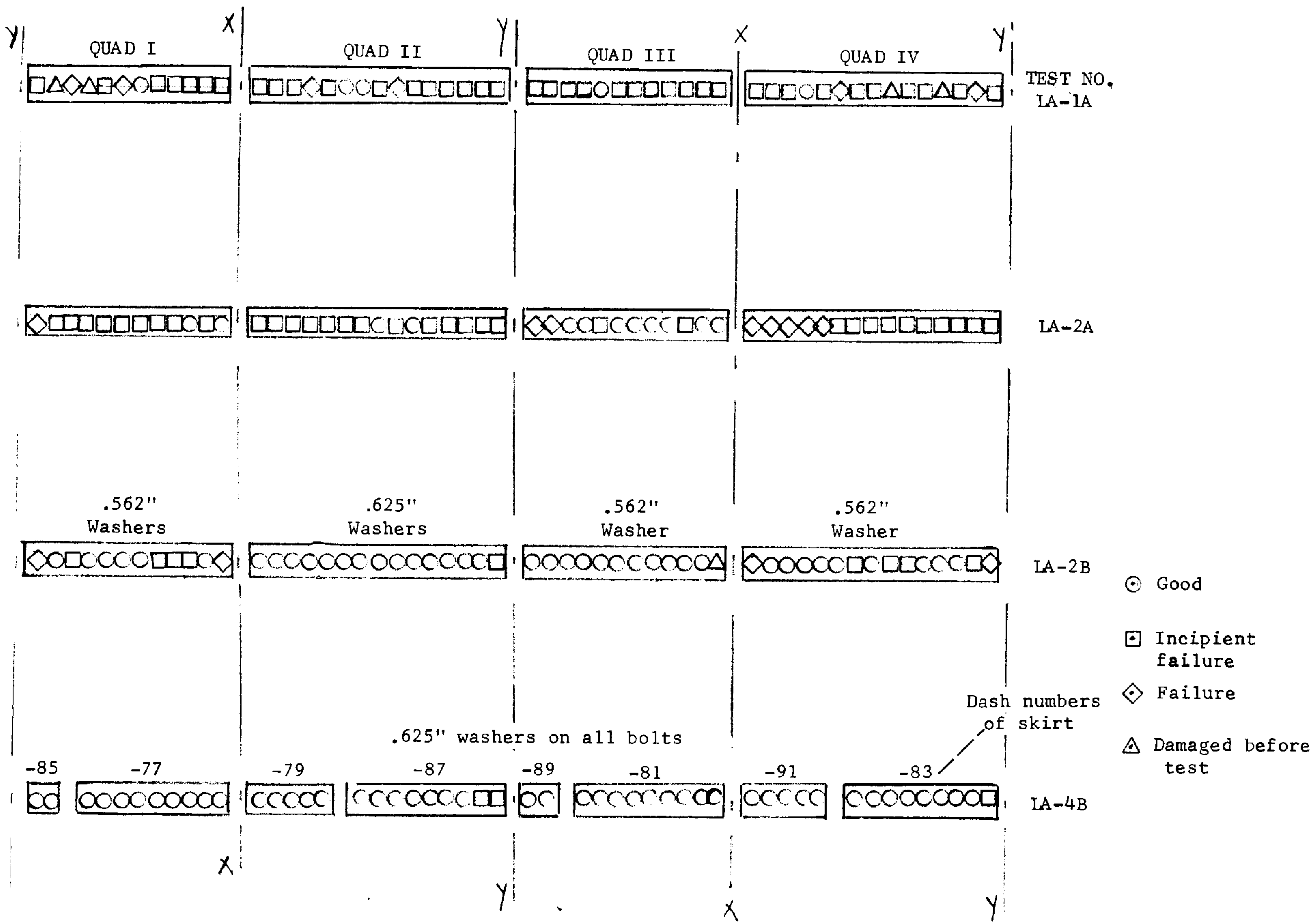

Figure 43. - Location and types of bolt bearing failures on the shaped charge skirt for all the shaped charge tests.

E-3897

Figure 44. - Detonator shown separated from the mounting pad as a result of test LA-2A.

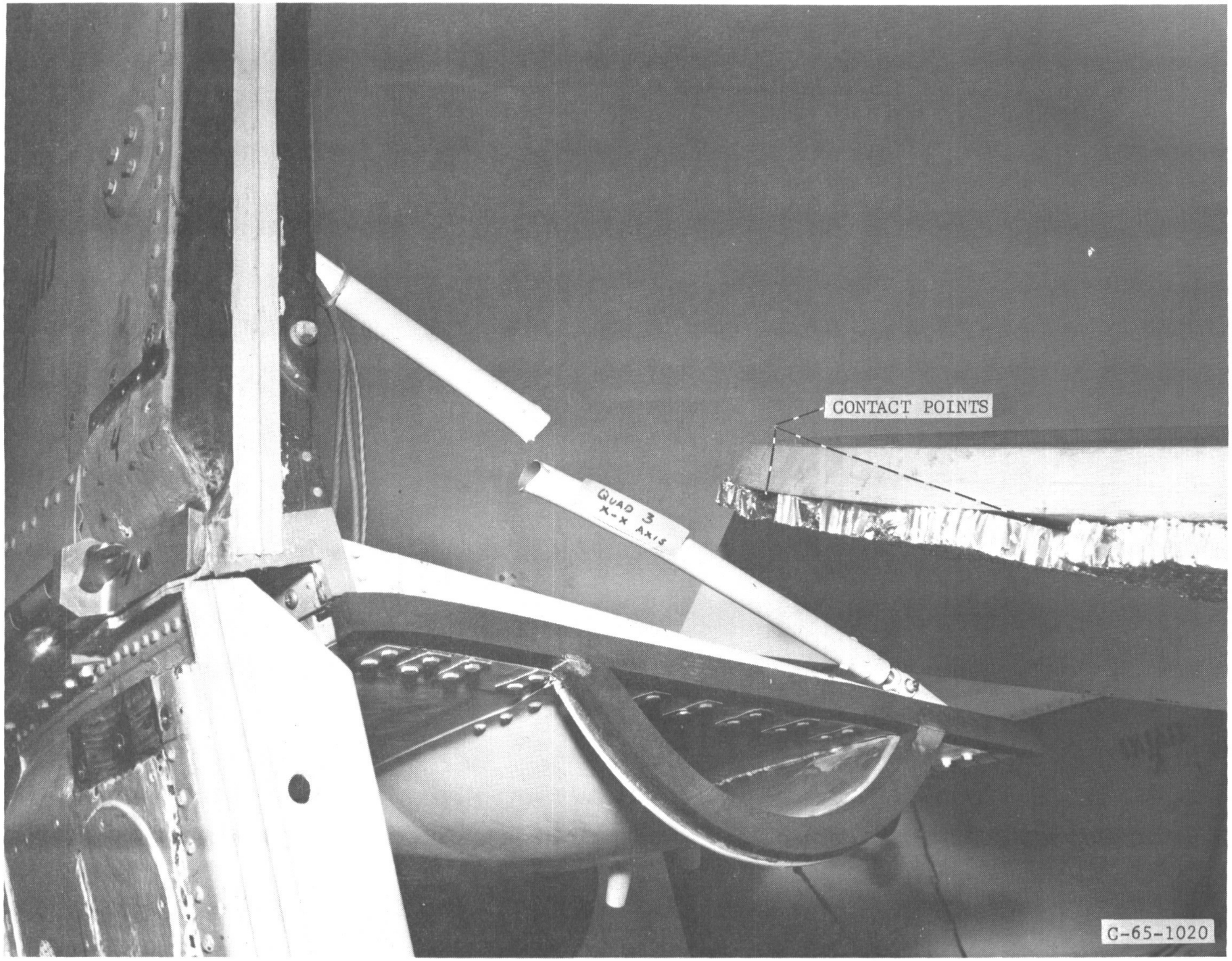

Figure 45. - Broken thermal bulkhead strut, test LA-2D.

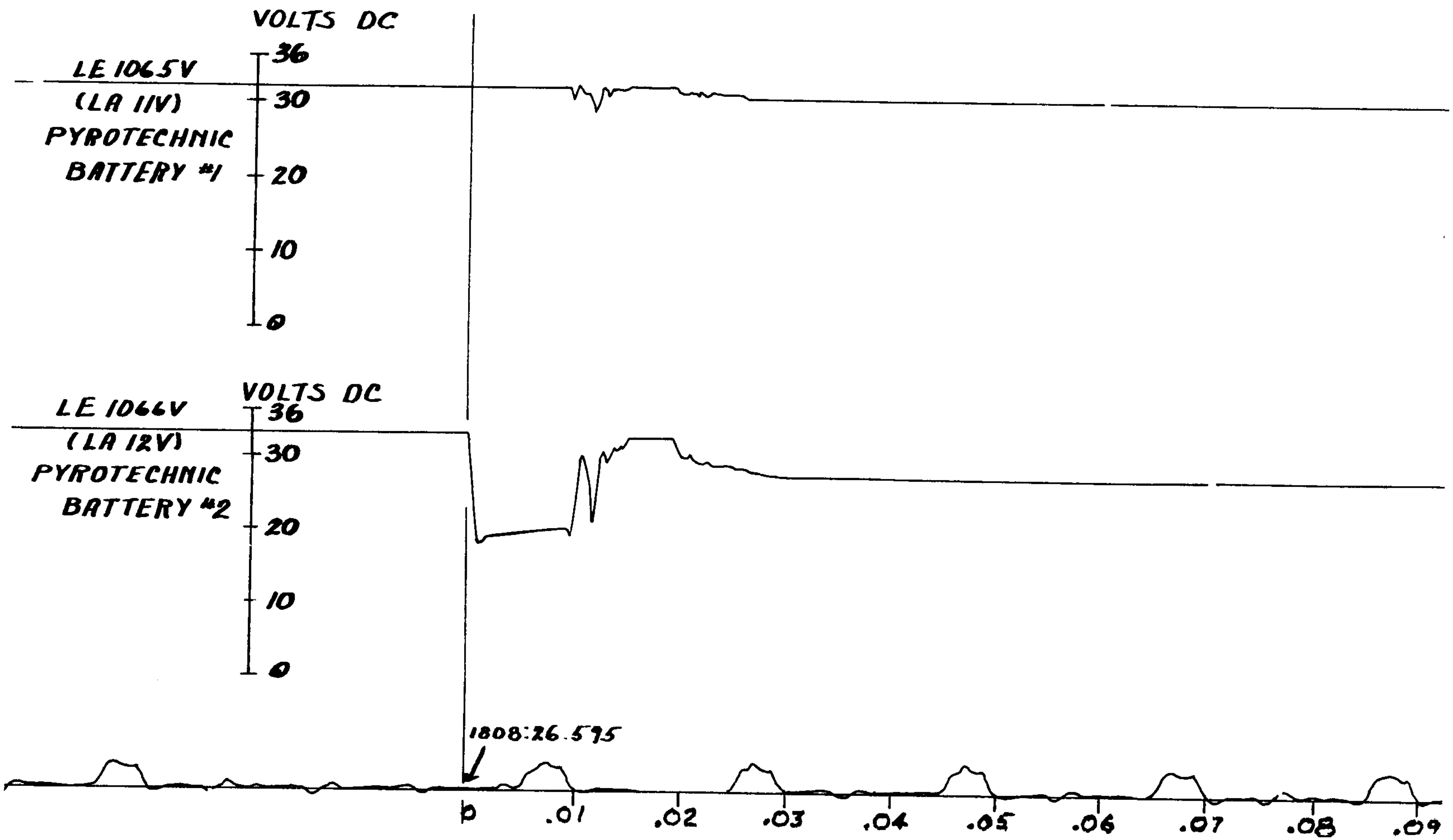

(a) Battery voltages, test LA-2A.

Figure 46. - Data for test. All LA-2 tests.

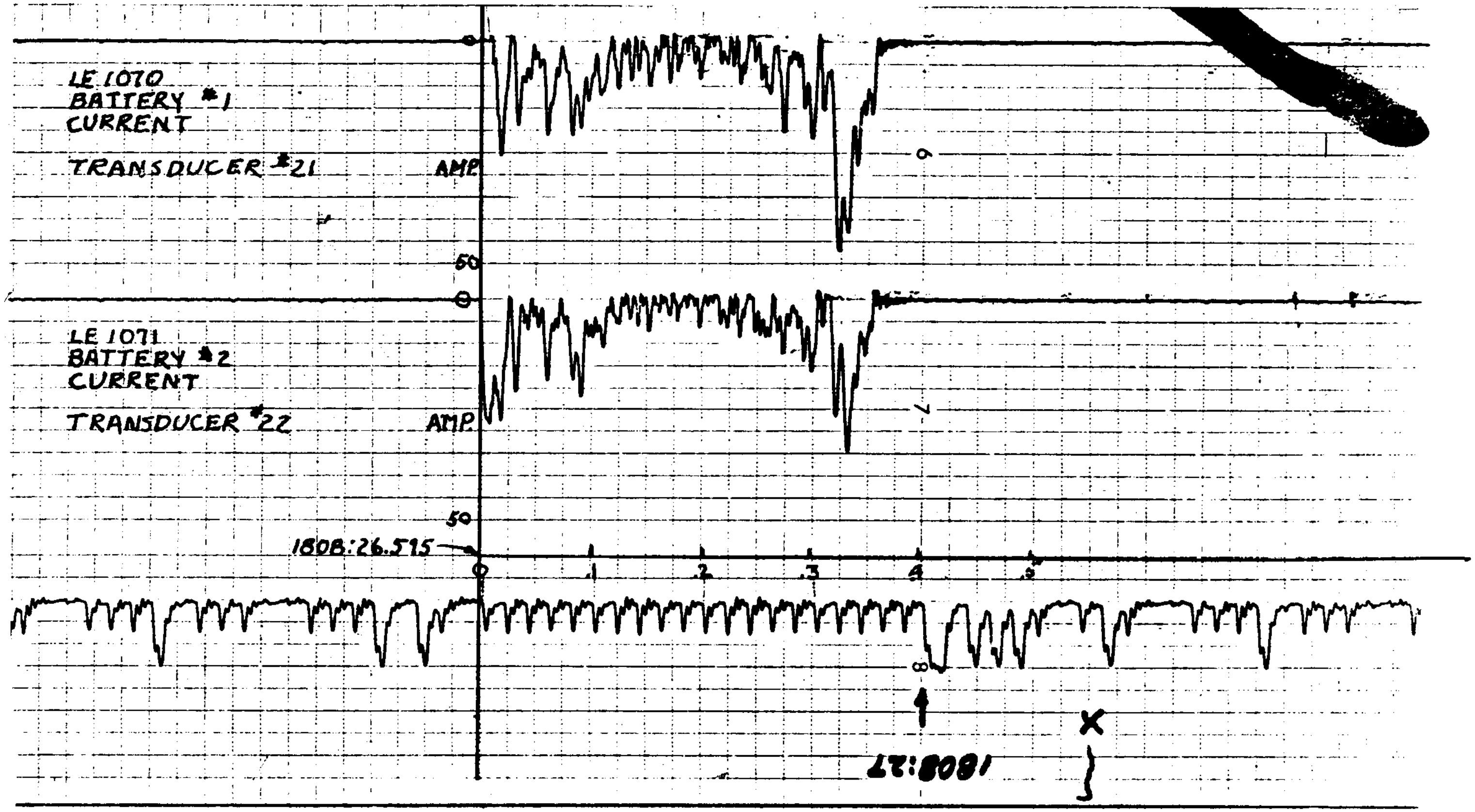

(b) Battery currents, test LA-2A.

Figure 46. - Continued. Data for test. All LA-2 tests.

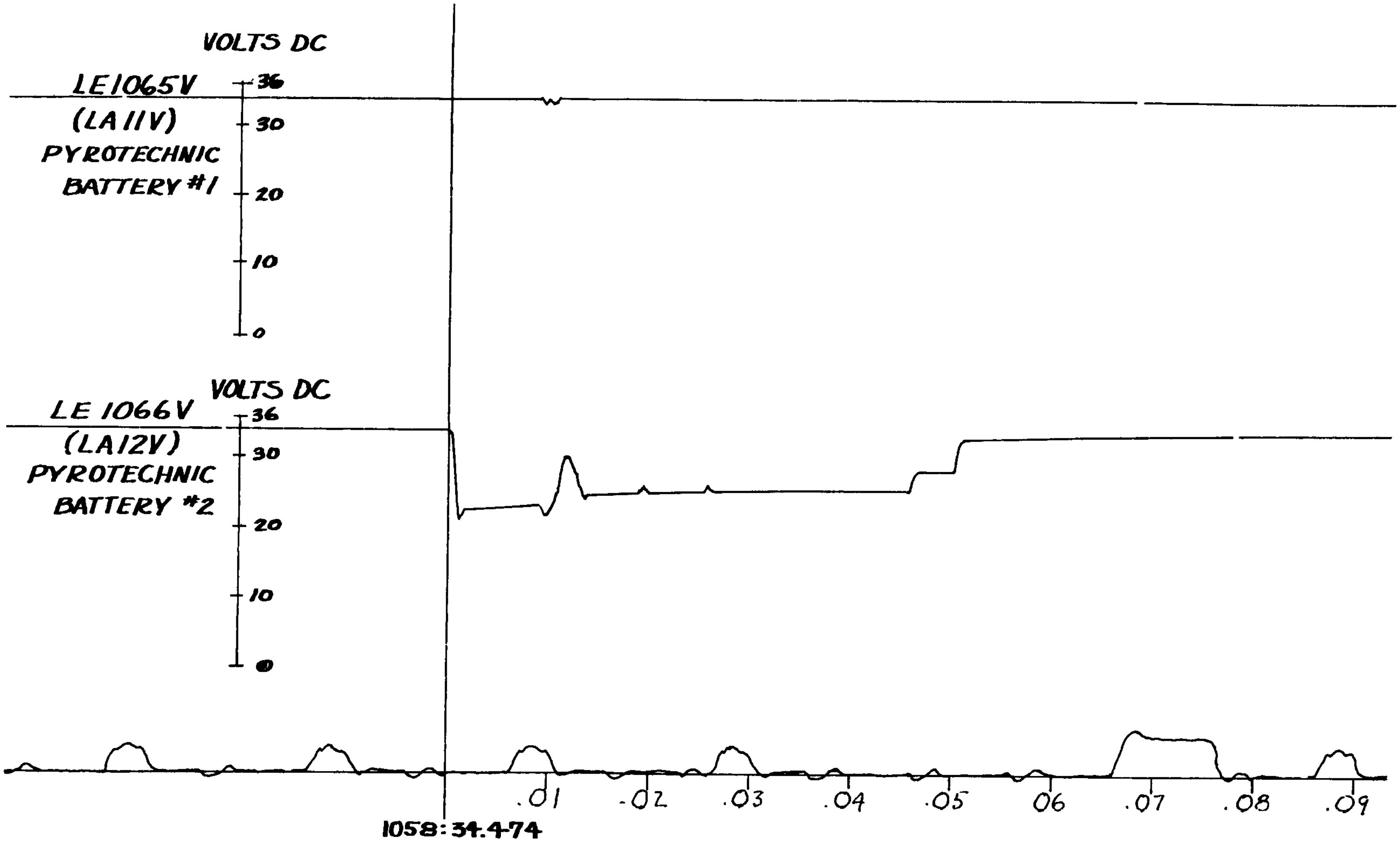

(c) Battery voltages, test LA-2B.

Figure 46. - Continued. Data for test. All LA-2 tests.

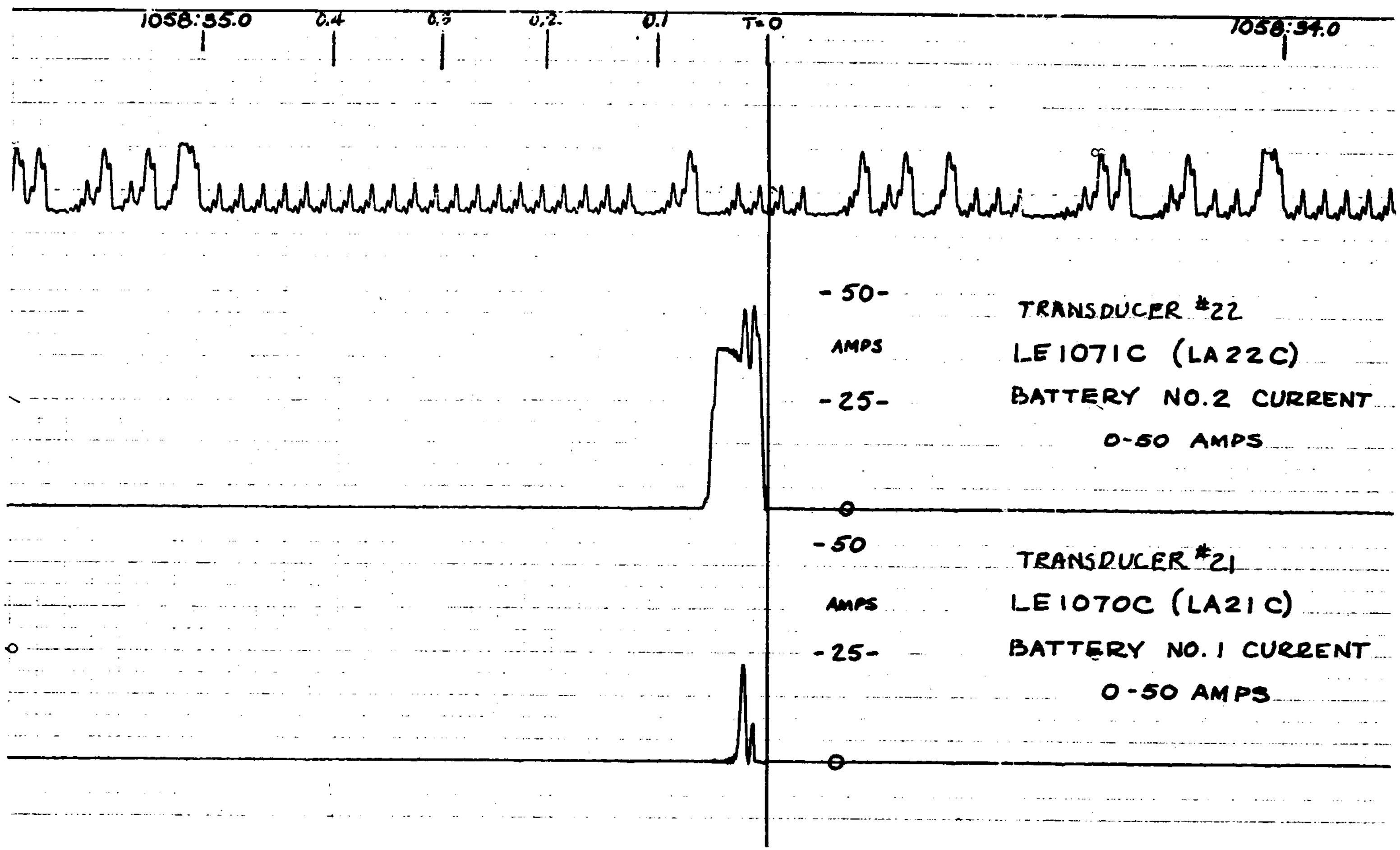

(d) Battery currents, test LA-2B.
Figure 46. - Continued. Data for test. All LA-2 tests.

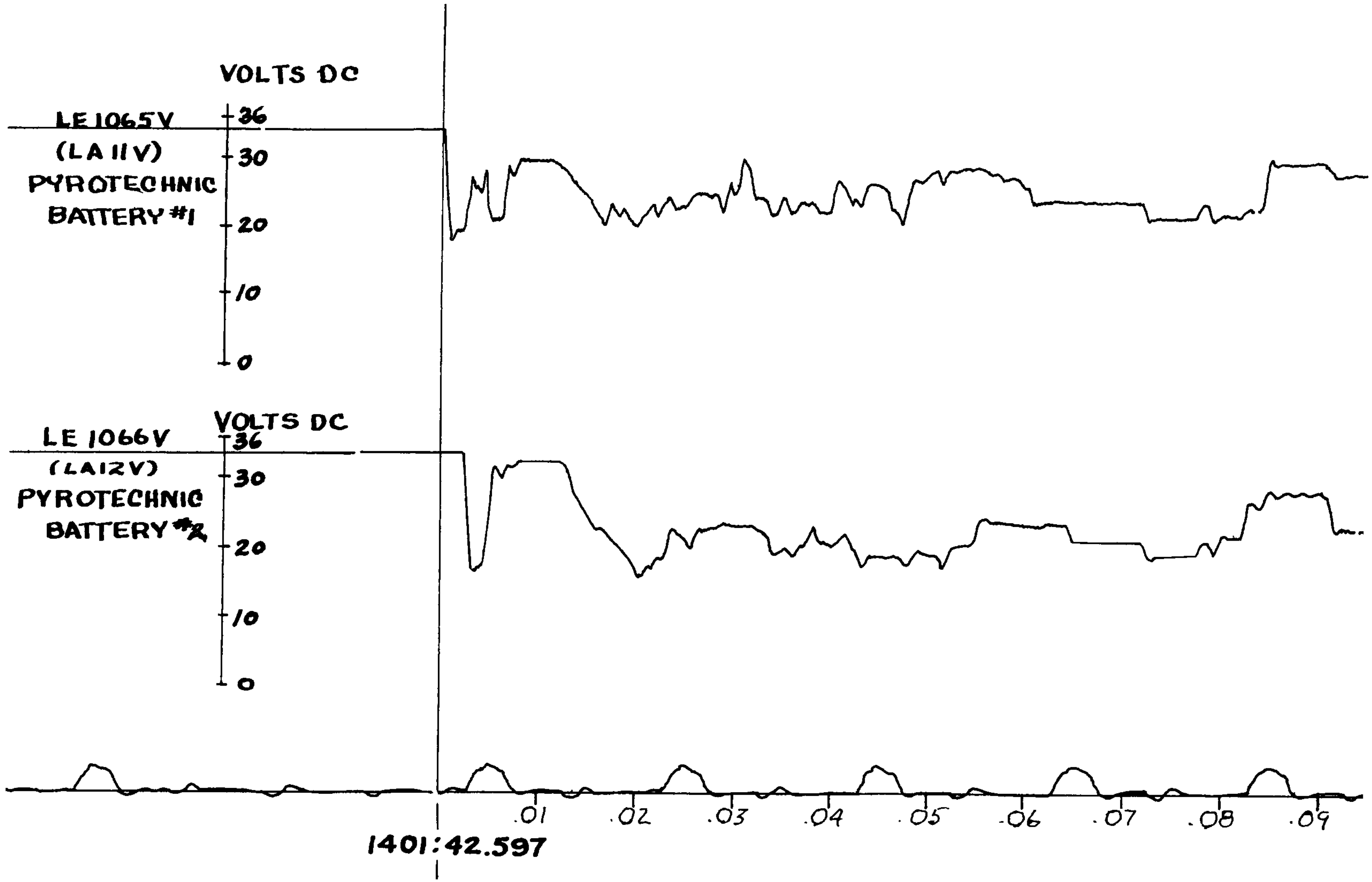

(e) Battery voltages, test LA-2C

Figure 46. - Continued. Data for test. All LA-2 tests.

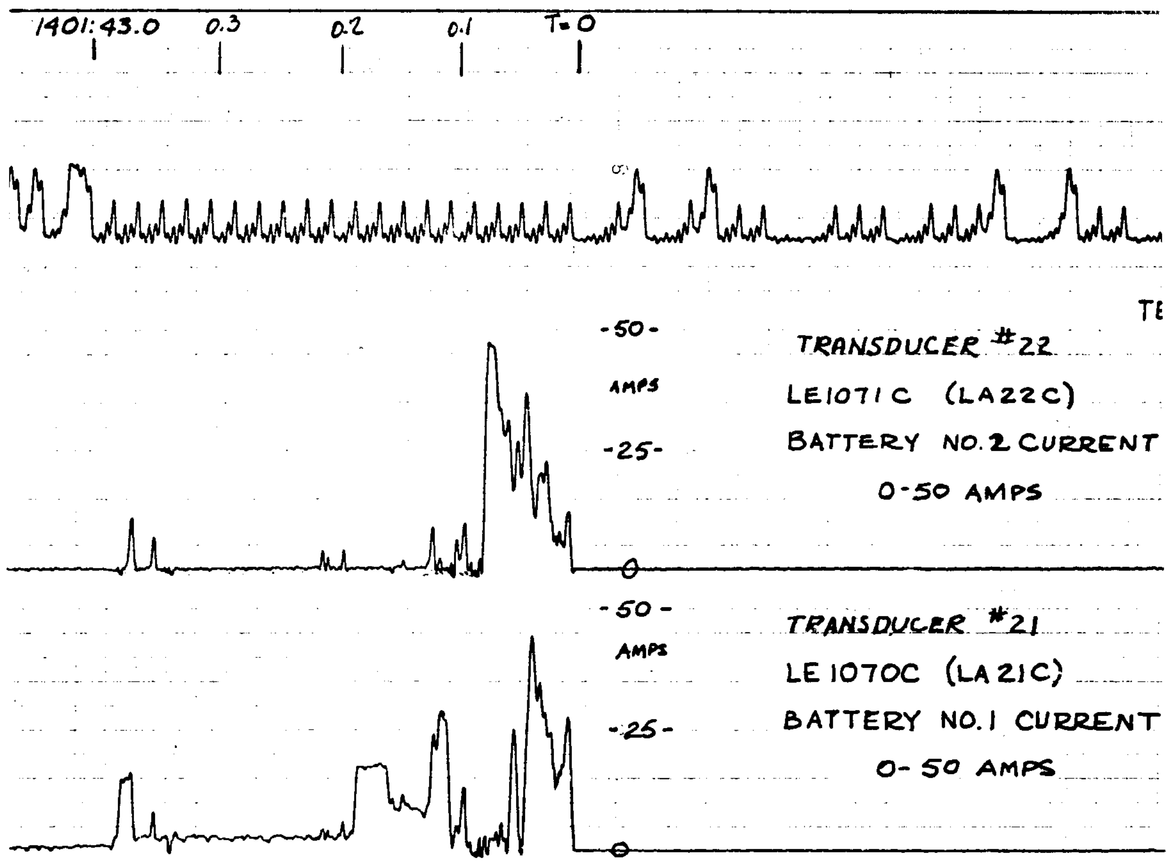

(f) Battery currents, test LA-2C.

Figure 46. - Continued. Data for test. All LA-2 tests

E-3897

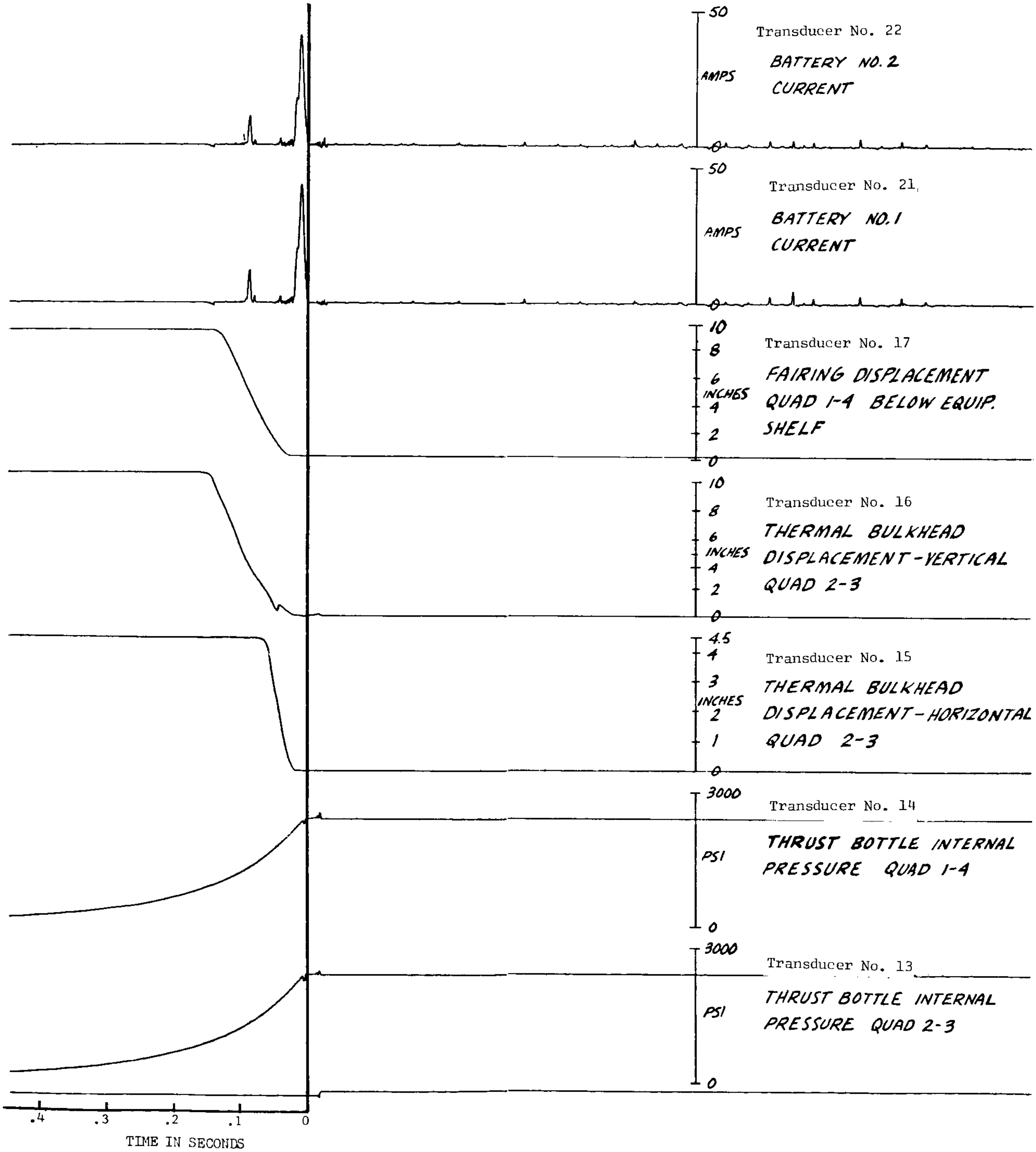

(g) Transducers 13, 14, 15, 16, 17, and battery currents for test LA-2D.

Figure 46. - Continued. Data for test. All LA-2 tests.

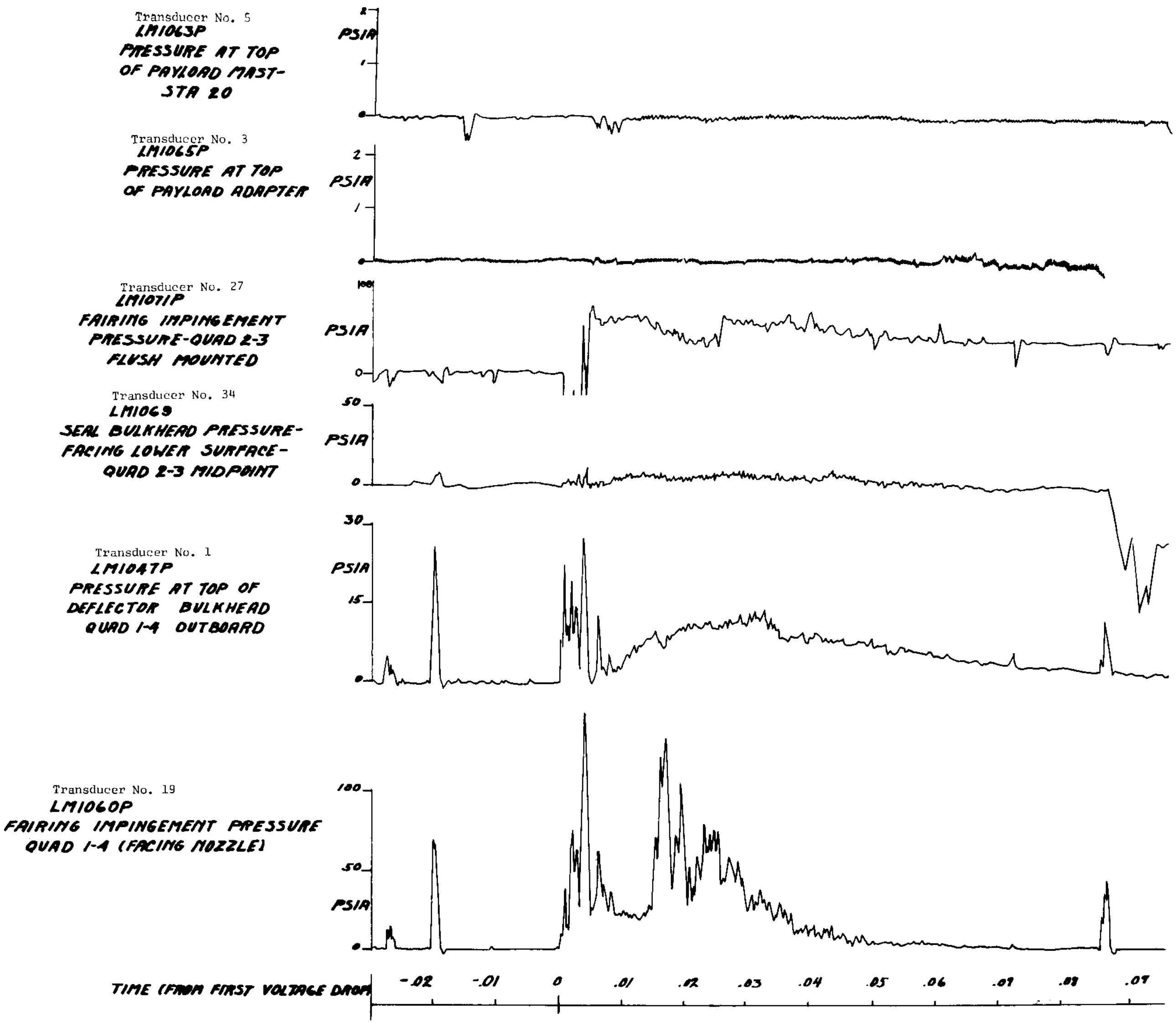

(h) Transducers 1, 3, 5, 19, 27, and 34 for test LA-2D.
Figure 46. - Continued. Data for test. All LA-2 tests.

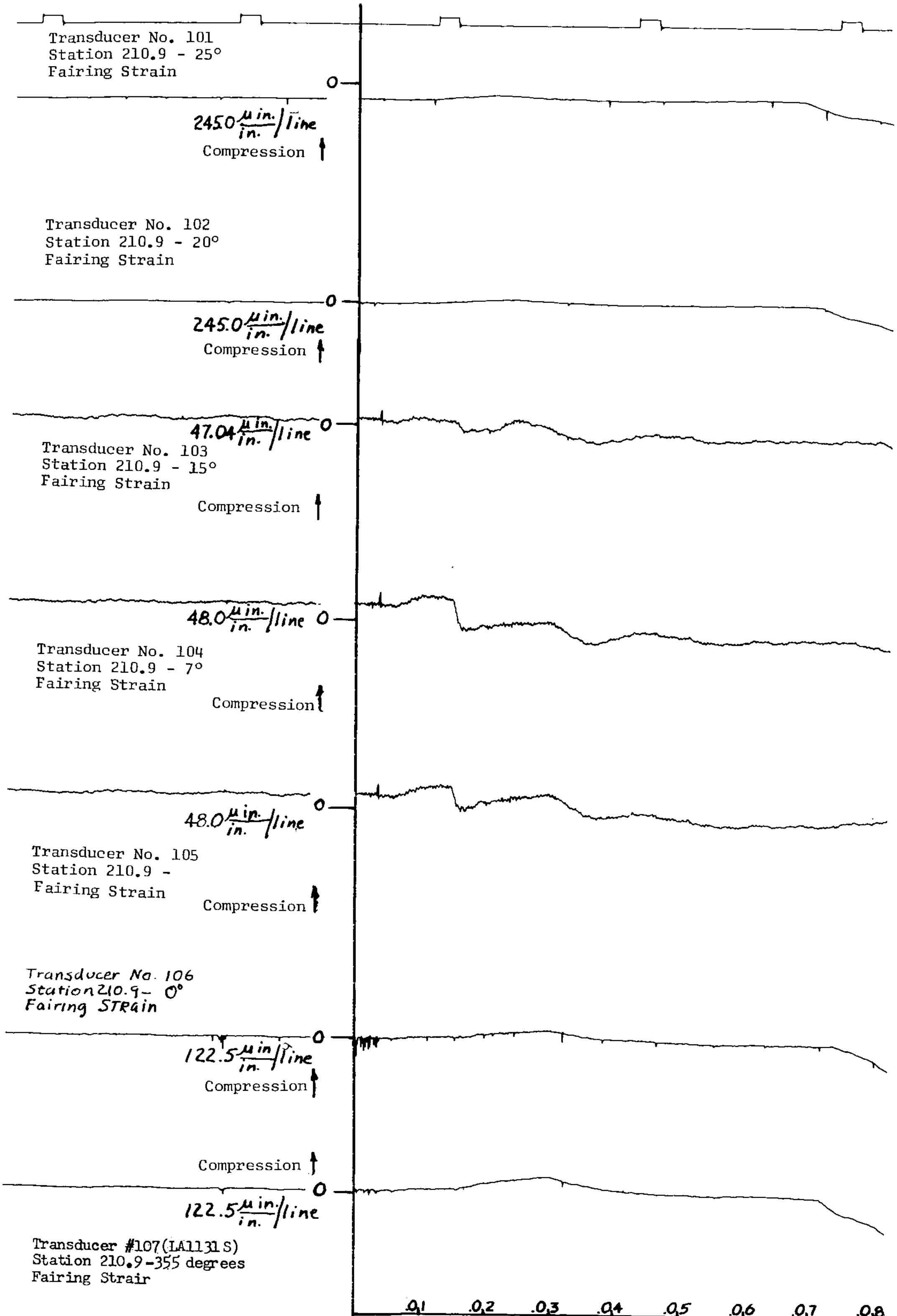

(i) Transducers 101, 102, 103, 104, 105, 106, and 107 for test LA-2D.

Figure 46. - Continued. Data for test. All LA-2 tests.

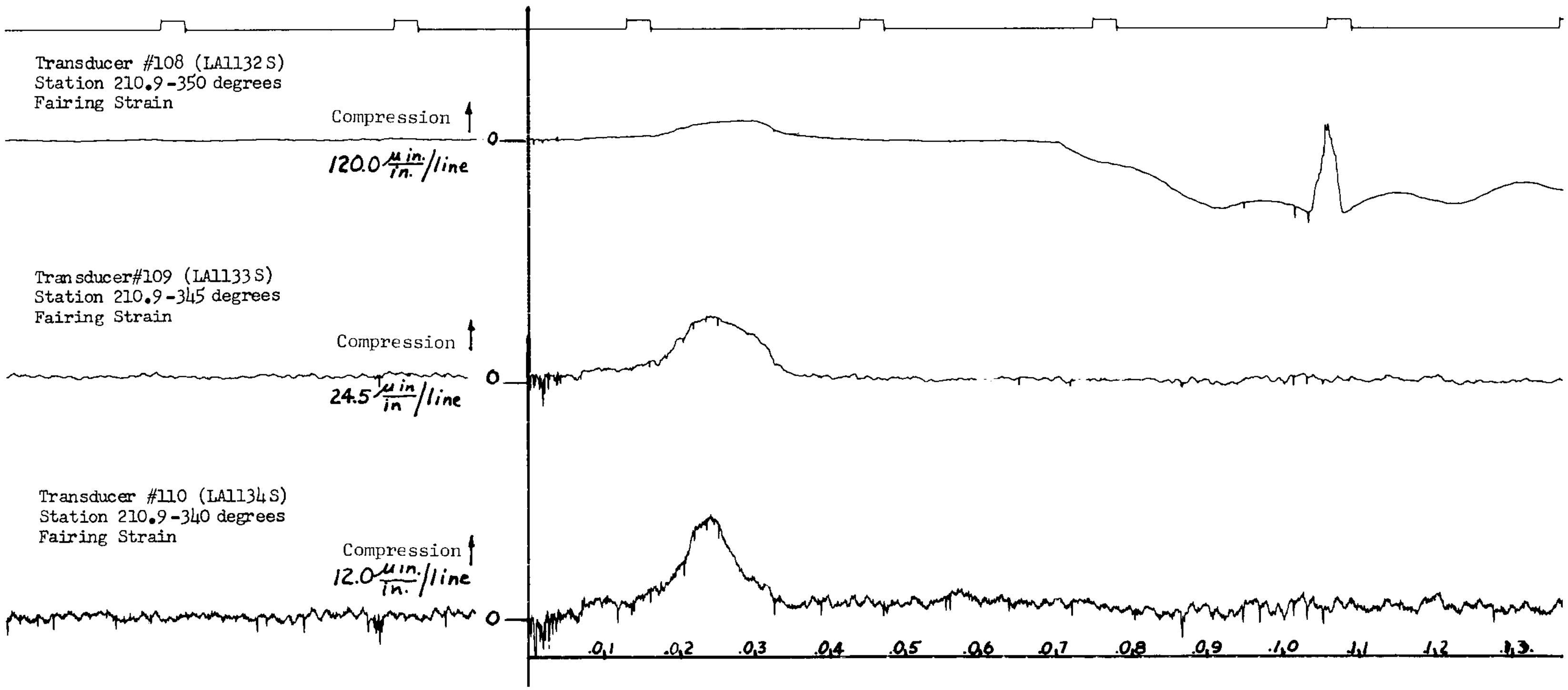

(j) Transducers 108, 109, and 110 for test LA-2D.

Figure 46. - Continued. Data for test. All LA-2 tests.

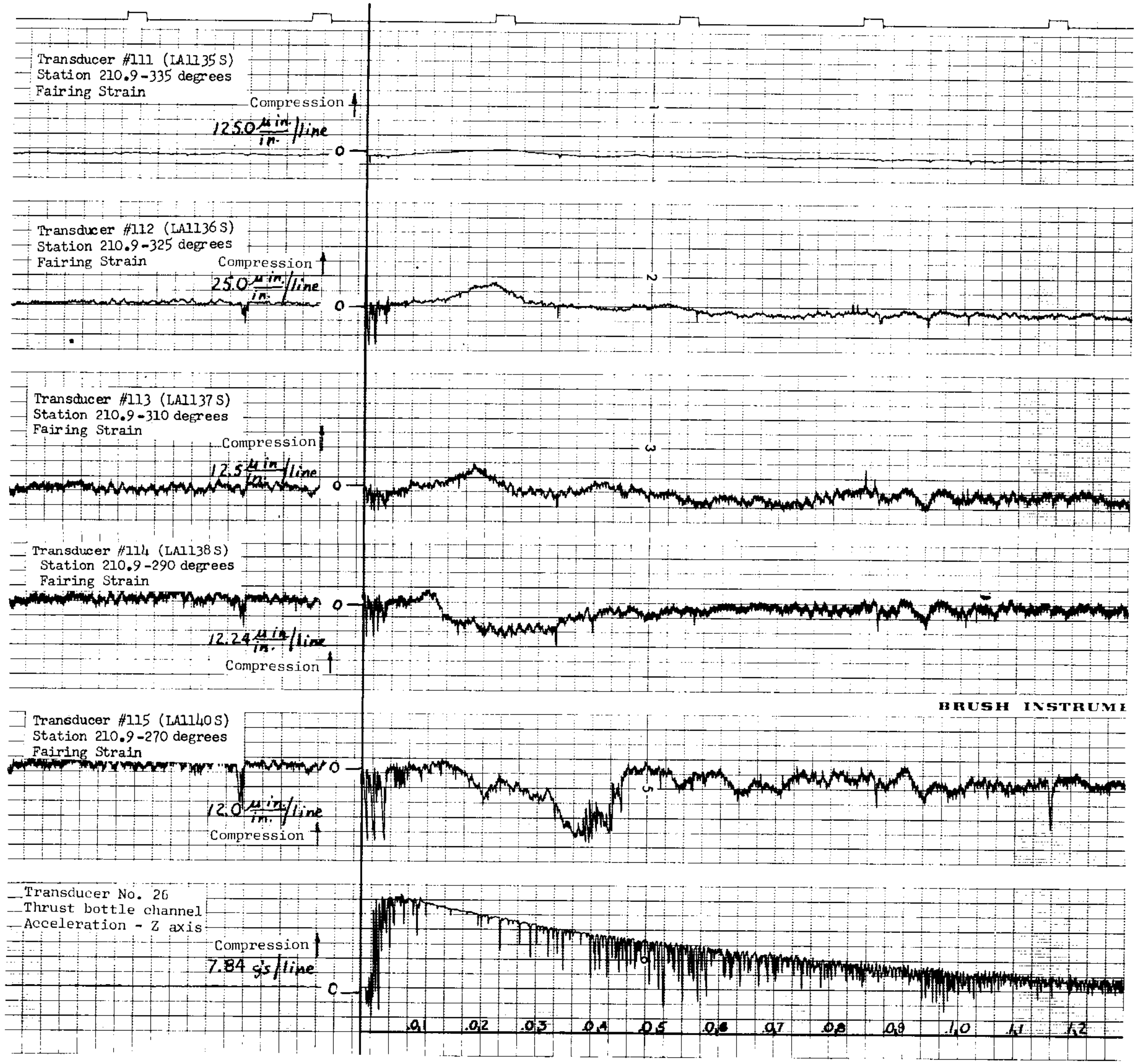

(k) Transducers 26, 111, 112, 113, 114, and 115 for test LA-2D.

Figure 46. - Continued. Data for test. All LA-2 tests.

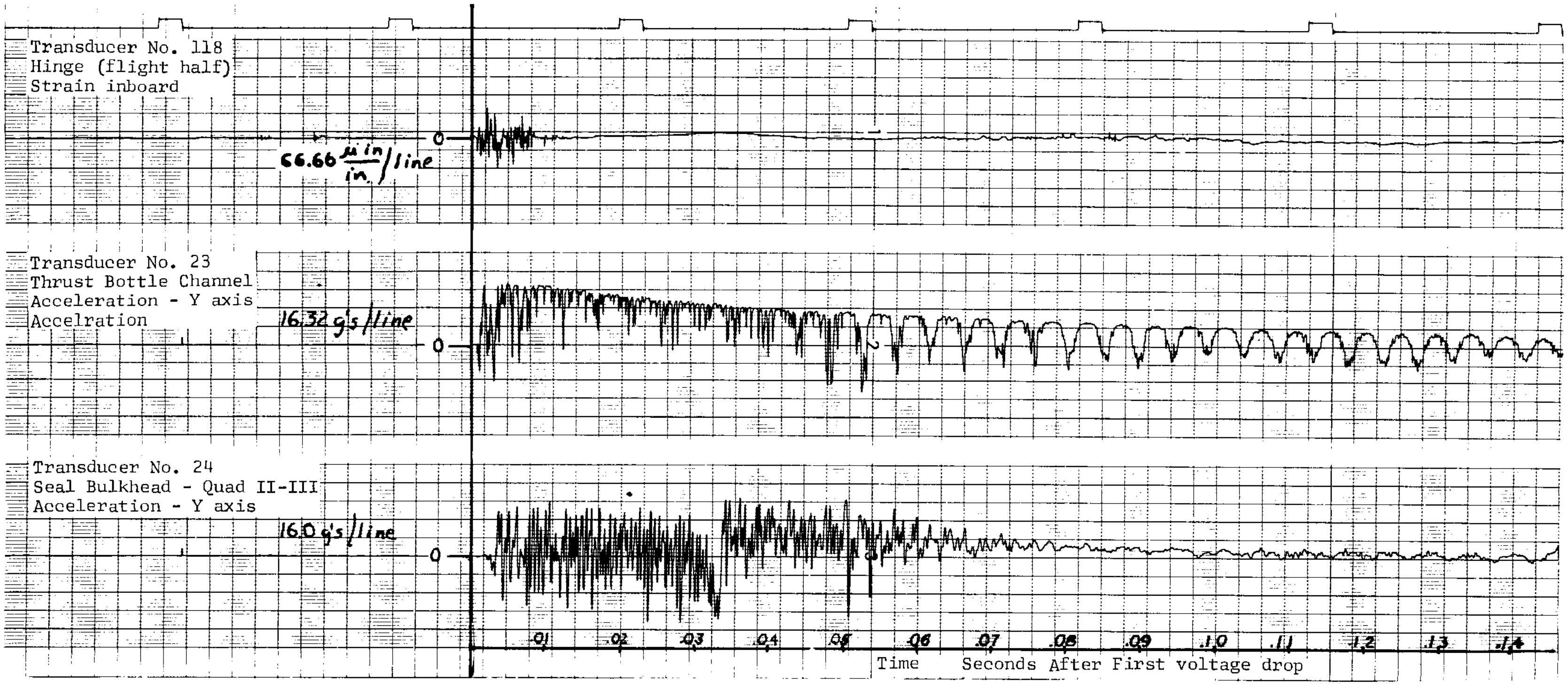

(1) Transducers 23, 24, and 118 for test LA-2D.

Figure 46. - Concluded. Data for test. All LA-2 tests.

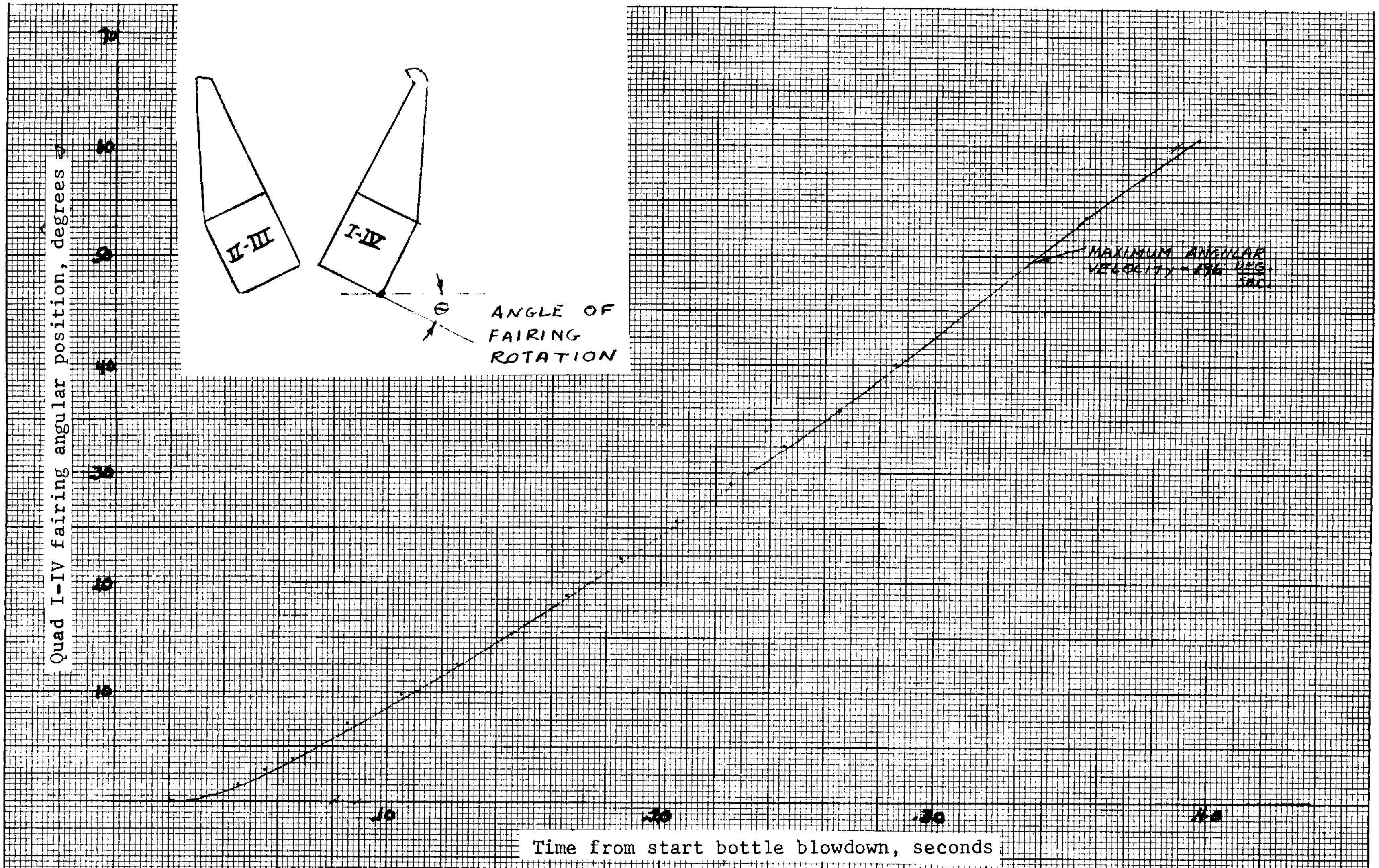

Figure 47. - Nose fairing angular position vs. time, Test LA-2D, (measured at the I-IV hinge point).

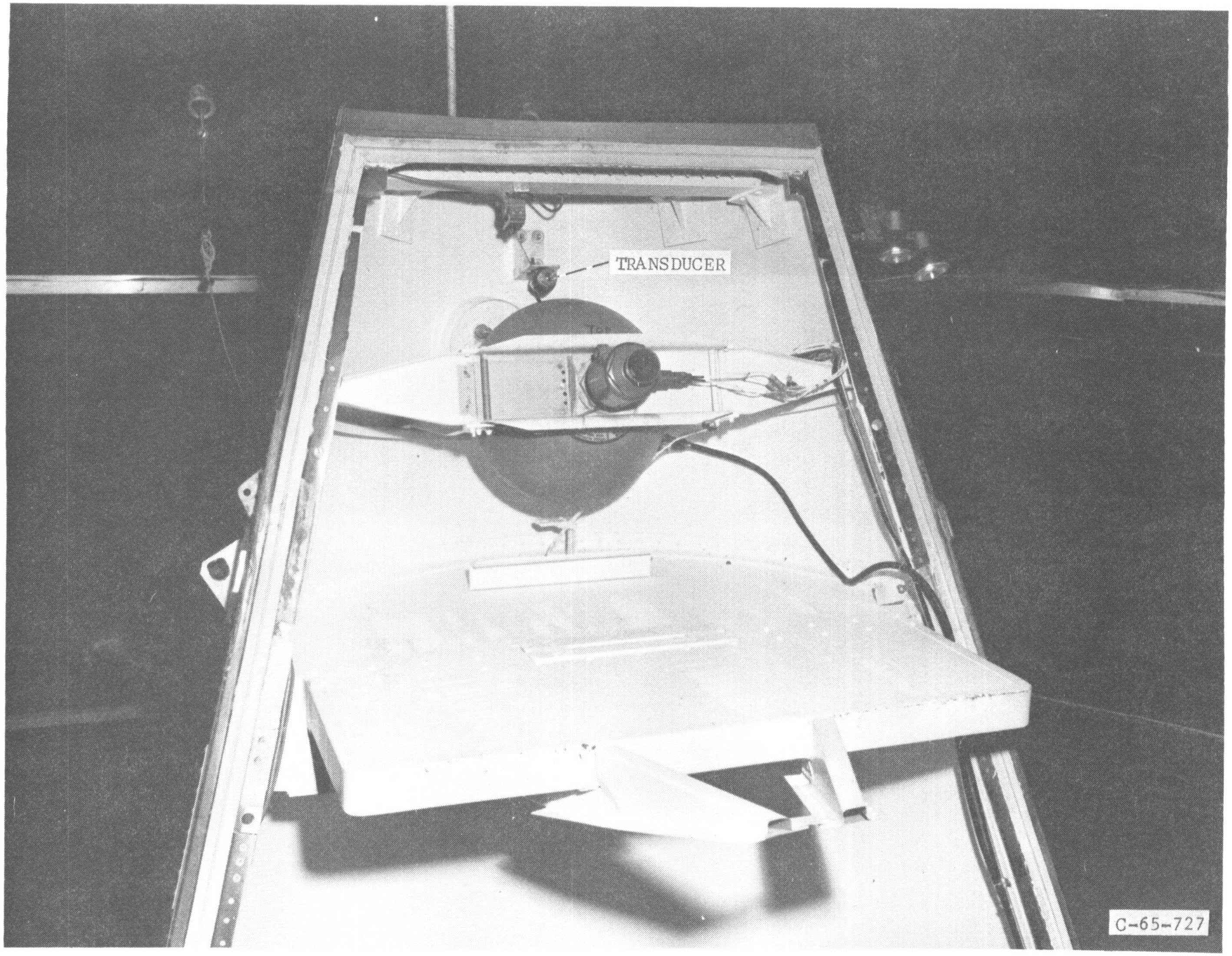

(a) Test LA-1B and LA-2D.
Figure 48. - Total pressure transducer installation opposite jettison bottles.

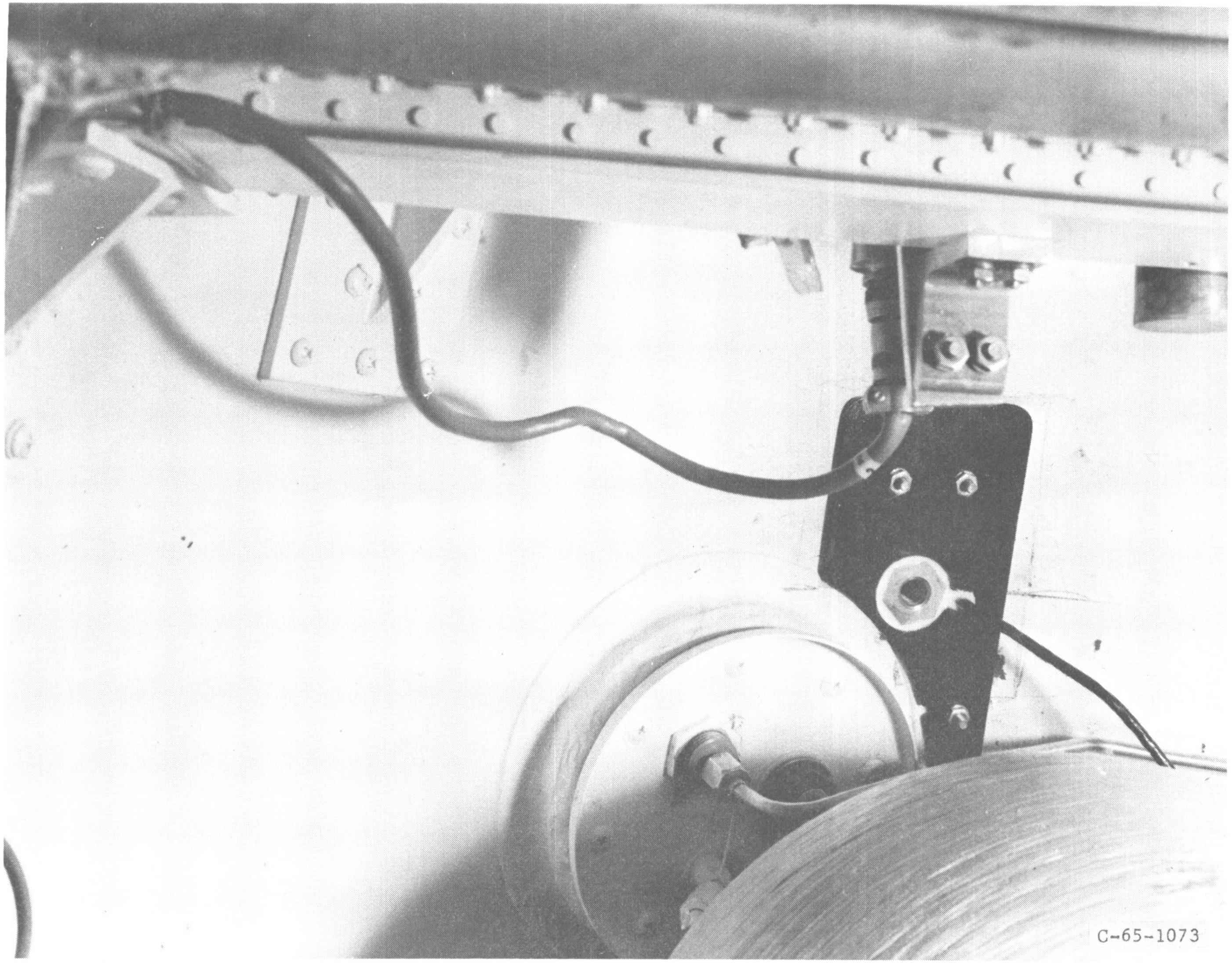

(b) Interior installation for test LA-3 and LA-4A.

Figure 48. - Continued. Total pressure transducer installation opposite jettison bottles.

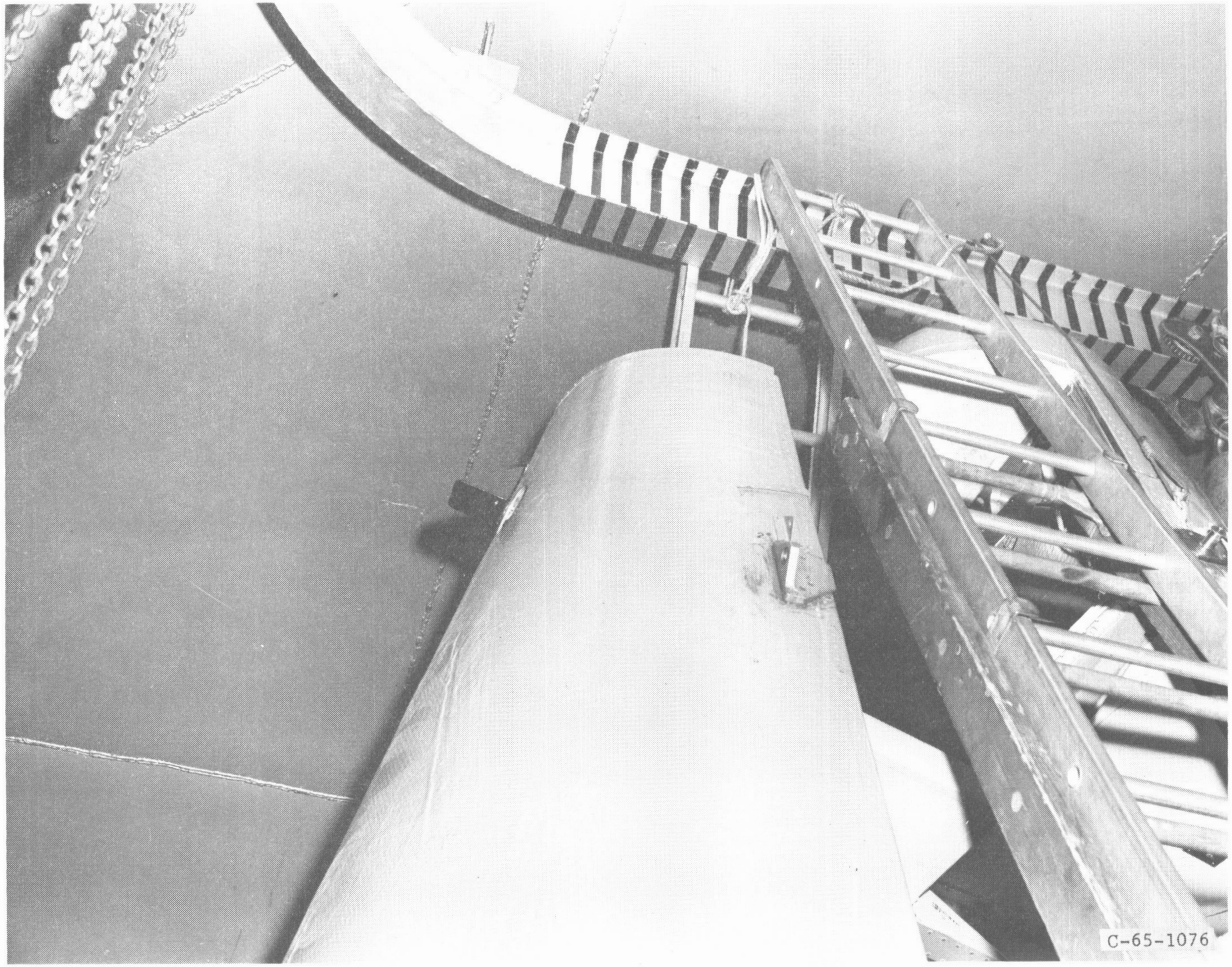

(c) Exterior installation for test LA-3 and LA-4A.

Figure 48. - Continued. Total pressure transducer installation opposite jettison bottles.

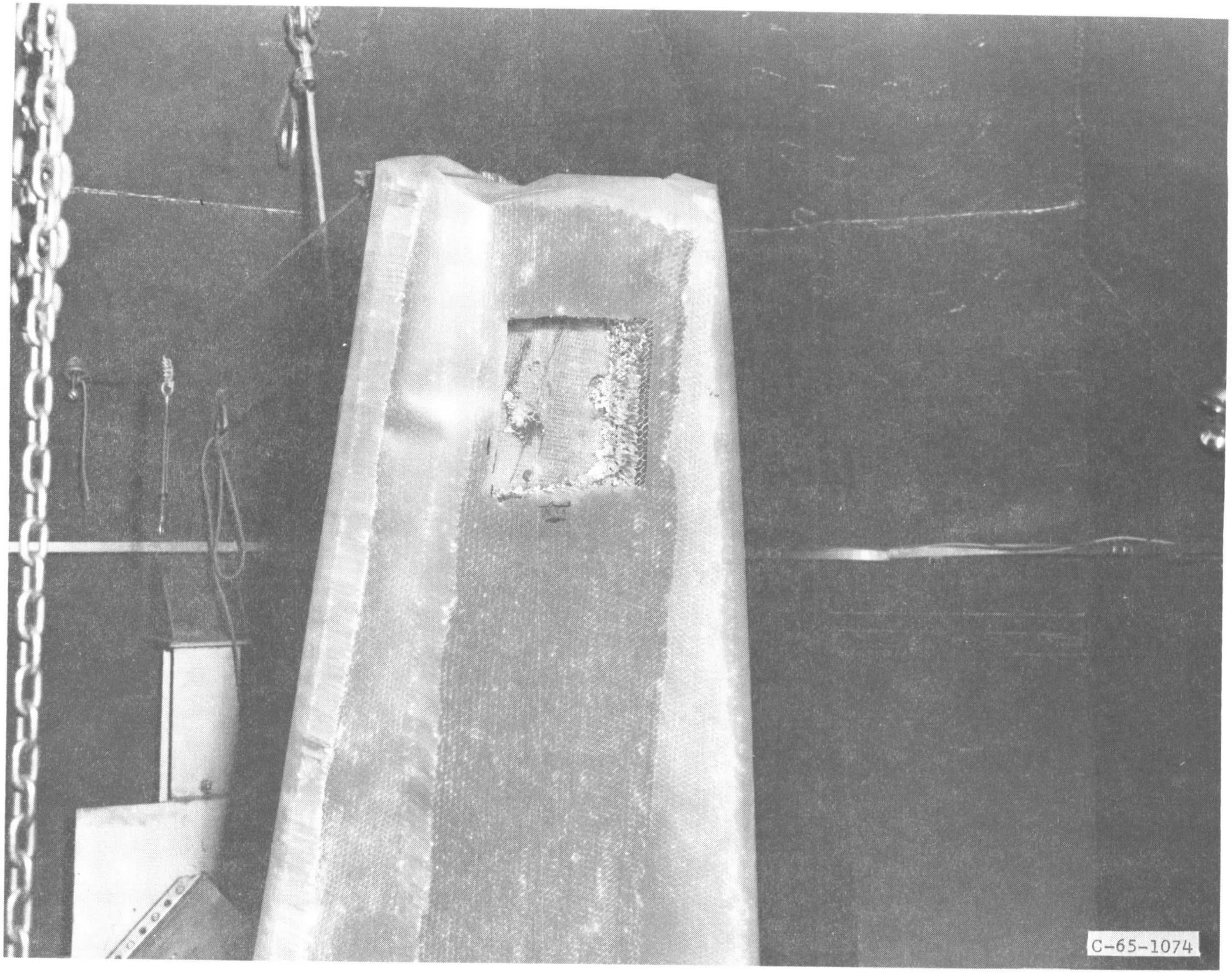

(d) Modification to catcher shoe for test LA-3 and LA-4A.

Figure 48. - Concluded. Total pressure transducer installation opposite jettison bottles.

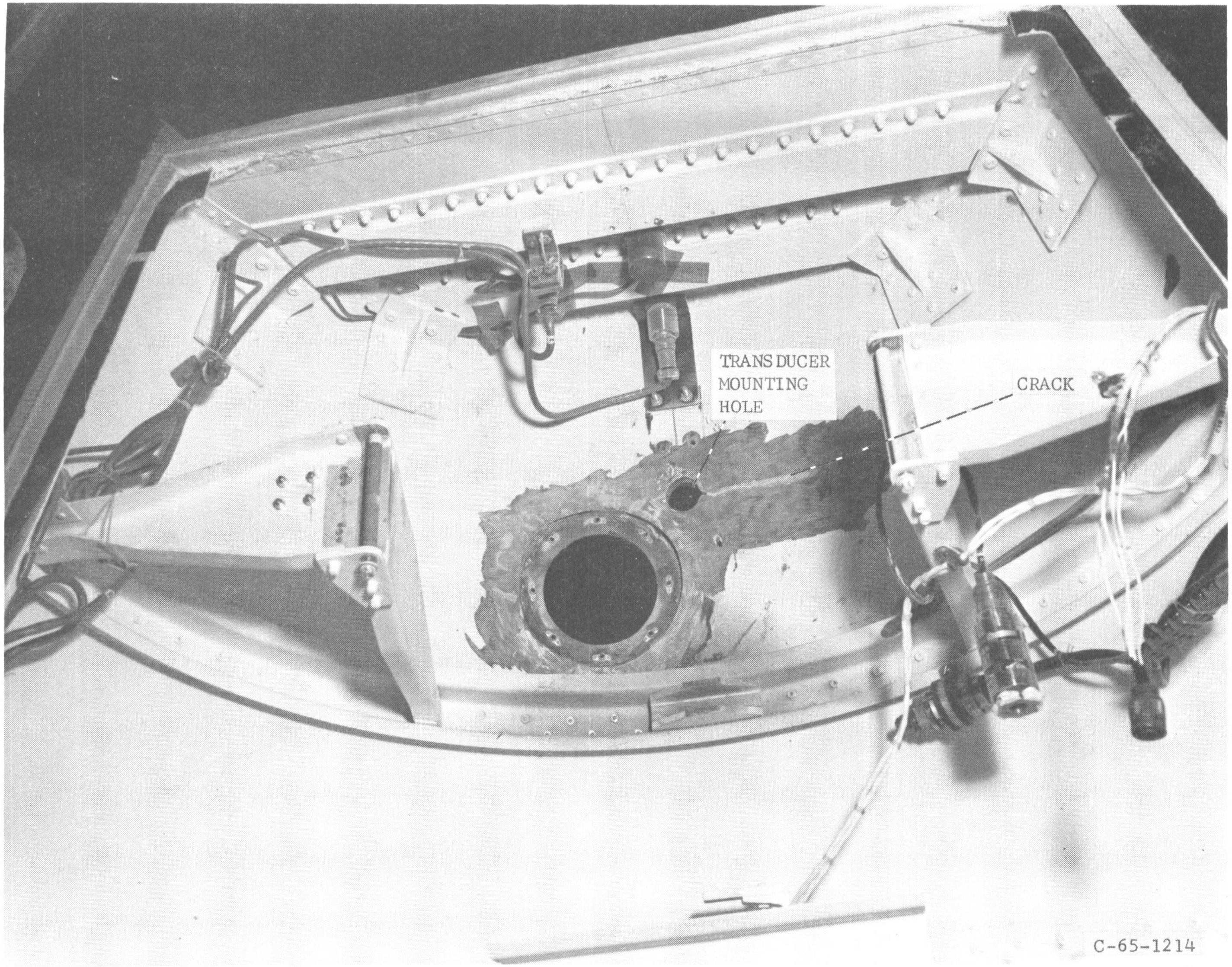

Figure 49. - Crack in fairing wall caused by the transducer contact with catcher, test LA-3.

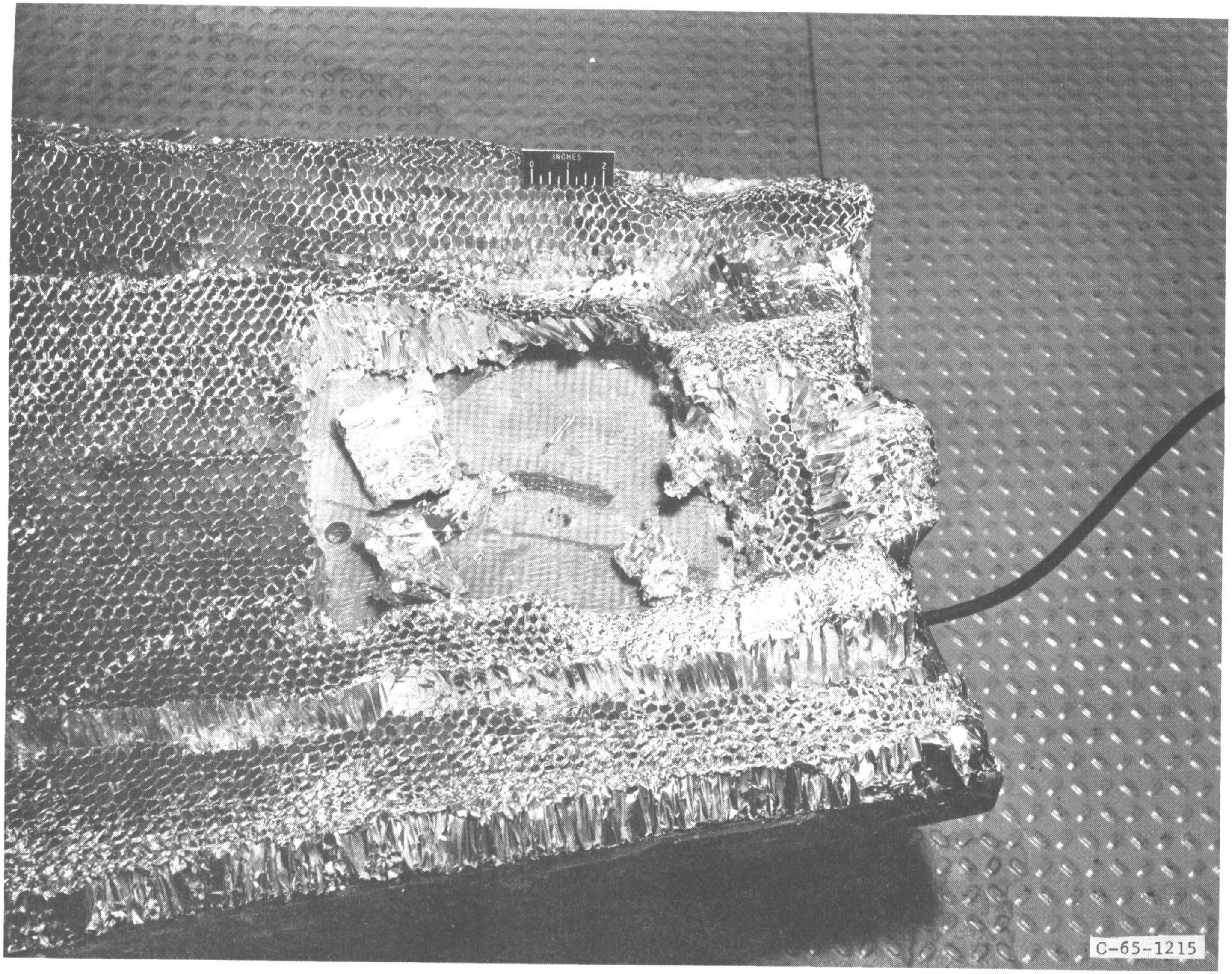

Figure 50. - Catcher after damage to fairing, test LA-3.

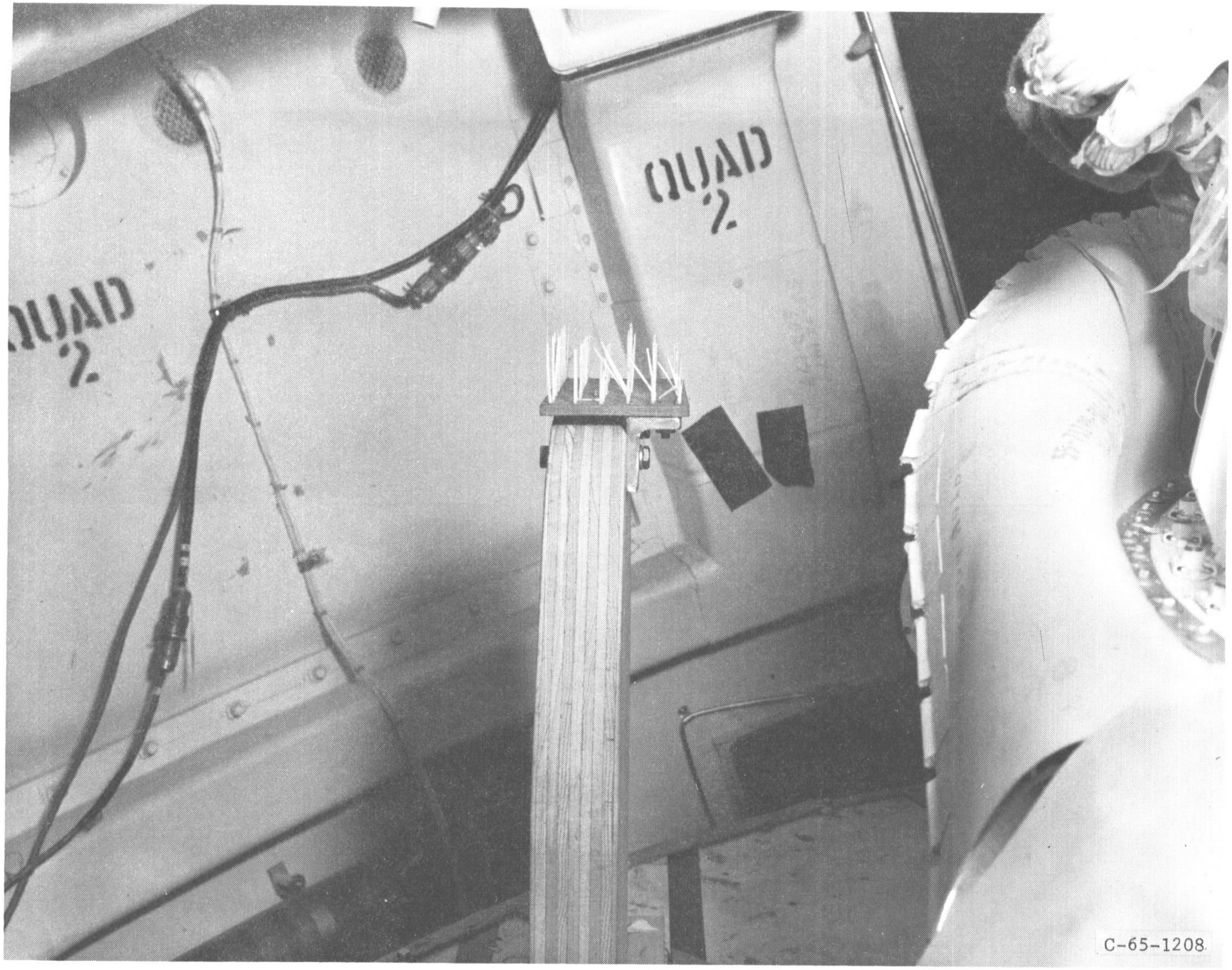

Figure 51. - Broken toothpicks on the guidance platform model after test LA-3.

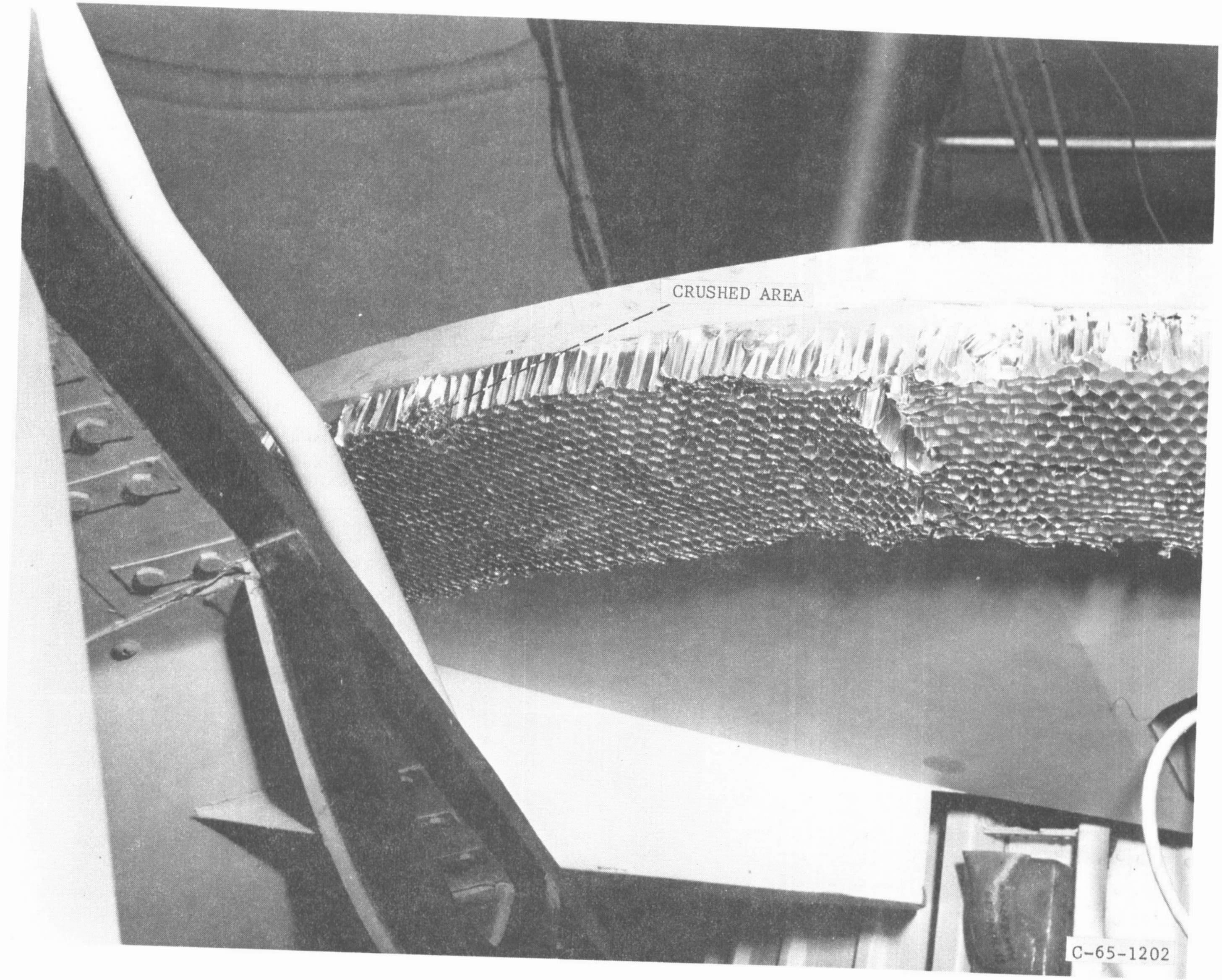

Figure 52. - Honeycomb installed on the Surveyor envelope model (Quad III), test LA-3.

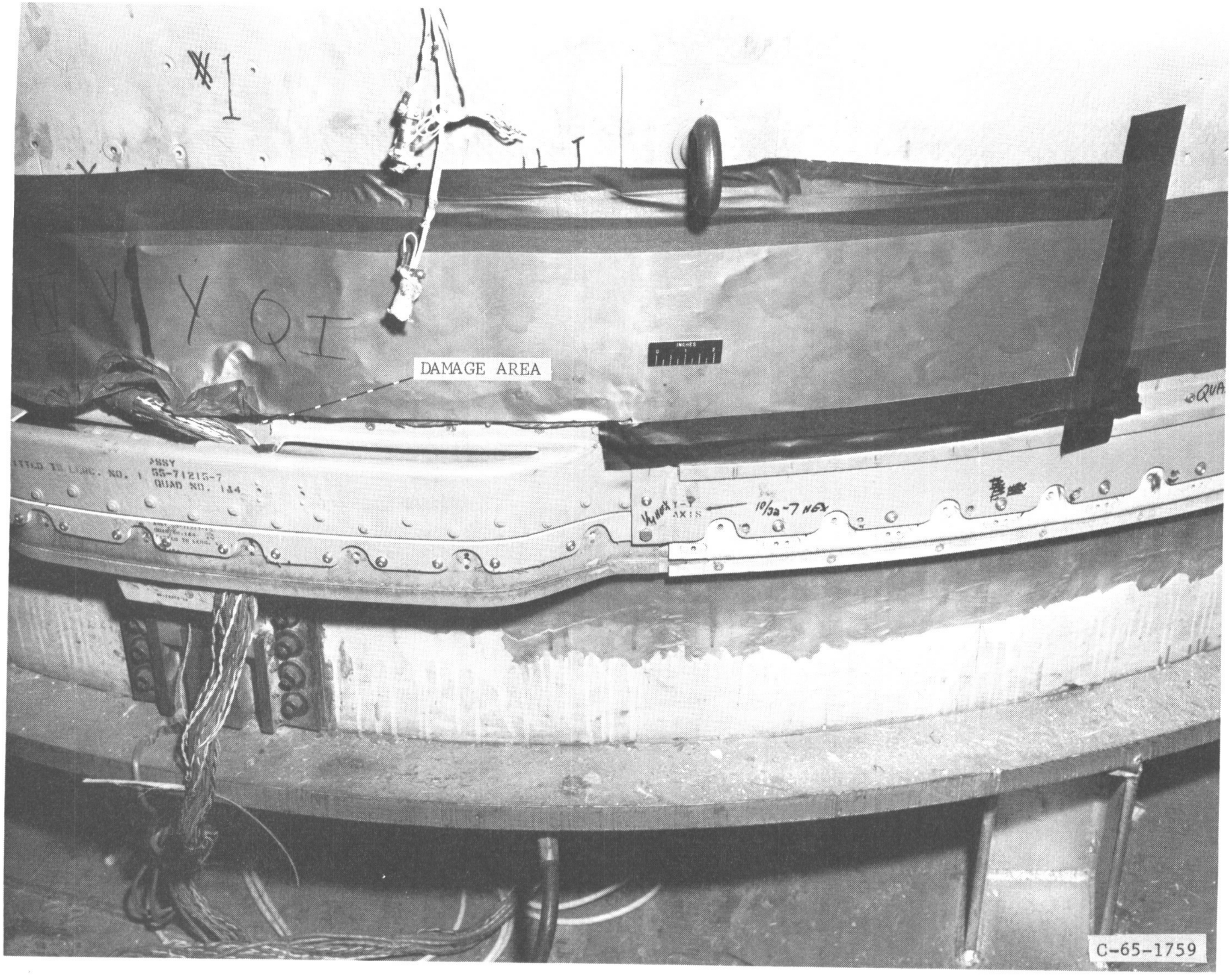

Figure 53. - Damage to the hinge pad fairing, test LA-3.

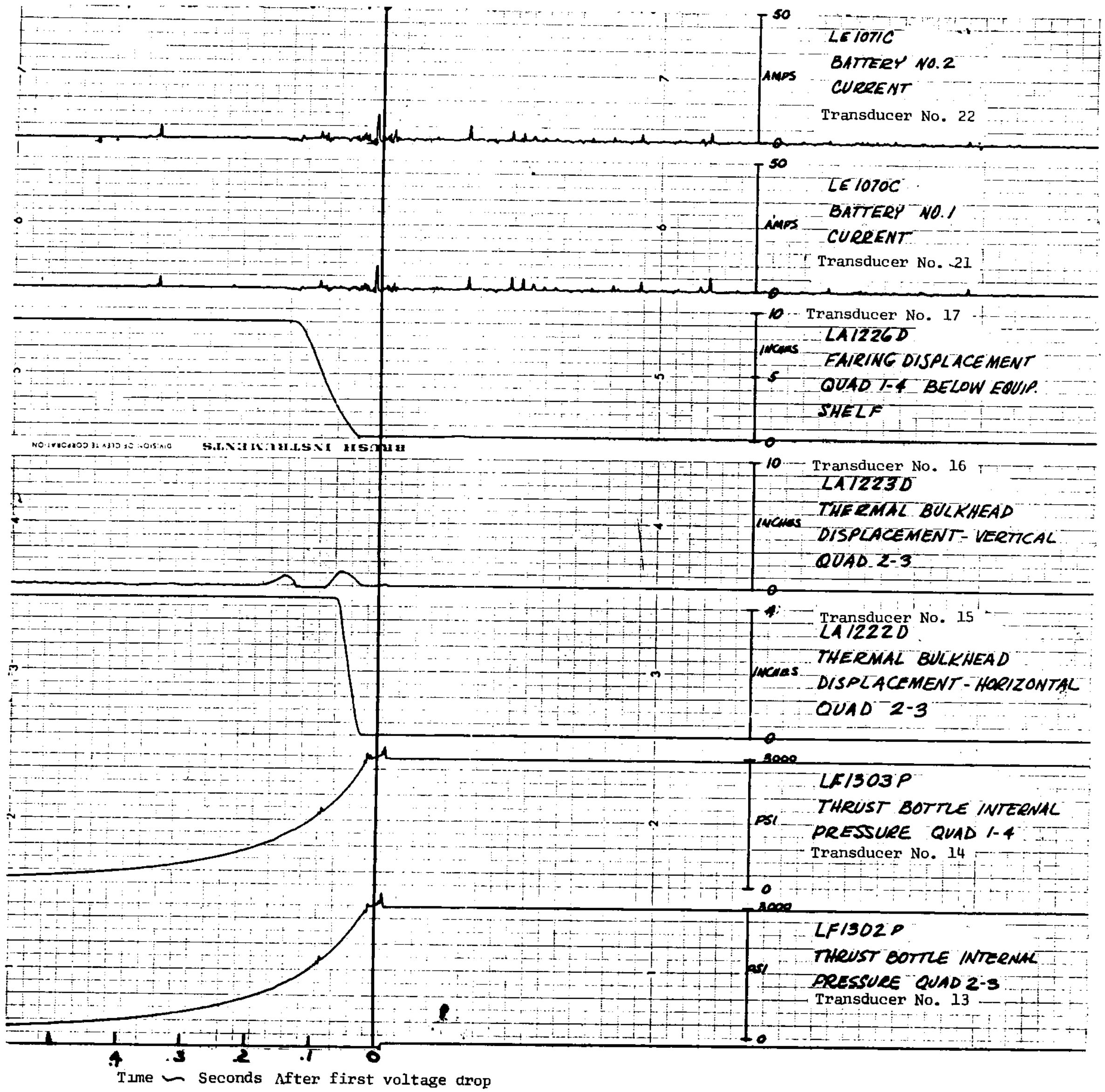

(a) Transducers 13, 14, 15, 16, 17, 21 and 22.

Figure 54. - Data for test LA-3.

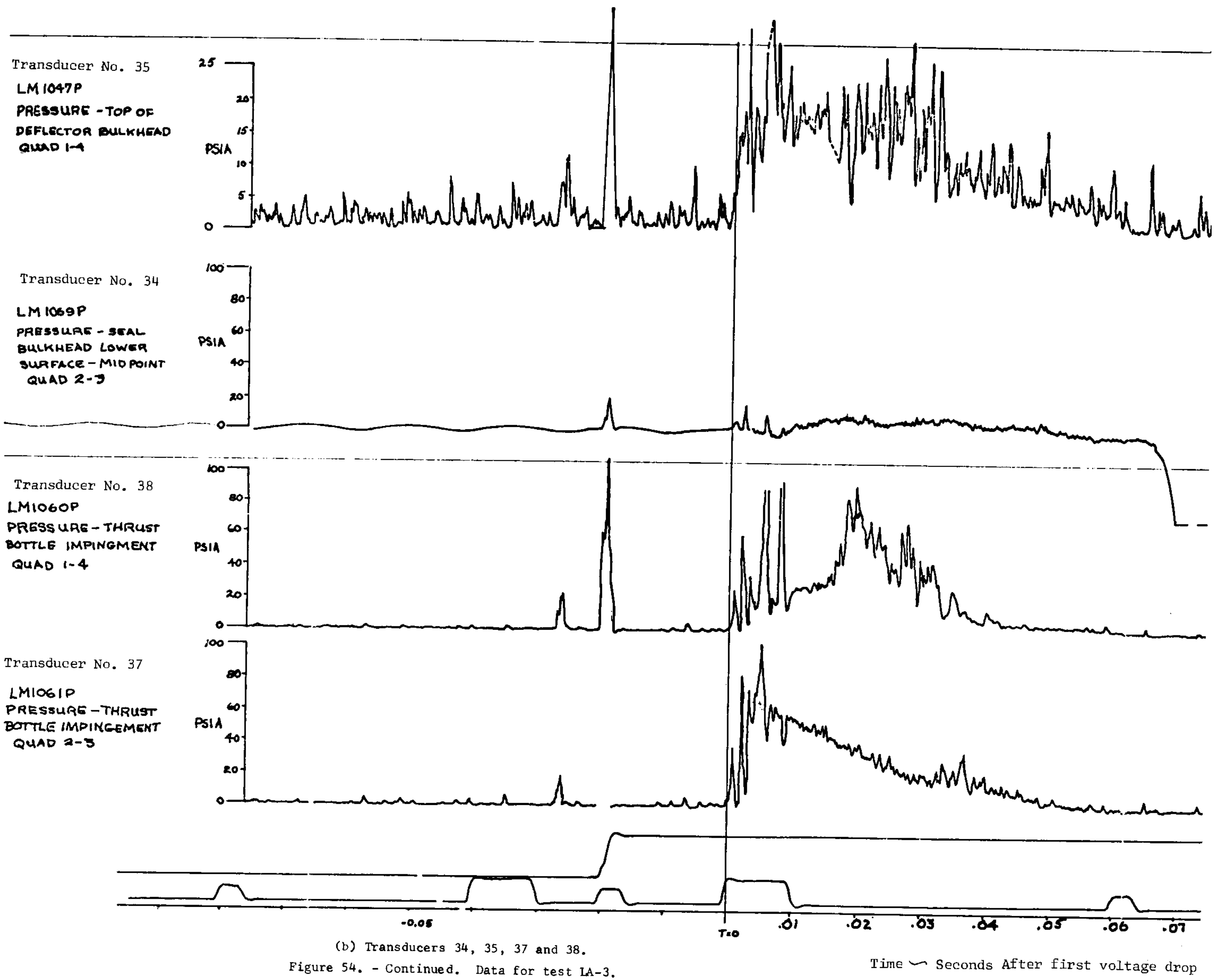

(b) Transducers 34, 35, 37 and 38.

Figure 54. - Continued. Data for test LA-3.

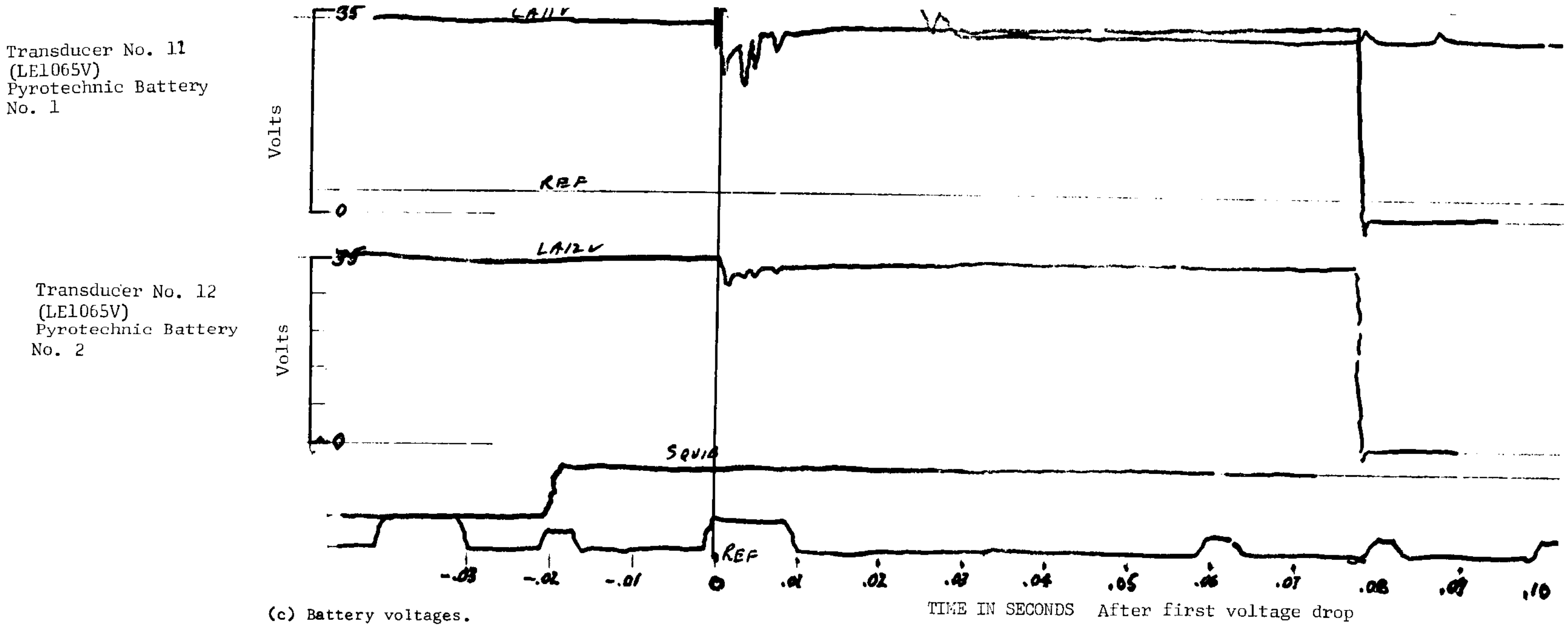

(c) Battery voltages.

Figure 54. - Continued. Data for test LA-3.

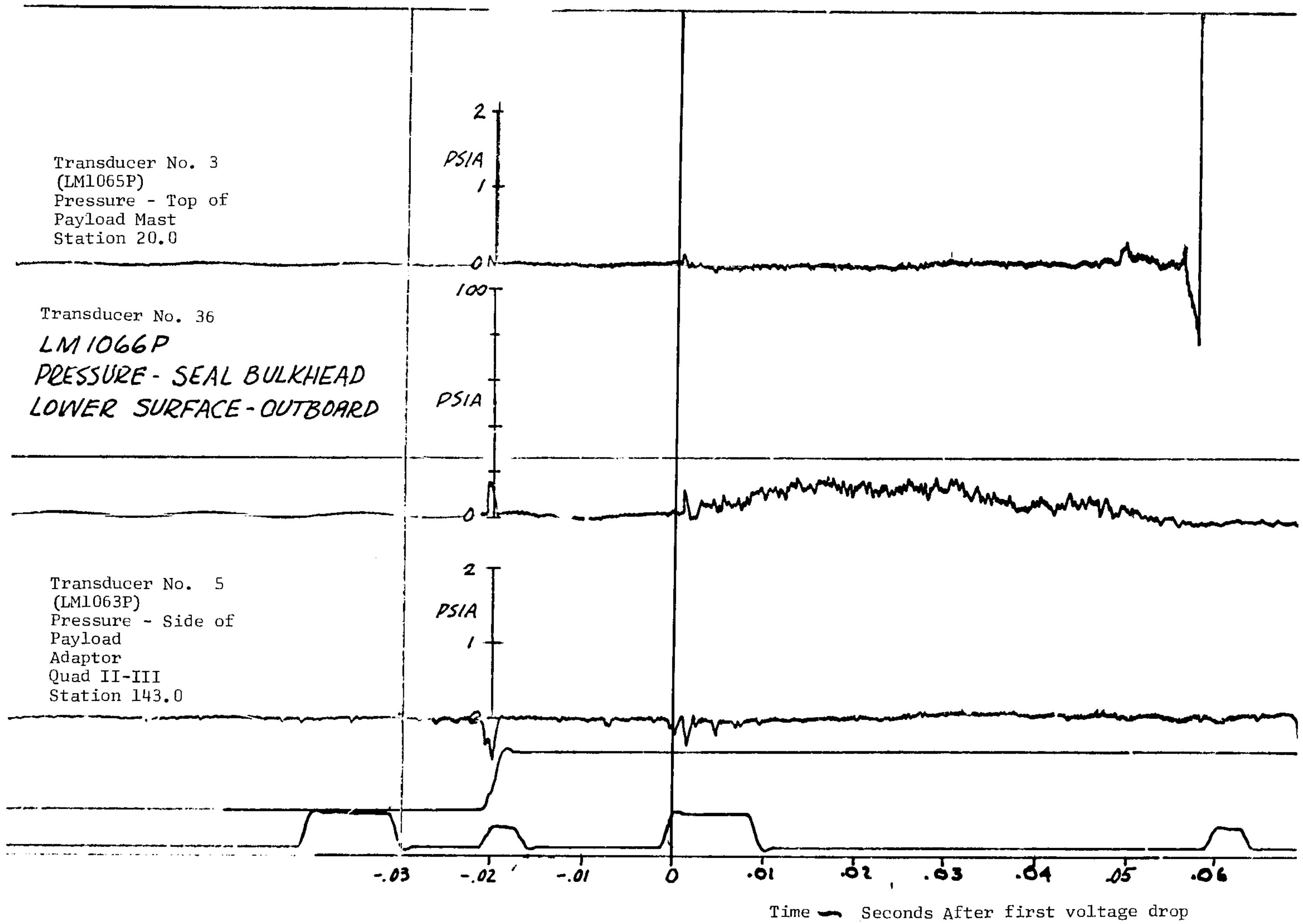

(d) Transducers 3, 5, and 36.
Figure 54. - Continued. Data for test LA-3.

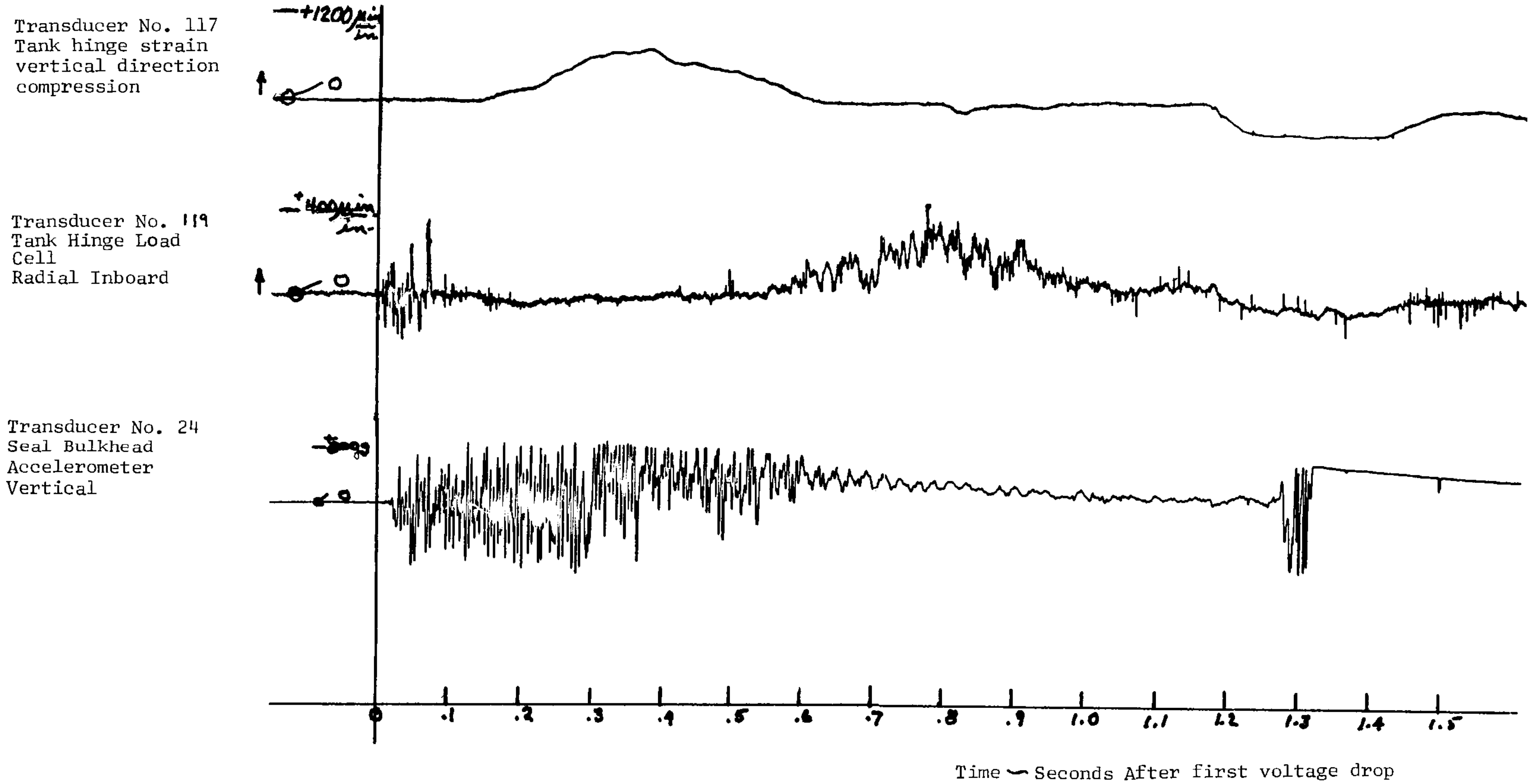

(e) Transducers 24, 117 and 119

Figure 54. - Concluded. Data for test LA-3.

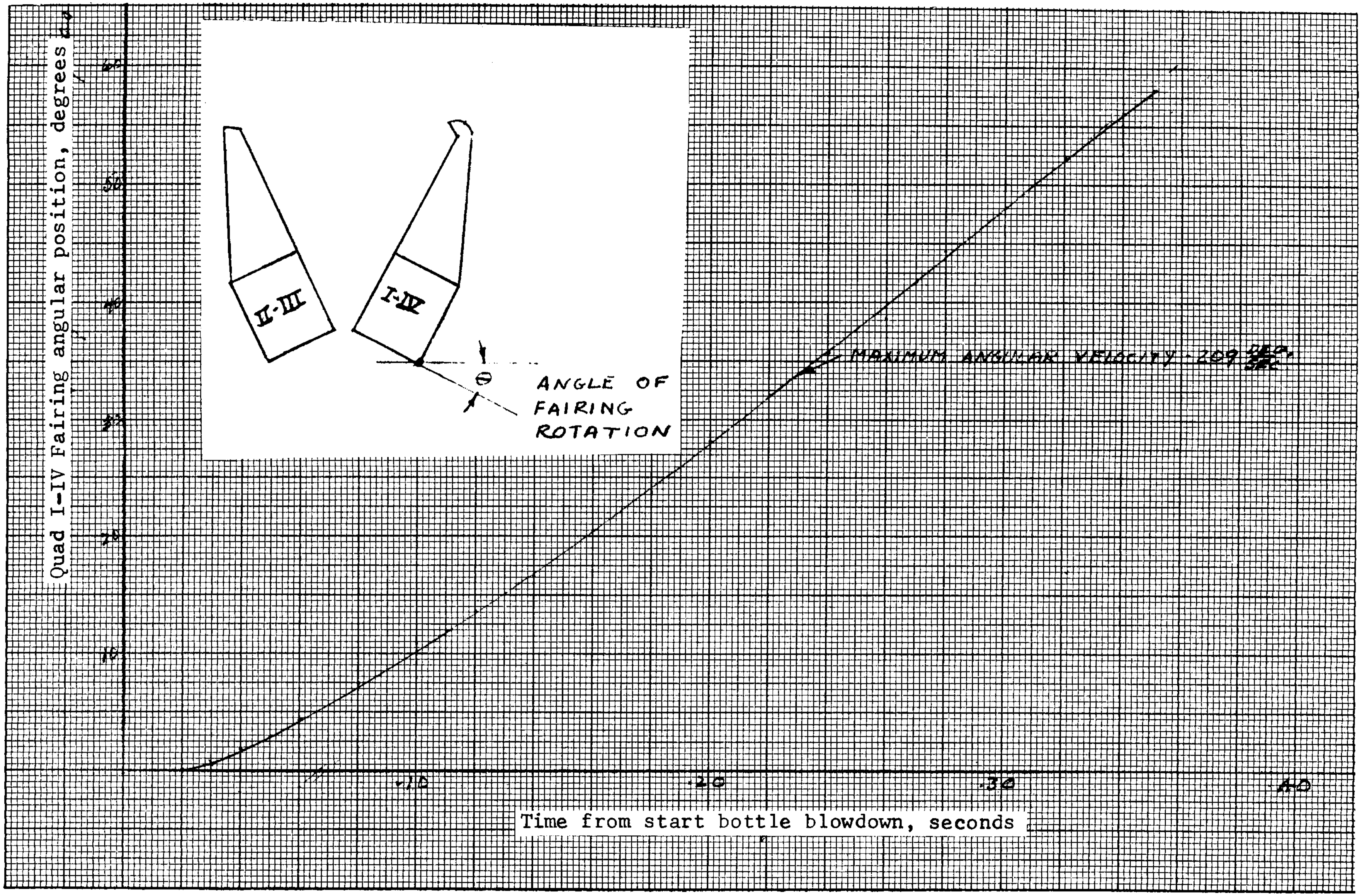

Figure 55. - Nose fairing angular position vs. time, test LA-3 (measured at the I-IV hinge point.)

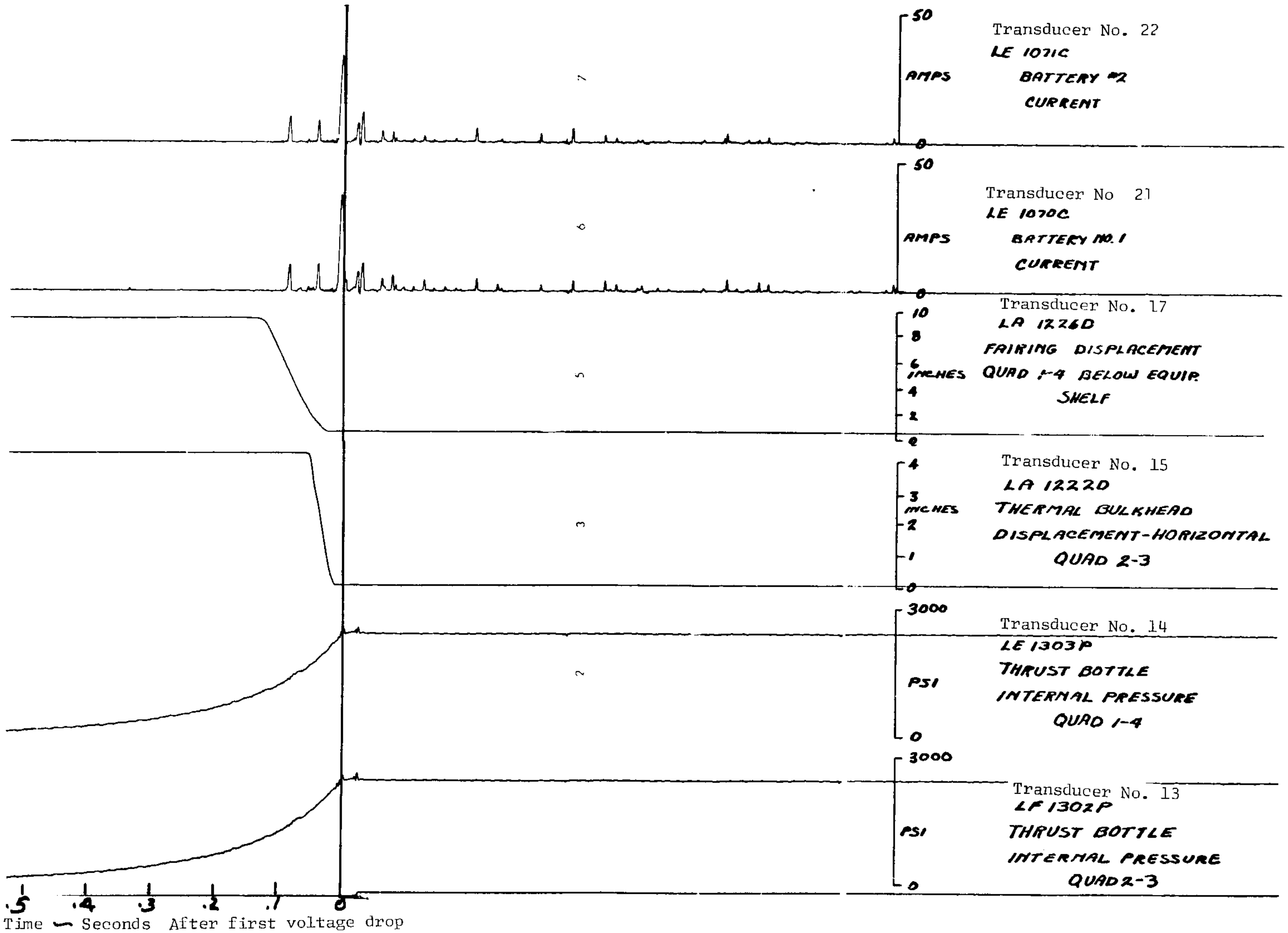

(a) Transducers 13, 14, 15, 17, 21 and 22.

Figure 56. - Data for test LA-4A.

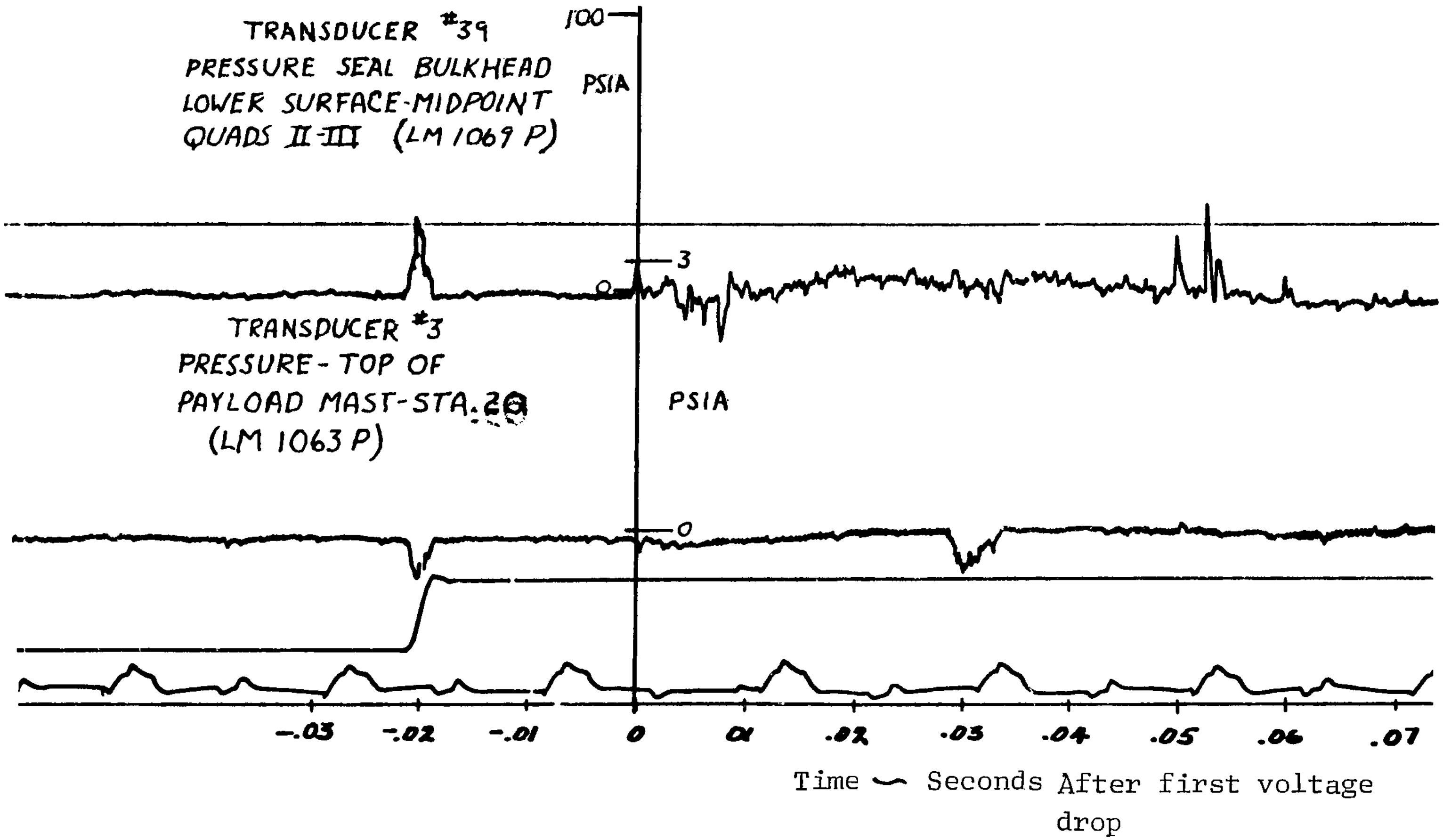

(b) Transducers 3 and 39.

Figure 56. - Continued. Data for test LA-4A.

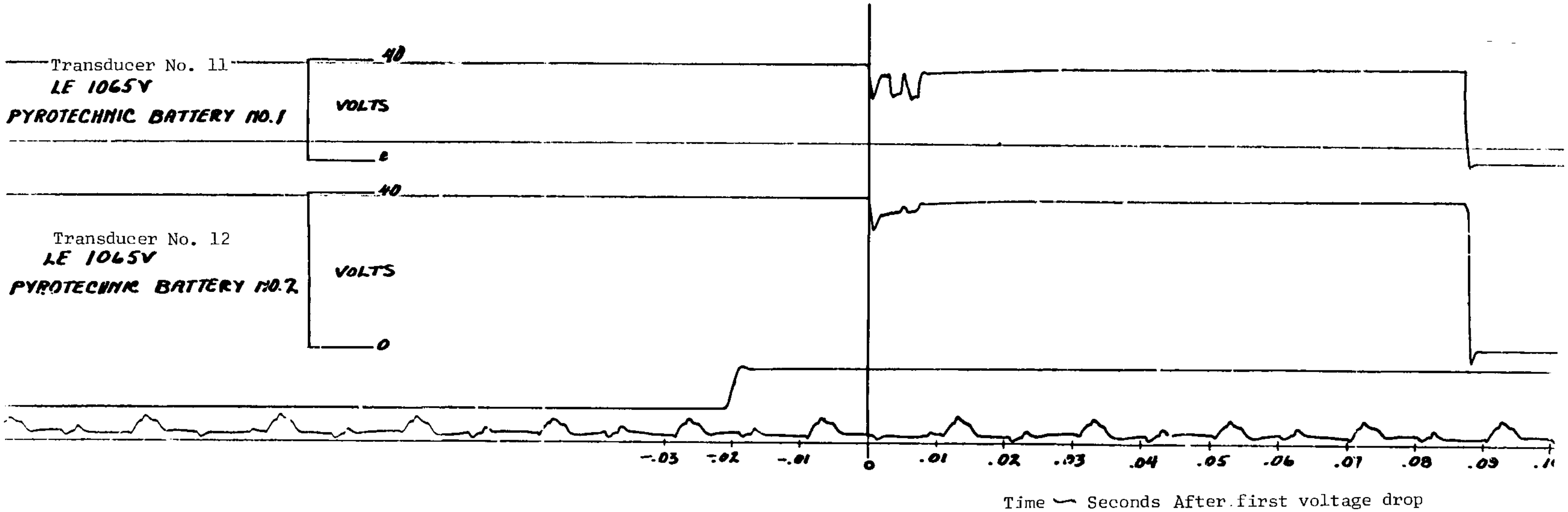

(c) Transducers 11 and 12.
Figure 56. - Continued. Data for test LA-4A.

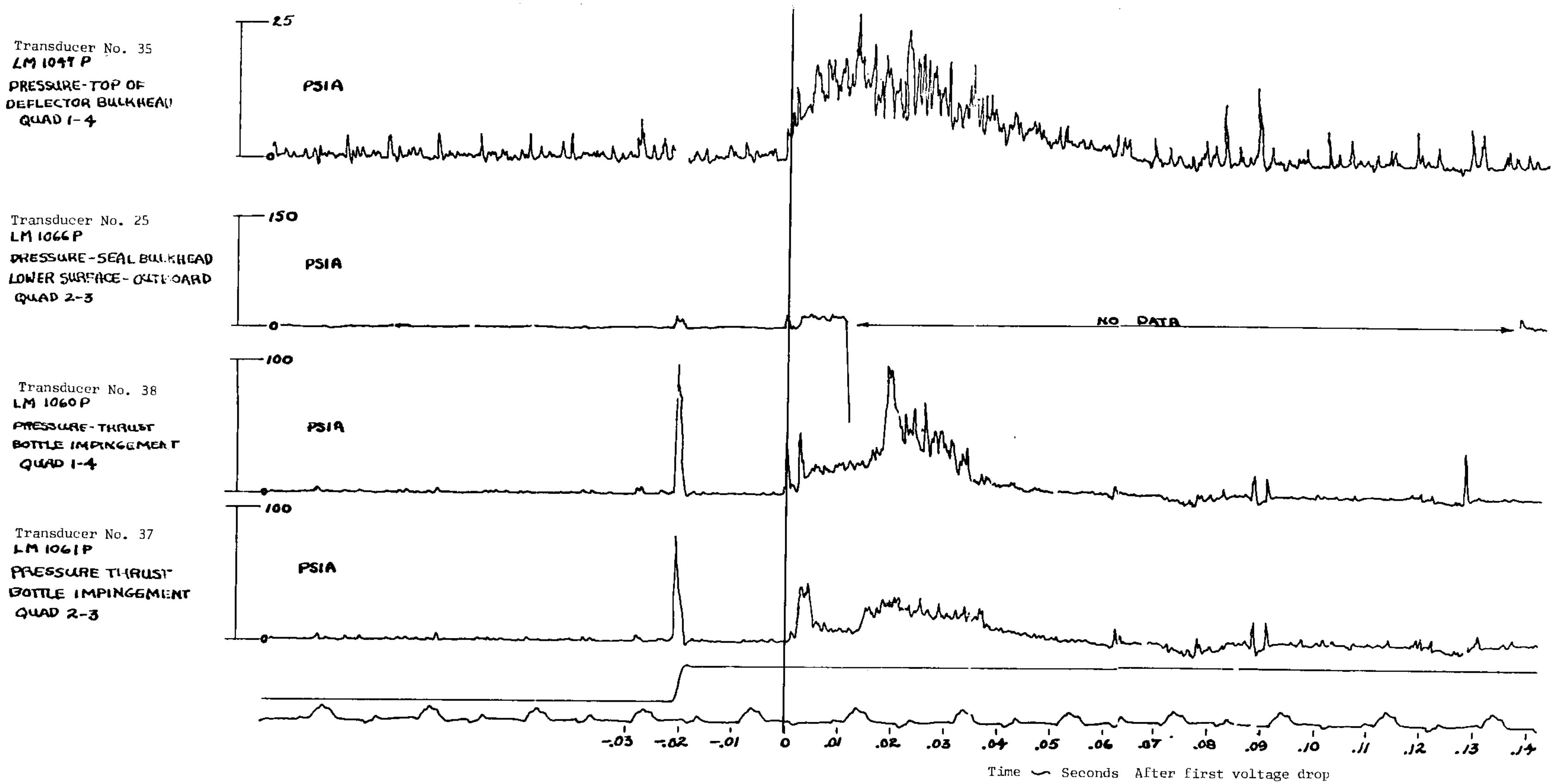

(d) Transducers 25, 35, 37 and 38.
Figure 56. - Continued. Data for test LA-4A.

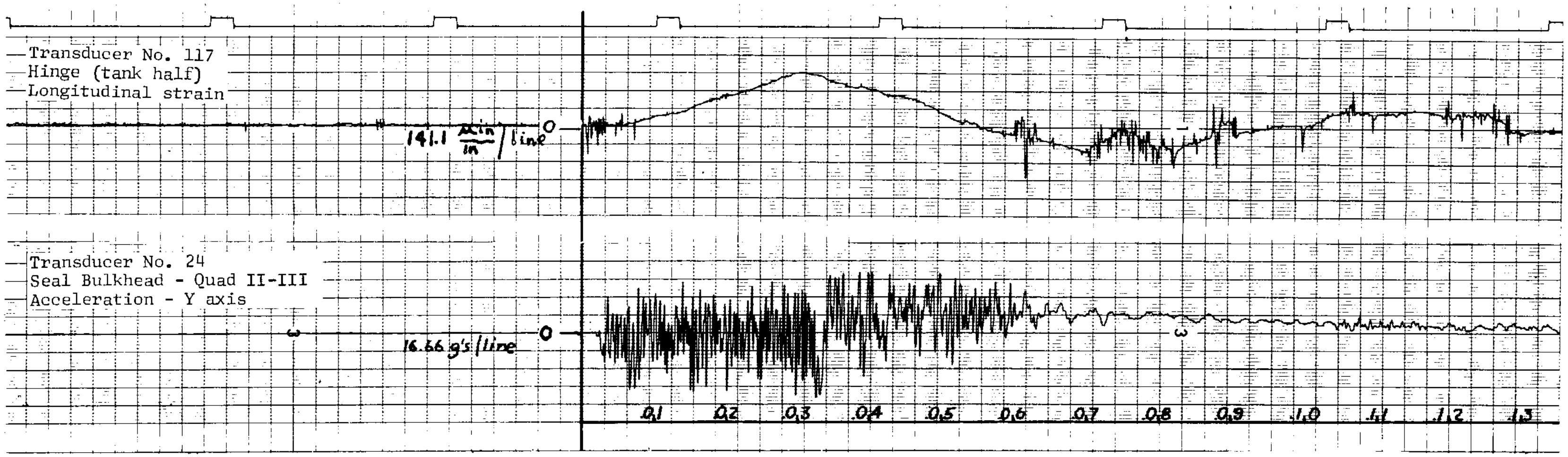

(e) Transducers 24 and 117.

Figure 56. - Concluded. Data for test LA-4A.

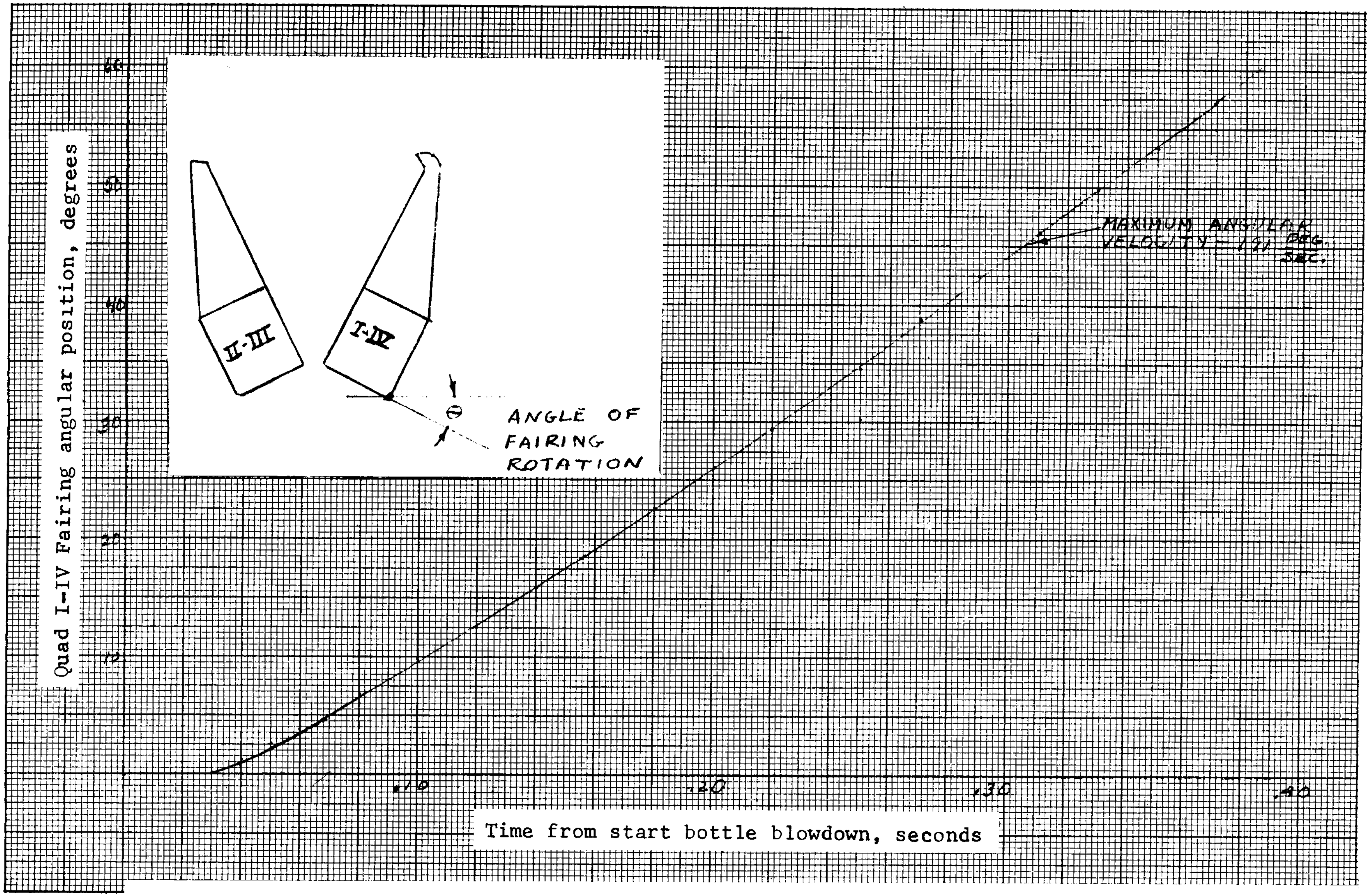

Figure 57. - Nose fairing angular position vs. time, test LA-4A (measured at the I-IV hinge point).

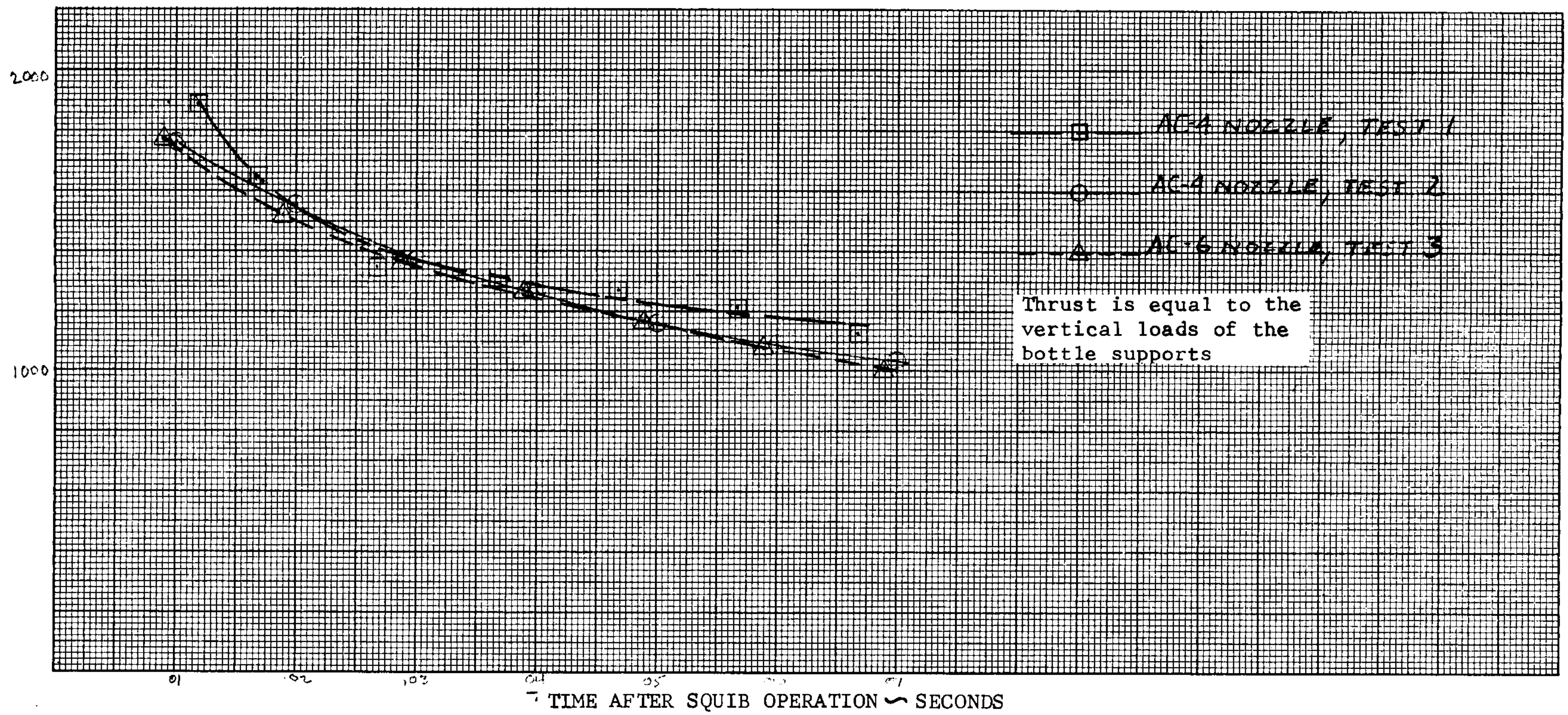

Figure 58. - Comparison of thrust, using AC-4 and AC-6 thruster bottle nozzles.

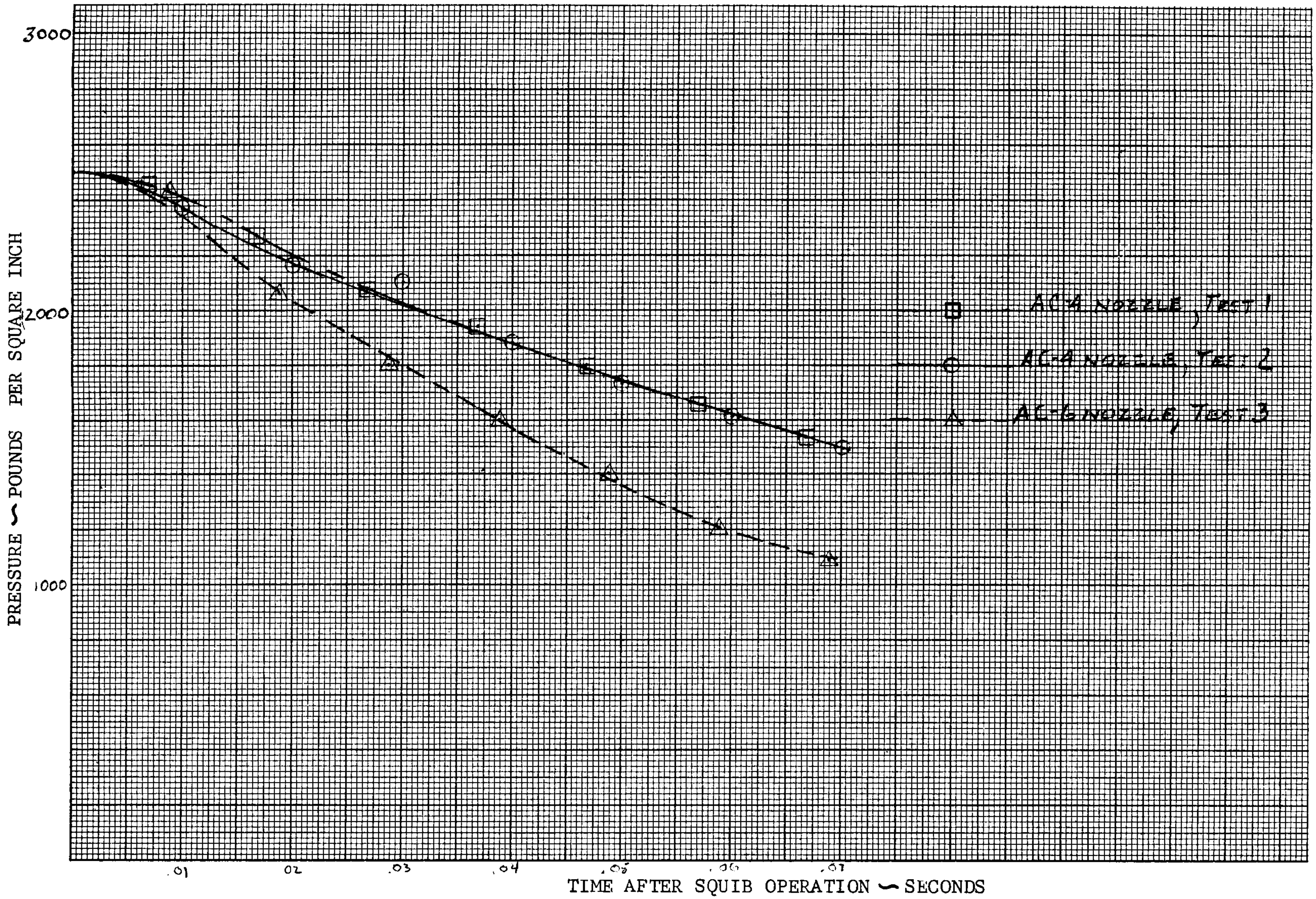

Figure 59. - Comparison of blowdown pressure, using AC-4 and AC-6 thruster bottle nozzles.

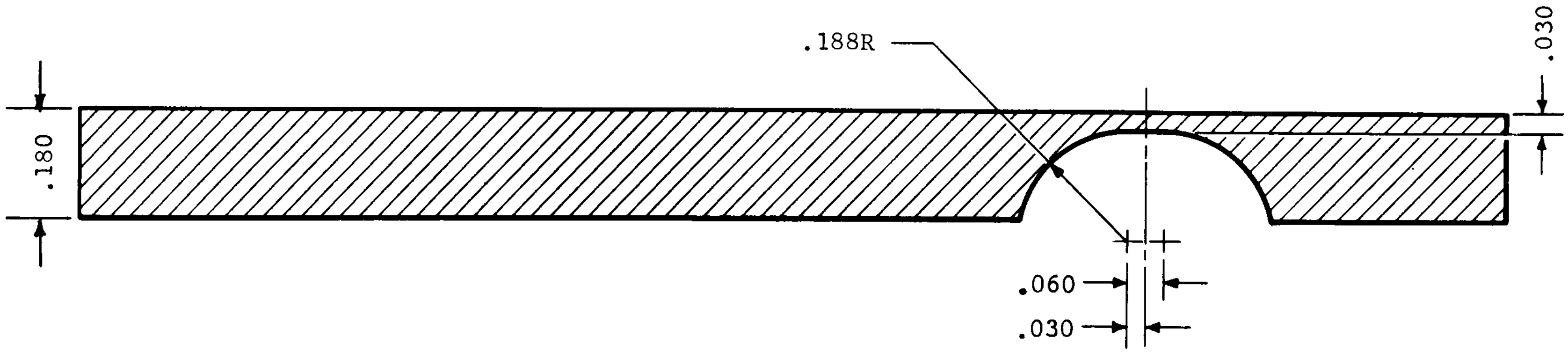

a) Tension tie as used in tests LA-1A, LA-2A, and LA-2B.

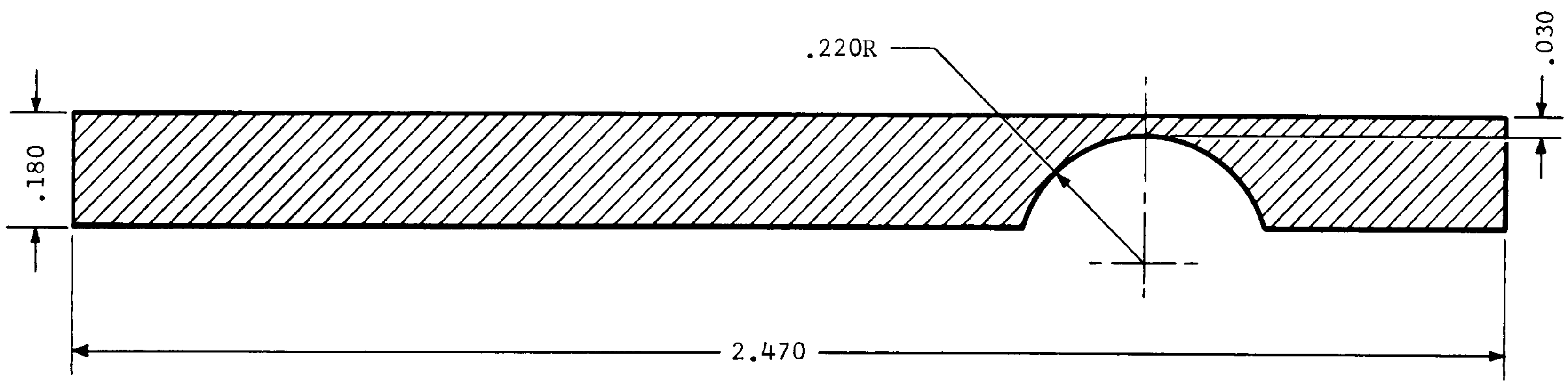

a) Tension tie as used in test LA-4B.

CD-8402

Figure 60. - Detailed view of the tension tie grooves for all AC-6 tests.

E-3897

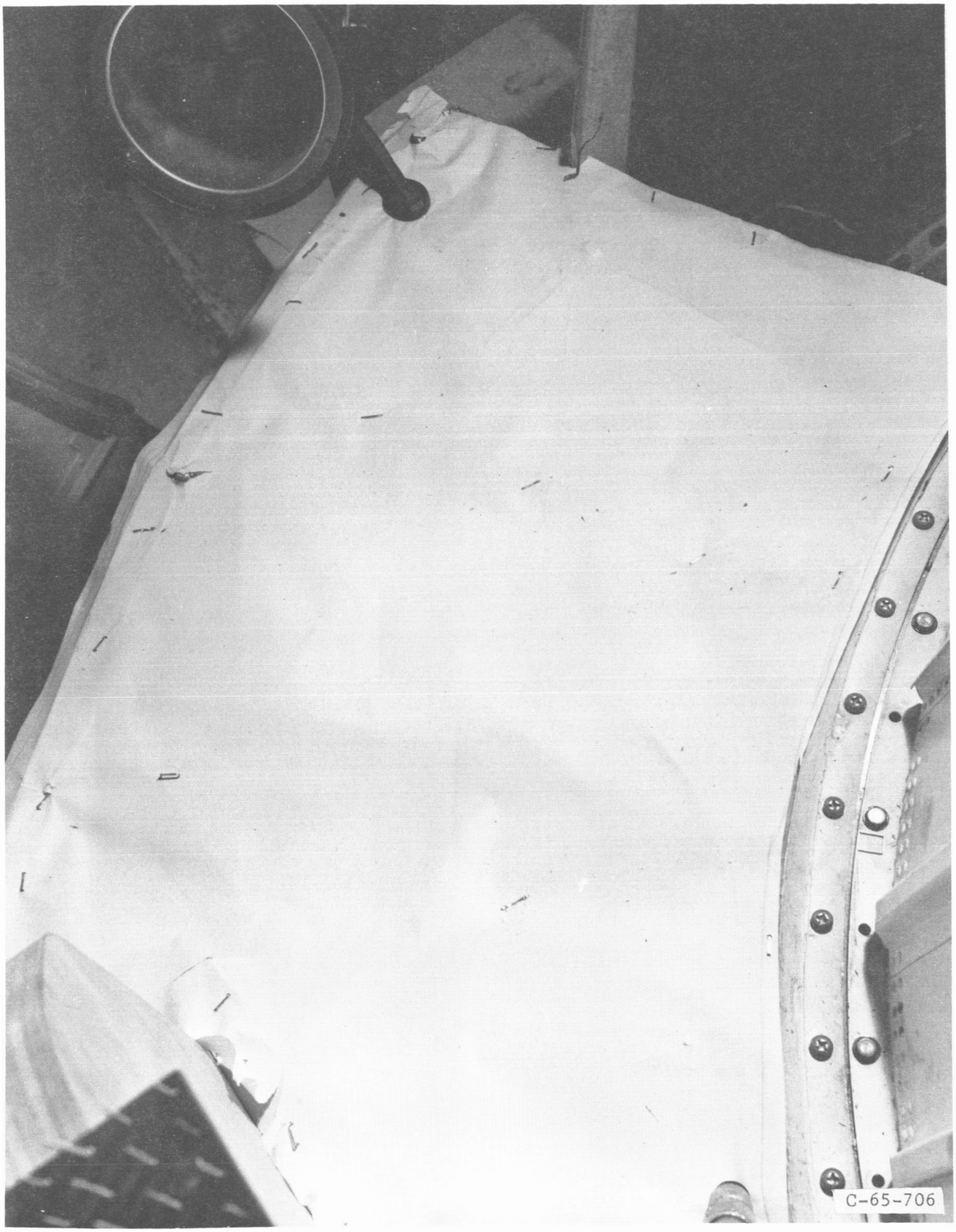

Figure 61. - Debris found on paper covering equipment shelf after test LA-1A.

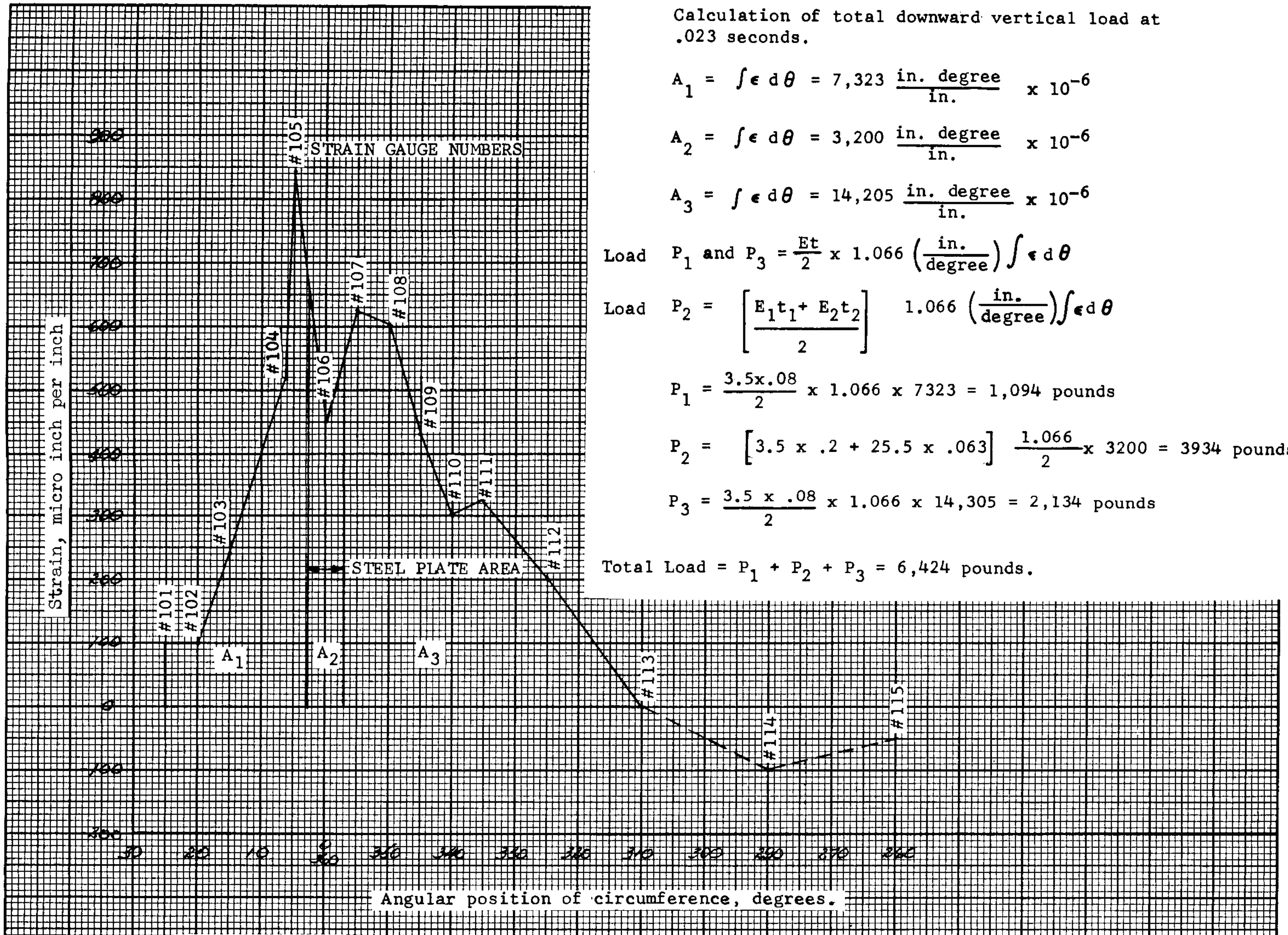

Calculation of total downward vertical load at .023 seconds.

$A_1 = \int \epsilon \, d\theta = 7{,}323 \ \frac{\text{in. degree}}{\text{in.}} \times 10^{-6}$

$A_2 = \int \epsilon \, d\theta = 3{,}200 \ \frac{\text{in. degree}}{\text{in.}} \times 10^{-6}$

$A_3 = \int \epsilon \, d\theta = 14{,}205 \ \frac{\text{in. degree}}{\text{in.}} \times 10^{-6}$

Load P_1 and $P_3 = \frac{Et}{2} \times 1.066 \left(\frac{\text{in.}}{\text{degree}}\right) \int \epsilon \, d\theta$

Load $P_2 = \left[\frac{E_1 t_1 + E_2 t_2}{2}\right] \ 1.066 \left(\frac{\text{in.}}{\text{degree}}\right) \int \epsilon \, d\theta$

$P_1 = \frac{3.5 \text{x} .08}{2} \times 1.066 \times 7323 = 1{,}094$ pounds

$P_2 = \left[3.5 \times .2 + 25.5 \times .063\right] \frac{1.066}{2} \times 3200 = 3934$ pounds

$P_3 = \frac{3.5 \times .08}{2} \times 1.066 \times 14{,}305 = 2{,}134$ pounds

Total Load $= P_1 + P_2 + P_3 = 6{,}424$ pounds.

Figure 62, Plot of fairing strain gauge reading and calculation of load for test LA-2D at .023 seconds after firing.

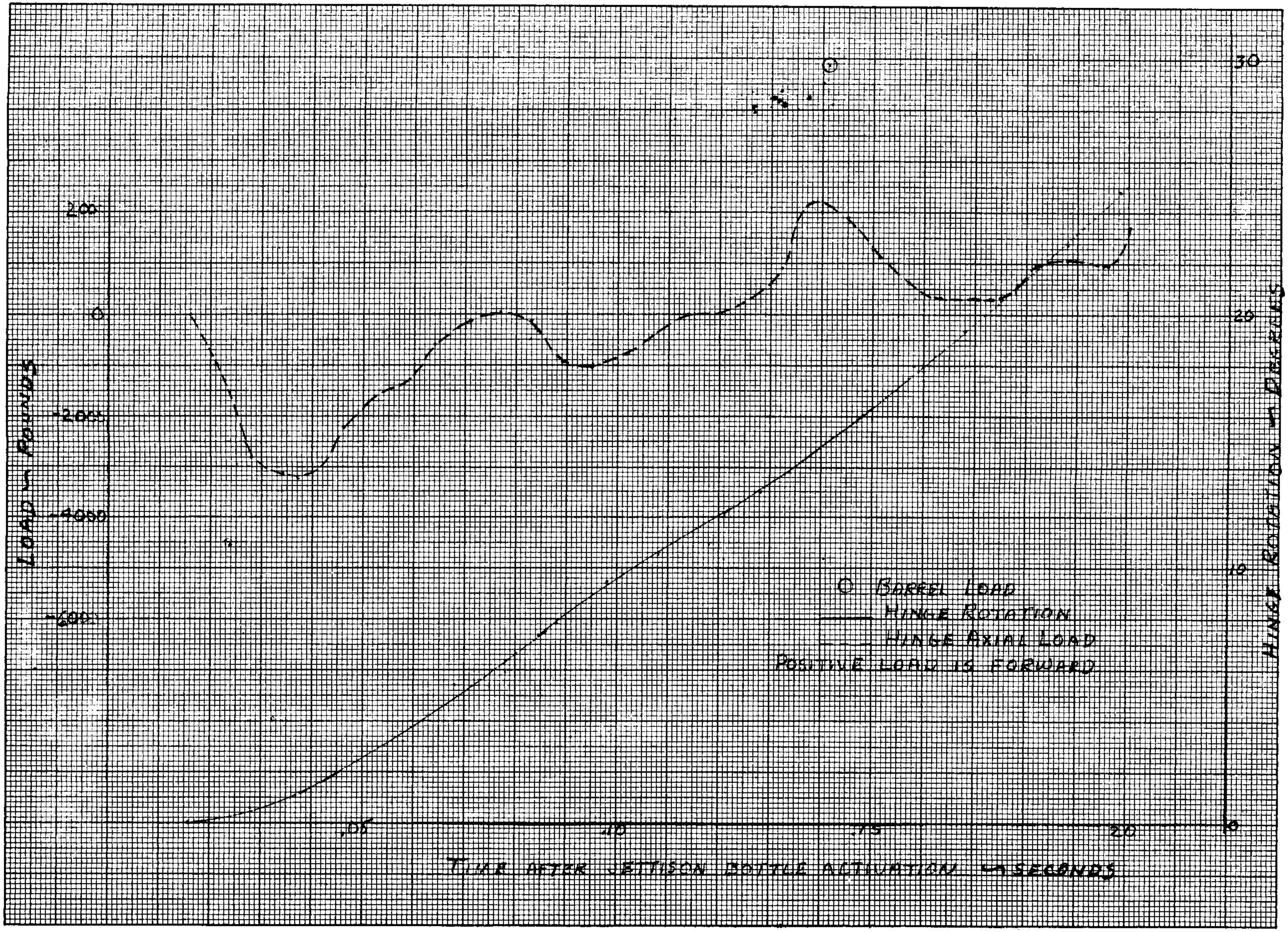

Figure 63. - Hinge and barrel loads and the rotation of fairing (Quad I-IV), test LA-1B.

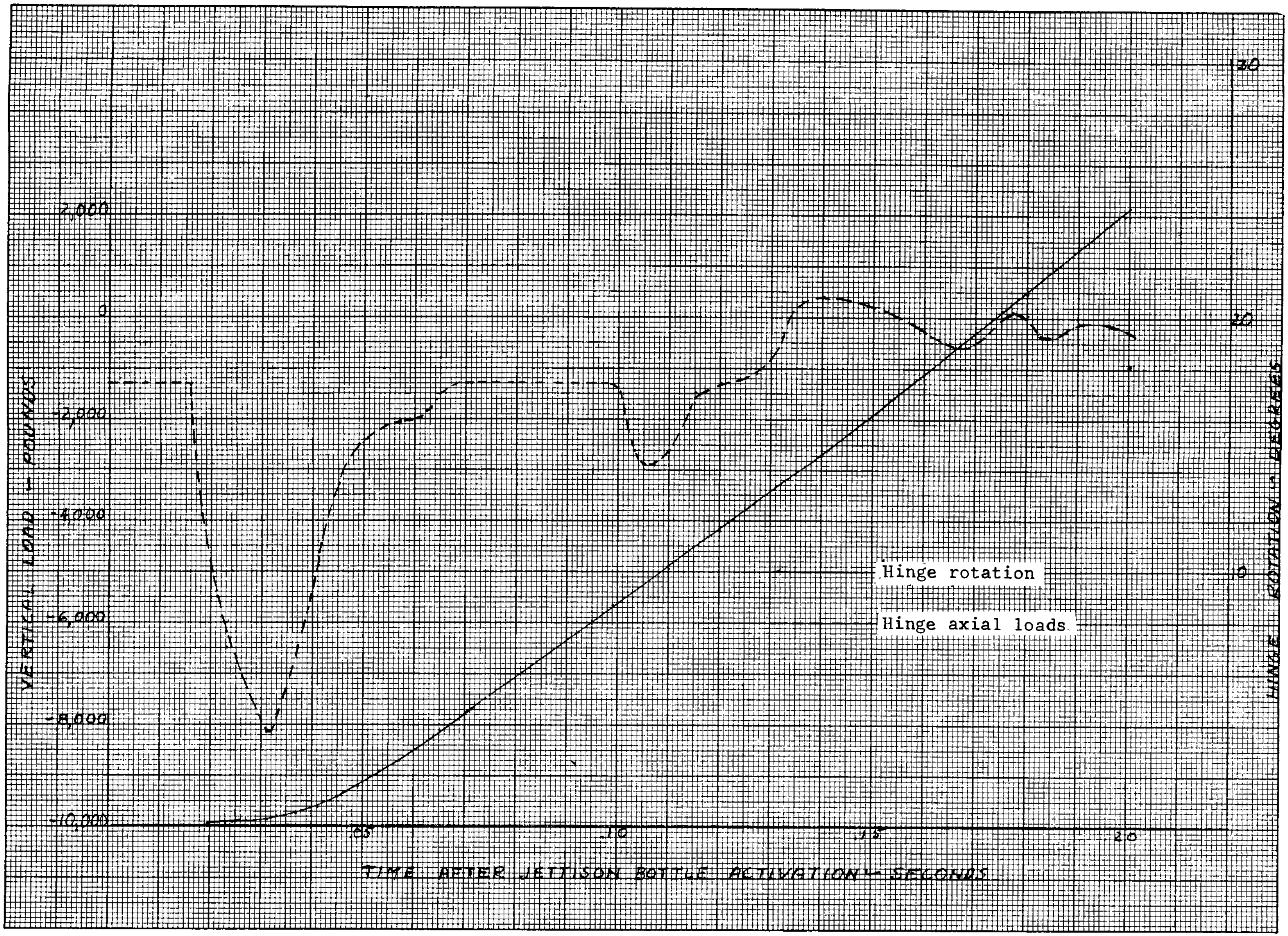

Figure 64. - Hinge and barrel loads and the rotation of fairing (Quad I-IV), test LA-2D.

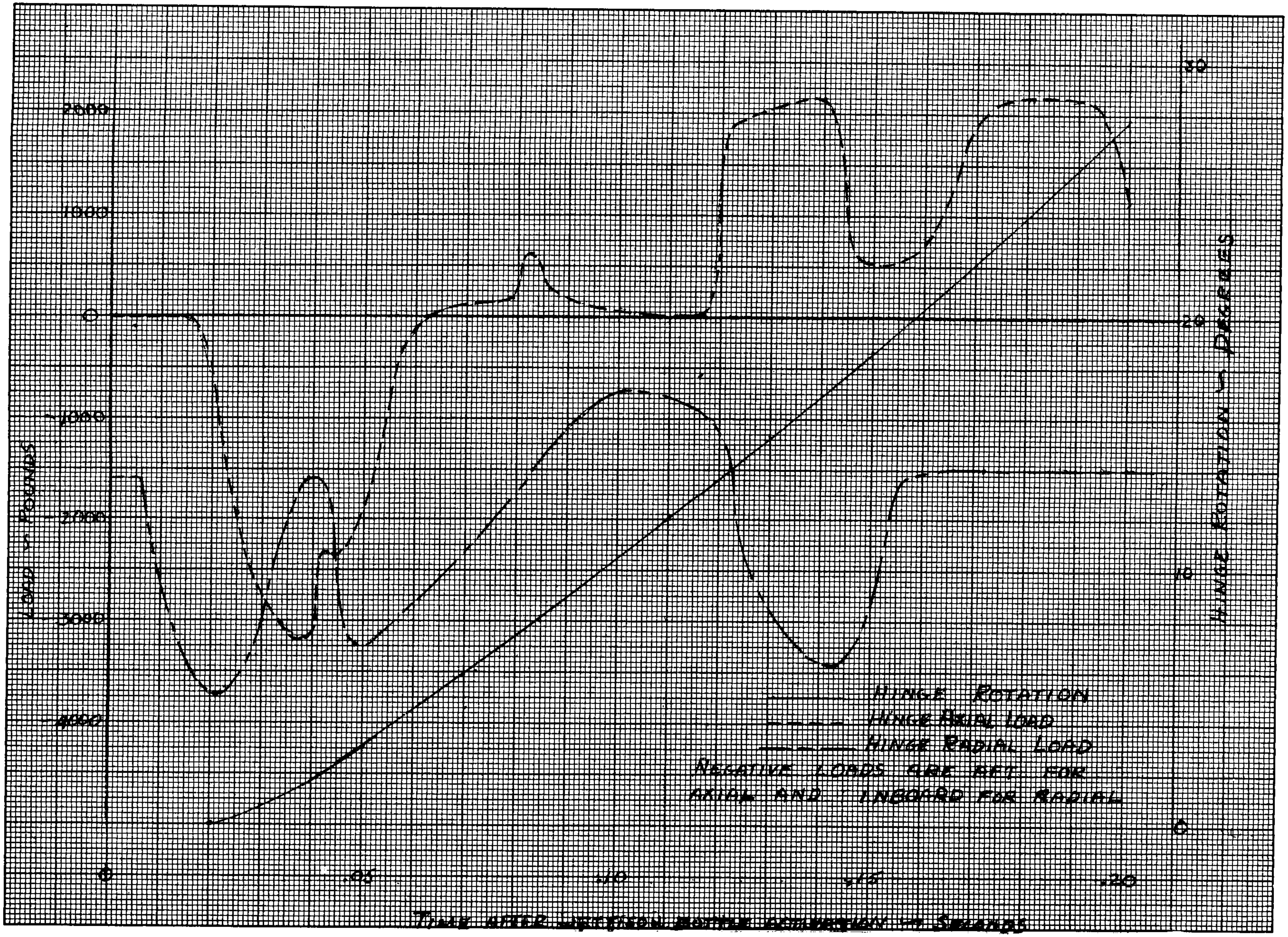

Figure 65. - Hinge loads and rotation of fairing (Quad I-IV), test LA-3.

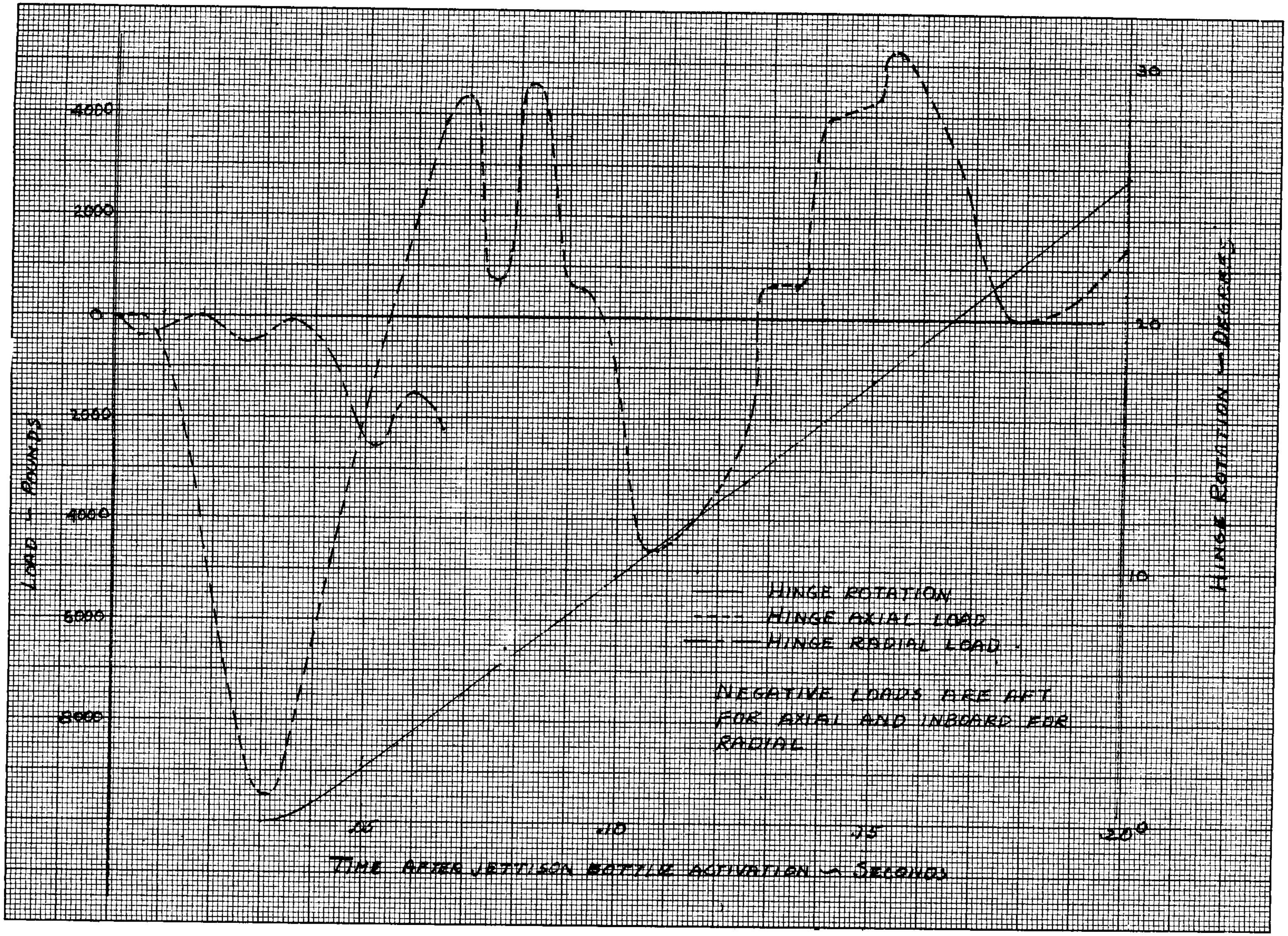

Figure 66. - Hinge loads and the rotation of fairing (Quad-I-IV), test LA-4A.

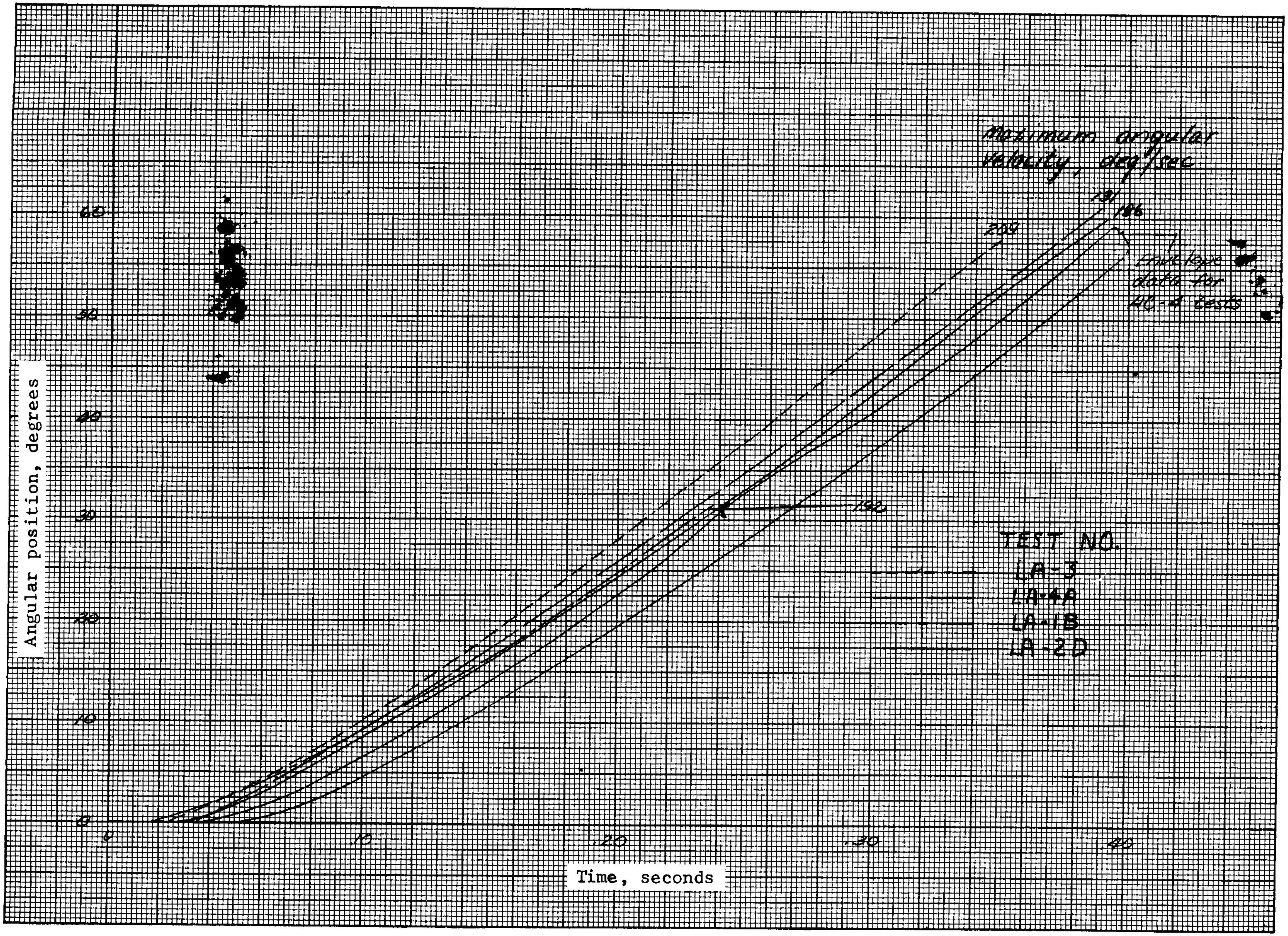

Figure 67. - Comparison of AC-4 fairing test angular positions with the AC-6 fairing test angular positions.

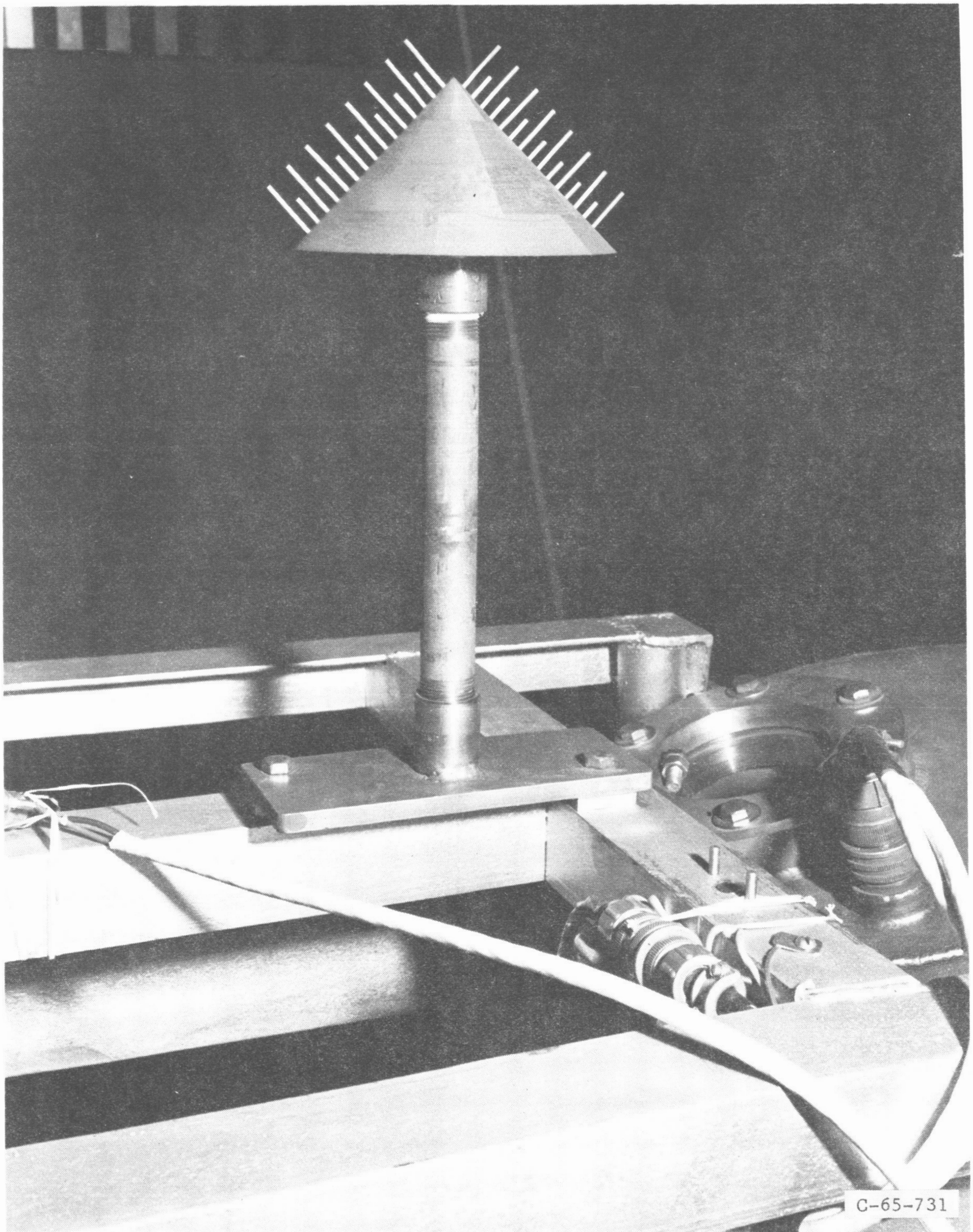

Figure 68. - Model of omni-directional antenna used in AC-6 tests.

E-3897

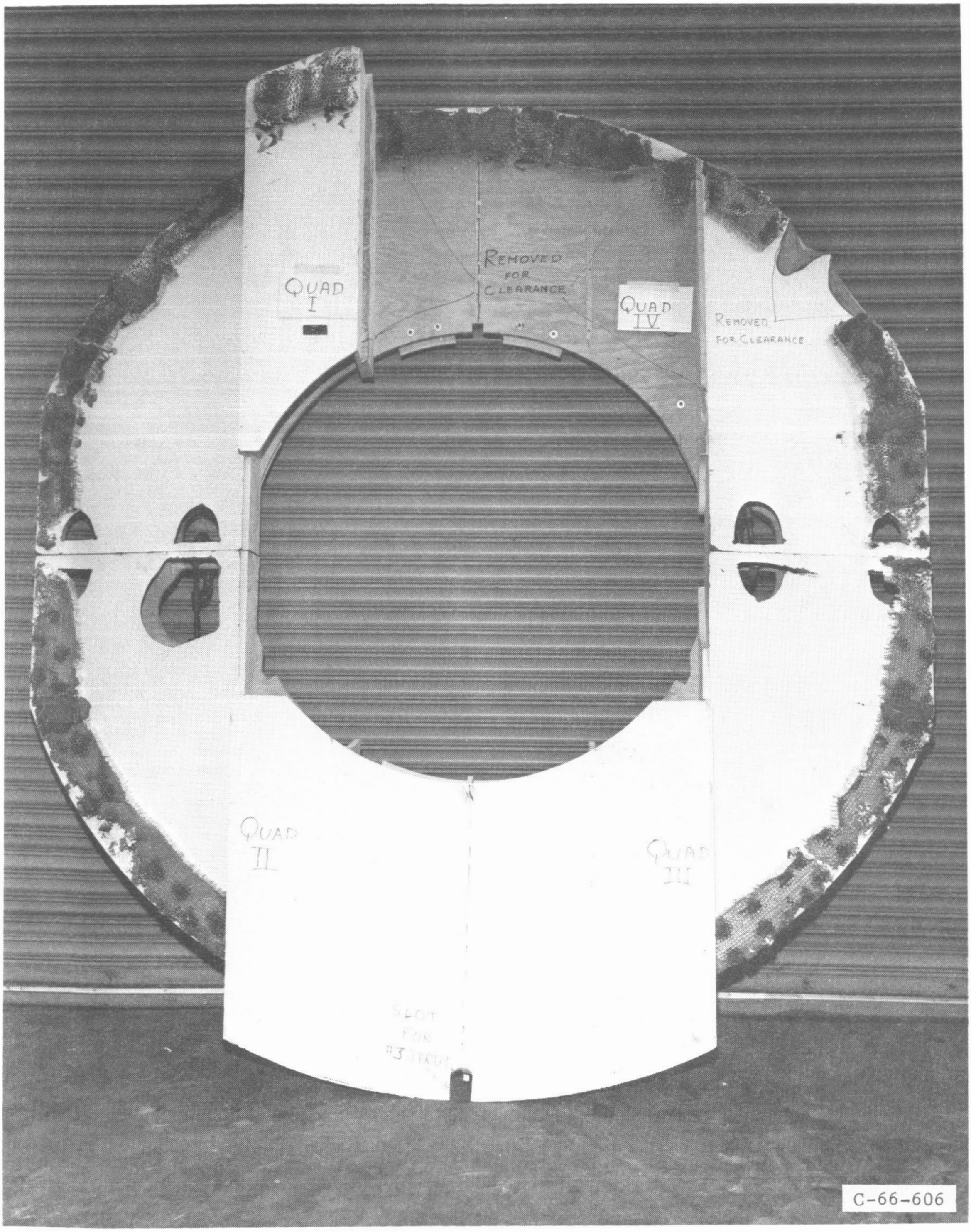

Figure 69. - Model of the Surveyor envelope and required changes.

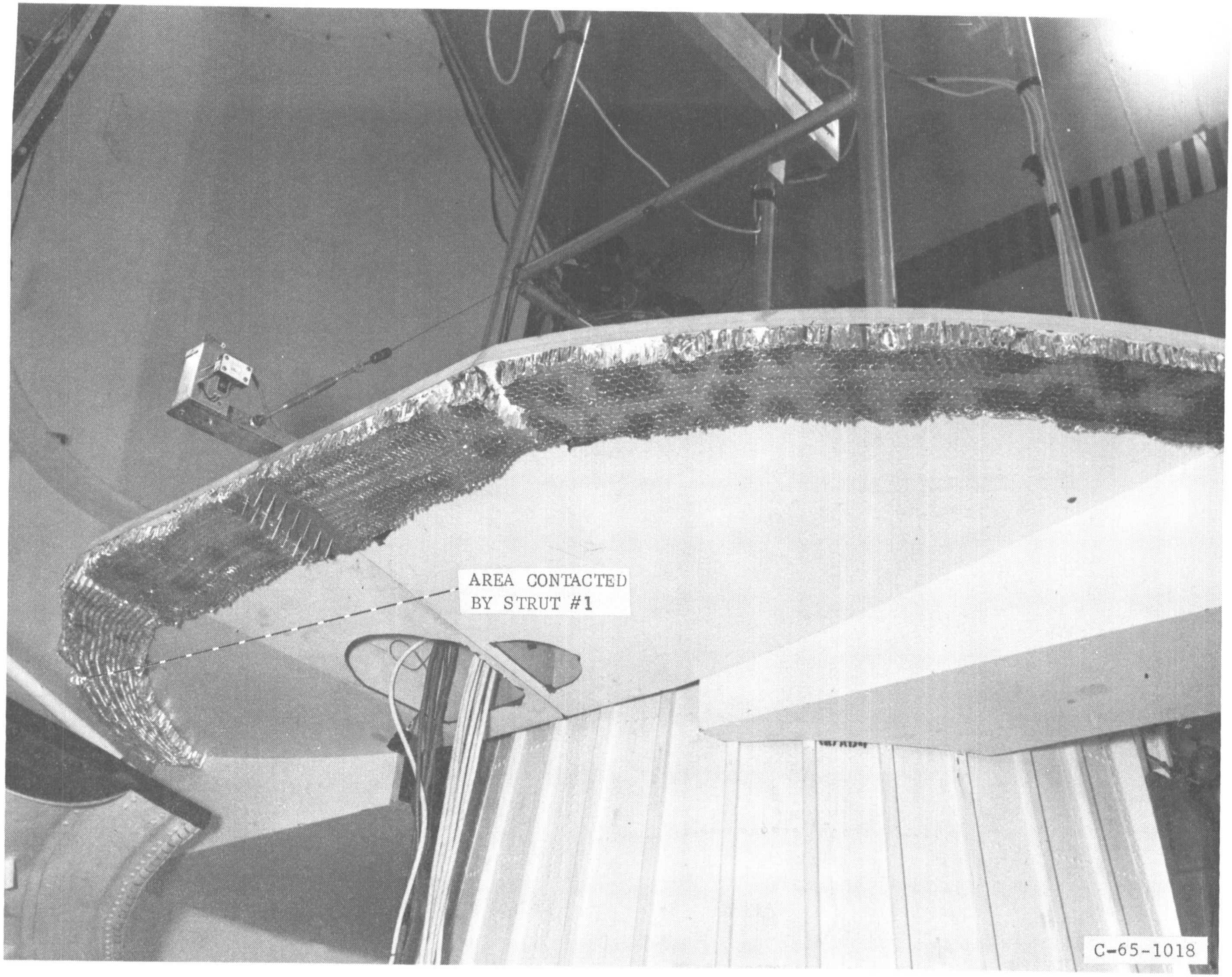

Figure 70. - Honeycomb on the envelope model after test LA-2D.